DTNH22-95-H-07002

COOPERATIVE AGREEMENT TO FOSTER THE DEPLOYMENT OF A HEAVY VEHICLE INTELLIGENT DYNAMIC STABILITY ENHANCEMENT SYSTEM

Interim Report

January 1998

Prepared by:
The University of Michigan
Transportation Research Institute
2901 Baxter Road, Ann Arbor, MI 48109-2150
under Cooperative Agreement: DTNH22-95-H-07002

for:
National Highway Traffic Safety Administration
U.S. Department of Transportation
400 7th Street S.W.
Washington, D.C. 20590

TABLE OF CONTENTS

LIST OF FIGURES

LIST OF TABLES

1.0 INTRODUCTION

This document provides an Interim Report on the Cooperative Agreement to Foster the Deployment of a Heavy Vehicle Intelligent Dynamic Stability Enhancement System. This project strives to develop, characterize, and demonstrate physical prototypes of two forms of intelligent subsystems that would enhance a truck driver's ability to obtain stable operations with an articulated heavy duty road vehicle. The systems in question address the potential instabilities of A) quasi-steady-state rollover and B) rearward amplification of lateral acceleration (especially in multiply-articulated trailer combinations.) Both forms of instability have been broadly documented through prior research and both are known to directly influence the crash record.

The "cooperative agreement" funding mechanism is established between the sponsor, the National Highway Traffic Safety Administration (NHTSA) and the University of Michigan Transportation Research Institute (UMTRI), in association with six industrial companies which each has interest in the commercial potential for dynamic stability enhancement products. The commercial partners and the contexts of their respective interests in this work are the following:

- Freightliner Corporation, North America's highest-volume manufacturer of heavy duty trucks and tractors in the U.S., which is interested in tractor-based stability enhancements as a further area of improvement in the safety performance of its vehicles;
- Hendrickson-Turner, the leading U.S. manufacturer of truck suspensions, which is interested in augmenting its air spring suspension products with sensory features that will enable rollover proximity assessments;
- Holland Hitch Company, the major supplier of fifth wheel hitches and other coupling components to the trucking industry, which is interested in instrumented fifth wheel products that may support an active stability enhancement function;
- Midland-Grau, a major supplier of brake components to U.S. and European markets, which seeks to find value-added improvements in the functionality of electronic braking systems for heavy duty vehicles;
- Rockwell Autonetics Division, a U.S. developer of micromachined inertial sensing instruments for automotive applications, which is interested in intelligent truck applications for such products;
- TRW's Commercial Steering Division, the largest seller of integral steering gears for the North American truck market, which is interested in enhanced features that may add value to steering system.

This Interim Report presents the conceptual basis for each of the two stability enhancements plus the progress made on the development of each system. Initial versions of both system types are described, as they have each been prototyped on a heavy-duty vehicle during the first portion of the study. Results from the preliminary testing of each system are also presented and discussed. While there is clearly room for substantial improvement on each system concept, the early results show that both system types are, indeed, viable from a technical point of view. The report concludes with an outline of steps remaining for further upgrading performance as well as for realizing certain configurational improvements in both systems.

2.0 THE ROLLOVER STABILITY ADVISOR SYSTEM

The first of the two stability enhancement systems is called the Roll Stability Advisor (RSA) system. In section 2.1, below, the concept of the system function and implementation is discussed as is the background rationale for selecting this function as a high-priority enhancement for modern trucks.

Given a statement of the RSA functionality, in general terms, the remainder of this section reports on progress to date in support of its realization. In section 2.2, laboratory measurements that were undertaken to quantify vehicle parameters and mechanical characteristics are presented. These measurements have been used in support of full-scale experiments by which prototype forms of the RSA system are evaluated.

In section 2.3, the first prototype of the RSA system is described. This system is based upon sensing roll-related responses at only the axle of a semi-trailer. Section 2.4 then presents the methods employed and the results obtained from testing this so-called "trailer-based" RSA system.

In preparation for the converse design approach in a *tractor-based* RSA system, section 2.5 summarizes an extensive analytical task by which a system identification technique was developed for deriving a roll stability assessment from the continuous measurement of roll-related responses on the tractor, only. The analysis considers differing approaches for estimating rollover threshold using real-time sensor data, one avenue of which is via a fifth-wheel load cell which is being developed within this project, as discussed in section 2.6. Implementation of a tractor-based RSA prototype, employing the new fifth wheel load cell and the associated processing algorithm will follow in the final portion of the project, including the conduct of full scale tests for evaluating this system's performance.

2.1 Concept and Rationale for Roll Stability Advisor

By way of introduction and background to the RSA system, we present below its underlying concept as well as the rationale linking such a system function to the potential for actually improving the safety record if such systems were in use.

2.1.1 RSA Concept

The RSA concept involves a real-time measurement and analysis of the roll-related properties of a vehicle, as it travels down the road which is done for the sake of displaying to the driver those aspects of this information that will enable the driver to properly appraise rollover risks. The concept requires the operation of sensing devices whose electronic output signals are processed through some form of *system-identification* algorithm in order to derive the display information. The algorithms will first automatically determine the as-loaded roll stability limit of the vehicle within the first few minutes of driving (i.e., after a new payload or a new trailer has been applied to the power unit.) The deduced rollover threshold of the vehicle is then presented and sustained as one aspect of the display.

As the vehicle is driven during the ensuing trip, the real-time proximity of maneuver severity, or *demand*, to this threshold value is captured and presented on the driver's display, with supplemental audio and perhaps modulated steering torque as attention-getting cues where appropriate. Assuming that the driver is unable to pay much attention to any visual display during the rare dramatic maneuver, the advisory system display is made to be inherently retentive such that an after-the-fact review of the rollover proximity that prevailed in the prior maneuver is available at a glance.

Clearly, the RSA concept as outlined here implies a training, or conditioning, instrument in contrast to, say, an automatic-rollover-avoidance system that can actually intervene to circumvent a rollover crash. The collaborators in this project have tended toward the view that systems of the automatic intervention type are commercially infeasible as rollover countermeasures for the foreseeable future. Further, it should be noted that the described RSA function goes well beyond that of *rollover warning* which is invoked only when an instability is pending. In fact, it is felt that warning of an imminent rollover is likely to have minimal safety benefit because rollover-precipitating conditions, once established, tend to avail little opportunity for driver correction.

Accordingly, the RSA concept is targeted to address the classical problem of the driver's failure to perceive: (a) the as-loaded stability level of the vehicle in relation to, (b) the roll-inducing demands actually imposed while underway. This approach recognizes that the driver has a general need to recognize and appreciate the rollover margin, especially with each new load that is carried. While this *appreciation* must eventually become intuitive, it is hypothesized that an intelligent advisory system can cultivate an accurate intuitive grasp of the essential rollover conflict issue within a reasonable term of system

usage. After a few months of exposure to the RSA system just described, it is expected that the typical driver would cease to consult the rollover-proximity display with any frequency and would, instead, simply note the as-loaded stability level as a sort of "calibration" before beginning a trip with a new load. At this stage, the driver would be making it a point to observe the as-loaded stability indicator as a regular in-trip supplement to the walk-around, pre-trip inspection of the rig.

2.1.2 Rationale underlying selection of the RSA concept for study

The RSA rationale begins with the observation that the low level of roll stability in heavy duty trucks constitutes the *principal manifestation* of dynamic limitations in this vehicle class. Further, the compelling size of the safety problem that is posed by truck rollover crashes is recognized as the principal argument suggesting a potential market for an RSA product. On the other hand, as stated earlier, the development of a product for automatically controlling the vehicle to avoid a pending rollover calls for too large a technological stretch (especially for the historically very conservative commercial truck market) and thus is seen as posing a commercially-unrealistic goal. Further, a simple system that would only warn when rollover is imminent would probably offer little value as a countermeasure. A further assumption was that any system requiring a *cooperative infrastructure* or even a roadway database that incorporates a sufficient level of detail on road curvatures and superelevation to supplement on-board dynamic measurement is too futuristic to qualify as a state-of-the-art implementation.

The primary fact arguing that the RSA approach would offer value as a strategic sort of countermeasure to rollover-risky driving arises from the probabilistic nature of the demand for rollover resistance, from one maneuver to the next. The probability density of roll-stability demands is known to be distributed in a manner very much like that which has been documented in many other domains of driver control behavior.[1] Thus, for every steering maneuver that demands 0.3 gs of lateral acceleration, for example, there are perhaps 20 that have demanded 0.25 gs, 400 that demanded 0.2 gs, and maybe 8,000 that demanded 0.15 gs. [e.g. 2] Accordingly, the very high incidence of sub-limit demand levels offers a great opportunity within which to train, or at least acquaint, the driver with an accurate and current illustration of his/her proximity to rollover.

In an era when there is a high rate of entry of inexperienced drivers into the trucking industry, the value of an RSA system was seen as unusually high. Thus, while it is suspected that even very experienced truck drivers could benefit from RSA advice, there is no question that a special market stimulus derives from the high state of flux in the truck driving population.

One can imagine that many fleets might wish to equip at least a few of their tractors with RSA systems simply for upgrading their drivers, or introducing new ones, to a high

state of rollover-proximity awareness. At the same time, it is assumed that the RSA concept is not devalued significantly by the background risk of rollover that will prevail while the "training phase" of a driver's first use of an RSA system is underway. It is noted, for example, that the absolute risk of rollover averages around six per 100 million miles of tractor-semi-trailer operation.[3] In, say, the first month of RSA-assisted training on rollover-proximity awareness, a driver covering 5000 miles would have otherwise had only a 1-in-3,000 chance of rollover. Thus, such a system which gives on-the-job safety-training is not significantly reduced in value by the fact that the safety risk prevails (as with all on-the-job exposures) throughout the training period, itself.

On the matter of rationalizing an RSA system configuration, it is useful to reflect on the vehicular platform upon which differing portions of the system investment might be made. Firstly, it is highly pertinent that tractors are replaced in the larger fleets every 3-5 years while semi-trailers turn over in fleet inventory on a schedule of, say, 15 to 20 years. Thus, if one is to create a marketing strategy for introducing a new stability-enhancement package, the commercial opportunity for rolling out a stand-alone, tractor-based system is much greater than for a system requiring matched tractors and trailers in cooperation.

Further, the tractor manufacturers have engineering groups that are growing in technical sophistication and are moving inexorably to play major roles in the integration of chassis and drivetrain controls. Thus, this project was designed to emphasize the development of an RSA system based upon a tractor-only implementation as a priority goal. At the same time, the project also included a provision for considering trailer-based measurements in deriving the roll-proximity information. This latter approach is more straightforward in terms of the mechanics of the problem but it poses a marketing strategy that will be difficult to realize. Nevertheless, the project was set up to address alternative approaches for implementing the rollover-proximity concept.

2.2 System Design For The Trailer-Based RSA Approach

The goals of the trailer-only RSA system (i.e., the RSA system lacking a fifth-wheel load transducer) are to (1) estimate the lateral accelerations (right and left) at which left and right wheels on the trailer axle would lift off the road surface, and (2) display these estimates plus the current lateral acceleration of the vehicle to the driver. These estimated lateral accelerations are not likely to be exactly equal to the actual rollover thresholds. However, given fairly even fore/aft load distributions in the trailer, they are expected to be close to, and somewhat less than, the actual limits.

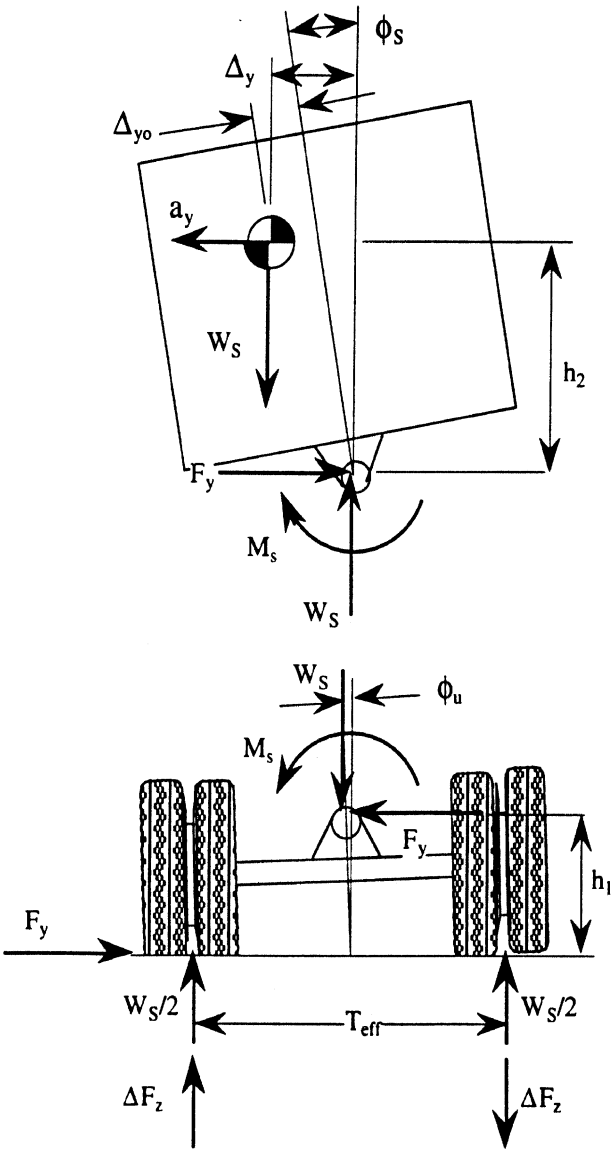

Figure 1. A roll model of the trailer sprung and unsprung masses

Figure 1 shows a simplified, steady-state model for predicting liftoff of the tires of the trailer axle. Freebody diagrams of the sprung and unsprung masses are shown separately. The sprung mass represents only that portion of the trailer supported by the trailer suspension. The unsprung mass is the trailer axle assembly. These two bodies are connected at a pivot joint, the so-called roll center. The total effective weight of these elements (i.e., the weight carried by the trailer suspension, W_S) is lumped in the sprung mass. Other nomenclature in the figure are as follows.

a_y	is lateral acceleration
F_y	is the total side force acting on the axle,
h_1	is the effective height of the roll center,
h_2	is the height of the center of gravity of the mass above the roll center,

M_s is the suspension roll moment about the roll center,

T_{eff} is the effective track width,

ΔF_z is the vertical load transferred from right-side to left-side tires

Δy is the lateral offset of the sprung mass from the center of the track at the ground,

Δy_o is the lateral offset of the sprung mass from the centerline of the trailer (i.e. at the zero-roll condition)

ϕ_S is the roll angle of the sprung mass, and

ϕ_U is the roll angle of the unsprung mass.

The condition of static equilibrium applied to the sprung mass requires that

$$F_y = a_y W_S , \tag{1}$$

$$M_s = a_y h_2 W_S + \Delta y W_S . \tag{2}$$

By the geometry of the figure, and assuming linear roll behavior,

$$\Delta y = \Delta y_o + \phi_S h_2 = \Delta y_o + a_y k_{\phi S} h_2 , \tag{3}$$

where $k_{\phi S}$ is the effective roll rate of the sprung mass with respect to lateral acceleration.

By combining these three equations, it can be shown that

$$M_S = a_0 + a_1 a_y , \tag{4}$$

where $$a_0 = (\Delta y_o W_S)/(1- k_{\phi S} h_2 W_S) , \qquad a_1 = (h_2 W_S)/(1- k_{\phi S} h_2 W_S) . \tag{5}$$

Static equilibrium of the unsprung mass of figure 1 requires

$$\Delta F_z T_{eff} = M_S + h_1 F_y + W_S \phi_U h_1 , \tag{6}$$

which, by using equation 1, can be restated as

$$\Delta F_z T_{eff} = M_S + h_1 W_S a_y + W_S \phi_U h_1 . \tag{7}$$

In equation 7, the third term on the right side is generally small and can be neglected. This can be shown by further substituting equation 2 and factoring W_S to obtain

$$\Delta F_z T_{eff} = W_S[a_y (h_1 + h_2) + \Delta y + \phi_U h_1] . \tag{8}$$

Near tire liftoff, the value of $[a_y (h_1 + h_2)]$ is typically at least 20 inches and Δy may be large or small. However, the value of $[\phi_U h_1]$ is always small–on the order of 0.5 inch. Thus, the following approximation of equation 7 is justified.

$$\Delta F_z = b_1 M_S + b_2 W_S a_y , \tag{9}$$

where $$b_1 = 1/ T_{eff} , \qquad b_2 = h_1/T_{eff} . \tag{10}$$

By definition, at tire liftoff:

$$\Delta F_z = \pm W_S/2 \,. \tag{11}$$

Equations 4, 10, and 11 can be solved for a_y at liftoff as follows:

$$a_{ylift} = \frac{\pm W_S/2 - a_0 b_1}{a_1 b_1 + b_2 W_S} \,. \tag{12}$$

Equation 12 is the basis on which the RSA system predicts the lateral acceleration at which trailer tires will lift off the road surface. The parameters b_1 and b_2 are obtained from preliminary "calibration" of the suspension. They become permanent constants of the RSA routine for a given trailer. The values of W_S, a_0, and a_1 are obtained on board the operating vehicle in real time. The prediction process goes on continuously, and the resulting value of a_{ylift} is continuously updated. (Note that in this process, the values of a_0, a_1, b_1, and b_2 are all found directly. That is, there is no need to determine all the individual components that appear on the right-hand sides of equations 5 and 10.)

The sensor for determining vertical load, W_S, is a pressure transducer that continually measures the internal pressure of the air springs. Figure 2 is a freebody diagram of a typical air-suspension axle in the side view. Summing moments about the trailing arm pivot reveals that the force applied by the air spring is a function of the vertical load supported by the axle and that axle's longitudinal (braking/driving) force. F_{as} is obviously also a function of the internal pressure of the air spring (P_{as}). That is,

$$F_{as} = \ell_1/\ell_2 \, W_S + h/\ell_2 \, F_x = f(P_{as}). \tag{13}$$

If F_x is known to be nearly zero, then 13 can be written as

$$W_S = \ell_1/\ell_2 \; f(P_{as}) = g(P_{as}) \,. \tag{14}$$

The function, g, can be found directly from calibration experiments, and W_S can be determined in real operation using air spring pressure measured when F_x is known to be small.

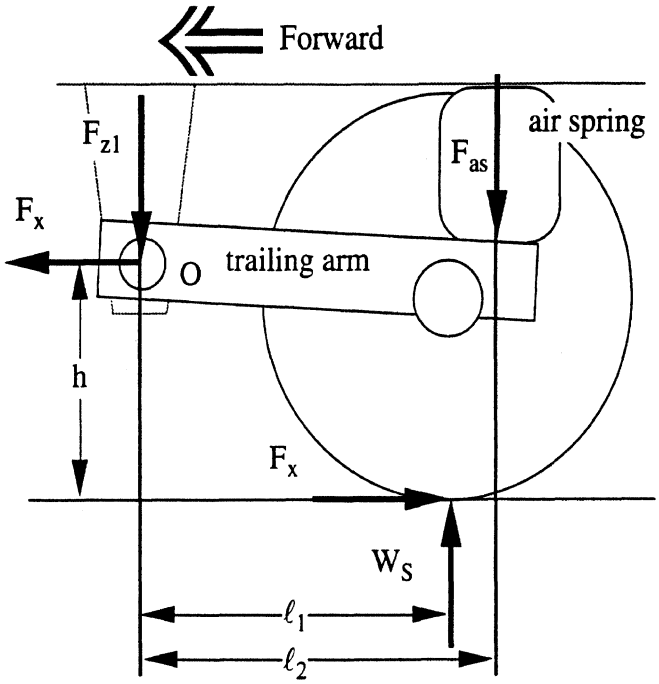

Figure 2. Freebody of a typical air suspension

The parameters a_0 and a_1 are determined by regression analysis based on equation 4 and using data from of continuous measurements of a_y and M_S. A conventional accelerometer, mounted on the trailer axle, is used to determine a_y. (The accelerometer is mounted on the axle to maintain its sensitive axes as nearly parallel to the road surface as practical.) Strain gauges applied to the trailer axle are used to obtain a signal representing M_S.

Figure 3 is a sketch of the overall suspension assembly showing the conventional components as well as the location of the strain gages. In air suspensions, the air springs themselves are so compliant that they provide very little resistance to rolling. Consequently, roll stability must be derived mostly from an *auxiliary roll stiffness* mechanism. Use of auxiliary roll stiffness is common in automotive suspensions where it is embodied in the so-called anti-sway bar. In the modern truck air suspension, the assembly composed of the right-side trailing arm, axle tube, and left-side trailing arm acts as a very stiff anti-sway bar and provides most of the roll stability of the suspension. As the vehicle rolls, the left and right trailing arms must rotate in opposite directions about the axle centerline. For this to happen, the axle tube between the trailing arms must "wrap up" and suffer a resulting torsional load. Strain gauges can be applied to the axle to sense this torsion. This measured torsion is *not*, itself, suspension roll moment. However, because this signal is expected to be proportional to suspension roll moment, it can be used as a roll-moment sensor in the same sense that the air-pressure transducer discussed above can be considered a vertical load sensor.

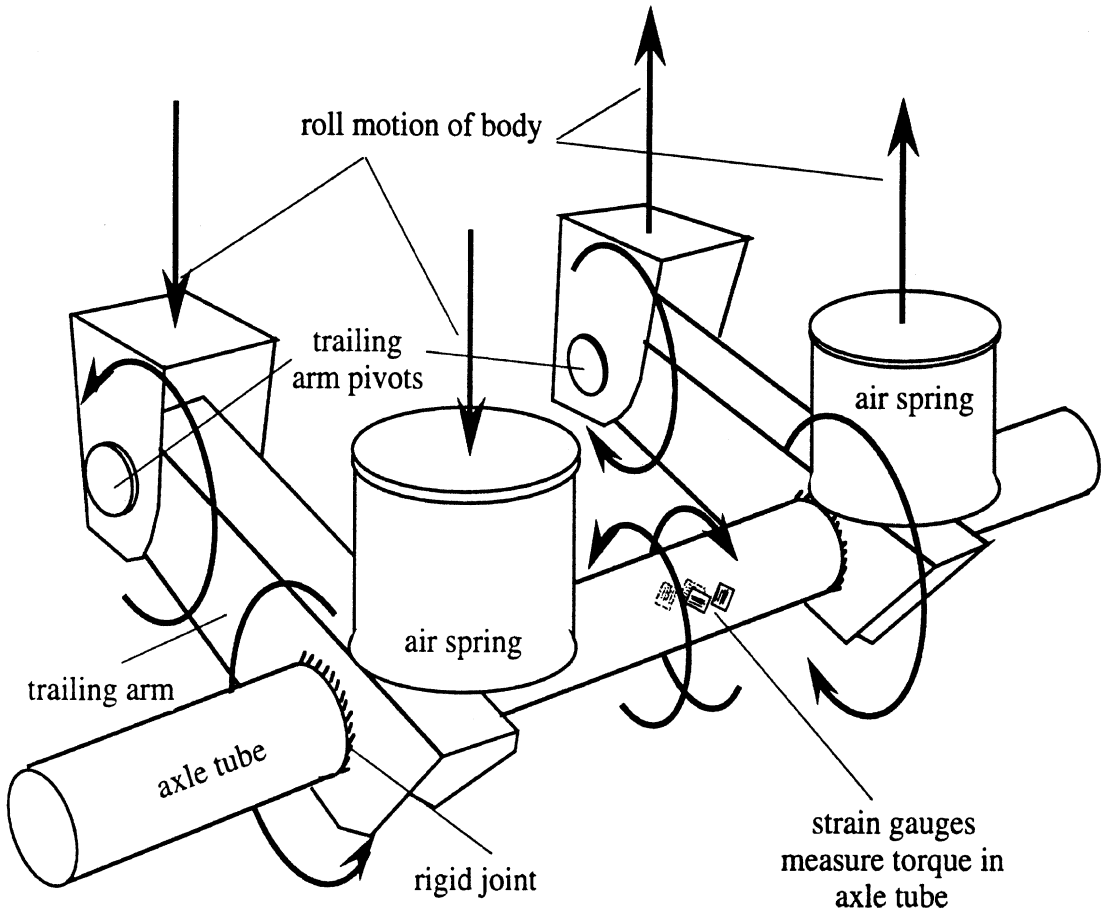

Figure 3. The axle tube of a trailing-arm air suspension experiences torsional stress during roll motion

2.3 Laboratory Experiments Supporting The Development Of The RSA

The following series of laboratory experiments have been undertaken in support of the development of the RSA system:

- evaluation of the partner-supplied, instrumented fifth wheel,
- measurement of the tractor and trailer suspension properties (including evaluation and calibration of instrumentation on the trailer suspension (strain gages and pressure transducer),
- tilt-table tests of the test vehicle.

2.3.1 Evaluation Of The Partner-Supplied, Instrumented Fifth Wheel

UMTRI received an instrumented fifth wheel, intended to measure the four primary loads transmitted between tractor and trailer through the fifth wheel (F_{x5}, F_{y5}, F_{z5}, M_{x5}). The design approach was one in which loads were sensed at the so-called *chairs* of the fifth wheel. The chairs of the fifth-wheel assembly are the two pieces which sit atop, and are firmly attached to, the left and right frame rails of the truck, respectively and, in turn,

support the fifth wheel plate. In this case, the chairs were each strain-gauged for measuring x, y, and z forces. Corresponding fifth-wheel forces were to be obtained by adding signals from the left and right chairs; overturning moment (M_{x5}) was to be obtained by subtracting left and right F_{z5} signals.

As is UMTRI's typical practice (and especially in this case, since UMTRI was to be the first user of the fifth-wheel transducer), it our intended that the transducer be thoroughly calibrated prior to using it in the research program. The general plan was to first calibrate the device in the laboratory with the assembly firmly installed on a bed plate. After this was completed, the device would be installed on the test vehicle and calibrated again in situ. Each calibration would provide data adequate to (1) check the calibration factors of the individual load cells within the assembly which had been provided by the manufacturer, StressTek, and (2) determine the precisely appropriate constants to apply for determining moments about the longitudinal and vertical axes of the fifth wheel.

The initial set up on the bed plate was for the application of lateral load to the fifth wheel plate. This would be done both with and without accompanying moment about the vertical axis (that is, with the line of action of the reference load in the plane of the plate surface and through the kingpin axis, and, respectively, with fore/aft displacement of the line of action). Several repeats of these tests were conducted and the resulting data examined prior to changing the experimental setup.

Review of this first set of data revealed that the output of the transducer assembly was very erratic and highly nonlinear. This initial experience led to an examination of the individual chairs as separate transducers. The fifth wheel plate was removed from the assembly so that loads could be applied to the individual chairs. Findings of the subsequent measurements were:

1) The output of the Fx channel of the individual cells were sensitive to both the applied lateral load and the moment about the long axis of the cell, that is to the load and to the vertical position of the line of action of the load.

2) The output of the Fy channels were also sensitive to both the applied lateral load and to the vertical position of the line of action of that load.

3) There was a substantial mechanical cross talk between left and right cells even when the 5th wheel plate was in place.

Items 1 and 2 implied that the design approach of the individual chairs was not appropriate for application in realistic situations. The contact of real fifth wheels with their chairs takes place at relatively crude, casted surfaces. It is therefore to be expected that the lines of action of the contact forces will migrate with, on the one hand, the relative motion of tractor and trailer , and on the other, with continuing wear of the parts in use. Item 3

strongly implied that the problems observed in the laboratory could be expected to multiply several times when the load-cell assembly was mounted on a highly flexible truck frame.

Given these difficulties, plans for the use of this fifth-wheel load cell were abandoned.

2.3.2 Measurements Of Suspension Properties

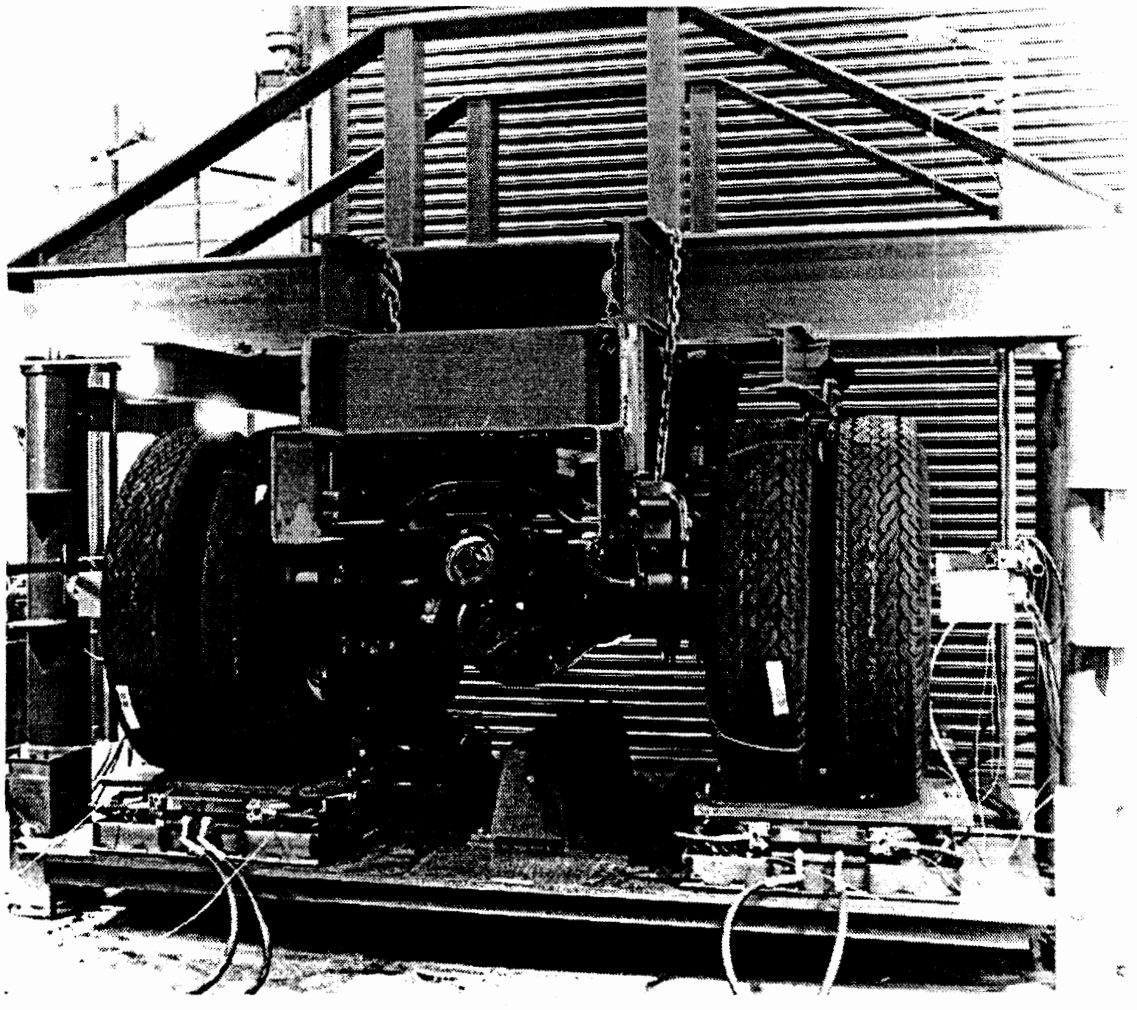

Figure 4. UMTRI heavy vehicle suspension measurement facility

Suspension properties of the test tractor and the test trailer were measured using the UMTRI heavy vehicle suspension measurement facility (figure 4). These measurements included calibrations of special instrumentation applied to the suspensions as well as measurement of standard suspension properties associated with roll stability. The former were used directly in the development of the RSA system while the later were used to describe the test vehicle in simulations of the vehicle for both RSA and RAMS development.

Measurements made on the tractor and the trailer suspensions included determination of vertical spring rate, total and auxiliary roll rates, roll-center height, and lateral compliance.

Graphical presentations of test data and reduced numerics associated with these properties are presented in appendix A. Special measurements to (1) relate vertical load to air-spring pressure for both the tractor and trailer suspensions and (2) evaluate the strain-gages installed for roll moment measurement on the trailer suspension were also accomplished.

Both the tractor drive axle and trailer axle suspensions on the test vehicle are air suspensions. Air suspensions include a height-sensing valve which controls inflation and deflation of the air springs in order to establish a specific ride height regardless of loading condition. The valve works very slowly so that, in effect, inflation takes place only in response to changes of static load brought about by changes in cargo. Virtually, no inflation/deflation takes place in response to the dynamic load changes which occur as the vehicle turns or travels over uneven road surfaces.

Of course, while this valve establishes the ride height, the internal air-spring *pressure* is dependent on vertical load—both statically and dynamically. As shown in the previous discussion, air spring pressure is also a function of braking and/or drive forces. (See equations 13 and 14 and the related discussion.) Therefore, the following discussion deals with data from tests in which braking/driving forces were maintained at virtually zero.

Figure 5 presents data from five different vertical-rate tests of the trailer suspension which show the relationship between vertical load and air-spring pressure. In each test, a nominal static condition was established by setting the suspension at its specified ride height and inflating the air springs to the pressure required to obtain a desired static axle load. The air system was then sealed and the suspension exercised vertically. Axle load and vertical motion were measured and are plotted (not shown) to obtain vertical spring rate for the particular static conditions. Simultaneously, internal air spring is measured and is plotted in figure 5 against axle load. This procedure was repeated for five different static conditions. All five plots of load versus pressure are superimposed in the figure. Additionally, the five open square data points indicate the five static test conditions.

The data of the figure show that the relationships between load and pressure which apply to dynamic load changes operating on the "sealed" air springs is substantially nonlinear and changes with the static condition. The relationship between load and pressure in the static conditions is very orderly, but different from any of the individual dynamic relationships. Regression analysis of the five static data points yields the following relationship for the trailer suspension.

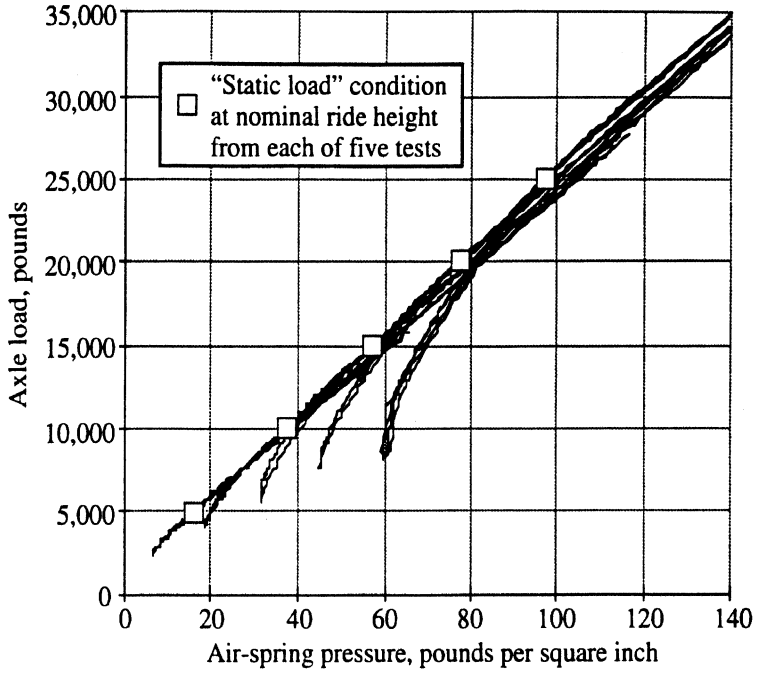

Figure 5. Axle load versus air-spring pressure for five tests of the trailer suspension

$$W_S = 1290 + 230.2\ P_s + 0.144\ P_s^2\ , \qquad (15)$$

where W_S is the static axle load in pounds and P_s is the static air-spring pressure in pounds per square inch. The similar relationship derived for the tractor suspension is:

$$W_S = 2627 + 173.8\ P_s + 0.996\ P_s^2\ . \qquad (16)$$

These relationships are used by the RSA system—within a statistical context and with certain constraints—to determine vertical load on the suspensions in operational conditions.

Prior to suspension testing, strain gauges were installed on the trailer suspension for the purpose of sensing roll moment. (See figure 3 and the associated discussion.) Assuming that the transducer signal, S, is proportional to roll moment about a roll center, then equation 6 can be rewritten as

$$S\ k_S = M_S = \Delta F_z\ T_{eff} + W_S\ \phi_U\ h_1 + h_1\ F_y\ , \qquad (17)$$

where k_S is the transducer gain, that is, the constant of proportionality.

The suspension measurement program included a series of tests to verify equation 17. Tests included (1) rolling the suspension such that ΔF_z varied while F_y remained essentially zero, (2) applying F_y while ΔF_z was held equal to zero, and (3) simultaneously altering F_y

and ΔF_z. In each case, W_S was held constant during the test, but each test was repeated for five values of W_S from 6000 to 24,000 lbs.

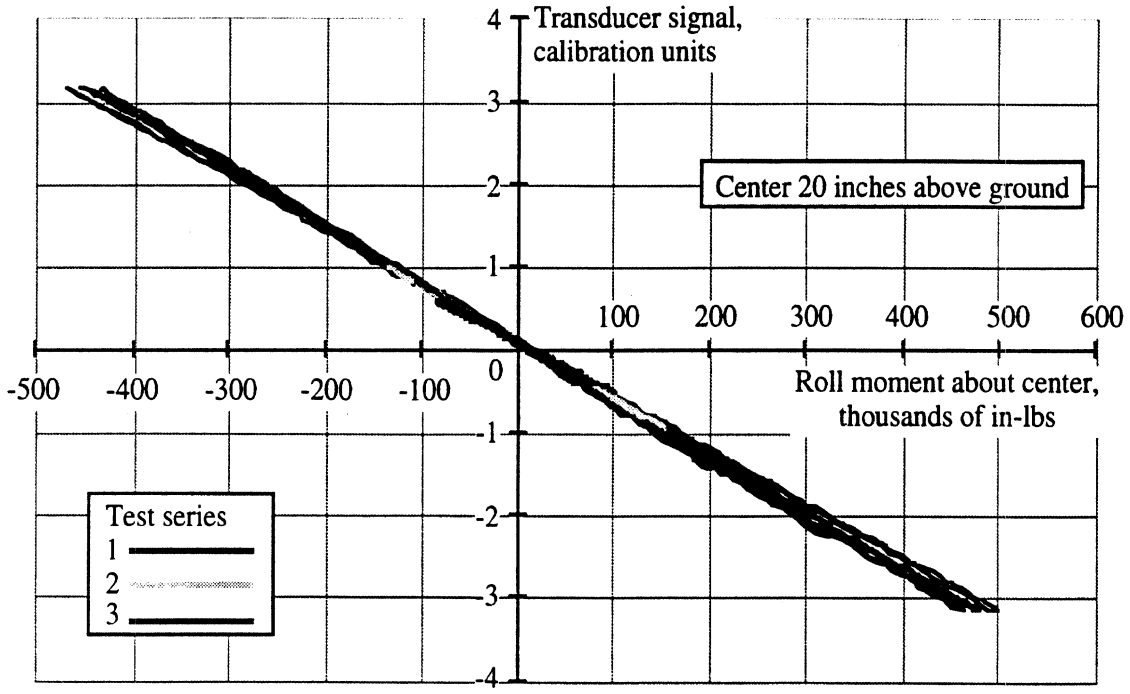

Figure 6a. Strain gauge signal versus roll moment; susp. loads from 6000 to 25,000 lbs

Data from all of these tests are superimposed in figure 6a. In this figure, M_s has been calculated based on h_1 = 20 inches (as determined by trial and error) and has been plotted on the horizontal axis. The strain gage signal is plotted on the vertical axis. (This signal is shown in arbitrary calibration; one calibration unit is equal to the signal strength obtained by placement of the calibration shunt resistor across the strain-gauge bridge.) The rather consistent proportionality between signal and moment (as indicated by the equally constant slope of the plot) implies that the gauges constitute a reasonable transducer of roll moment about a center 20 inches above the ground. Two deviations from the RSA model are apparent in this data, however. (1) The spread in the data at large roll moments (all series-1 data) indicates the transducer has some sensitivity to vertical load. (2) Other elements of the suspension measurement program show the roll center of the suspension to be nominally 25 inches above the ground, implying that the "center" of the transducer and the roll center are not superimposed.

Using the same test data as the figure (and interpreting M_S in transducer calibration units), regression analysis yields values of 1850 and 0.2763 for the parameters b_1 and b_2, respectively. These values and the measured roll moment (i.e., S) and side force (F_y) can be used in equation 9 to estimate ΔF_z. Figure 6b shows the rather good agreement between this estimated value and the measured value of ΔF_z in the three test series.

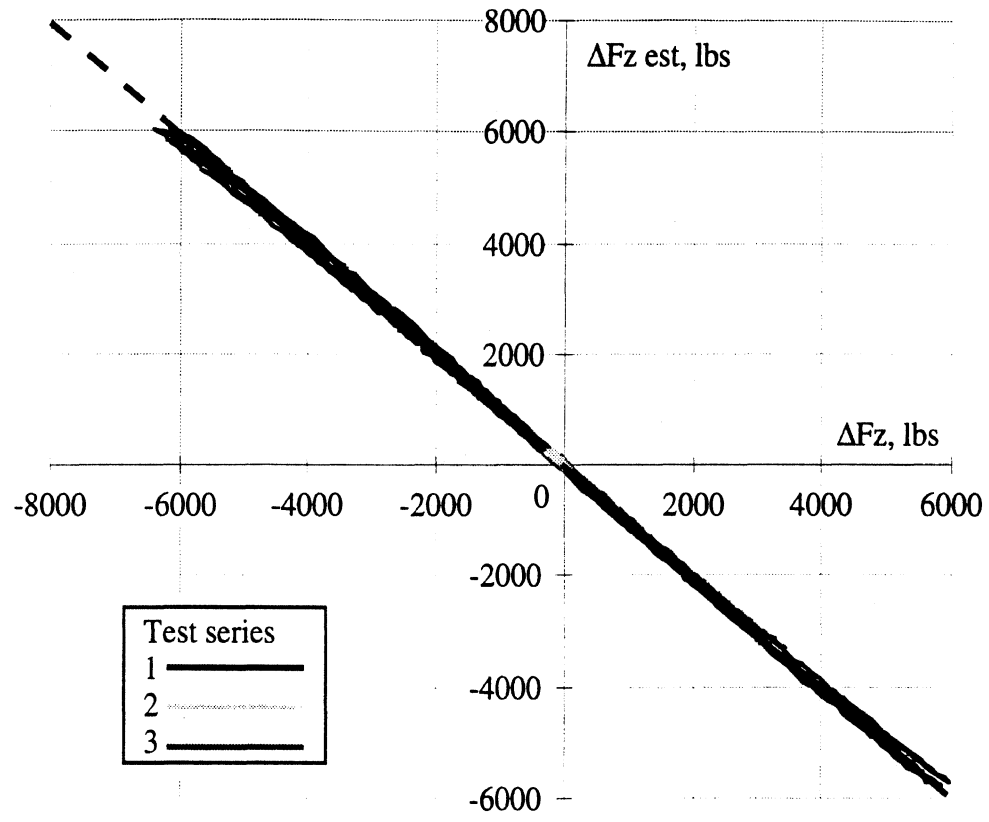

Figure 6b. Measured and estimated ΔF_z from suspension measurements

2.3.3 Tilt Table Tests

The test vehicle was subject to a series of tilt table tests as a further calibration check of the trailer-only RSA system.

Figure 7 presents a simplified diagram of the tilt table experiment. The tilt-table methodology is a physical simulation of the roll plane experience of a vehicle in a steady turn. The vehicle is placed on a tilt table and is very gradually tilted over in roll. As shown in the figure, the component of gravitational forces parallel to the table surface provides a simulation of the centrifugal forces experienced by a vehicle in turning maneuvers. The progressive application of these forces by slowly tilting the table serves to simulate the effects of quasi-statically increasing lateral acceleration in steady turning maneuvers. The tilting process continues until the vehicle reaches the point of roll instability and "rolls over." Tilt angle at which special events (in this case, the lift off of tires on the trailer axle) occur are also noted.

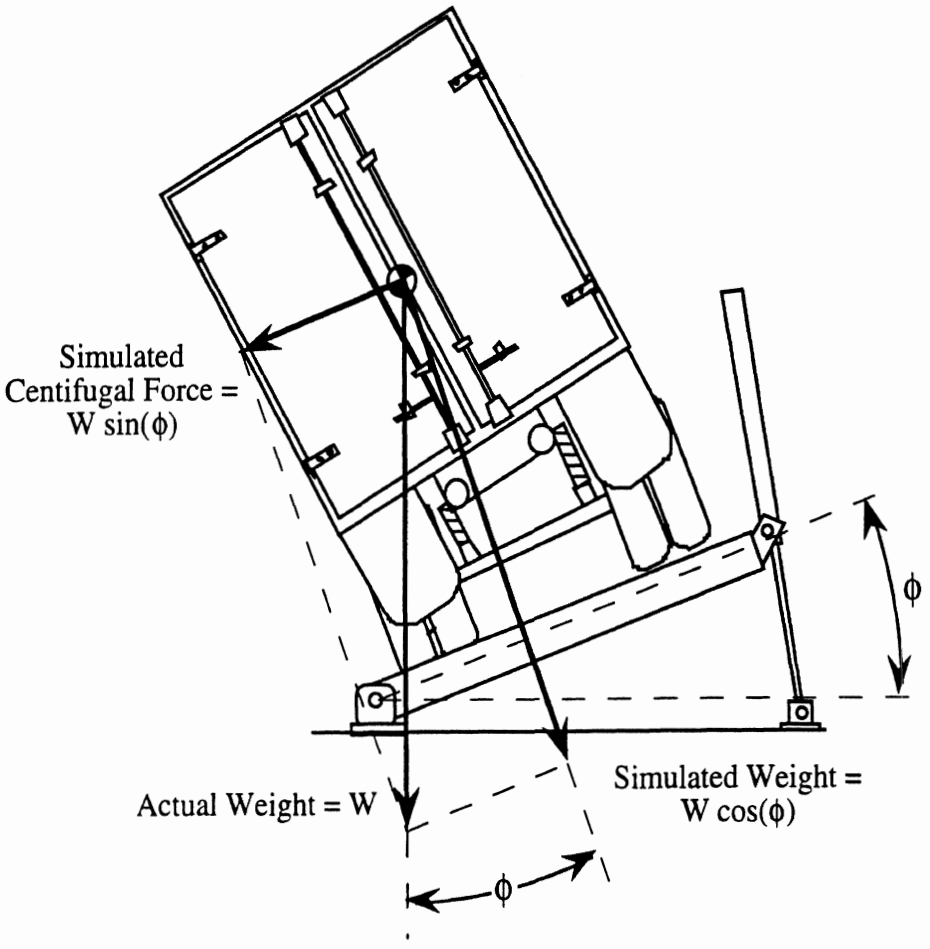

Figure 7. The tilt-table experiment

When the table is tilted, the component of gravitational forces parallel to the table surface, $W \bullet \sin(\phi)$, simulates lateral forces, and the weight of the vehicle itself is simulated by the component of gravitational forces that are perpendicular to the table (i.e. $W \bullet \cos(\phi)$, where W is the actual weight of the vehicle and ϕ is the roll angle of the table relative to the true gravitational vector). Thus, the vertical suspension loads acting during the tilt-table test are *scaled down* by a factor of $\cos(\phi)$. Since the most fundamental mechanisms of actual rollover depend on the *ratio* of the centrifugal forces to the vertical, gravitational forces, it is appropriate to take the ratio of the simulated lateral acceleration forces to the simulated weight to represent lateral acceleration when interpreting the results of a tilt-table experiment. That is:

$$a_{ys} \equiv \tan(\phi) = W \bullet \sin(\phi) / W \bullet \cos(\phi), \qquad (18)$$

where:

- a_{ys} is the simulated lateral acceleration (expressed in gravitational units),
- ϕ is the roll angle of the tilt table,
- W is the actual weight of the vehicle.

The test trailer (including the actual suspension whose properties had been measured in the laboratory) was equipped with a load rack which allowed adjustment of both the weight and the height of the center of gravity of a ballast load. Test were conducted with two different gross loads, each at three different cg. heights. Two tests were conducted in each of these six conditions. Results are reviewed in table 1.

As was done with the suspension measurement data, the tilt-table results can be used to obtain values for the parameters b_1 and b_2. Regression of the F_y, S, and ΔF_z data from table 1 yields values of 5468 and 0.4683 for b_1 and b_2, respectively. Surprisingly, these values of b_1 and b_2 are substantially different from those obtained from the suspension measurements. An interpretation of these new values is that the strain-gauge transducer now appears to measure roll moment about a center which is some 39 inches above the ground as opposed to the height observed in the suspension measurements—20 inches for the transducer's measurement center and 25 inches for the suspension roll center.

The discrepancy between suspension measurements and tilt table results is not understood at this time. One possible explanation involves the suspension mounting. On the suspension facility, the suspension components are mounted directly to the very stiff superstructure of the facility. On the vehicle, the suspension is mounted to the (probably) more compliant subframe and floor structure of the trailer. Compliance in these elements may very well result in a change in height of the effective roll center and/or measurement center of the suspension.

Regardless of the reason—and as will be seen in following sections—the RSA system appears capable of rather good, on-road prediction of the lift off of trailer tires when the b_1 and b_2 values from the tilt table tests are used.

2.4 Experimental Operation Of The Trailer-Based RSA System

The basic physical analysis underlying the RSA system was presented in section 2.2. This analysis culminates in the simple expression of equation 12 which is used to predict the lateral acceleration at which trailer tires will lift off the road surface. The equation is repeated here.

$$a_{ylift} = \frac{\pm W_S/2 - a_0 b_1}{a_1 b_1 + b_2 W_S} \quad . \tag{12}$$

The parameters b_1 and b_2 are properties of the vehicle determined by calibration experiments performed on the tilt table (section 2.3). W_S is the load carried on the trailer axle and the parameters a_0 and a_1 are related to (1) the lateral offset and (2) effective height of that load, respectively. These three parameters are, of course, functions of the vehicle loading condition and, therefore, must be determined on board the vehicle during operation.

Table 1. Results from tilt table tests

Test No	Trailer GVW, lbs	Trailer axle GAW, lbs	Est. trailer sprung mass cg height, in	At lift off of trailer axle tires: Tilt angle, degrees	Simulated a_y, gs	Simulated W_S, lbs	Simulated F_y, lbs	Roll transducer S, cal units	Simulated ΔF_z, lbs	At rollover: Tilt angle, degrees	Simulated Ay, gs
1	29,460	15,660	93.5	na	na	na	na	na	na	na	na
2	29,460	15,660	93.5	17.85	0.322	14,906	4,800	1.181	7,453	20.71	0.378
3	29,460	15,660	90.0	18.88	0.342	14,817	5,068	1.167	7,409	21.70	0.398
4	29,460	15,660	90.0	18.93	0.343	14,813	5,081	1.170	7,406	21.45	0.393
5	29,460	15,660	82.9	21.36	0.391	14,585	5,703	1.108	7,292	23.70	0.439
6	29,460	15,660	82.9	21.16	0.387	14,604	5,652	1.090	7,302	23.51	0.435
7	35,920	18,840	96.5	16.33	0.293	18,080	5,297	1.442	9,040	19.49	0.354
8	35,920	18,840	96.5	16.33	0.293	18,080	5,297	1.453	9,040	19.49	0.354
9	35,920	18,840	88.5	18.37	0.332	17,880	5,936	1.368	8,940	21.06	0.385
10	35,920	18,840	88.5	18.42	0.333	17,875	5,952	1.372	8,937	21.26	0.389
11	35,920	18,840	80.4	20.96	0.383	17,594	6,738	1.272	8,797	23.17	0.428
12	35,920	18,840	80.4	20.96	0.383	17,594	6,738	1.273	8,797	23.27	0.43

W_S is determined from measurements of air spring pressure based on the following expression (from section 2.3).

$$W_S = 1290 + 230.2\, P_s + 0.144\, P_s^2 . \qquad (15)$$

The parameters a_0 and a_1 are determined from measurements of suspension roll moment and lateral acceleration which are related by the expression,

$$M_S = a_0 + a_1\, a_y . \qquad (4)$$

These two expressions are valid only for steady-state operating conditions. Further, equation 15 is limited to conditions in which driving and/or braking forces are small. Since these conditions do not generally exist in normal operation, selective use of the sensor data is required.

In the prototype RSA system, the signals from the three primary sensors (air pressure transducer, accelerometer, and strain gauge bridge) are conditioned with appropriate analog anti-aliasing filters and then sampled digitally every 0.25 seconds. The forward velocity on the vehicle and the brake-light voltage are also monitored in the same manner. The signals are further smoothed with appropriate digital filtering routines and then used to determine the needed parameters as explained below.

When in motion, drive thrust is virtually never present at the trailer axle but braking forces may be. Further, when parked, the trailer axle may experience longitudinal forces in either direction for a variety of reasons. (With parking brakes on, brake forces may act in either direction, or the vehicle can be parked with trailer wheels against a curb or in a hole.) Also, air brakes, particularly on trailers, may require a substantial fraction of a second to fully release. Therefore, the RSA system discards pressure data taken when either (1) velocity is less than 2 mph or (2) the brake-lights have been on within the last 1 second. Vertical load is then estimated using equation 15 and the average pressure over the last 2500 valid data points (i.e., the last 10.4 minutes of valid data) (or all the data available if less than 2500 points have yet to be collected). Thus, the RSA system accounts for changes in load (due to deliberate cargo loading or unintended shifting of payload) within a bit over ten minutes of operation.

The parameters a_0 and a_1 are determined by conventional statistical regression of the strain-gauge and lateral-acceleration data in accordance with equation 4. This regression analysis uses the most recent 3600 sets of strain gauge and accelerometer data points (i.e., 15 minutes worth) collected when the vehicle is traveling faster than 40 mph. (At the initiation of the routine, regressions are performed and results output with data from as little as one minute) Only data from these higher speeds are used because, at lower speeds, lateral acceleration measured at the trailer axle and the roll moment at that axle may be significantly out of phase. By way of explanation, imagine a tractor-semi combination

rounding a city intersection. At the start of the maneuver, the tractor can be rounding the curve while the rear of the trailer is still traveling virtually straight ahead. The trailer may be rolling, however, because of the roll of the tractor and the centrifugal forces acting on the forward end of the trailer mass. Thus, the onset of roll moment in the trailer suspension leads the development of lateral acceleration at the suspension. Similarly, in exiting the maneuver, the roll moment can be expected to subside before lateral acceleration. The details of this relationship depend a good deal on unknown properties of the tractor and trailer (unknown to the trailer-only RSA system, that is). Analysis of the data shows that the influence of this phasing becomes rather insignificant above 40 mph due to the natural growth in path radii with increasing speed.

The details of the calculation routines described were developed using data gathered during eleven trips around a specified course of public roads in and about Ann Arbor, Michigan. The course started in the parking lot at the UMTRI facility and proceeded through several blocks of suburban streets including multiple stops and turns at intersections. The course then proceeded to Dearborn, Michigan via restricted, multi-lane highways including two high-speed interchanges. After a brief interlude of urban driving in Dearborn, the vehicle returned over the same network. (A map of the test course appears in appendix B.) The trip typically required approximately one hour and twenty minutes. The eleven trips covered the same course, but with different loading conditions and different known (from tilt table tests) reference values of the lateral acceleration required for lift off of trailer tires. The loading conditions and the reference lateral accelerations appear in table 2.

Table 2. Trailer loading condition and reference lateral acceleration for lift off of trailer tires in road tests

Test No	Trailer GVW, lbs	Trailer GAW, lbs	Est. trailer sprung mass cg height, in	Reference a_{ylift}, gs
1	21,350	11,710	71.9	0.489
2	21,350	11,710	82.1	0.420
3	29,460	15,660	72.2	0.452
4	35,920	18,840	80.4	0.357
5	35,920	18,840	96.5	0.285
6	29,460	15,660	82.9	0.391
7	29,460	15,660	93.5	0.323
8	29,460	15,660	86.4	0.365
9	29,460	15,660	79.3	0.397
10	35,920	18,840	72.4	0.434
11	35,920	18,840	88.5	0.307

Figure 8 presents a time history of the lateral acceleration required for liftoff of the trailer tires as estimated by the RSA system in trip number 7. The reference lateral acceleration is also shown. The first estimates appear after about 8 minutes of driving above 2 miles per hour. This would have coincided with the time in this particular run at which one full minute of travel above 40 mph had occurred. Based on only a minute's data, the estimate is changing rapidly but settles down to a rather consistent estimate when sufficient data for the moving, 15-minute average becomes available. At about 40 to 50 minutes into the test, the vehicle reaches the end of the out-bound highway run and spends 10 minutes or so at less than 40 mph. As a result, the estimate stays virtually constant during this time.

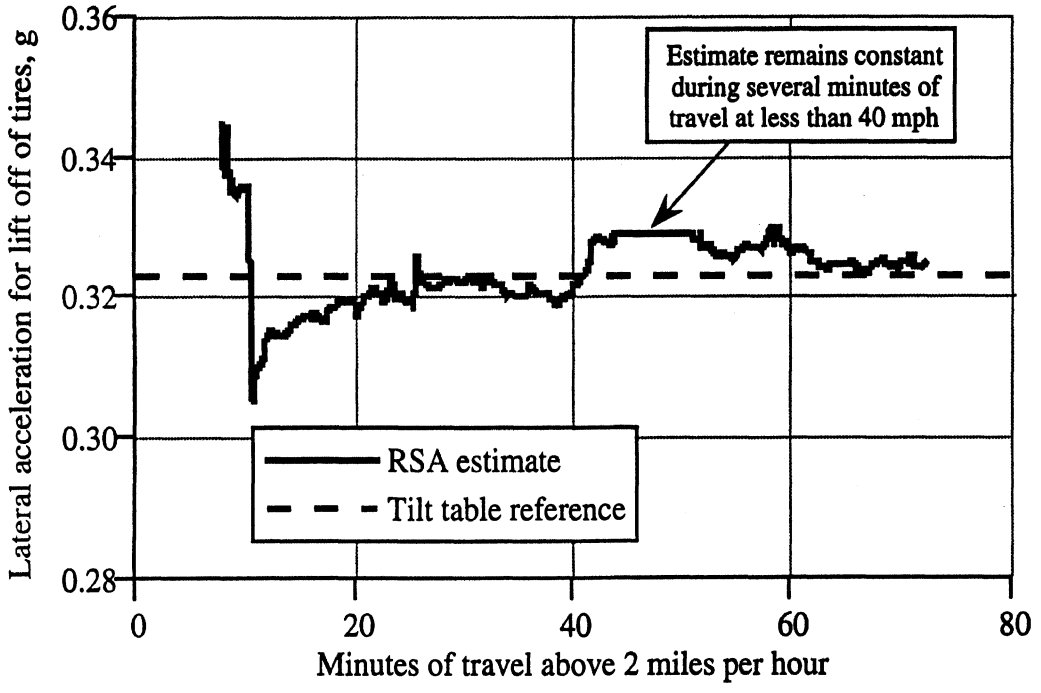

Figure 8. RSA system estimate of lateral acceleration for lift off of trailer wheels

Figure 9 is a composite presentation of all eleven development test runs. In order to show all runs on the same scale, the vertical axis is no longer the estimated acceleration itself, but rather the error in the estimate relative to the reference for the loading condition. The figure shows that the RSA system typically homes in on an estimate within +0.02 to -0.04 g of the reference. In fact, we believe that part of the reason for this range of error is associated with insufficient attention to "zeroing" of instrumentation signals prior to some of the test runs, and that a range of ±0.02 g is likely to be a more appropriate description of the quality of the RSA routine.

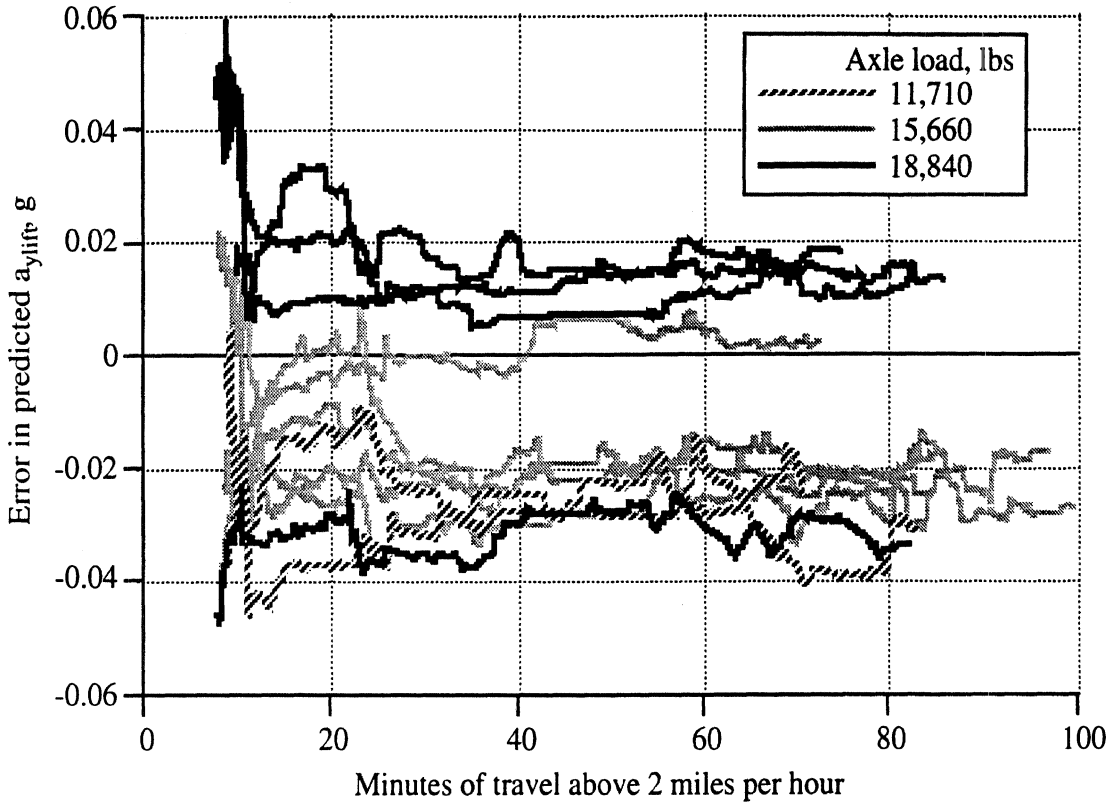

Figure 9. Estimation error of RSA system in eleven development runs

All eleven of the development tests runs were conducted with left-right symmetric loads in the trailer. Two additional check runs (runs 12 and 13) were conducted with loads deliberately placed off the center line of the trailer. Table 3 gives the particulars of the loading conditions. Figure 10 shows that the RSA system estimates different liftoff thresholds for left- and right-going turns in these additional runs. Estimates for the more stable right-hand turns (left wheel lift) are seen to be quite accurate. Estimates for the right wheel lift-off are nominally within 0.02 g and estimates for the left wheel lift-off are seen to be even more accurate. (Closer attention was given to proper zero calibrations prior to these two final test runs.)

Table 3. Trailer loading condition and reference lateral acceleration for road tests with off-center loading

Test No	Trailer Properties				Reference a_{ylift}, gs	
	GVW, lbs	GAW, lbs	Est. sprung mass cg hght., in	Equiv. lat. offset of axle load, in	right	left
12	35,940	18,700	90.8	8.74	0.360	0.279
13	35,940	18,700	84.1	8.74	0.398	0.309

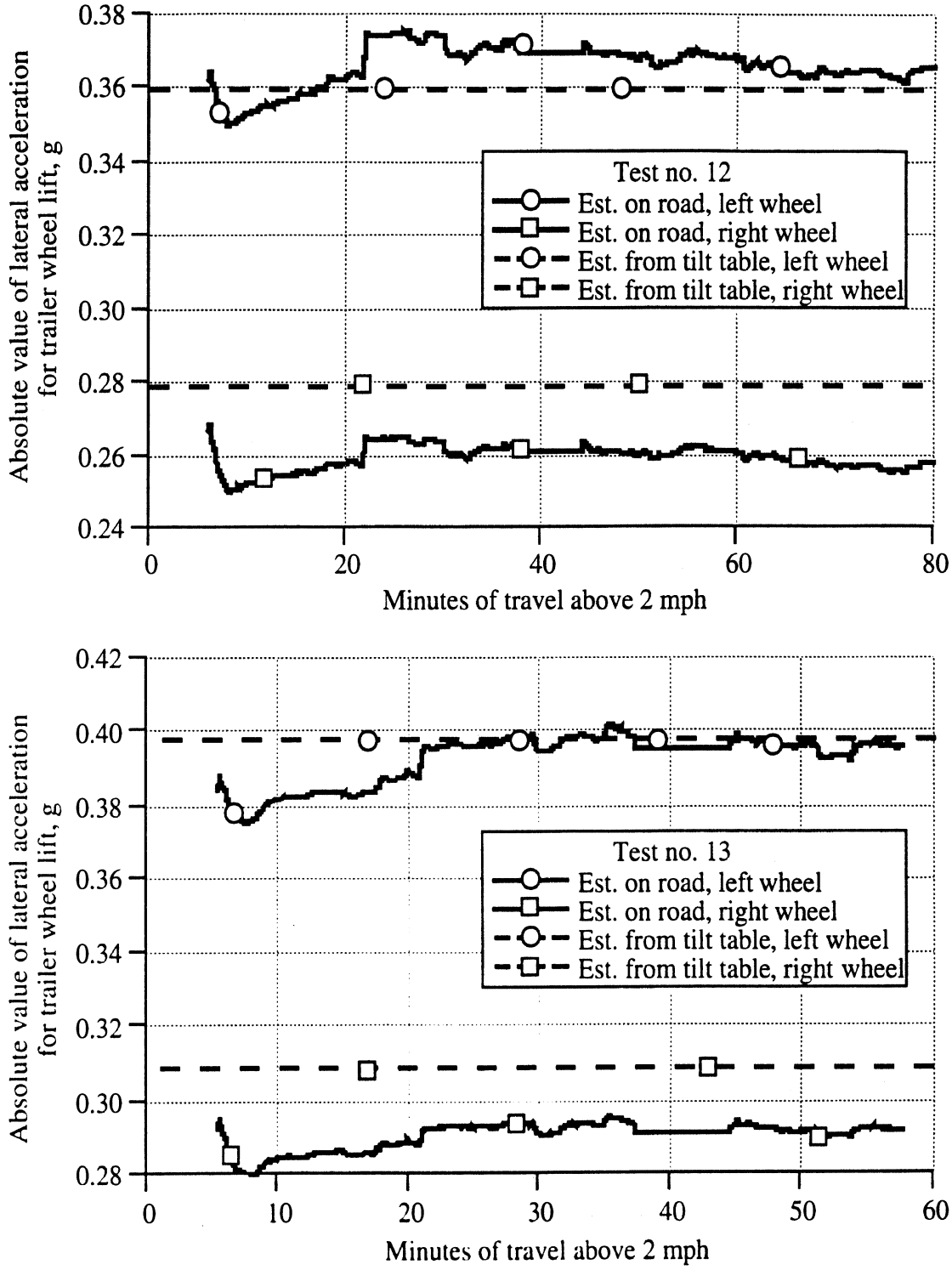

Figure 10. RSA time histories for test runs with asymmetric loading

2.5 Preliminary Analysis for RSA System Identification

A preliminary analysis of the feasibility of developing the RSA system using only information available at the tractor and no direct knowledge of trailer properties was conducted, using simulation studies. A detailed description of the analysis and its results

are presented in appendix C. This section summarizes the findings of this portion of the initial study and indicates the steps for further progress based on those results.

The approach taken in the preliminary study was to use measurements made at the fifth wheel of the tractor-trailer combination to derive parametric values for trailer properties, such as trailer mass, wheelbase, and the height and lateral offset of the trailer center of gravity. From the derived properties, and from knowledge of the dynamics of the rollover process, the minimum lateral acceleration that would induce roll over to either the right or the left was estimated.

Trailer wheelbase was estimated by using the fact that the vertical forces measured at the fifth wheel are related to the response of tractor axles 2 and 3 passing over the same road profile, separated in time by a period inversely proportional to vehicle speed. Therefore the autocorrelation function of the signal from a fifth wheel vertical force transducer shows a peak at a time delay equal to this period. It was shown that the wheelbase could be reliably estimated with minimal error using this property.

Measurements relating to two main modes of dynamic behavior of the semi-trailer, namely the (i) pitch plane motions and (ii) roll plane motions, were considered for estimating the remaining trailer parameters.

Analysis based upon the pitch-plane motions attempted to derive trailer properties from measurements available from the portion of the driving regime that involved longitudinal acceleration of the tractor-trailer combination. Simulation studies were conducted using realistic road profiles as described in appendix C. It was found that only by using measurements of trailer pitch and vertical acceleration could trailer parameters be estimated with reasonable accuracy. However, the measurement of such responses would be difficult in practice and would substantially complicate the system configuration, driving up the cost. When a simplified and more realistically-implementable model was used, very poor estimates were obtained for all parameters except the trailer mass. Thus it appeared that roll stability assessment based simply upon pitch plane measurements is not a practical option.

The converse analytic approach focusing upon roll plane motions relies on vehicle behavior during turning maneuvers and was seen to produce considerably better results. The height of the trailer center of gravity, for example, could be estimated to within 10% of its actual value. However, the center of gravity was assumed to have no lateral offset and further analysis will be necessary to evaluate the feasibility of simultaneously estimating both center of gravity height and lateral offset.

In both of the above cases a recursive parameter estimation scheme was used. Further work in the project must address the implications of recursive estimation on the computing power that is needed on board the vehicle.

The preliminary study has also indicated that obtaining an estimate of the trailer's propensity for axle lift-off from tractor based measurements may be feasible. Since this initial work was done on the basis of statics only, however—thus neglecting vehicle dynamic behavior—the resulting estimates of rollover threshold values may differ considerably from actual values. Further, all the results obtained so far have been from simulation studies and do not include the effect of measurement noise that is inevitably present in practice. The effect of such noise will be to increase the bounds of uncertainty in the estimated parameters and thus eventually in the bounds of the values of the critical acceleration likely to cause roll over.

Based on the above findings, the next phase of the project will focus on (i) studying the sensitivity and noise characteristics of the new fifth wheel load cell (discussed below) that is being constructed and (ii) evaluating the dynamic responses of the vehicle. From a study of the sensor characteristics, those measurements that show the maximum signal to noise ratio can be selected. Dynamic analysis of vehicle behavior is likely to be more complicated, but it is also possible that the greater richness of information contained in measurements obtained under such conditions may improve the parameter estimates.

The effectiveness of the roll stability advisor will ultimately depend upon the tightness with which the estimate of the rollover threshold can be bounded and how much more useful such an estimate is than that based on a driver's feel and experience.

2.6 Design of the fifth-wheel load transducer

As of the time of this writing, UMTRI is in the midst of fabricating a fifth-wheel load cell system to measure all of the major loads between tractor and trailer at the fifth wheel. The loads, shown in figure 11, are:

- F_x longitudinal (fore/aft) force,
- F_y lateral (sideways) force,
- F_z vertical force,
- M_x overturning (roll) moment.

UMTRI's approach to measuring these loads will be to replace the standard fifth-wheel chairs with specially-made chairs which will each transduce four similar loads. Total fifth-wheel loads will be obtained through the appropriate adding and/or subtracting of the signals from left- and right-side transducers.

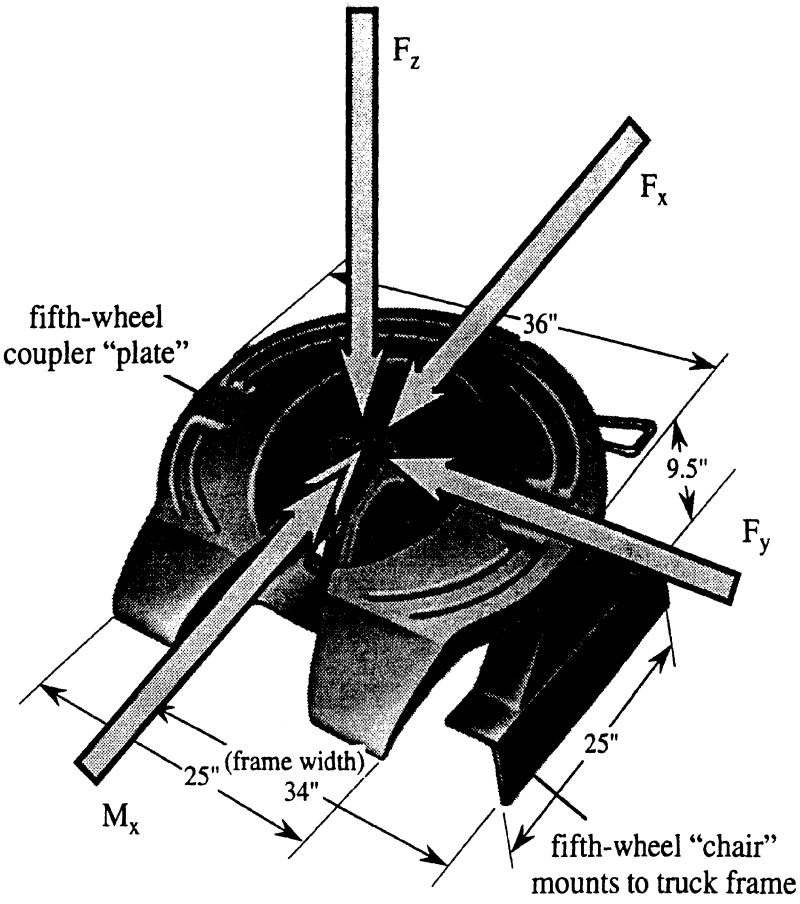

Figure 11. A standard fifth-wheel with loads and nomenclature

Figure 12 is a sketch which reviews the general design of an individual transducer. The transducer has approximately the same overall dimensions as the standard chair shown in figure 11. However, this chair will be cut from a solid block of high-strength steel in a manner such that all loads applied to it by the fifth-wheel plate will flow down into the truck frame through four precisely-machined posts. Each post will have 12 strain gauges applied to it, 3 on each face. These gauges will be wired into three resistive bridges as shown in figure 12. Bridges i and k respond to shear loads in the post and will, therefore, measure longitudinal and lateral loads, respectively. Bridge j will respond to tension/compression of the post and will measure vertical loads. The i-bridge signals on all four posts will be summed to obtain the total F_x of one chair. Similarly, j-bridge and k-bridge signals sum to yield F_z and F_y, respectively. Local M_x in the chair is obtained by combining j-bridge signals after the fashion of (postA+postC-postB-postD).

A detailed mechanical design drawing for the load-cell chair appears in figure 13. Fabrication of two replications of this piece is currently in progress.

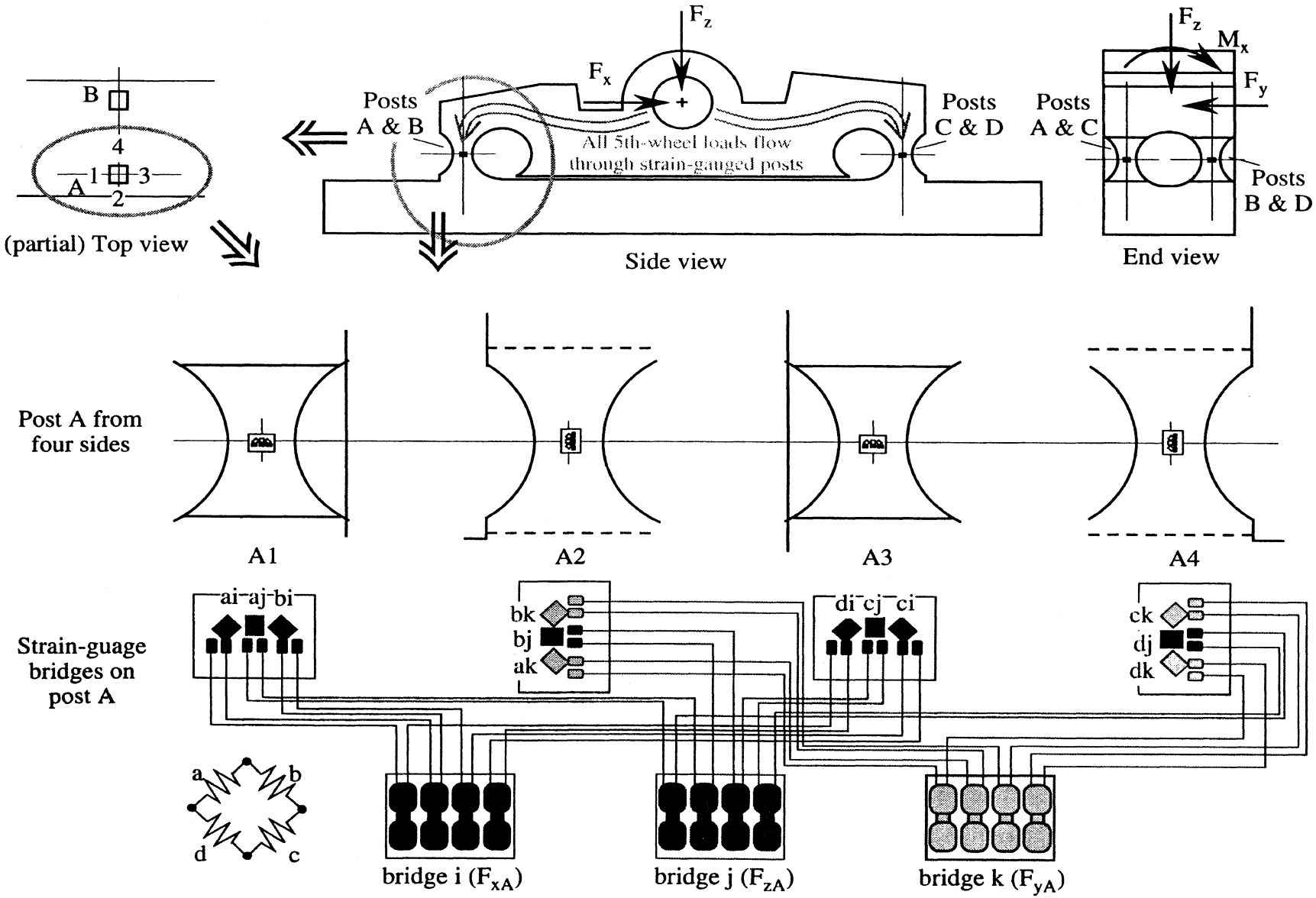

Figure 12. A sketch describing the design approach of the fifth-wheel load transducer chairs

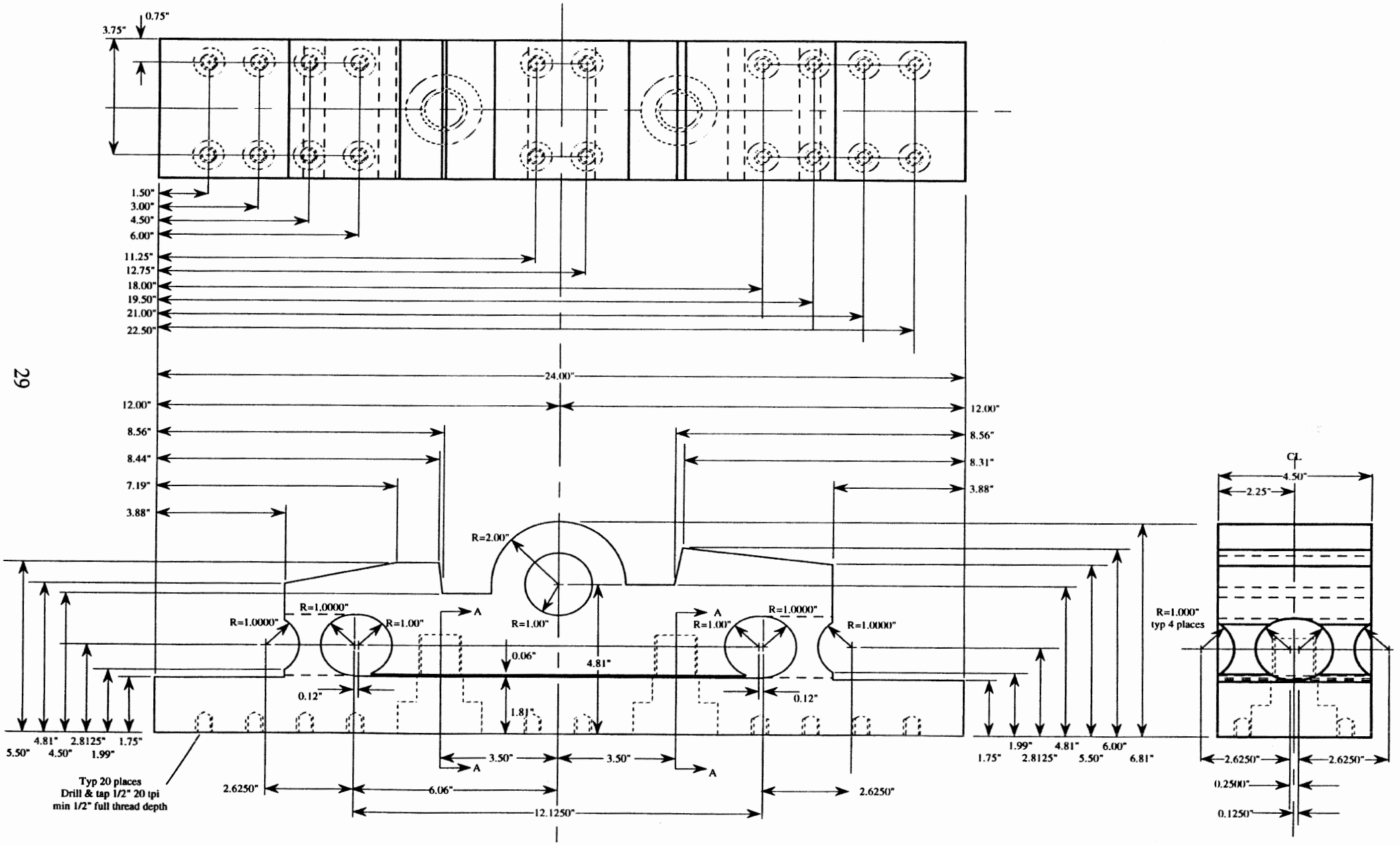

Figure 13. Mechanical design drawing of the fifth-wheel load transducer chair

3.0 REARWARD AMPLIFICATION SUPPRESSION SYSTEM

The project has also developed an automatic intervention system for Rearward AMplification Suppression (RAMS) in multi-trailer combinations. The RAMS concept involves measurement of steering input and forward speed at the tractor, followed by computations which determine whether a significant rearward amplification event is pending. If it is, the control algorithm then establishes a sequence of carefully phased brake applications at selected trailer wheels so as to induce yaw moments that oppose the rearward-amplifying motions of trailers and dollies. The concept requires electronically-controlled brake systems (ECBS) at trailer and dolly axle positions and requires placement of and communications with yaw rate sensors in individual trailer and dolly units. If successful, the system would obviate the need for innovative dollies or other countermeasures for taming the rearward amplification behavior of multi-trailer combinations.

3.1 Rationale for Suppressing Rearward Amplification

While it is known that rearward amplification is a very real stability problem occurring with commonly-employed doubles and triples equipment, NHTSA's crash data show that the total scope of the safety issue does not compare with that of rollover, per se. Nevertheless, the rearward amplification problem is serious and it is seen as one of the major deficiencies preventing the nationwide allowance of triple trailer combinations.

As a technical backdrop to the RAMS application, it has been known for fifteen years that rearward amplification does not simply derive from low levels of yaw damping, as is the case with many other modal oscillations of trailers (for example, in the case of rhythmic yaw motions of recreational trailers having negligible tongue load). Rather the motion of concern constitutes a forced vibration that is stimulated peculiarly by steering inputs that lie in the frequency zone near 0.5 Hz.[e.g. 4] This technical detail is highly fortuitous because 0.5Hz steer inputs, of any significant amplitude, are exceedingly rare. Thus the prospect of "false alarms", in terms of unneeded and perhaps disruptive brake applications from a RAMS controller, is made inherently improbable by the rare-but-pronounced nature of the critical input conditions. The RAMS system can look for those conditions, and only those, with little concern that the condition can be mistaken for some other non-threatening type of steering input.

Further, it is highly significant that the RAMS function might enable widespread triples usage—by a scheme that may involve a modest cost increment beyond that of an all-axle antilock system. Such aspirations are in concert with industrial progress in ECBS hardware, and other developments as mentioned below.

ECBS products are scheduled for introduction on European-manufactured trucks within the next few years and efforts are well underway to develop corresponding products for the U.S. market. As with so many other electronic control advances involving powertrain or chassis functions, ECBS technology powerfully elevates the potential for integrating vehicular control functions in behalf of new, whole-vehicle, performance goals such as stability enhancement. In the passenger car market, for example, both foreign and domestic manufacturers offer automatic yaw control systems in certain luxury models based upon inertial motion sensing and ECBS braking. And, of course, a number of vehicles across the passenger vehicle and truck spectrum have already implemented automatic traction control. In the heavy vehicle application involving multiply-articulated trailer combinations, the addition of a RAMS functionality may help in tilting the balance of value vs. cost in favor of upgrading to ECBS equipment.

The possibility of taming rearward amplification without replacing the conventional dolly is also expected to provoke a substantial interest from the large commercial operators of doubles and triples. Especially in the case of the major LTL carriers who wish dearly to operate triples nationwide, the chance to "do it all" for the ball-park price of an ECBS system may be attractive, indeed. Thus one can imagine an outcome in which a convincing demonstration of the RAMS concept would underpin a legislative initiative to allow triples on, say, the designated highway system if they were required to implement the RAMS package—perhaps pending confirmation of the commercial readiness of the concept by means of a field operational test.

3.2 Development of a RAMS Controller

This section describes the system design process employed in developing the initial design of this RAMS system. The next section (3.3) presents results used to provide a first evaluation of the initial design. The ideas involved in the creation of the design (section 3.2) and the evaluation of the design (section 3.3) are unified by considering five levels of abstraction ranging from a statement of functional purpose (at the level of objectives) to a description of the physical form of the design (its appearance, the location of the parts, etc.). These levels of abstraction and their relationships with regard to creating a design and then evaluating it are presented in figure 14.

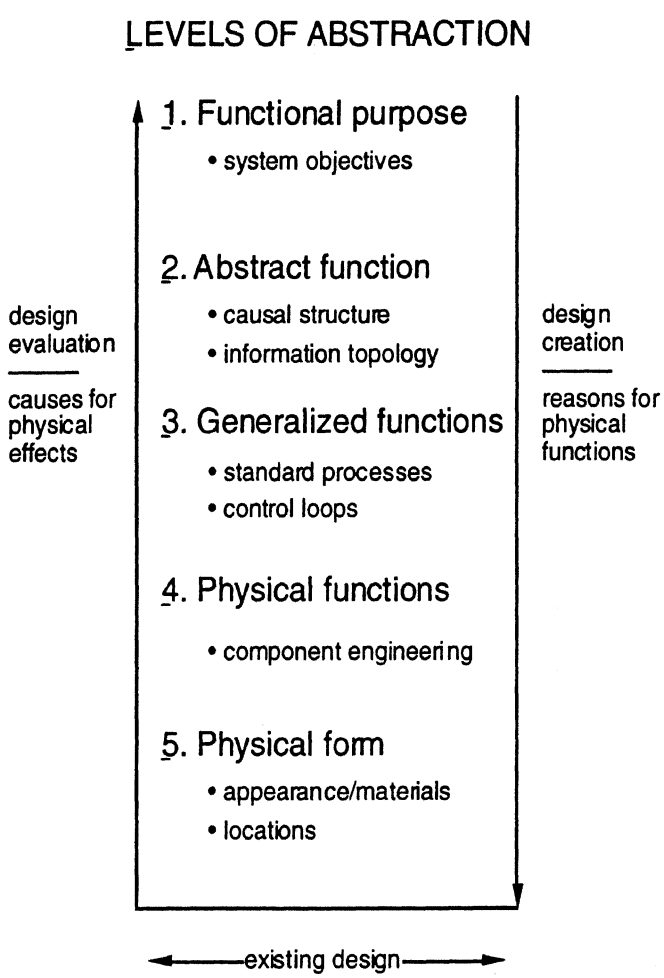

Figure 14. Creating and evaluating the design of the RAMS system

The right side of figure 14 pertains to the design process. The design process involves decisions that are based primarily on reasons for physical functions. According to this portrayal of the design process, one goes from an abstract idea of what the system is to do to a real system that is expected to perform the desired function. Although there could be many different systems that will perform the desired function with some degree of fidelity and satisfaction, the design consists of only one particular system out of the multitude of possible systems.

In order to explain the RAMS system that has been developed in this project, the following subsections discuss matters associated with each of the five levels of abstraction listed in figure 14. In general the design process has proceeded from objectives on the top to a system on the bottom as illustrated by the down arrow at the right in figure 14. However, in actual practice the time sequence of design events tends to jump back and forth from one level of abstraction to another as the physical form of the design becomes clearer. The initial form of the design is arrived at when enough "reasons" (choices, constraints, etc.) have been specified to allow the assembly of one specific system.

3.2.1 Functional Purpose

The purpose of the RAMS design is to create a system that will reduce rearward amplification of multiply articulated heavy trucks thereby reducing the tendency for these vehicles to rollover and/or sweep out a large path in a severe obstacle avoidance maneuver.

Figure 15 illustrates the concept of rearward amplification.

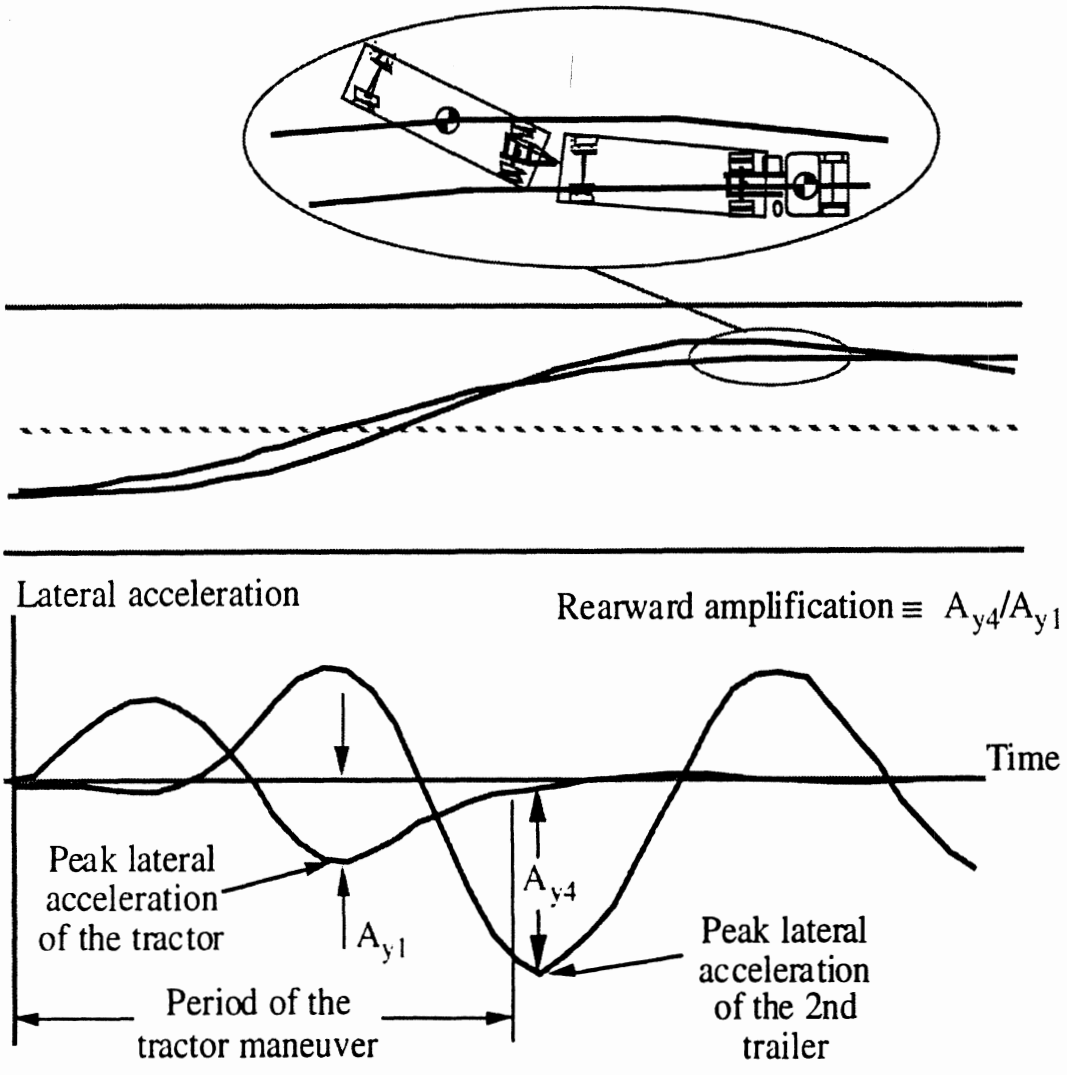

Figure 15. Rearward amplification is the ratio of the maximum lateral acceleration of the last trailer to the maximum lateral acceleration of the tractor.

Currently the design goal may be stated in terms of bounds on distinct levels of lateral acceleration occurring in prescribed maneuvers. Specifically, the current objective is as follows:

"For a maneuver in which the driver steers to follow a path defined by an 8 ft lateral translation in 200 ft–kinematically corresponding to a peak lateral acceleration of 0.25 g at

55 mph (80 ft/sec)–the lateral acceleration of the center of the floor of the rear trailer should not exceed 0.3 g."

An objective of this type is now known to be reasonable, given experience with testing a prototype system. In a sense the process of describing and developing the system is circular in that new ideas and findings feedback to put more specificity into the design concept.

3.2.2 Abstract function

The RAMS system may be envisioned as an assembly of sensors, control system components, and brake actuators that modify vehicle behavior in a manner that reduces rearward amplification. Figure 16 provides a very simplified overview of the causal structure and information flow for this system. At this level of abstraction there could be many systems that could be represented by figure 16. The figure itself illustrates how abstraction can be viewed as a means of simplification. Nevertheless, and even though the figure is very simple, it conveys a great amount of information concerning the basic form of the system being created.

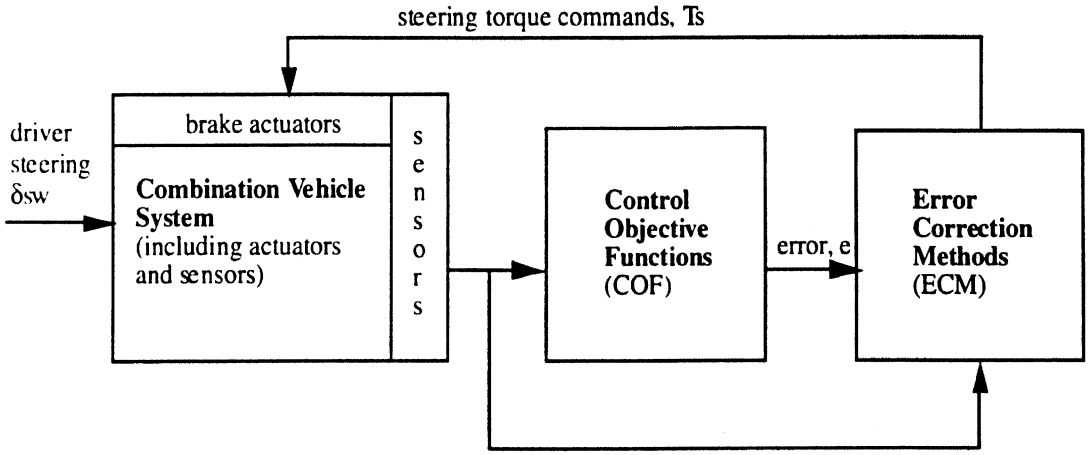

Figure 16. Overview of RAMS structure

The system consists of a battery of sensors whose outputs provide the information needed to compute corrective commands to brake actuators that will apply torques that tend to steer the units of the combination vehicle in a manner that reduces rearward amplification. The control objective functions (included in figure 16) represent the rules used by the RAMS system to achieve its functional purpose. The formulations of these control objective functions are the primary inventive steps in the process of designing the RAMS. Their formulation represents a jump in insight that unifies physical form with functional meaning. They are at the heart of this invention of a RAMS system. The functional quality of the RAMS depends upon the quality of the control objective functions employed in the system.

3.2.3 Generalized functions

The actual RAMS system uses a number of standard subfunctions to achieve its purpose. There is a wide variety of devices that could be suitable for performing these subfunctions. In this project the choices of equipment are influenced by the availability of standard equipment from the partners in the program. For example, the brake actuation process employs electronically-controlled brake system (ECBS) components developed by Midland-Grau. Although not immediately apparent to the vehicle dynamicist, the development of a working system depends upon the process of communicating information to where it is needed. The tractor supplied by Freightliner has a communication bus that conforms to SAE Standard J1708/J1587. With regard to sensing the needed information, the air suspensions provided by Hendrickson-Turner have devices indicating the pressure in the air bags installed on the axles on the trailers. These electronic signals can be processed to reflect the load on individual axles. In addition, standard commercially available sensors have been employed to measure the other vehicle dynamics variables used in the control loops that will be discussed next.

The inventive part of the RAMS design involves the development of suitable control loops. In this project, a vehicle simulation was developed and utilized to try out various control schemes. See references [5] and [6]. Linear analyses were also used to study the rearward amplification problem further. Furthermore, there exists a substantial literature on rearward amplification. (See references [7 though 11].) Reference [10] in particular provides test and analytical results indicating the proficiency of various mechanical linkage and constraint systems in reducing rearward amplification. All of this knowledge and understanding was used to envision and try a number of control objective functions. After a considerable amount of effort, it was predicted by evaluating simulation results that a RAMS system using ECBS systems on the axle of the first semi-trailer, the dolly axle, and the axle of the last semi-trailer in a doubles combination could be used to reduce rearward amplification to less than a value of 1.2 as compared to approximately 2.0 for a typical western doubles combination without a RAMS.

Of the many control objective functions that were tried, an arrangement that provided articulation rate damping to the axles of the first and last semi-trailers plus "steering" torque to the dolly axle was selected. These control objective functions could be evaluated using information from yaw rate sensors for each unit with a yaw degree of freedom (tractor, first semi-trailer, dolly, and last semi-trailer) plus measurement of the driver's steering input and the forward velocity of the vehicle. Attempts to use control objective functions using measurements of lateral acceleration directly did not succeed but this does not mean that such an arrangement cannot work. It just means that we do not know how to use lateral acceleration measurements to build a workable system.

Two ideas providing the basis for the jumps of insight leading to the control loops employed in the RAMS are:

(1) rearward amplification is a crack-the-whip phenomenon that can be reduced by damping the articulation motion occurring at the hitching joints at the front of each semi-trailer.

(2) the motion of the full trailer can be controlled to tend to mimic that of the tractor by applying steering torque to the dolly axle.

There does not seem to be any method short of simulation and testing to show that a RAMS system based upon these ideas will work well. We do not know of any way to guarantee success prior to experimenting with the real thing or experimenting with models (simulation). Since simulation and initial testing indicate that this RAMS will work satisfactorily, we will describe the control loops for manifesting this concept of the RAMS system.

There is a separate control loop for each of the axle sets on the trailing units of the combination. Each control loop has its own control objective function. However, the control objective functions for the axles on the semi-trailers only differ in the yaw rates they use in evaluating the rate of change of the pertinent articulation angle. The purpose of these control loops is to damp the articulation rates of the semis with respect to the unit ahead in the multiply-articulated vehicle. This purpose is implemented by the choice of the functional form of the control objective function. The chosen functional forms are listed in figure 17.

The control objective function for the dolly axle is more complicated in that its purpose is to steer the dolly axle in a manner that will cause the full trailer to follow the path of the tractor. In order to explain this, it is convenient to think of the unit that evaluates the control objective function as a "planner" because it performs the first step in executing a control plan. The plan involves determining a desired articulation angle between the dolly and the last semi (Γ_{Cd}). The difference between the desired angle and the actual articulation angle(Γ_C) is the difference between what we want and what we have, that is, the error. Because it is believed to be difficult to measure articulation angle satisfactorily the articulation angle has been computed using the integral of the difference in yaw rates r3 and r4. The desired articulation angle depends upon how the driver steers the tractor as expressed by the steering wheel angle δ_{SW}. There are two parameters used in the equations for desired articulation angle as given in figure 17. One is the distance, L, from the front axle of the tractor to the dolly axle. The other is K, the ratio of the wheel base of the full trailer to that of the tractor. The purpose of these parameters is to cause the full trailer to maneuver at the same place on the road where the tractor maneuvered and to control the amount of lateral motion so that it approximates that of the tractor. These parameters directly address the meaning and functional purpose of the RAMS.

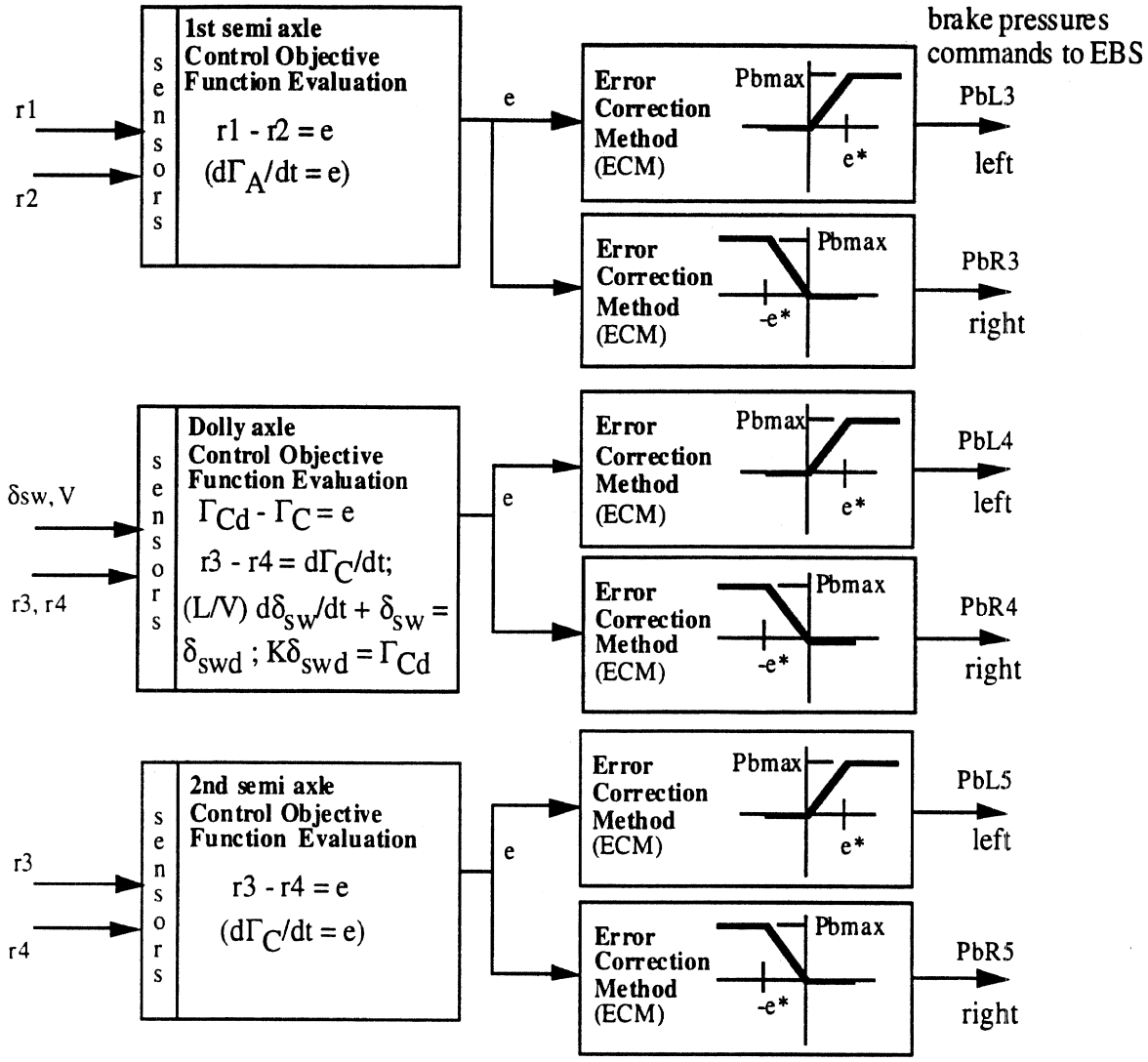

Figure 17. Planners and controllers for the loops controlling braking in the RAMS

Each of the control evaluation units (constituting part of a central processor) develops a control signal, e, that is used in an error correction method specially tailored to the RAMS application. See figure 17. In general, each error correction unit employs a gain factor as need to perform a proportional control function. Studies were made trying more sophisticated control methods including a modified sliding mode control method but the results show that the sophisticated control methods produce very little improvement in suppressing rearward amplification at the expense of a great deal of control activity that could be detrimental to the control valves in the braking system.

In addition, each of the error correction units employs compensation for the gain of the brake and the time needed to pressurize the brake chambers. This compensation provides the means for applying "steering" (i.e., via yawing torque) of the desired magnitude and at the desired time for performing the RAMS function. Since the polarity of the torque depends upon which brake is actuated, there is a logical operation called a "splitter" that

splits the pressure commands to provide the proper polarity of steering torque throughout a period of RAMS activity. Furthermore there is a limiter that limits the maximum braking command so that the RAMS system will not tend to lockup the wheels on lightly loaded axles. These features of the error correction method are illustrated cryptically by the graphs included in the ECM blocks in figure 17.

Although there are three separate control loops (one for each axle), they work together and do not tend to fight each other. The arrangement of damping and steering works much better than using one or the other alone. Fortunately, the simulations show a synergy such that the combination of damping and steering works better than might be expected based upon results for damping or steering individually.

3.2.4 Physical functions

The components of the RAMS system have been implemented in a truck combination. This means that certain properties of these components are known in detail. One overall system aspect of the engineering properties of the components has to do with communication of information. The informational properties of this RAMS system are summarized by saying that the system operates at an update rate of once every 0.01 seconds (100 samples per second). The signals generally have 8 bits for resolving values over their range of interest. Simulation experiments were used in choosing these levels. The results showed that the system would work, but with some degradation at 50 samples per second. On the other hand, 16 bit resolution did not provide much improvement over 8 bit resolution. This appears to mean that timing is more important than resolution in the context of the levels of timing and resolution studied.

In the final documentation of the system the physical properties of the components will be described further. Given that this is a prototype, proof of the actual mechanical, electrical, and environmental toughness qualities of the components is not as important as it would be if this were a finished product. Nevertheless, the components used in the RAMS prototype appear to be strong enough and sufficiently resistant to extraneous influences to survive and perform in the truck environment encountered at a proving grounds.

Perhaps a good way to summarize the description of the physical functions performed within this RAMS system is by means of the block diagram of the communication system shown in figure 18.

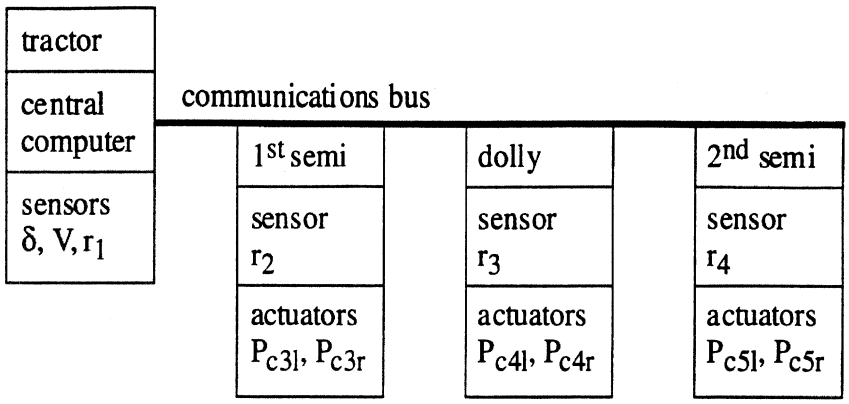

In addition, lateral accelerations A_{y1} and A_{y4} are also measured to evaluate the system.

Figure 18. Communication diagram

The actuators shown in figure 18 involve the ECBS system, including compensation for the properties of the brake system as in the manner illustrated in figure 19.

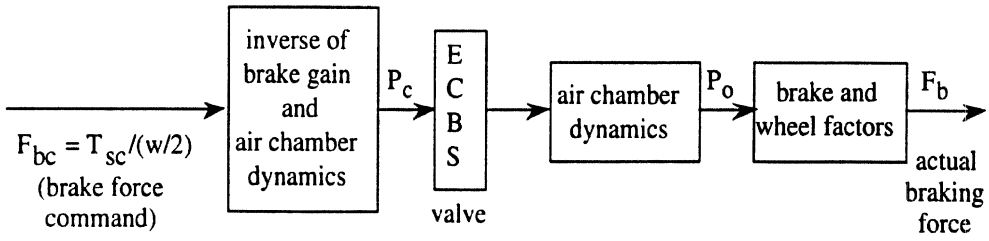

Figure 19. Compensation for brake properties

3.2.5 Physical form

The locations and appearance of the RAMS components will be observed at a later demonstration. The actual dimensions and mounting does not appear to be a problem but these are issues to be considered in later development if the concept is carried forward to deployable systems. At this time in the development of the system, it is most important to know where to mount the sensors and how to obtain information for evaluating the system. To the extent that many of the components are already either products or near-production versions of products, their physical properties have been checked for operation in service. In general, many practical and pragmatic aspects of the final form of a deployable RAMS system are beyond the scope of this project.

3.3 Experimental Results from Initial RAMS Testing

This section presents a first evaluation of the design of the RAMS system using results from an initial set of vehicle tests. The form of the evaluation refers back to figure x1 on the levels of abstraction. However this time the emphasis is on causes for physical effects rather than on reasons for physical functions. In a sense, analysis of the test results is like

troubleshooting the system to see how it works and to compare that with what the system is intended to do. At the higher levels of abstraction, the discussion of the comparison between actual function and desired function need not be very complicated since the data show that this RAMS system satisfies its functional purpose. Nevertheless, there are aspects of component engineering and system development that need attention. After introducing the test procedure, there are subsections addressing each of the levels of abstraction but not strictly in the bottom up sequence implied by the upward arrow shown in figure 14.

The process for examining the performance of the RAMS system involves a modified version of SAE recommended practice J2179 entitled "A Test for Evaluating the Rearward Amplification of Multi-Articulated Vehicles." This test procedure specifies the layout of a test course (path) for the driver to follow. The design of the course is based upon a lateral acceleration function of time corresponding to one cycle of a sine wave. The path obtained from this type of lateral acceleration is a lateral displacement maneuver. If the time period of the maneuver is short, the path is representative of an emergency obstacle avoidance maneuver. A kinematic analysis of this maneuver indicates that the time period of the maneuver T, the amount of lateral displacement Y, and the maximum value of lateral acceleration A (expressed in consistent units) are related by the following equation:

$$Y = A\,T^2/2\pi \tag{19}$$

The J2179 procedure is based upon a lateral acceleration of 0.15 g and a time period of 2.5 seconds when the vehicle is driven at a speed of 55 mph (80 ft/sec). This maneuver nominally yields a lateral displacement of 4.8 ft in a course that is 200 ft long. Although there were some tests done at 0.15 g and 4.8 ft, the procedure was modified to do a more aggressive maneuver. The course was widened to 8 ft yielding a lateral acceleration of 0.25 g. This elevated level of lateral acceleration provides a more demanding test for challenging the capabilities of the RAMS system.

The results presented here are for the 8 ft and 0.25 g course. (This corresponds to the maneuver used in the simulation runs since we wanted to challenge the RAMS design in the simulation runs.) Note that drivers may be able to follow the 0.25 g course with minimal errors in position and only employ a maximum of approximately 0.2 g at the tractor. However this is not a problem here because the results are interpreted in terms of the lateral acceleration actually achieved and furthermore the purpose of this initial testing is to evaluate the viability of the design concept regardless of the test procedure.

For these tests the trailers were loaded to provide an 80,000 lb vehicle but the weights were placed in a low position such that the center of mass was lower than it would be for typical cargo. This helps to keep the vehicle from rolling over. The low position of the load has some limited affect on rearward amplification but the test conditions were the same for

tests with and without the RAMS system in operation. Since outriggers were used here, the vehicle could have been tested with a higher placed payloads without the danger of rolling over the last trailer. We expect to employ higher loads in the demonstration tests planned for this spring in order to graphically illustrate the potential for rollover. However, this was not a critical requirement in the context of the initial tests.

3.3.1 Functional purpose

The ultimate test of performance is to look at the lateral acceleration time histories for the tractor and the last semi-trailer. Figure 20 shows results from a test run without the RAMS system in action. Examination of the time history for the tractor shows that the driver did employ approximately 0.2 g in steering the tractor to follow the course with an 8 ft translation in lateral position. Examination of the time history of lateral acceleration for the last trailer shows clearly that the last trailer did not make the goal of no more than 0.3g of lateral acceleration. The last trailer has a peak lateral acceleration that is greater than 0.45 g.

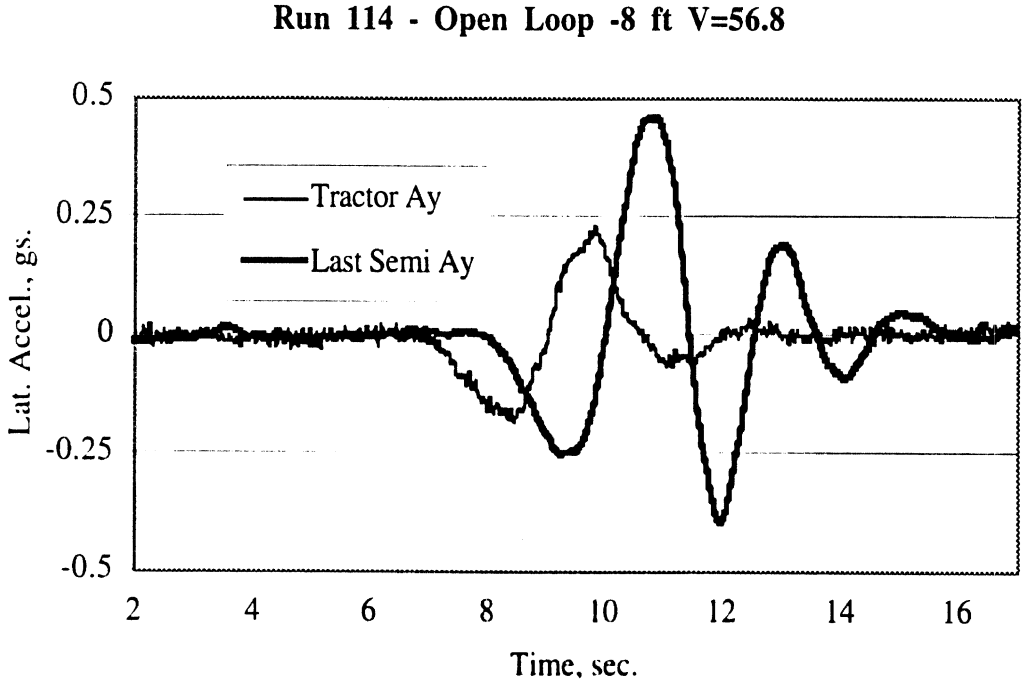

Figure 20. Lateral acceleration without RAMS

If this last trailer were to have been in a "cubed-out-maxed-out" condition, it would have rolled over (or, rather, would have tilted onto the outriggers in our test configuration). For typical doubles combinations, one might expect a steady-turn rollover-threshold at or above 0.3 g when the vehicle is fully laden with a moderate-density cargo. This

observation is part of the rationale for using 0.3 g as an objective for assessing the ability of the RAMS system to satisfy its functional purpose.

Figure 21 shows an example of the performance of the vehicle in the 8 ft maneuver with the RAMS system functioning. In this run the tractor again achieved approximately 0.2 g but the peak lateral acceleration of the last trailer was 0.3 g with the RAMS system in operation.

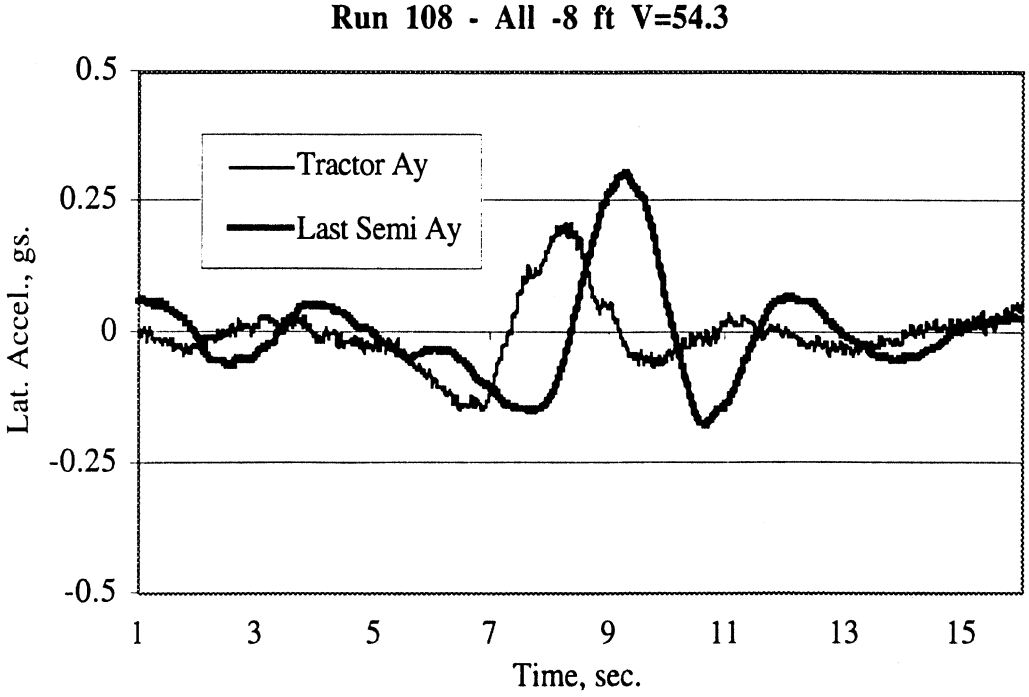

Figure 21. Lateral acceleration with RAMS

In summary, these results alone indicate that this design of the RAMS system appears to be a viable approach for suppressing rearward amplification. Nevertheless, further examination of the test findings will identify some areas in which the system did not behave completely as intended.

3.3.2 Physical Form

In going from functional purpose (section 3.3.1) to physical form (this section), the discussion skips from the most abstract to the least abstract. The reason for putting the evaluation of functional purpose first is to set the tone for viewing further details of the test results knowing that the system works. Once functionality is established, it seems reasonable to address ways to improve the performance of the system.

With regard to physical form there is not much to infer from the test results directly. The fact that the vehicle could be run and tested represents evidence that the location of the

parts did not interfere with normal operation of the truck. At the simplest level, the ability to operate the system in a dynamic environment shows at least a minimal level of practicality to the physical form of the system. Based upon our experience exercising the vehicle with the RAMS in action, we have no suggestions for changing the physical layout of the equipment or its appearance.

3.3.3 Physical Functions

The ability to operate at 100 samples per second did not come easily. Laboratory testing, troubleshooting, and evaluation were needed to get the sensor and actuator data on and off of the communications bus in a timely manner. However, once these problems were corrected in the laboratory, intra-vehicle communications were not a problem during the initial testing exercise.

The electronic braking equipment did show some temperature sensitivity in the beginning of the installation of the equipment on the vehicle. These difficulties were resolved in so far as the system was tested without incident in cold winter weather at TRC in Ohio.

Clearly, the initial testing did not constitute an endurance test nor did it involve checking out electrical or mechanical specifications for the equipment. Rather the initial testing showed that the components worked as a system. Their basic physical functions did not need to be investigated to solve operational problems that would cause the system to malfunction.

3.3.4 Generalized Functions

Once the basic functional performance was established, the primary value of the initial testing was the opportunity to observe how well the control loops and associated processes performed in an obstacle avoidance maneuver.

Even when the RAMS was not engaged, performance of the sensors could be checked and results could be obtained to aid in understanding the differences between driving with and without the RAMS. Figure 22 shows the yaw rate signals from the transducers mounted on each of the articulating units of the doubles combination. These data are for the same test (run 114) as the data presented in figure 20. A notable feature of these time histories is that the yaw rates of the dolly and the last semi are much larger than those of the tractor and the first semi. There is also an amplification of rotational motion of the last semi compared to that of the tractor. Also the yawing motion of the last semi takes several seconds to damp out. As indicated in the figure, the amplitude of the first half cycle of oscillation is less than that occurring during the second half cycle. This is typical behavior indicating that the heading correction required to return to the original direction of travel is more severe than that used to initiate the maneuver.

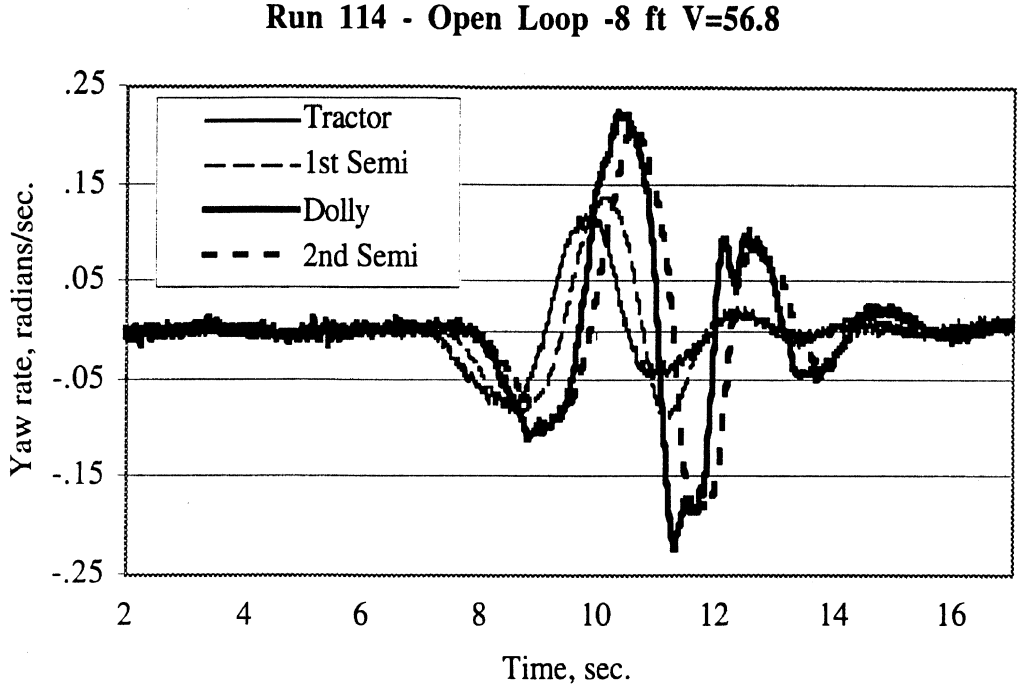

Figure 22. Yaw rate signals without RAMS

With regard to the components and processes of the RAMS system, these data indicate that the yaw rate transducers work, their signals are communicated properly to the central processing unit, and the vehicle behaves as expected.

Figure 23 shows the same yaw rate signals but with the RAMS in operation. The lateral acceleration signals for this run were presented in figure 21. One can see by comparing the time histories in figures 22 and 23 that the RAMS suppresses and damps the yaw rates particularly for the full trailer consisting of the dolly and the last semi. This is an indication that the control loops are having the intended effect on the motion of the vehicle.

Insight into the operations of the control objective function for the dolly can be obtained by examining figure 24. These data show the steering of the front wheels of the tractor as well as the delayed (lagged) steering signal and the computed articulation angle. The reason why the signals for the lagged steer angle and the dolly angle start and end as seen in the data is because the RAMS system exercises an interrupt function and, thus, does not operate all of the time. If it was continuously active, it could overheat and wear out the brakes. RAMS operation is triggered by a sudden steering action in which the steering wheel angle exceeds a preset threshold in a preset period of time. Once the RAMS is engaged it stays on for 10 seconds and then disengages.

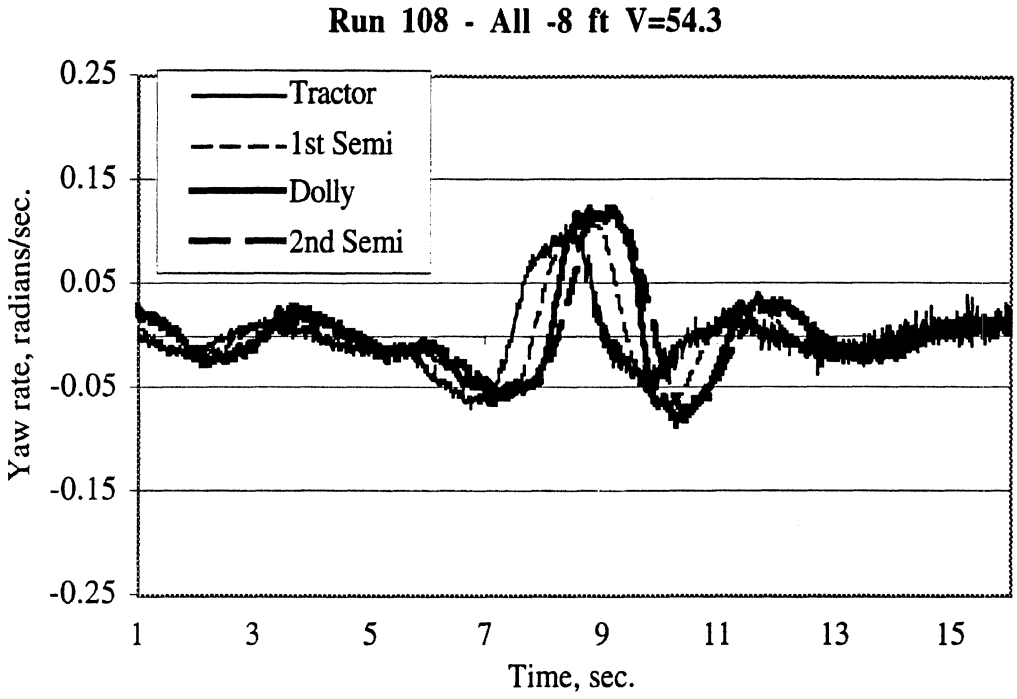

Figure 23. Yaw rate signals with RAMS

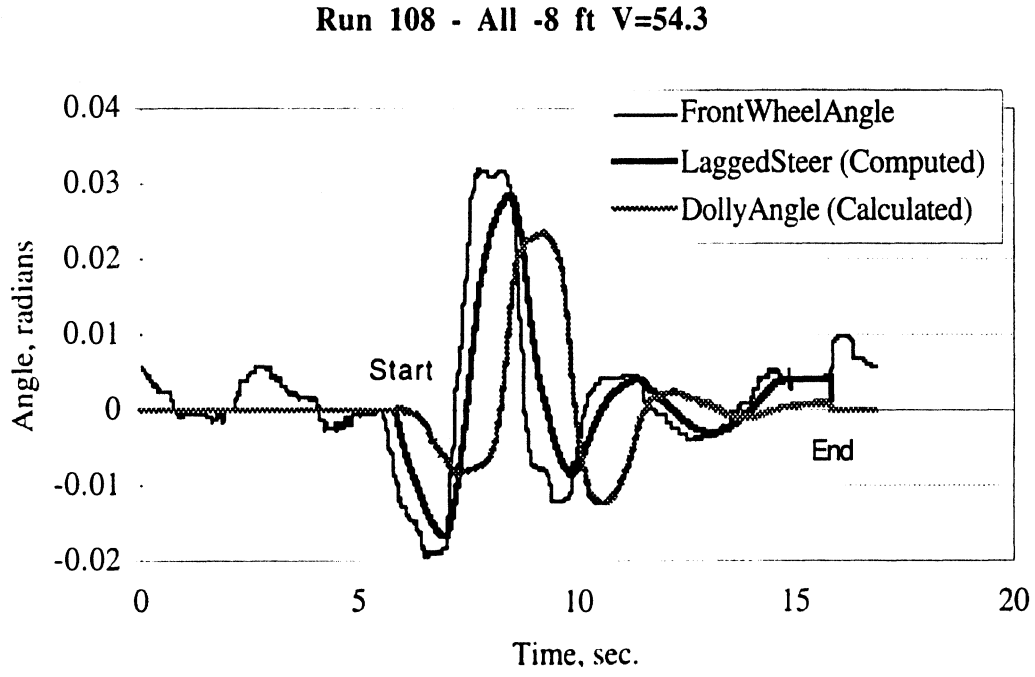

Figure 24. Signals pertaining to the dolly's control objective function

These data look qualitatively reasonable except that there appears to be a large difference between the lagged steer and the calculated dolly articulation angle. Although it is not obvious, these data indicate that we do not have exactly the correct values for the time delay and the tractor steering gain in the system. Fortunately, the control loop is fairly robust in the sense that it will still work even if the gains and delays are not perfect. Nevertheless we anticipate that adjusting the delay and the gain will result in some improvement in rearward amplification suppression.

For this run (number 108), the rearward amplification is approximately 1.4 to 1.5. The computer simulations predicted that the RAMS system would be capable of a rearward amplification of 1.2 or less in this maneuver. This leads us to believe that adjustment in the steering control for the dolly will help to reduce rearward amplification.

Insight into the performance of the error correction and ECBS systems has been gained by examining figures 25 through 27. These figures show the pressure responses obtained in the left and right brake chambers of the axles on the first semi, the dolly, and the last semi, respectively. The pressures are going on and off at roughly the intended times. They are switching between the right and left brakes as expected. This means that the splitters are functioning properly. In hindsight we see (although it is not obvious) that the value of lead used in compensating for the lag in pressure involved with filling the brake chambers may be too long. We will correct this if necessary before testing again but it is not expected to make a major change in performance.

An eye-catching feature of the braking action is the magnitude and steepness of the pulses of braking pressure shown in figures 25 through 27. Magnitudes over 70 psi are surprising because 70 psi was intended to be the limiting value of brake pressure. Computer simulation had shown that pressures up to the limit were to be expected, but obviously pressures over the limit are not to be expected. Troubleshooting this symptom indicates that the interaction of the limiter circuit and the pressure signal from the suspension airbags is not proper. We will need to examine this circuit further to see if we want to leave it as is or change it. It appears that we have neglected to consider that braking torque gets reacted in the suspension in a manner that increases the air bag pressure suddenly. The original intention in using the air bag pressure was to adjust the brake gain to aid in preventing wheel lockup on an axle having a light static load.

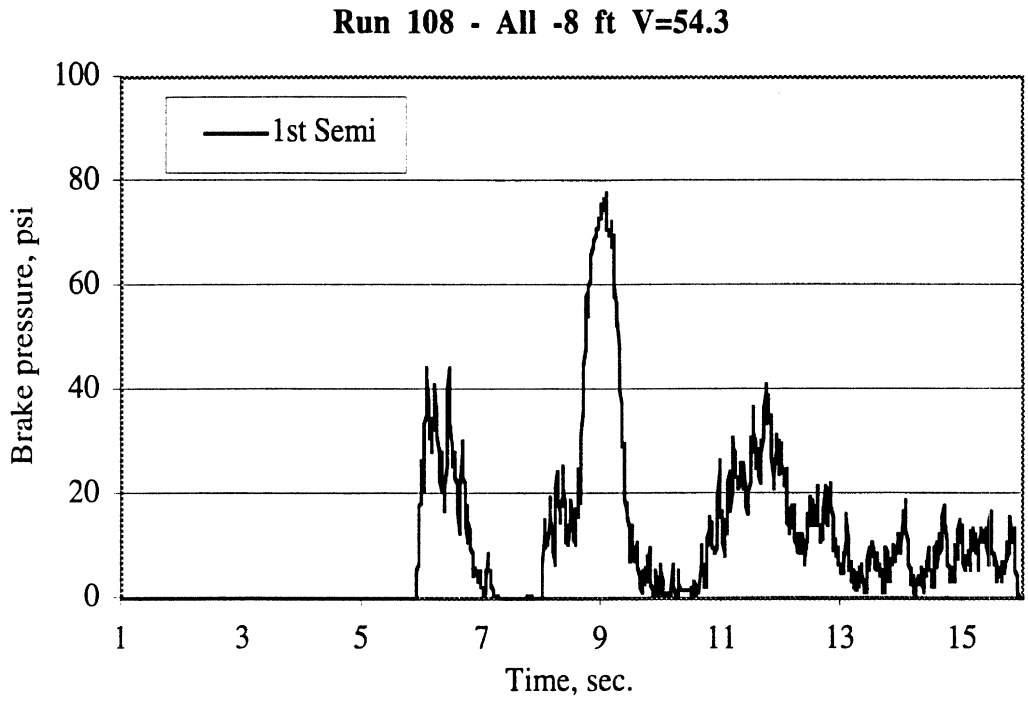

Figure 25a. RAMS–controlled brake pressure at the left wheels of the axle on the first semi-trailer

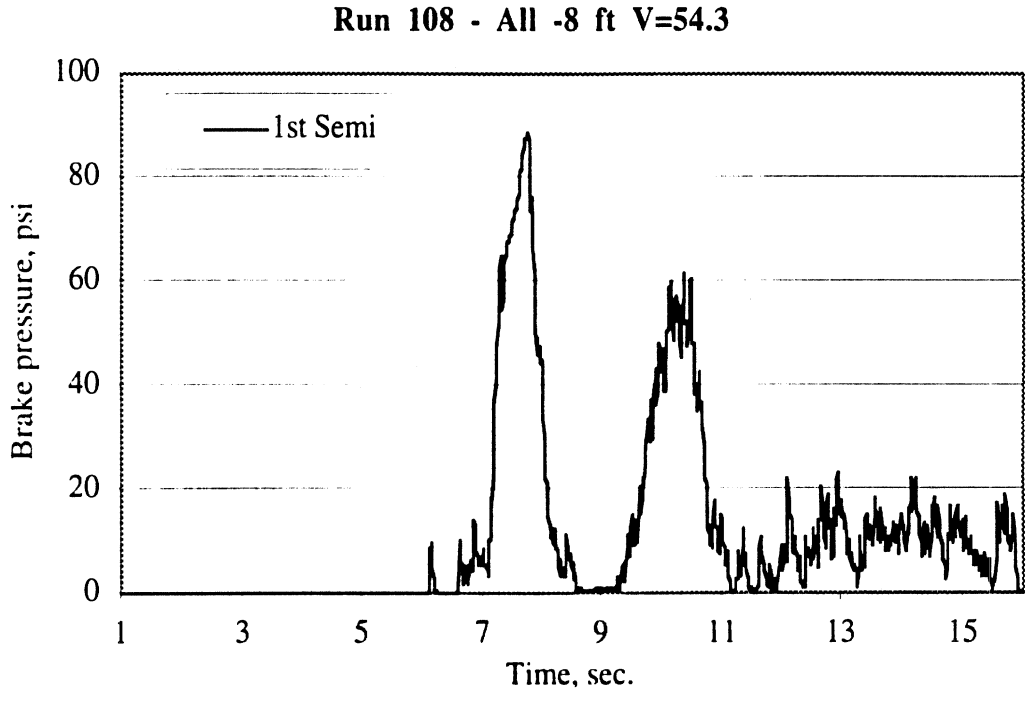

Figure 25b. RAMS–controlled brake pressure at the right wheels of the axle on the first semi-trailer

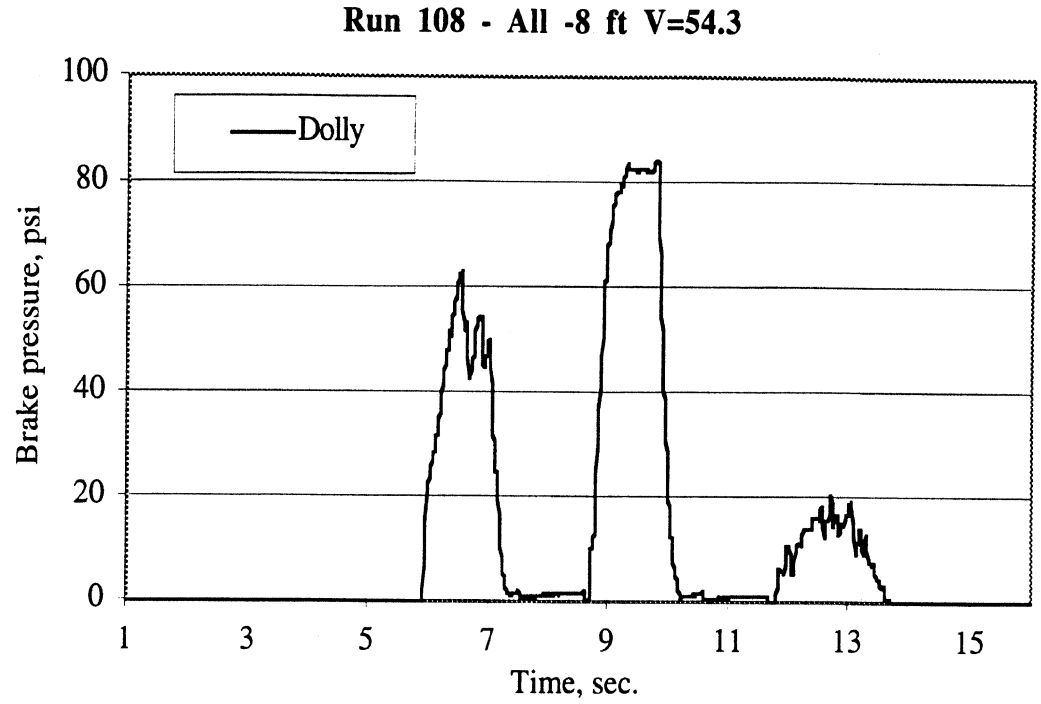

Figure 26a. RAMS–controlled brake pressure at the left wheels of the axle on the dolly

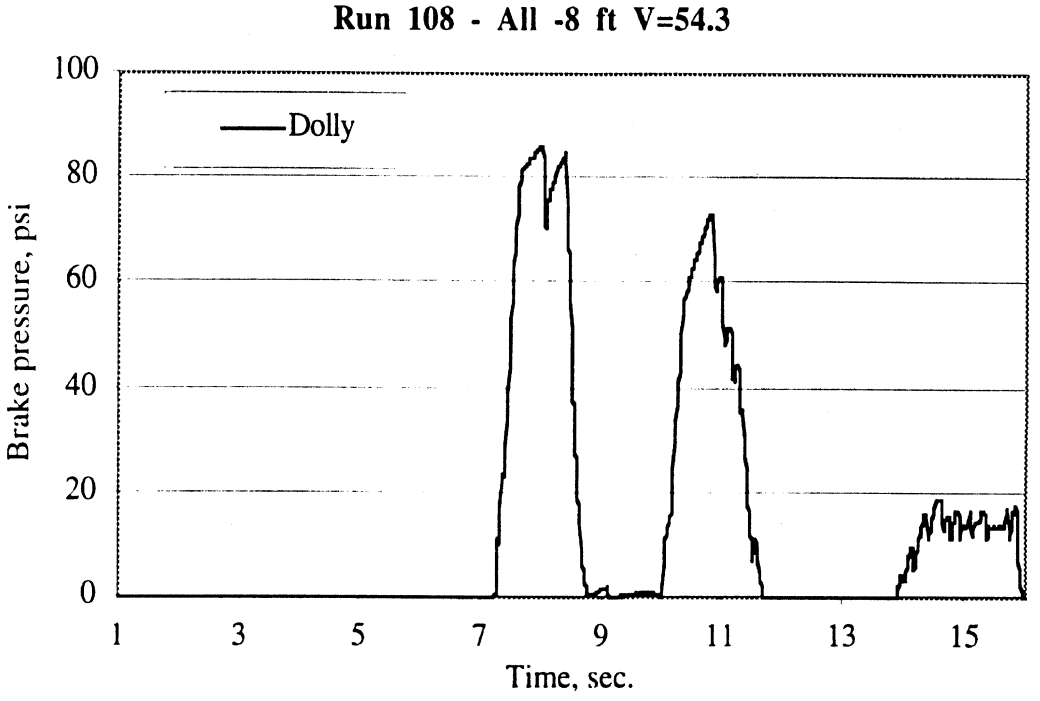

Figure 26b. RAMS–controlled brake pressure at the right wheels of the axle on the dolly

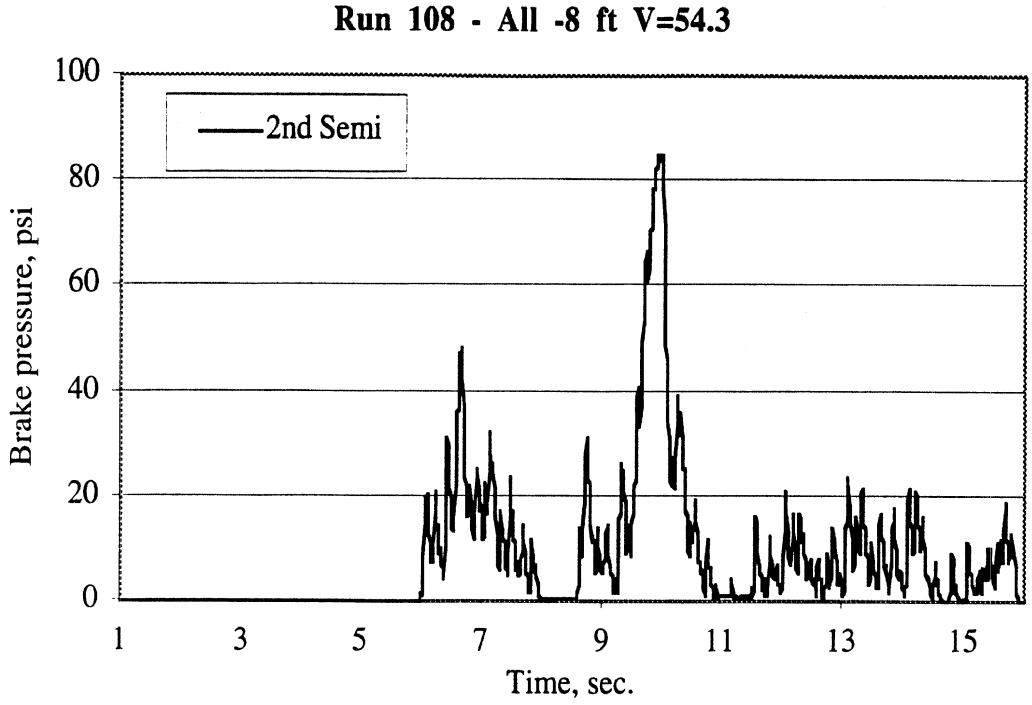

Figure 27a. RAMS–controlled brake pressure at the left wheels of the axle on the last semi-trailer

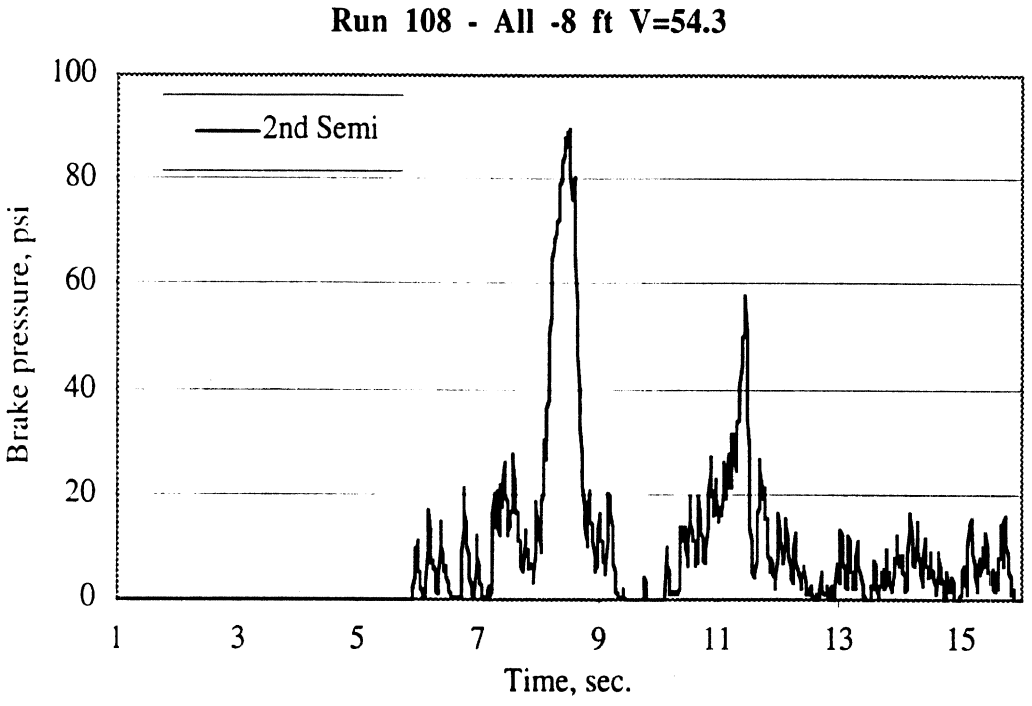

Figure 27b. RAMS–controlled brake pressure at the right wheels of the axle on the last semi-trailer

However, the steepness of the braking pulses indicates that the system is in effect acting more or less as a bang-bang controller. This means that the timing of the onset and fall of each pulse is more important than the magnitude as long as the magnitude is large enough. Clearly, when the pulse is limited to a maximum amplitude, an increase in gain will not change the control action. Because of this, it may be that changing the value of the limit on braking pressure could be as important as a change in gain. However, there is probably not a lot of improvement to be gained by changing the system, although even a little improvement to a rearward amplification of 1.3 or 1.2 is thought to be important.

One other test run illustrates important considerations for correcting and improving the system. Namely, we see in run 106 that the RAMS system did not trigger on the first half cycle of steering activity. This can be seen by examining figure 28. (Also, in this case, we note that the driver did not initiate the maneuver as aggressively as was done in run 108.)

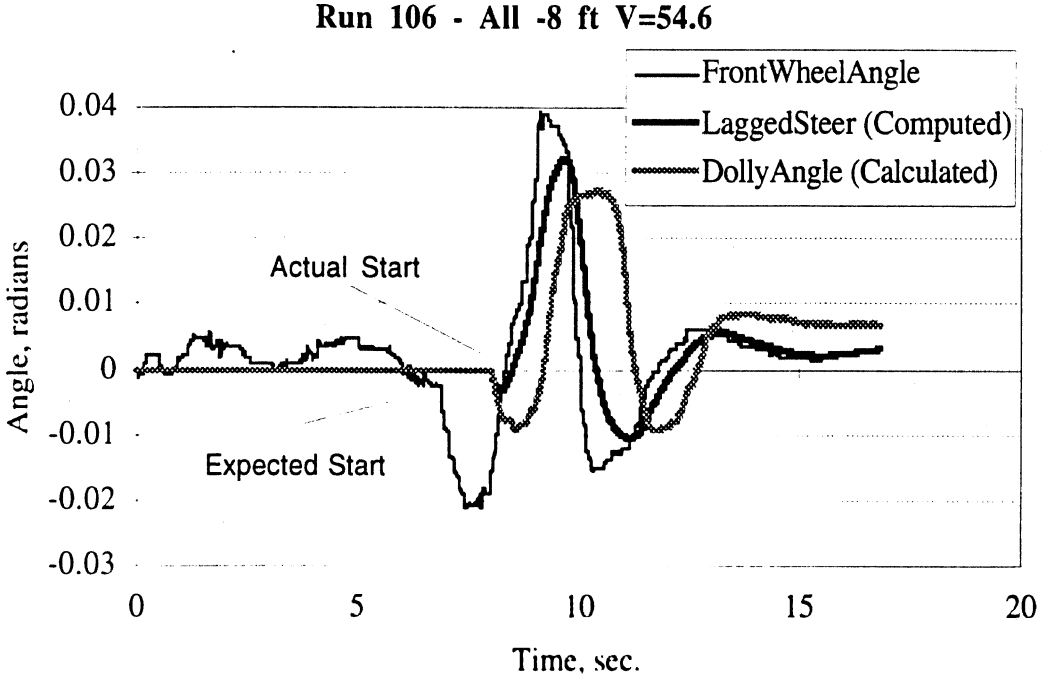

Figure 28. Example of late triggering of RAMS

Nevertheless, the vehicle's response in Run 106, as shown in figure 29, indicates that the RAMS still did very well in suppressing rearward amplification well below 0.3 g in this maneuver. This is further indication of the robustness of the control system, but it also indicates the need to reexamine the triggering criteria to better understand its influence on RAMS performance. We may find that there is something to be gained by a more accommodating arrangement of the triggering criteria.

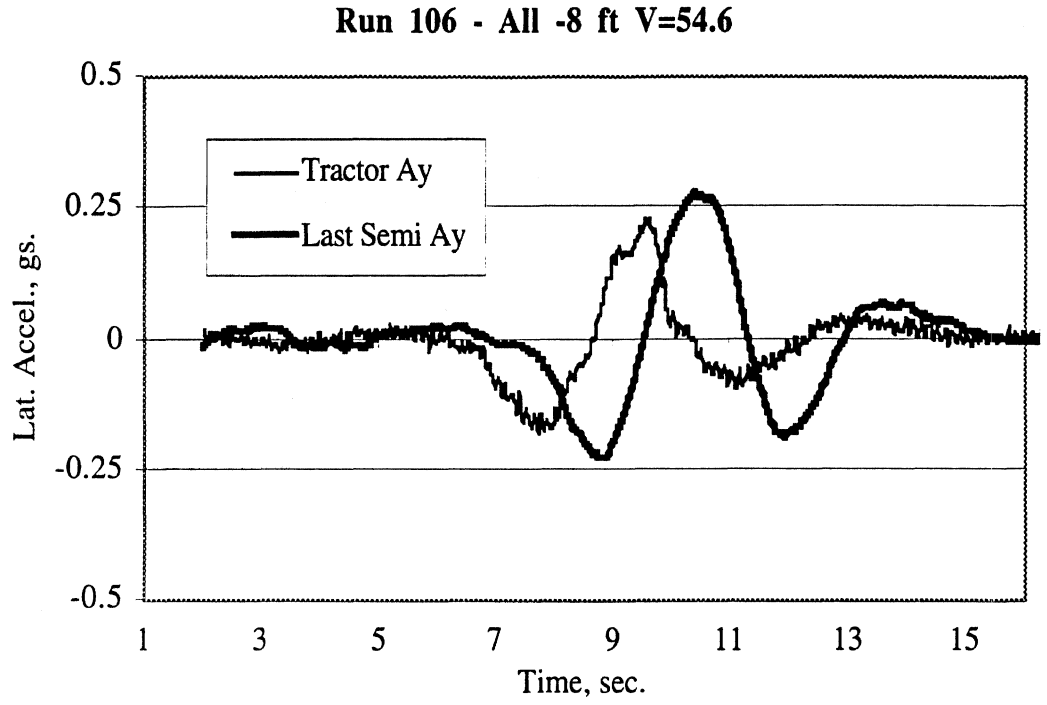

Figure 29. Rearward amplification for the second half cycle of Run 106

In summary, we have found a few items to examine for improving the operation of the control loops. It is conceivable that with corrections and adjustments in timing, the RAMS will act to contain rearward amplification values within a maximum of approximately 1.2.

3.3.5 Abstract Function

After having performed the initial tests it seems appropriate to offer another view of the RAMS structure in contrast to the perspective provided by figure 16. This view is provided by figure 30. Figure 30 situates the activation rules as the enabler of RAMS control and shows the information flow to each of the articulating units of the vehicle. Since the initial design has now been evaluated for the first time, there exists a better feel for what is important and how to portray the system. In particular, the work has progressed through the hierarchy of abstractions in the context of design considerations and back through that same hierarchy in the context of evaluating the performance of the RAMS system. This process has confirmed that the functional purpose and the abstract function need not be changed in any significant manner. Nevertheless, they have clarified how our next iteration of this cycle of design and evaluation can be aimed at improving and optimizing the design of the RAMS system.

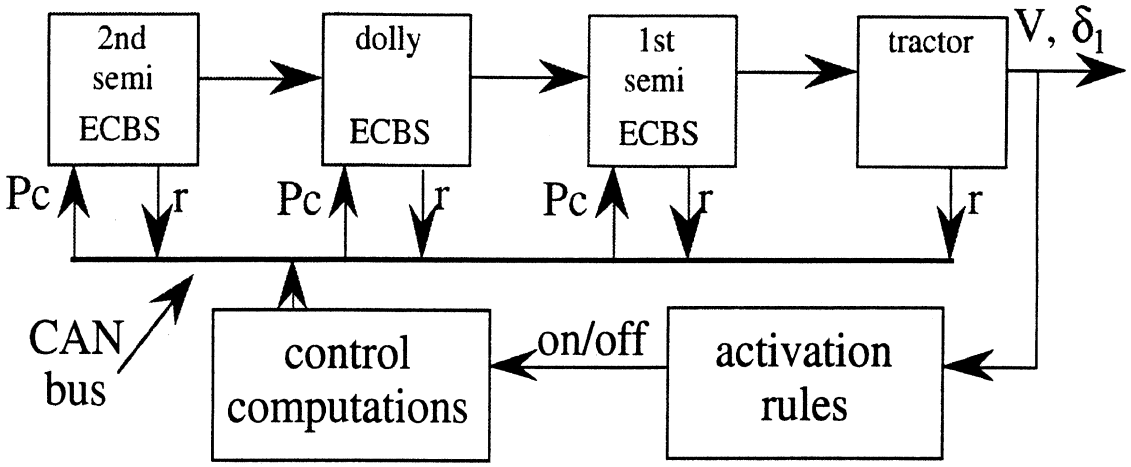

Figure 30. Connectivity diagram of the RAMS system currently being tested

4.0 Plans for Project Completion

The remainder of the project calls for preparation of the complete, tractor-based RSA system, refinement of the RAMS control system, and final testing and demonstration of both. Each of these efforts is outlined below.

4.1 Preparation of the RSA System

The key components comprising the complete RSA system are 1) the fifth wheel load cell, 2) the revised processing algorithm, and 3) the display-related elements for presenting the advisory information to the driver. Having completed design of the fifth wheel load cell, the remaining effort involves machining, strain gage placement and calibration using laboratory fixtures. After calibration, this device is to be mounted as the fifth wheel element coupling the test tractor and a loaded semi-trailer for initial over-the-road operations producing exemplar output data whose noise content must be scrutinized for adapting a suitable processing algorithm.

The algorithm for utilizing this cell's output data, together with other tractor state variables, would be brought to a complete and working version. Next, the vehicle will be run over a route of some fifty miles of normal driving, in various states of trailer loading, to produce data showing the extent of accuracy in the RSA's estimation of the vehicle's rollover threshold. As with earlier tests of the trailer-based RSA system, "accuracy" is expressed by the comparison of system-derived estimates with actual roll stability limits measured for this tractor semi-trailer combination using UMTRI's tilt table facility.

Following whatever iterations are needed on the algorithm coding, the driver-display element will be added for operation of the complete RSA system. Field exercises based upon normal driving over the local road system will be undertaken to establish the final

state of readiness of the system and to collect data documenting its performance in rapidly updating the rollover threshold estimate, following any type of reset condition (such as coupling a new trailer or changing the payload).

4.2 Refinement of the RAMS System

The successful demonstration of the RAMS prototype in December, 1997 indicates that only a few revisions in the control code are necessary for completion of the RAMS portion of the project work. Following the revisions, the full system function will be checked out in preparation for final testing.

4.3 Final Testing and Demonstration

The test vehicle, equipped for both RAMS and RSA functionality, will be taken to the TRC test facility in Ohio and subjected to a final set of tests. Test data are to be collected principally to confirm the final state of performance of the revised RAMS controller. A specific day will also be arranged for demonstration of both functions to representatives of NHTSA and the industrial partners to this cooperative agreement.

4.4 Final Report

Following analysis of the final data sets and evaluation of results, a final report will be prepared documenting the methods, results, findings, and recommendations from this work.

5.0 REFERENCES

1. Ervin, R. D.,Winkler, C. B. The influence of braking efficiency on the probability of wheel lockup. 1987. 13 p. SAE Transactions Paper No. 870334. Volume 96.
2. Winkler, C.B, Bogard, S.E., Bowen, M.A., Ganduri, S.M., Lindquist, D.J. "An operational field test of long combination vehicles using ABS and C-dollies." Final technical report to the National Highway Traffic Safety Administration, U.S. Department of Transportation. University of Michigan Transportation Research Institute. Ann Arbor, MI. November, 1995.
3. Ervin, R. D., Mathew, A. Reducing the risk of spillage in the transportation of chemical wastes by truck. Final report. 1988. 25 p. Sponsored by Rohm and Haas, Bristol, Pa. Report No. UMTRI-88-28.
4. Mallikarjunarao, C., Fancher, P.S. Analysis of the Directional Response Characteristics of Double Tankers. SAE Paper No. 781064, December 1978.
5. Fancher, P, Winkler, C, Ervin, R, Zhang, H. "Using Braking to Control the Lateral Motions of Full Trailers" 15th IAVSD Symposium. *Proceedings.* The Dynamics of Vehicles on Roads and Tracks. Budapest. 1997.

6. Fancher, P, Zhang, H, Winkler, C. "The Use of Braking for Controlling the Lateral Motion of Full Trailers" AVEC'96. *Proceedings.* International Symposium on Advanced Vehicle Conrol. Aachen. 1996. pp 527-545.

7. Hazemoto, T. "Analysis of lateral stability for doubles." Mitsubishi Motors Corporation, Japan. 1973. 18 p. SAE 730688.

8. Strandberg, L.; Nordstroem, O.; Nordmark, S. "Safety problems in commercial vehicle handling." Statens Vag- och Trafikinstitut, Linkoping, Sweden. 1975. 66 p. Commercial Vehicle Braking and Handling Symposium. Proceedings. Ann Arbor, HSRI, 1975. Pp. 463-528.

9. Ervin, R.D.; Fancher, P.S.; Gillespie, T.D.; Winkler, C.B.; Wolfe, A. *Ad hoc study of certain safety-related aspects of double-bottom tankers.* Final report. Highway Safety Research Institute, Ann Arbor, Mich. 1978. 78 p. UM-HSRI-78-18-1.

10. Winkler, C B; Fancher, P S; Carsten, O; Mathew, A.; Dill, P. *Improving the dynamic performance of multi-trailer vehicles: a study of innovative dollies.* Final report. University of Michigan Transportation Research Institute, Ann Arbor. 1987. 246 p. UMTRI-86-26/I. DTFH-61-84-C-00026.

11. Winkler, C B; Fancher, P S; Bareket, Z; Bogard, S; Johnson, G; Karamihas, S; Mink, C. *Heavy Vehicle Size and Weight—Test Procedures for Minimum Safety Performance Standards* Final report. University of Michigan Transportation Research Institute, Ann Arbor. 1992. 246 p. UMTRI-92-13. NTIS report no. DOT HS 807 855

APPENDIX A TRACTOR AND TRAILER SUSPENSIONS MEASUREMENTS

APPENDIX B MAP OF THE RSA TEST COURSE

APPENDIX C SYSTEM IDENTIFICATION ANALYSIS FOR THE RSA SYSTEM

Appendix A: "Smart Truck" Suspension Tests

This document reports on suspension testing performed for the Smart Truck project. The steer axle, trailing drive axle, and one of the trailer axles of a 6-axle doulbes combination were tested. The tests were performed primarily to characterize suspension properties relevant to roll stability of the vehicle. Table A-1 summarizes the axles that were tested.

Table A-1. Smart Truck Suspensions.

Axle Class	Steer	Drive, Tandem†	Trailer, Single
Suspension Type	Single	Trailing Arm	Trailing Arm
Spring Type	Taper Leaf (2)	Air	Air
Rating (per axle)	12,000 lbs	20,000 lbs	20,000 lbs
Vehicle Manufacurer	Freightliner		Fruehauf
Vehicle ID	VIN 1FUYSXZB5UP556581		Model FBB9-F1-28

† Only the trailing axle of the tandem set was tested.

TESTING PROGRAM

Testing of the functional performance of the suspensions listed in table A-1 was done to measure: the vertical spring rate, suspension roll stiffness (including auxiliary stiffness), the roll center height, the roll steer performance, the lateral compliance, and the aligning moment steer. Table A-2 describes the measurement program for the steer axle. For the steer axle the roll motion and lateral force tests were performed at suspension loads of 14000, 12000, 10000, 7500, and 5000 lbs. The aligning moment test was performed at a suspension load of 12000 lbs. Table A-3 describes the measurement program for the drive and trailer axles. Only the trailing drive axle was tested. The vertical motion, roll motion, lateral force, and aligning moment, tests were performed at nominal suspension loads of 20000, 18000, 16000, 14000, 8000, and 4000 lbs for the drive axle. The vertical motion, roll motion, and tests were performed at nominal suspension loads of 25800, 20800, 15300, 10400, and 5900 lbs for the trailer axle. The aligning moment test for the trailer axle was performed at a suspension load of 20800 lbs.

The test results corresponding to each entry in the tables are reported in reduced and graphical form. The graphical data, provided at the end of this appendix, provide the functional relationships between the independent and dependent variables of interest. The reduced parameters, provided in the "Results" section, represent idealized (usually linear) stiffness or kinematic properties derived from the graphical data.

TEST DEFINITIONS

All suspension measurements were conducted using the UMTRI heavy vehicle suspension measurement facility. The facility is described in detail in SAE Technical Paper 800906. In all tests, the frame of the vehicle is held fixed and the suspension is exercised by moving the facility "table" vertically, in roll, or by applying tire shear forces using the "wheel pads."

Table A-2. Steer Axle Suspension Measurement Program.

Test	Measurement	Reduced Numerics	Data Plots
Vertical motion	Vertical rate	Boundary tables, beta, linear coefficients	F_Z vs Z
Roll motion	Roll rate	Total roll stiffness, Auxiliary roll stiffness	M_X vs Roll
	Roll center	Roll center height	Y_{REF} vs Roll
	Roll steer	Roll steer coefficient	Steer vs Roll
Aligning moment	Aligning moment steer	Linear coefficient, freeplay, model parameters	Steer vs M_Z
Lateral force	Lateral compliance	Linear coefficient	Y vs F_Y

Table A-3. Drive and Trailer Axle Suspension Measurement Program.

Test	Measurement	Reduced Numerics	Data Plots
Vertical motion	Vertical rate	Boundary tables, beta	F_Z vs Z
Roll motion	Roll rate	Total roll stiffness, Auxiliary roll stiffness	M_X vs Roll
	Roll center	Roll center height	Y_{REF} vs Roll
	Roll steer	Roll steer coefficient	Steer vs Roll
Lateral force	Lateral compliance	Linear coefficient	Y vs F_Y
	Lateral force steer	Linear coefficient	Steer vs F_Y
Aligning moment	Aligning moment steer	Linear coefficient	Steer vs M_Z

Force measurements are made with load cell systems located in each of the wheel pads. Thus, in general and except where noted, the reported forces in the data are absolute values measured at the tire/road interface. Resulting motions of the suspension and wheels are measured with several potentiometric devices. Generally, these motion measurements are relative (not absolute) and are referenced to the fixed frame of the vehicle.

The following paragraphs outline the test procedure for the four physical test types listed in tables A-2 and A-3.

Vertical motion: The suspension is exercised by vertical motion of the table. Table motion is controlled by a force and moment feedback servo-system so that roll moment applied to the suspension is held constant at zero while vertical load on the suspension is varied over the range of interest. Force and moment control servo-systems are also used to maintain zero levels of tire shear force and moment.

Roll motion: The suspension is exercised by roll motion of the table. Table motion is controlled by a force and moment feedback servo-system so that the total vertical load applied to the suspension is held constant at the desired value while total roll moment on the suspension is varied over the range of interest. Force and moment control servo-systems are also used to maintain zero levels of tire shear force and moment. This force and moment control mode allows the motion of the suspension to be determined by the suspension geometry, rather than by facility geometry.

Lateral force: The suspension is exercised by the application of lateral tire shear force. Prior to the test, the suspension is loaded vertically to the desired level (with zero roll moment). During the test, the table is controlled by feedback of the vertical position of the right and left axle spindles so that the *vertical and roll position of the axle is held fixed.* (As a result, vertical and roll motions, and especially their influence on steer, are not allowed to influence the test, but vertical load on individual tires will change some during the test. Total vertical load may also change slightly.) The force and moment control servo-systems of the wheel pads are used to vary the lateral force at each tire while longitudinal force and aligning moment are held fixed at zero. Lateral force loading is equal at each wheel throughout the test.

Aligning moment: The suspension is exercised by the application of aligning moments at each tire pair. Prior to the test, the suspension is loaded vertically to the desired level (with zero roll moment). During the test, the table is controlled by feedback of the vertical position of the right and left axle spindles so that the *vertical and roll position of the axle is held fixed.* (As a result, vertical and roll motions, and especially their influence on steer, are not allowed to influence the test, but vertical load on individual tires will change some during the test. Total vertical load may also change slightly.) The force and moment control servo-systems of the wheel pads are used to vary the aligning moment at each tire while longitudinal and lateral force are held fixed at zero. Aligning moment is equal at each wheel throughout the test.

RESULTS

The graphical data collected for the suspensions are provided at the end of this appendix. At least one graph is produced from each test. Each graph identifies the data file, test type, vertical load (if applicable), and other pertinent information. The graphs also provide definitions of the dependent and independent variables, including the units and sign convention. Any explanation needed for interpretation of the graphs is provided in this section.

Reduced data appear in tables A-5 through A-19, and are discussed in this section. Many of the reduced numerics are simply linear coefficients indicating the nominal slope of the related graphical data. The slopes presented are taken from the data at the nominal suspension operating point for the test, often at the origin of the data graph. Note that, due to nonlinearity of the graphical data, other values may be appropriate for "off-center" conditions.

Vertical Motion

The vertical force-deflection behavior is characterized during the vertical motion test. The functional relationship that results from the test is a plot of vertical load versus suspension deflection. The plots provide the suspension spring rate *as measured at the wheel spindle,* that is, they do not include compliance of the tire. In all plots, the vertical

load is measured at the ground, not at the spring, so it includes the unsprung weight of the suspension.

Vertical spring rate

The stiffness properties relevant to roll stability derived from the vertical motion test are linear spring rate and coulomb friction level at a specified operating point (see tables A-5 through A-7), and tables describing the compression and extension boundaries of the force-deflection data (see tables A-8 through A-19). The stiffness of the suspension springs, in combination with their lateral separation, determine the contribution of vertical rate to roll stiffness. The linear spring rate is simply the slope of the vertical force-deflection plot at the operating point. For the drive and trailer axles, a set of extension and compression boundaries is given of each nominal load condition, because each condition implies a different air bag pressure at ride height.

Roll Motion

The suspension total roll stiffness, auxiliary roll stiffness, roll center height, and roll steer coefficient are all reduced from the results of the roll motion test. (See tables A-5 through A-7.)

Total roll stiffness

The plots entitled "Axle Roll Rate" present roll moment about the suspension roll center versus the roll angle of the axle. The slope of this plot is the total roll stiffness of an axle.

The total roll stiffness of the steer axle decreased with nominal suspension load. This is because the auxiliary roll stiffness decreased with load. The total roll stiffness of the drive and trailer axles was fairly consistent over a broad range of suspension loads.

Auxiliary roll stiffness

The roll stiffness of most suspensions is higher than the stiffness dictated by the vertical spring rate of the suspension and the spring spacing. Some portion of the overall roll stiffness of a suspension can usually be attributed to auxiliary mechanisms, such as lateral links or stabilizer bars. Roll motion test data and vertical motion test data are applied to a simple suspension model (based on the UMTRI exponential spring model) to determine what portion of the total roll stiffness is accounted for by the vertical spring rate and what portion derives from auxiliary stiffness.

Most of the stiffness in the drive and trailer axles stems from resistance of the trailing arms to twisting. Thus, the auxiliary stiffness accounts for most of the total roll stiffness.

Roll center height

The roll center is defined as the *instant center of axle roll motion with respect to the fixed frame of the vehicle*. The roll center is assumed to be *on the centerline* of the vehicle and its height is relative to the simulated ground plane. Roll center height is determined from the slope of the Roll Center Height plot (lateral vs. roll motion of the axle). The slope

of the plot a zero roll angle is determined and used in the following formula to calculate h_{rc}, the height of the suspension roll center above the simulated ground plane.

$$h_{rc} = h_a + 57.3 \bullet \left.\frac{\partial y_a}{\partial \phi_a}\right|_{\phi_a = 0} \qquad \text{(A-1)}$$

where: ϕ_a is the roll motion of the axle, y_a is the lateral motion of the axle at an arbitrary height, h_a, above the simulated ground plane. As expected, the roll center height of the suspensions lowered with increasing load. The change is due largely to the compression of the suspension springs and tires (making the fixed frame closer to "ground").

Roll steer coefficient

The roll steer coefficient is the slope of the Roll Steer plots at zero roll angle. This coefficient indicates the steer response of the suspension that results from roll motion. For the steer axle roll steer was moderate and positive and decreased with suspension load. For the drive axle roll steer was moderate and negative and increased with suspension load. For the trailer axle roll steer was moderate and positive and increased with suspension load.

Lateral Force

Lateral force compliance coefficient

The lateral compliance coefficient given is the slope of the linear portion of the Lateral Force Compliance plot. (See tables A-5 through A-7.) That is, the coefficient indicates the lateral motion response of the axle as results from the sum of the two tire lateral forces. Note that the values reported in tables A-5 through A-7 are lateral motion of the axle per *total* lateral force applied to the suspension, not lateral force per side.

Although the lateral force compliance coefficient is given as a linear coefficient, the lateral force compliance behavior is often nonlinear. In such cases, a portion of the lateral motion of the suspension in response to lateral force is due to lash (restricted by coulomb friction). For the trailer axle, the lateral compliance characteristic showed a distict decrease in slope for lateral loads above 800 lbs per wheel. For this reason, a separate linear coefficient is given in table A-7 for lateral loads above and below 800 lbs per wheel.

Lateral force steer coefficient

The lateral force steer coefficient is the slope of the Lateral Force Compliance Steer plot at the zero lateral force condition. The coefficient indicates the steer response of the suspension that results from the from the sum of the two tire lateral forces. Note that the values reported in tables A-6 and A-7 are steer of the axle per *total* lateral force applied to the suspension, not lateral force per side. This test was not performed on the steer axle, because it was too difficult to obtain results that did not include the influence of aligning moment steer.

Aligning Moment

The aligning moment steer coefficient for the drive and trailer axles is the slope of the Aligning Moment Compliance Steer plots. (See tables A-6 and A-7.) Note that the aligning moment used is the average of that applied to the two wheel sets. The coefficient indicates the steer response of the suspension that results from the sum of tire aligning moments. Although the aligning moment compliance steer is given as a linear coefficient, the aligning moment behavior is sometimes nonlinear. In such cases, a portion of the steer of the suspension in response to aligning moment is due to lash.

The aligning moment compliance steer of the front axle was measured at a suspension load of 12000 lbs. The steering gear and tie rod stiffness values are derived from the slopes of the linear portions of the Aligning Moment Compliance Steer plots. The calculated spring values were deduced from the model shown in figure A-1 and the following:

$$K_S = 2 \bullet \left(\partial SAL / \partial MZAV\right)^{-1}$$

$$K_T = \left[\left(\partial SAR / \partial MZAV\right) - \left(\partial SAL / \partial MZAV\right)\right]^{-1} \qquad \text{(A-2)}$$

Table A-4 provides the results.

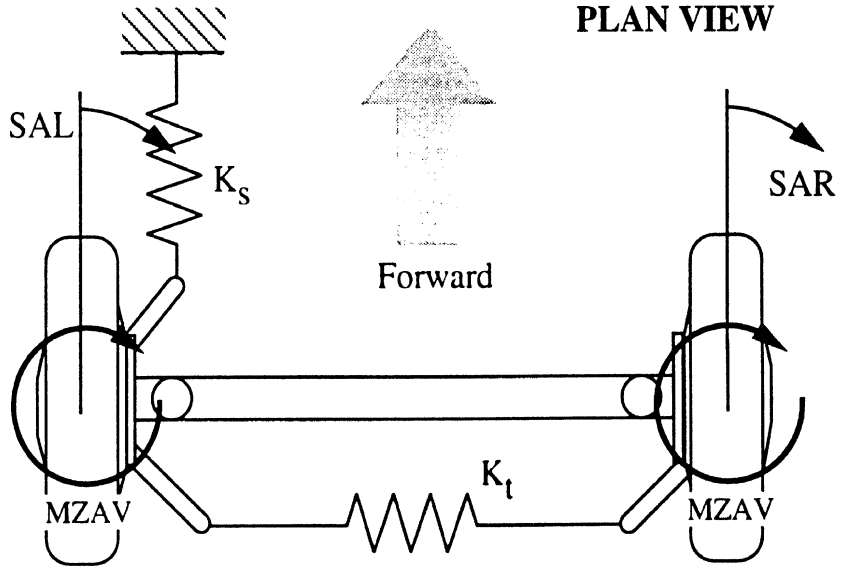

Figure A-1. Aligning moment compliance steer model.

Table A-4. Steering System Model Parameters.

Freeplay (deg)	*Measured Compliance (deg/in-lb)*		*Calculated Spring Values (in-lb/deg)*	
	$\frac{\partial SAR}{\partial MZAV}$	$\frac{\partial SAL}{\partial MZAV}$	K_S	K_T
.25	$.235 \times 10^{-3}$	$.194 \times 10^{-3}$	10,310	24,390

Table A-5. Reduced Data, Steer Axle.

At a Nominal Suspension Load of:	*5000 lbs*	*7500 lbs*	*10000 lbs*	*12000 lbs*	*14000 lbs*
Vertical Stiffness (lb/in)	1560	1510	1460	1445	1465
Coulomb Friction (lbs)	205	218	201	200	208
Total Roll Stiffness (in-lb/deg)	28,800	26,000	24,200	23,000	22,600
Auxiliary Roll Stiffness (in-lb/deg)	14,500	12,000	10,500	9,500	8,500
Roll Center Height, above ground (in)	21.2	20.0	19.2	18.5	18.0
Roll Steer Coefficient (deg/deg)	.145	.133	.104	.075	.059
Lateral Compliance Coeff (in/lb)	$.595 \times 10^{-4}$	$.600 \times 10^{-4}$	$.550 \times 10^{-4}$	$.580 \times 10^{-4}$	$.540 \times 10^{-4}$

Table A-6. Reduced Data, Trailing Drive Axle.

At a Nominal Suspension Load of:	*4000 lbs*	*8000 lbs*	*14000 lbs*
Nominal Air Bag Pressure (psi)	8	26	51
Vertical Stiffness (lb/in)	562	968	1460
Coulomb Friction (lbs)	416	560	780
Total Roll Stiffness (in-lb/deg)	110,500	109,500	106,500
Auxiliary Roll Stiffness (in-lb/deg)	107,500	105,000	100,000
Roll Center Height, above ground (in)	31.3	31.0	30.7
Roll Steer Coefficient (deg/deg)	-.125	-.125	-.108
Lateral Compliance Coeff (in/lb)	$.156 \times 10^{-4}$	$.163 \times 10^{-4}$	$.143 \times 10^{-4}$
Lateral Compliance Steer (deg/lb)	$.680 \times 10^{-5}$	$.106 \times 10^{-4}$	$.655 \times 10^{-5}$
Aligning Moment Steer Coeff (deg/in-lb)	$.485 \times 10^{-5}$	$.411 \times 10^{-4}$	$.494 \times 10^{-5}$

Table 6. (cont) Reduced Data, Trailing Drive Axle.

At a Nominal Suspension Load of:	*16000 lbs*	*18000 lbs*	*20000 lbs*
Nominal Air Bag Pressure (psi)	58	65	70.5
Vertical Stiffness (lb/in)	1605	1785	1980
Coulomb Friction (lbs)	735	640	755
Total Roll Stiffness (in-lb/deg)	105,000	106,000	107,000
Auxiliary Roll Stiffness (in-lb/deg)	95,000	95,000	95,000
Roll Center Height, above ground (in)	31.3	30.4	30.3
Roll Steer Coefficient (deg/deg)	-1.06	-.104	-.098
Lateral Compliance Coeff (in/lb)	$.139 \times 10^{-4}$	$.142 \times 10^{-4}$	$.143 \times 10^{-4}$
Lateral Compliance Steer (deg/lb)	$.710 \times 10^{-5}$	$.580 \times 10^{-5}$	$.616 \times 10^{-5}$
Aligning Moment Steer Coeff (deg/in-lb)	$.458 \times 10^{-5}$	$.434 \times 10^{-4}$	$.455 \times 10^{-5}$

Table A-7. Reduced Data, Trailer Axle.

At a Nominal Suspension Load of:	*5900 lbs*	*10400 lbs*	*15300 lbs*	*20800 lbs*	*25800 lbs*
Nominal Bag Pressure (psi)	20	40	60	80	100
Vertical Stiffness (lb/in)	760	1110	1540	1950	2580
Coulomb Friction (lbs)	345	535	780	610	560
Total Roll Stiffness (in-lb/deg)	124,000	119,000	119,500	124,000	125,000
Auxiliary Roll Stiffness (in-lb/deg)	117,000	111,000	106,000	104,000	105,000
Roll Center Height, above ground (in)	25.9	25.2	25.1	24.5	24.4
Roll Steer Coefficient (deg/deg)	.104	.125	.133	.143	.162
Lateral Compliance Coeff (in/lb)	$.735 \times 10^{-4}$	$.770 \times 10^{-4}$	$.850 \times 10^{-4}$	$.830 \times 10^{-4}$	$.790 \times 10^{-4}$
Lateral Compliance Steer (deg/lb)	$-.372 \times 10^{-4}$	$-.346 \times 10^{-4}$	$-.377 \times 10^{-4}$	$-.375 \times 10^{-4}$	$-.389 \times 10^{-4}$
Aligning Moment Steer Coeff (deg/in-lb)	–	–	–	$.656 \times 10^{-5}$	–

Table A-8. Steer Axle Spring Boundary Tables.

Compression Envelope		*Extension Envelope*	
Deflection (in)	Force (lbs)	Deflection (in)	Force (lbs)
.77	441	.84	441
1.23	1492	1.56	1695
1.88	2610	2.56	3220
3.28	4712	4.12	5492
4.65	6678	5.33	7288
5.54	8000	5.71	7966
5.74	8576	5.93	9085
5.90	9424		

Table A-9. Drive Axle Spring Boundary Tables, Nominal Load of 4000 lbs, Air Bags at 8 PSI.

Compression Envelope		*Extension Envelope*	
Deflection (in)	Force (lbs)	Deflection (in)	Force (lbs)
1.24	1180	1.37	712
2.82	1770	2.73	1058
3.96	2339	4.03	1525
4.98	2990	5.13	2237
5.85	3824	5.94	2929
6.74	4759	6.55	3783
6.95	5186	6.95	4658
6.99	6183	7.02	4983
		7.04	5898

Table A-10. Drive Axle Spring Boundary Tables, Nominal Load of 8000 lbs, Air Bags at 26 PSI.

Compression Envelope		*Extension Envelope*	
Deflection (in)	Force (lbs)	Deflection (in)	Force (lbs)
.82	1915	.96	1407
2.06	2932	2.06	2119
3.48	3847	3.48	2831
4.61	4932	4.36	3542
5.69	6424	5.29	4525
6.46	7746	6.01	5678
7.02	8932	6.69	7136
7.08	10458	7.08	8390
		7.15	10390

Table A-11. Drive Axle Spring Boundary Tables, Nominal Load of 14000 lbs, Air Bags at 50.5 PSI.

Compression Envelope		*Extension Envelope*	
Deflection (in)	Force (lbs)	Deflection (in)	Force (lbs)
.67	3420	.78	2946
1.93	4939	2.84	4892
3.74	7122	3.80	5793
4.72	8688	4.84	7217
5.75	10776	5.78	9115
6.71	13339	6.55	11251
7.20	15237	7.11	13434
		7.20	14573

Table A-12. Drive Axle Spring Boundary Tables, Nominal Load of 16000 lbs, Air Bags at 58 PSI.

Compression Envelope		*Extension Envelope*	
Deflection (in)	Force (lbs)	Deflection (in)	Force (lbs)
.92	3851	.85	3234
1.38	4610	2.43	5085
2.78	6556	3.67	6414
3.65	7742	4.61	7932
4.45	8976	5.25	9166
5.32	10780	6.12	11444
6.21	13105	6.63	13200
7.02	15668	7.02	15003

Table A-13. Drive Axle Spring Boundary Tables, Nominal Load of 18000 lbs, Air Bags at 65 PSI.

Compression Envelope		*Extension Envelope*	
Deflection (in)	Force (lbs)	Deflection (in)	Force (lbs)
.89	4224	.80	3573
1.79	5742	2.15	5308
4.04	9159	3.87	7532
5.07	11329	5.09	9810
6.03	13715	5.85	11871
6.88	16644	6.51	13986
		6.99	15885

Table A-14. Drive Axle Spring Boundary Tables, Nominal Load of 20000 lbs, Air Bags at 71.5 PSI.

Compression Envelope		*Extension Envelope*	
Deflection (in)	Force (lbs)	Deflection (in)	Force (lbs)
.83	4790	.89	4302
1.92	6634	2.71	6905
3.62	9400	4.12	8858
4.90	11949	5.09	10864
5.87	14444	5.76	12654
6.40	16125	6.53	15312
6.88	17807	6.92	17102

Table A-15. Trailer Axle Spring Boundary Tables, Nominal Load of 5900 lbs, Air Bags at 20 PSI.

Compression Envelope		*Extension Envelope*	
Deflection (in)	Force (lbs)	Deflection (in)	Force (lbs)
1.55	1232	1.71	1178
2.51	1720	3.47	1856
3.71	2398	4.69	2453
4.74	3076	5.75	3212
5.70	3917	6.48	3944
6.57	4893	7.30	5110
7.47	6276	7.83	6303
8.36	8093	8.36	7849

Table A-16. Trailer Axle Spring Boundary Tables, Nominal Load of 10400 lbs, Air Bags at 40 PSI.

Compression Envelope		*Extension Envelope*	
Deflection (in)	Force (lbs)	Deflection (in)	Force (lbs)
1.72	2386	1.70	2169
4.07	4664	3.53	3525
5.69	6617	4.73	4393
6.73	8461	6.05	5749
7.86	11281	6.91	7214
8.64	13776	7.47	8461
8.82	16434	8.28	11064
		8.76	13505
		8.84	16163

Table A-17. Trailer Axle Spring Boundary Tables, Nominal Load of 15300 lbs, Air Bags at 60 PSI.

Compression Envelope		*Extension Envelope*	
Deflection (in)	Force (lbs)	Deflection (in)	Force (lbs)
1.74	3464	1.86	3281
3.65	6088	3.41	4929
5.23	8529	4.91	6576
6.35	10786	5.95	8041
6.99	12434	6.79	9627
7.86	15180	7.63	11885
8.74	18658	8.16	13898
8.96	20000	8.94	17986
		9.12	20000

Table A-18. Trailer Axle Spring Boundary Tables, Nominal Load of 20800 lbs, Air Bags at 80 PSI.

Compression Envelope		*Extension Envelope*	
Deflection (in)	Force (lbs)	Deflection (in)	Force (lbs)
1.68	4441	1.78	4383
3.39	7495	3.28	6573
4.87	10549	4.94	9512
5.82	12739	5.86	11356
6.85	15966	6.64	13431
7.98	20173	7.19	15505
		8.23	20231

Table A-19. Trailer Axle Spring Boundary Tables, Nominal Load of 25800 lbs, Air Bags at 100 PSI.

Compression Envelope		*Extension Envelope*	
Deflection (in)	Force (lbs)	Deflection (in)	Force (lbs)
1.44	4671	1.48	4305
1.72	6014	1.74	5708
2.80	8332	2.62	7234
4.01	11444	3.79	9736
5.67	15837	5.01	12786
6.39	17973	5.91	15105
7.13	20597	6.61	17729
		7.21	20414

Measured by UMTRI for Smart Truck
Freightliner Tractor

Data file: FRTLNS00.ERD

Single Steer Axle Suspension

Aligning Moment Compliance Steer

6 April 96
Suspension: Taper-Leaf (2)

Suspension Load: 12000 lb.

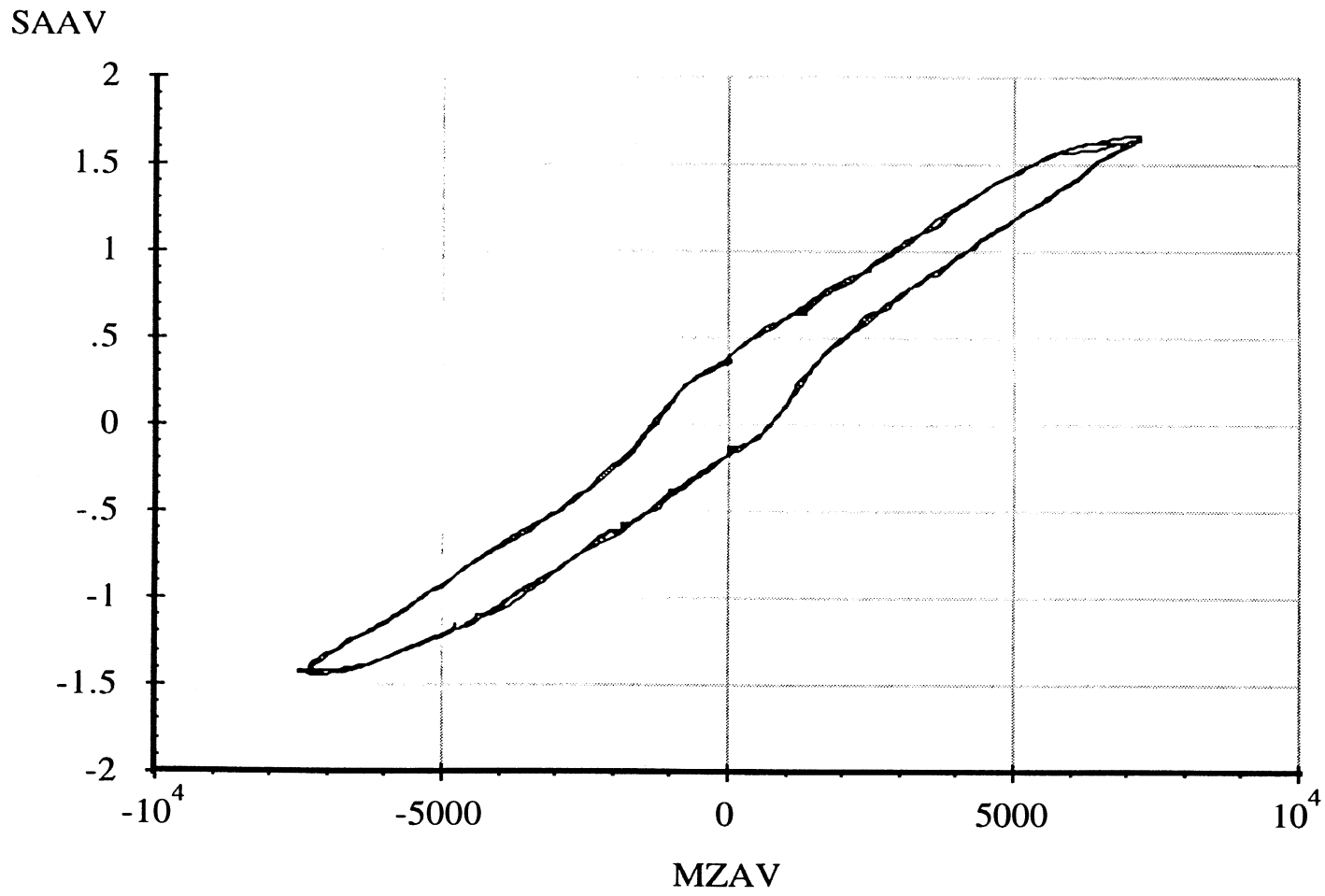

Abscissa (X): Average axle aligning moment (MZAV); in-lb per wheel; applied to both wheels simultaneously; downward (right hand rule) moment vector, positive.

Ordinate (Y): Average steer angle (SAAV); degrees; steer toward right, positive.

*Note: Brakes on. Engine on. Position Control. Steering Wheel Locked.

Measured by UMTRI for Smart Truck
Freightliner Tractor

Single Steer Axle Suspension

6 April 96
Suspension: Taper-Leaf (2)

Data file: FRTLNS00.ERD

Left Wheel Aligning Moment Compliance Steer

Suspension Load: 12000 lb.

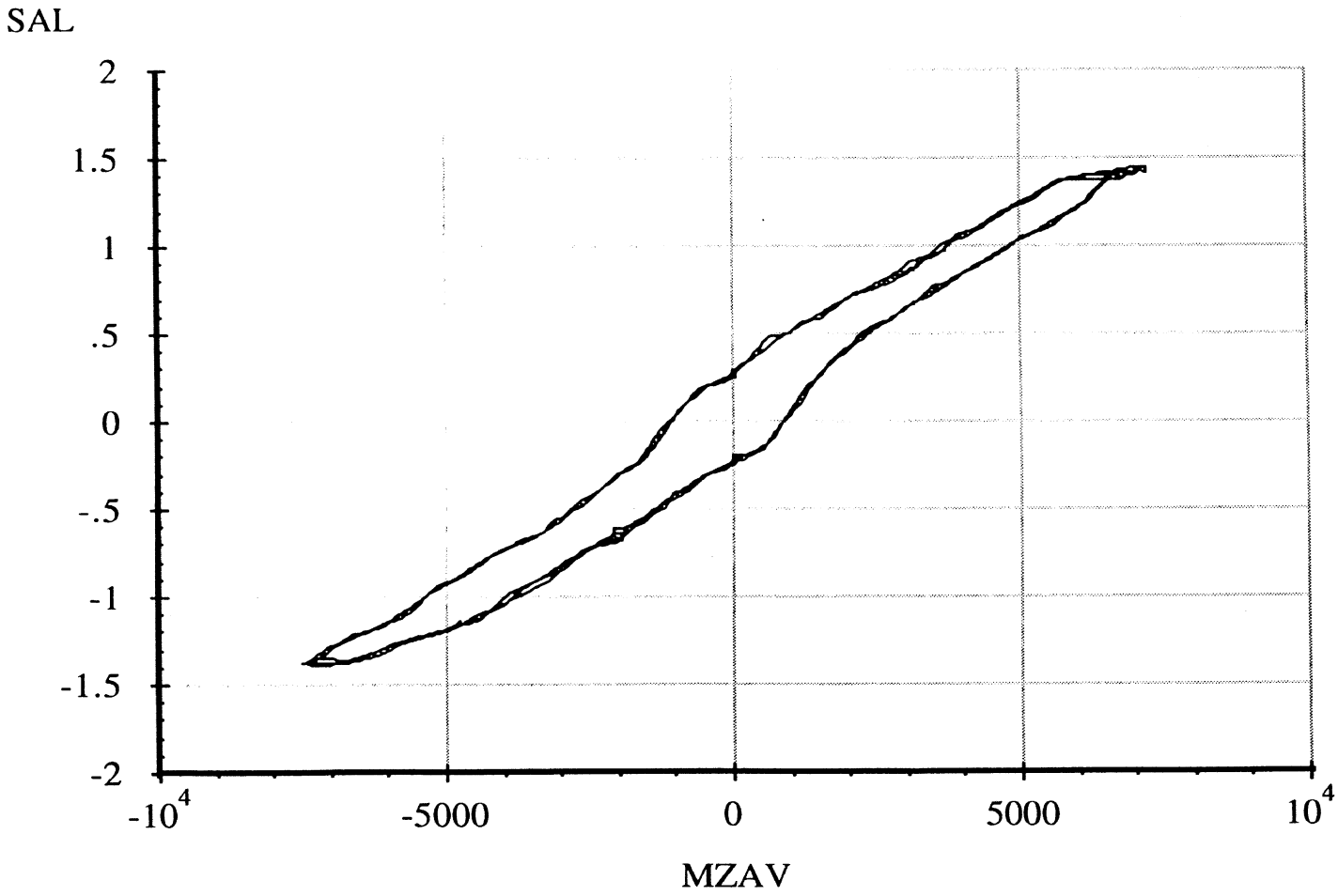

Abscissa (X): Average axle aligning moment (MZAV); in-lb per wheel; applied to both wheels simultaneously; downward (right hand rule) moment vector, positive.

Ordinate (Y): Left wheel steer angle (SAL); degrees; steer toward right, positive.

*Note: Brakes on. Engine on. Position Control. Steering Wheel Locked.

Measured by UMTRI for Smart Truck
Freightliner Tractor

Single Steer Axle Suspension

6 April 96
Suspension: Taper-Leaf (2)

Data file: FRTLNS00.ERD

Right Wheel Aligning Moment Compliance Steer

Suspension Load: 12000 lb.

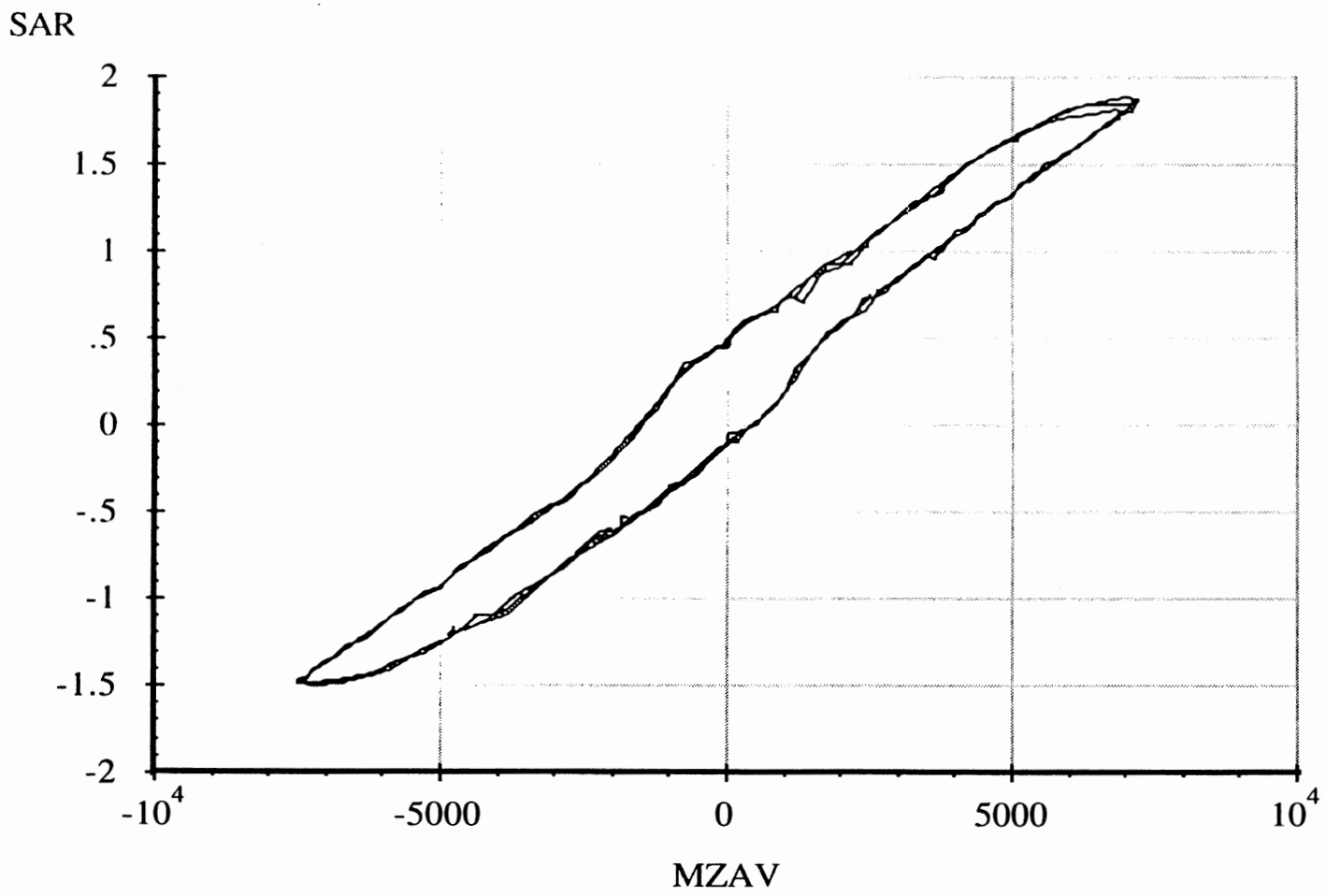

Abscissa (X): Average axle aligning moment (MZAV); in-lb per wheel; applied to both wheels simultaneously; downward (right hand rule) moment vector, positive.

Ordinate (Y): Right wheel steer angle (SAR); degrees; steer toward right, positive.

*Note: Brakes on. Engine on. Position Control. Steering Wheel Locked.

Measured by UMTRI for Smart Truck
Freightliner Tractor

Data file: FRTLNS01.ERD

Single Steer Axle Suspension

Average Vertical Spring Rate

6 April 96
Suspension: Taper-Leaf (2)

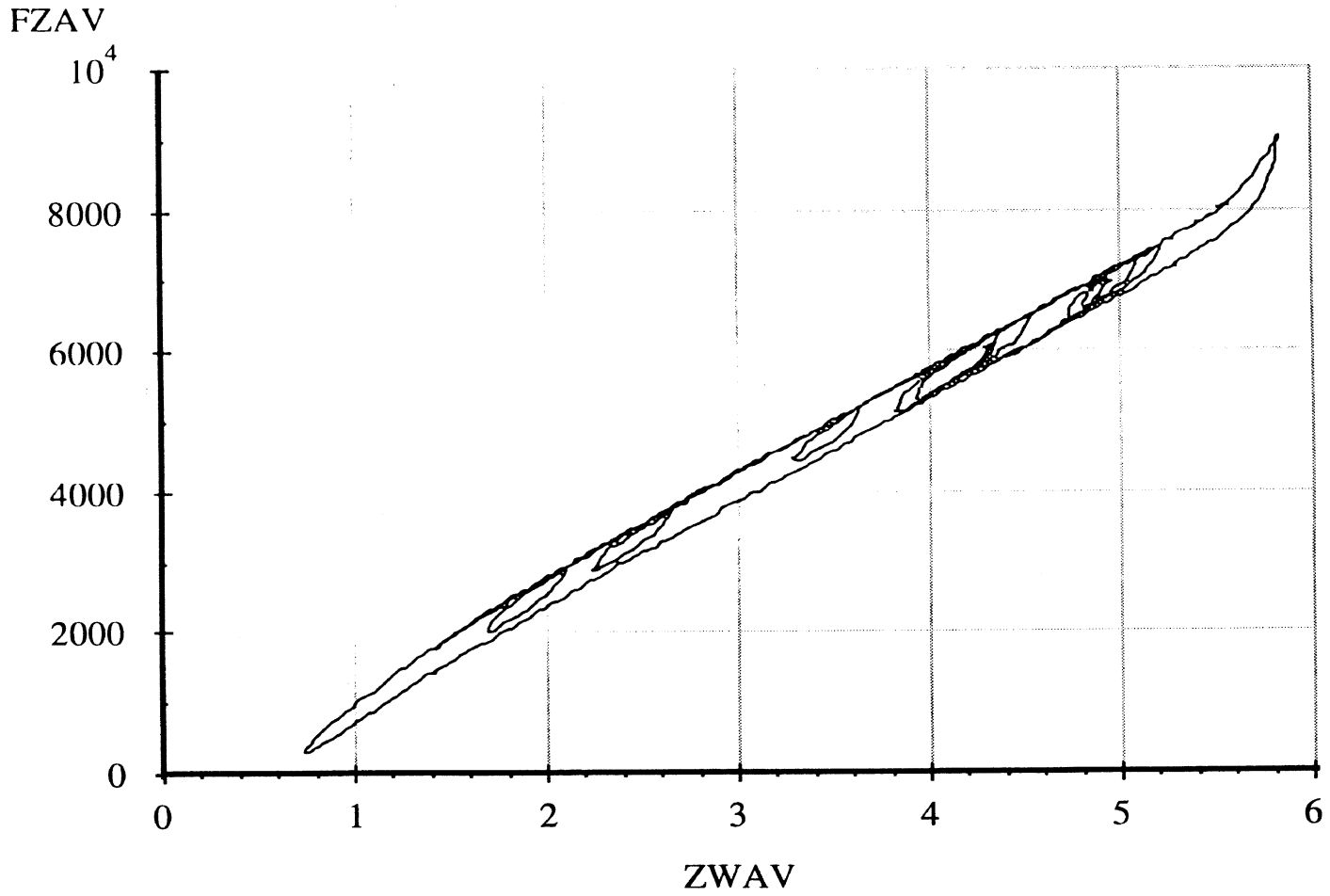

Abscissa (X): Average vertical wheel displacement (ZWAV); inches; spring compression, positive.

Ordinate (Y): Average vertical wheel load (FZAV); pounds; spring compression, positive.

*Note: Brakes on. Position control. Pitman arm blocked.

Measured by UMTRI for Smart Truck
Freightliner Tractor

Data file: FRTLNS06.ERD

Single Steer Axle Suspension

Axle Roll Rate

6 April 96
Suspension: Taper-Leaf (2)

Suspension Load: 14000 lb.

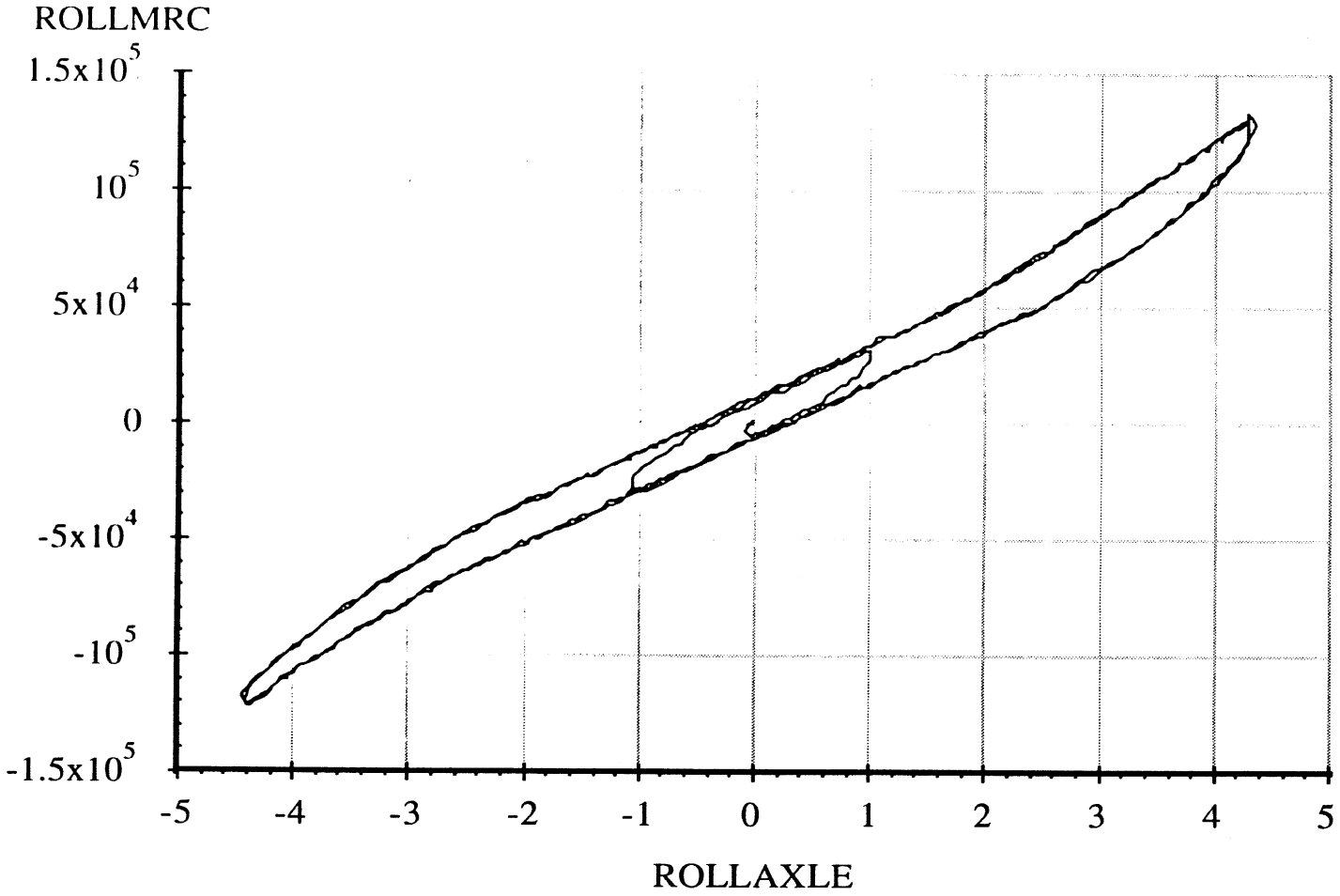

Abscissa (X): Axle roll angle (ROLLAXLE); degrees; right side compressed, positive.

Ordinate (Y): Axle roll moment about the roll center (ROLLMRC); in-lb; right side compressed, positive.

*Note: Brakes on. Force control. Pitman arm blocked.

Measured by UMTRI for Smart Truck
Freightliner Tractor

Data file: FRTLNS06.ERD

Single Steer Axle Suspension

Roll Center Height

6 April 96
Suspension: Taper-Leaf (2)

Suspension Load: 14000 lb.

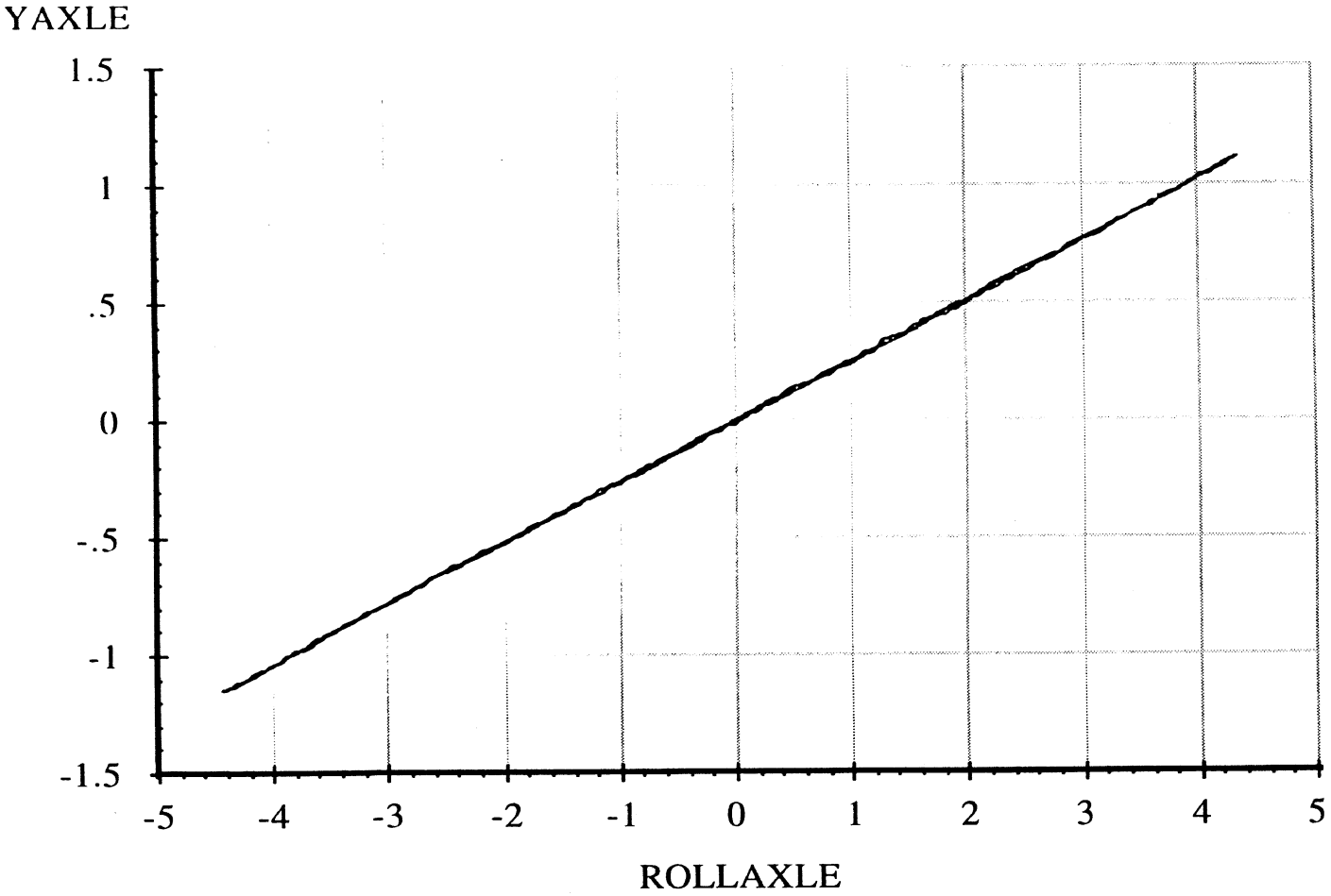

Abscissa (X): Axle roll angle (ROLLAXLE); degrees; right side compressed, positive.

Ordinate (Y): Axle reference point lateral translation (YAXLE); inches; motion toward right, positive.

*Note: Brakes on. Force control. Pitman arm blocked. Reference height of 3.25 inches.

Measured by UMTRI for Smart Truck
Freightliner Tractor

Data file: FRTLNS06.ERD

Single Steer Axle Suspension

Roll Steer

6 April 96
Suspension: Taper-Leaf (2)

Suspension Load: 14000 lb.

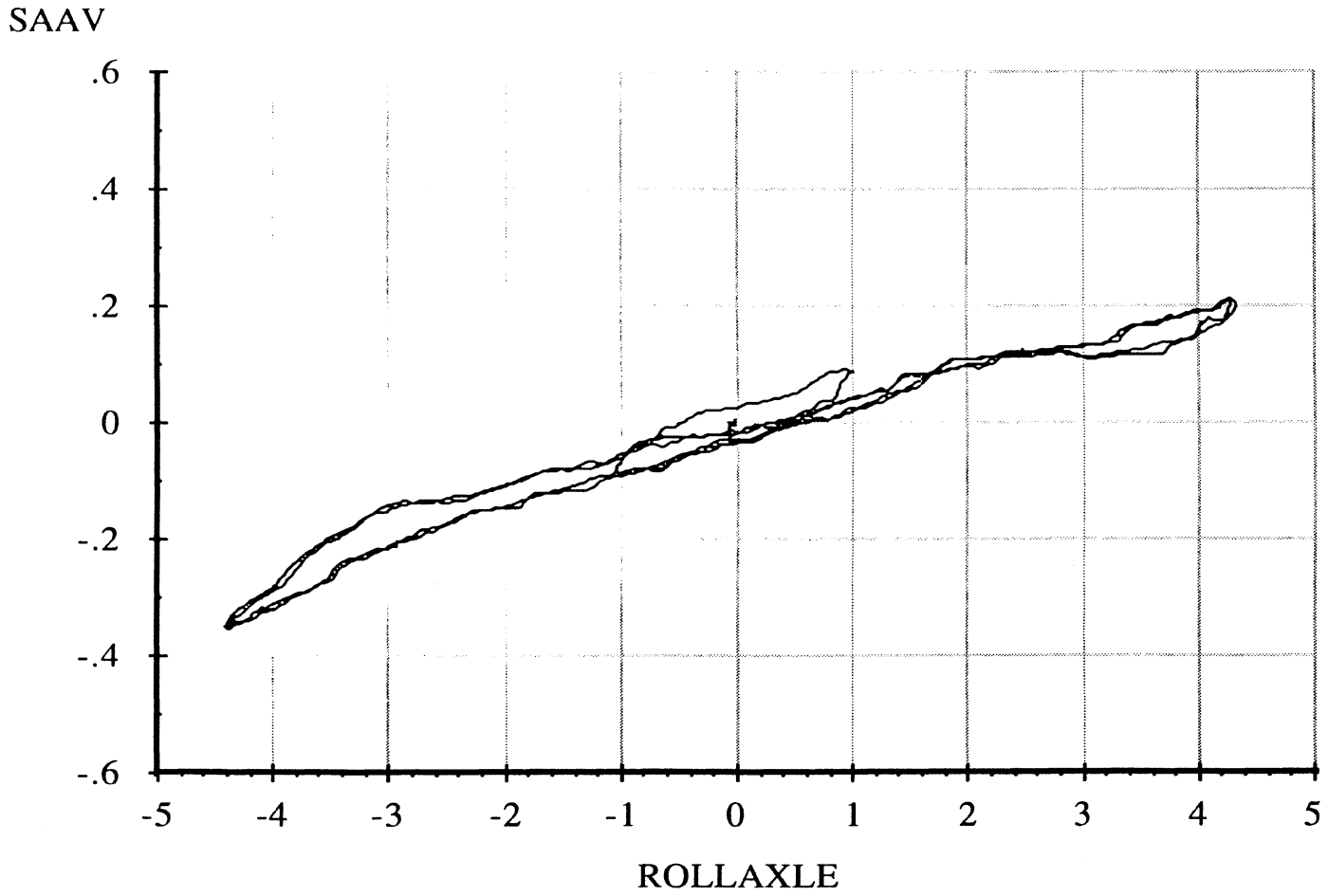

Abscissa (X): Axle roll angle (ROLLAXLE); degrees; right side compressed, positive.

Ordinate (Y): Average steer angle (SAAV); degrees; steer toward right, positive.

*Note: Brakes on. Force control. Pitman arm blocked.

Measured by UMTRI for Smart Truck
Freightliner Tractor

Data file: FRTLNS05.ERD

Single Steer Axle Suspension

Axle Roll Rate

6 April 96
Suspension: Taper-Leaf (2)

Suspension Load: 12000 lb.

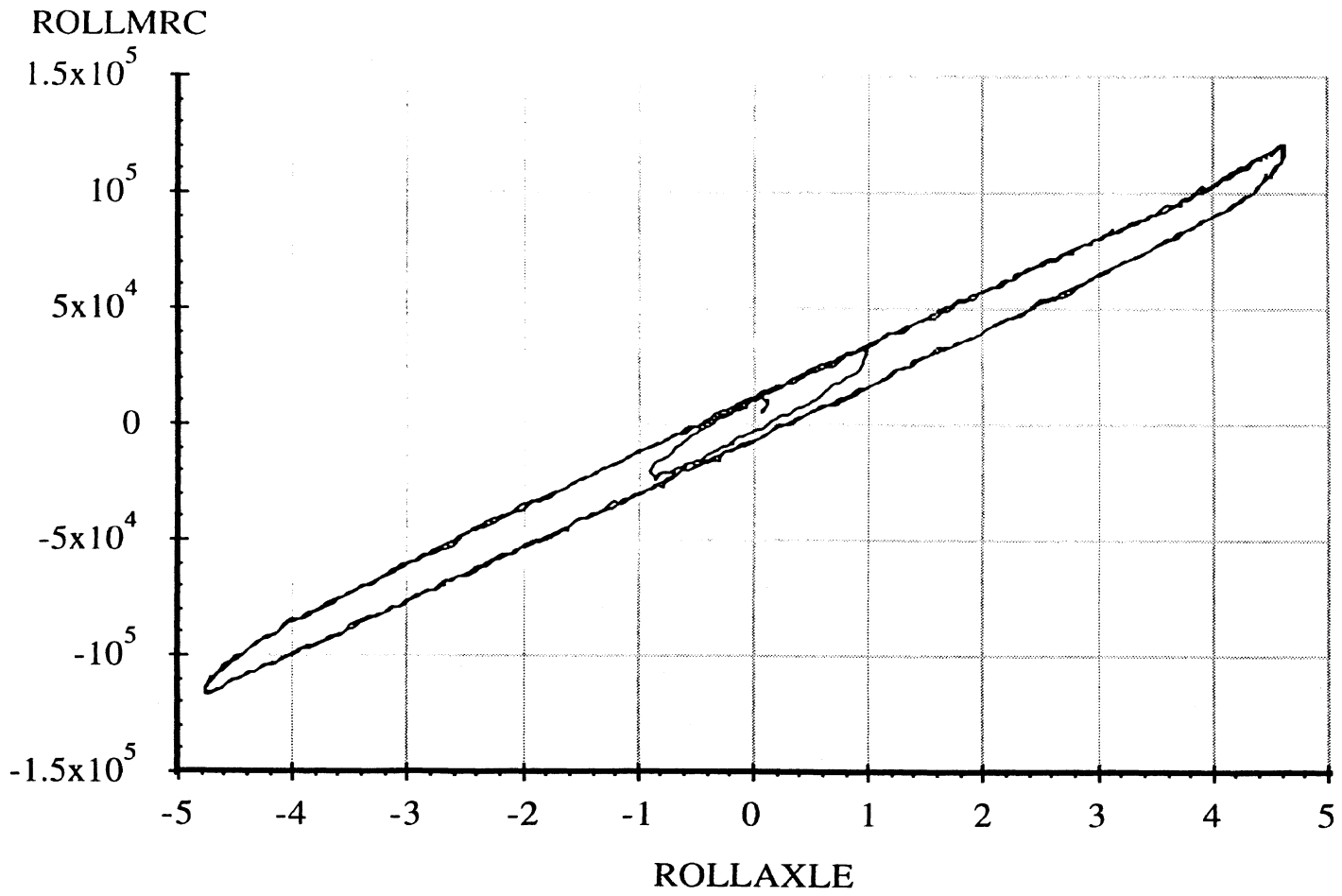

Abscissa (X): Axle roll angle (ROLLAXLE); degrees; right side compressed, positive.

Ordinate (Y): Axle roll moment about the roll center (ROLLMRC); in-lb; right side compressed, positive.

*Note: Brakes on. Force control. Pitman arm blocked.

Measured by UMTRI for Smart Truck
Freightliner Tractor

Data file: FRTLNS05.ERD

Single Steer Axle Suspension

Roll Center Height

6 April 96
Suspension: Taper-Leaf (2)

Suspension Load: 12000 lb.

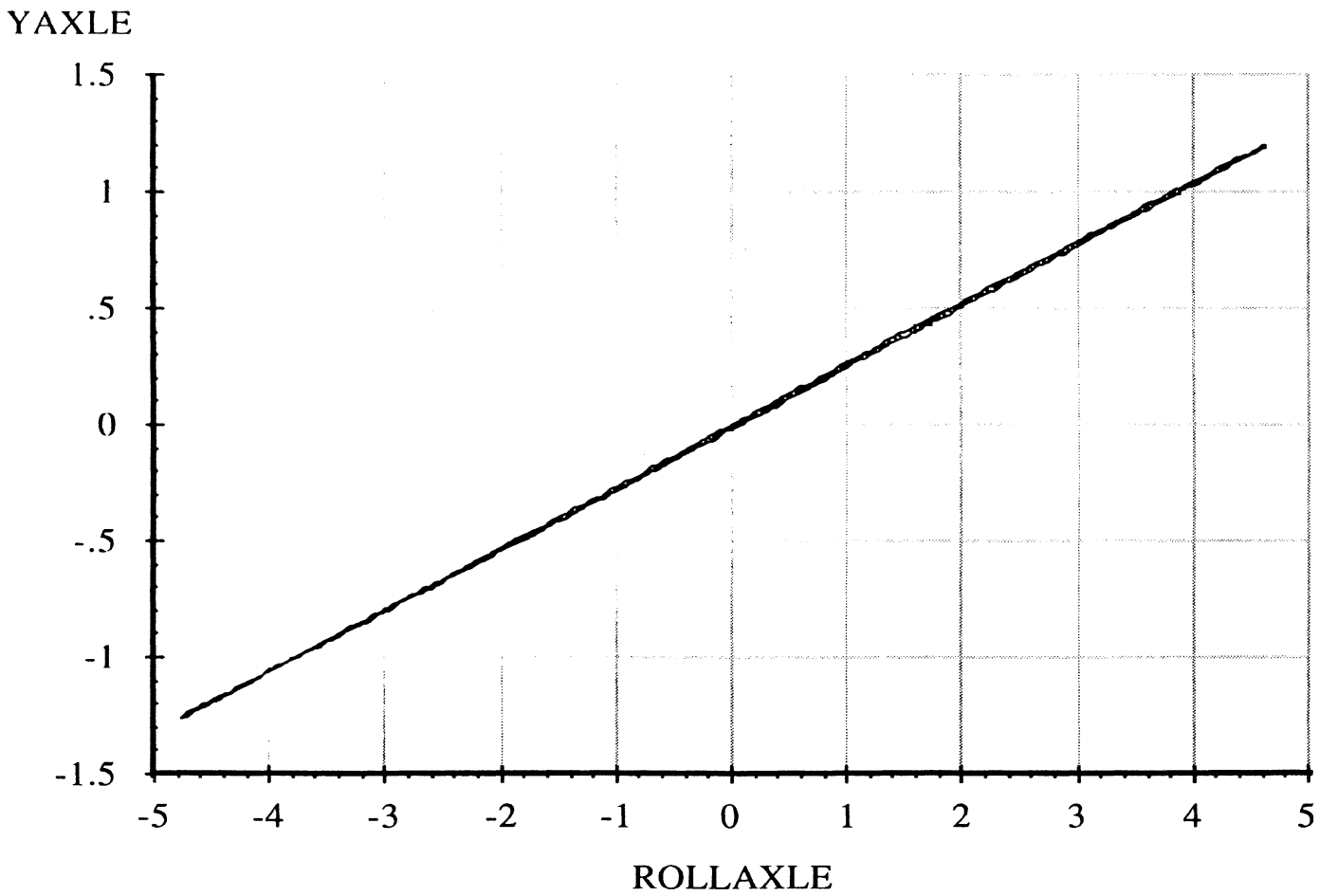

Abscissa (X): Axle roll angle (ROLLAXLE); degrees; right side compressed, positive.

Ordinate (Y): Axle reference point lateral translation (YAXLE); inches; motion toward right, positive.

*Note: Brakes on. Force control. Pitman arm blocked. Reference height of 3.44 inches.

Measured by UMTRI for Smart Truck
Freightliner Tractor

Data file: FRTLNS05.ERD

Single Steer Axle Suspension

Roll Steer

6 April 96
Suspension: Taper-Leaf (2)

Suspension Load: 12000 lb.

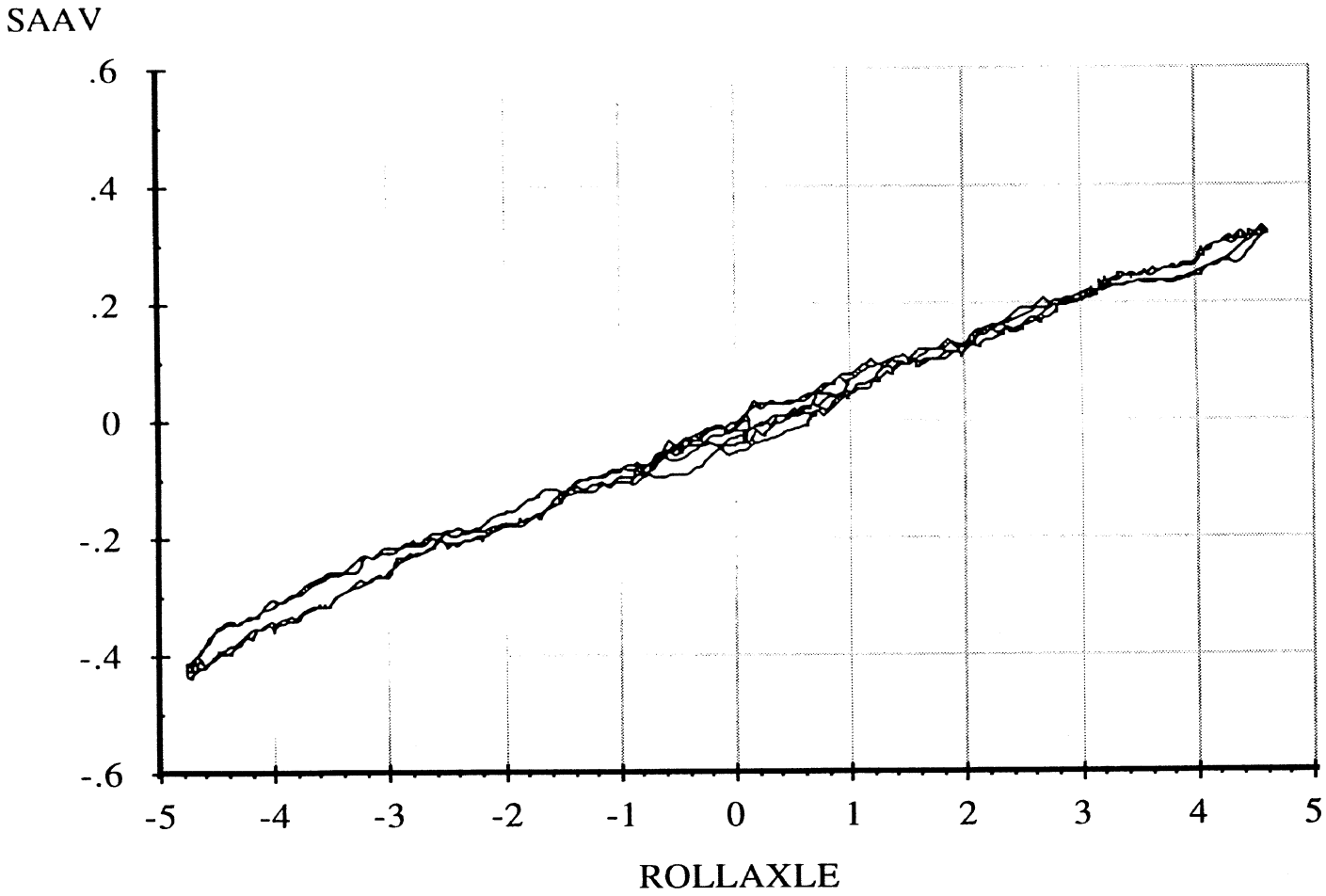

Abscissa (X): Axle roll angle (ROLLAXLE); degrees; right side compressed, positive.

Ordinate (Y): Average steer angle (SAAV); degrees; steer toward right, positive.

*Note: Brakes on. Force control. Pitman arm blocked.

Measured by UMTRI for Smart Truck
Freightliner Tractor

Data file: FRTLNS04.ERD

Single Steer Axle Suspension

Axle Roll Rate

6 April 96
Suspension: Taper-Leaf (2)

Suspension Load: 10000 lb.

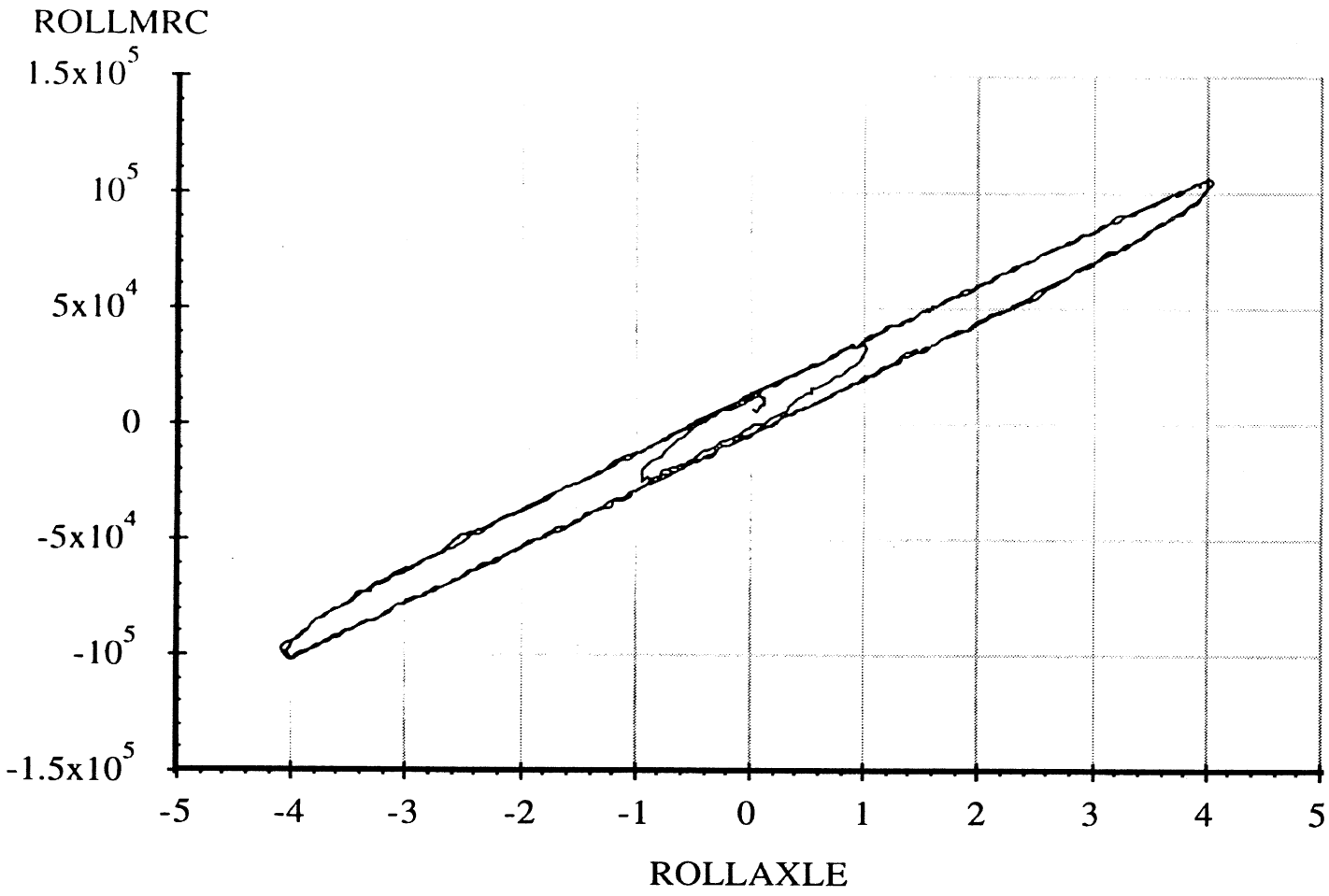

Abscissa (X): Axle roll angle (ROLLAXLE); degrees; right side compressed, positive.

Ordinate (Y): Axle roll moment about the roll center (ROLLMRC); in-lb; right side compressed, positive.

*Note: Brakes on. Force control. Pitman arm blocked.

Measured by UMTRI for Smart Truck
Freightliner Tractor

Data file: FRTLNS04.ERD

Single Steer Axle Suspension

Roll Center Height

6 April 96
Suspension: Taper-Leaf (2)

Suspension Load: 10000 lb.

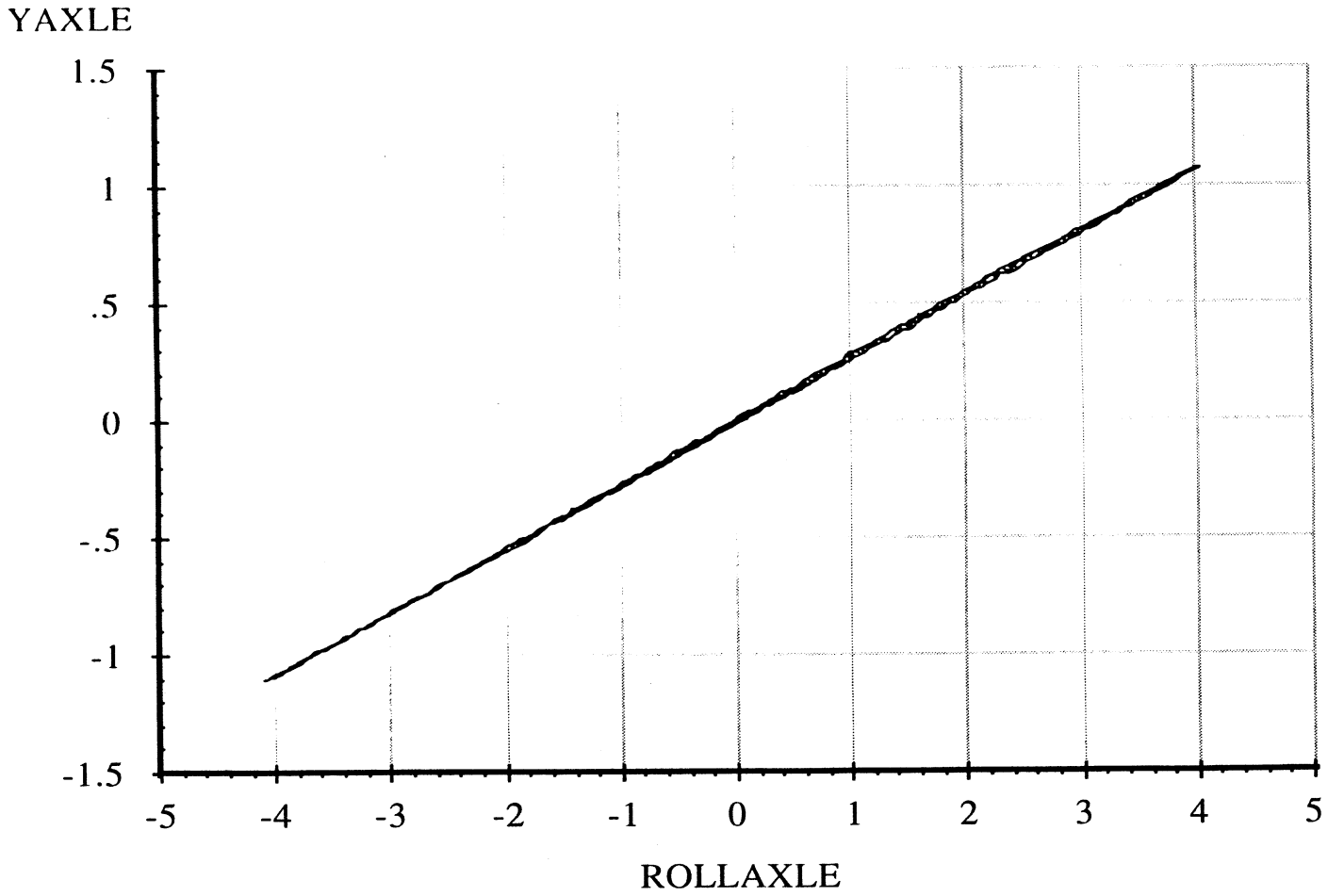

Abscissa (X): Axle roll angle (ROLLAXLE); degrees; right side compressed, positive.

Ordinate (Y): Axle reference point lateral translation (YAXLE); inches; motion toward right, positive.

*Note: Brakes on. Force control. Pitman arm blocked. Reference height of 3.75 inches.

Measured by UMTRI for Smart Truck
Freightliner Tractor

Data file: FRTLNS04.ERD

Single Steer Axle Suspension

Roll Steer

6 April 96
Suspension: Taper-Leaf (2)

Suspension Load: 10000 lb.

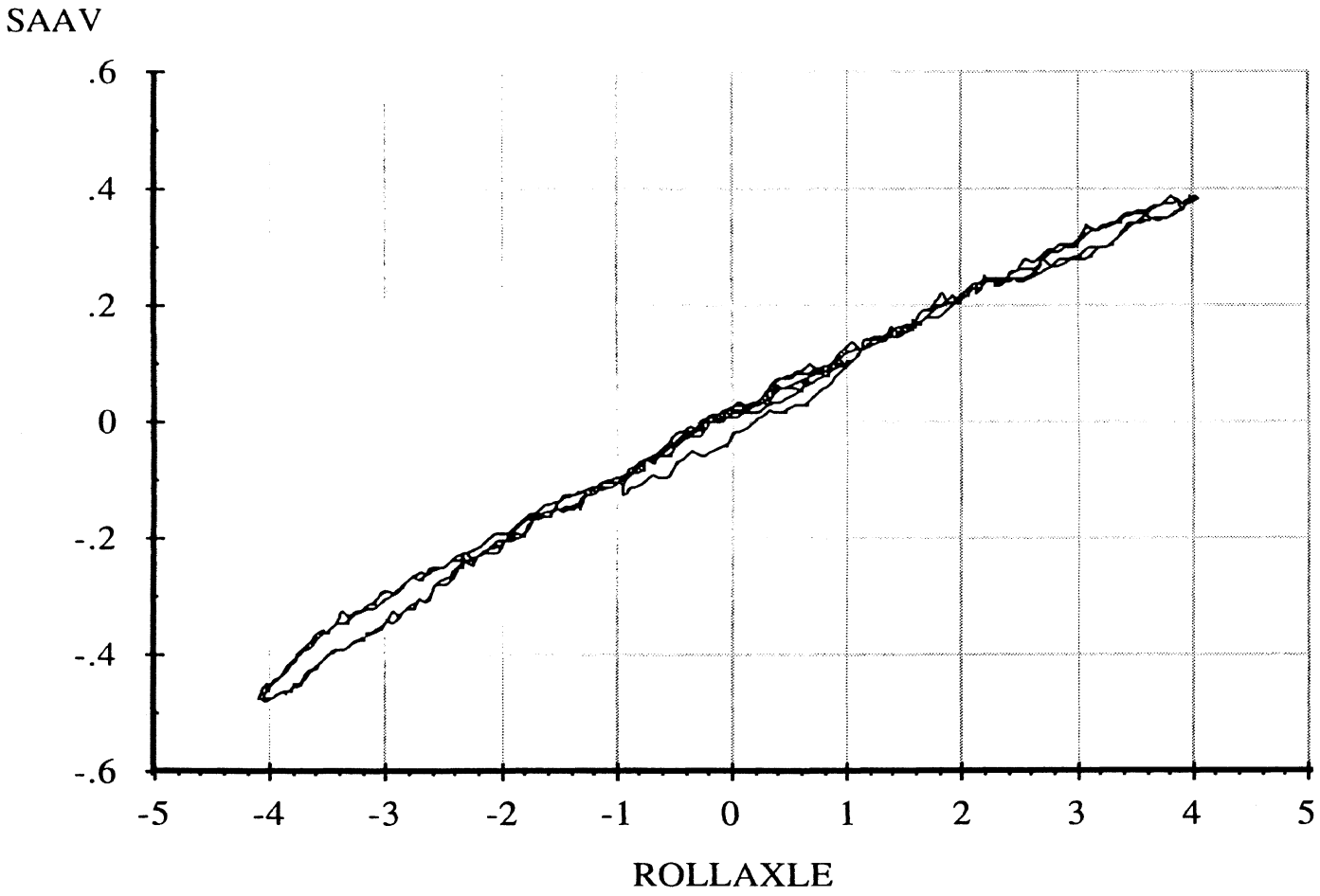

Abscissa (X): Axle roll angle (ROLLAXLE); degrees; right side compressed, positive.

Ordinate (Y): Average steer angle (SAAV); degrees; steer toward right, positive.

*Note: Brakes on. Force control. Pitman arm blocked.

Measured by UMTRI for Smart Truck
Freightliner Tractor

Data file: FRTLNS03.ERD

Single Steer Axle Suspension

Axle Roll Rate

6 April 96
Suspension: Taper-Leaf (2)

Suspension Load: 7500 lb.

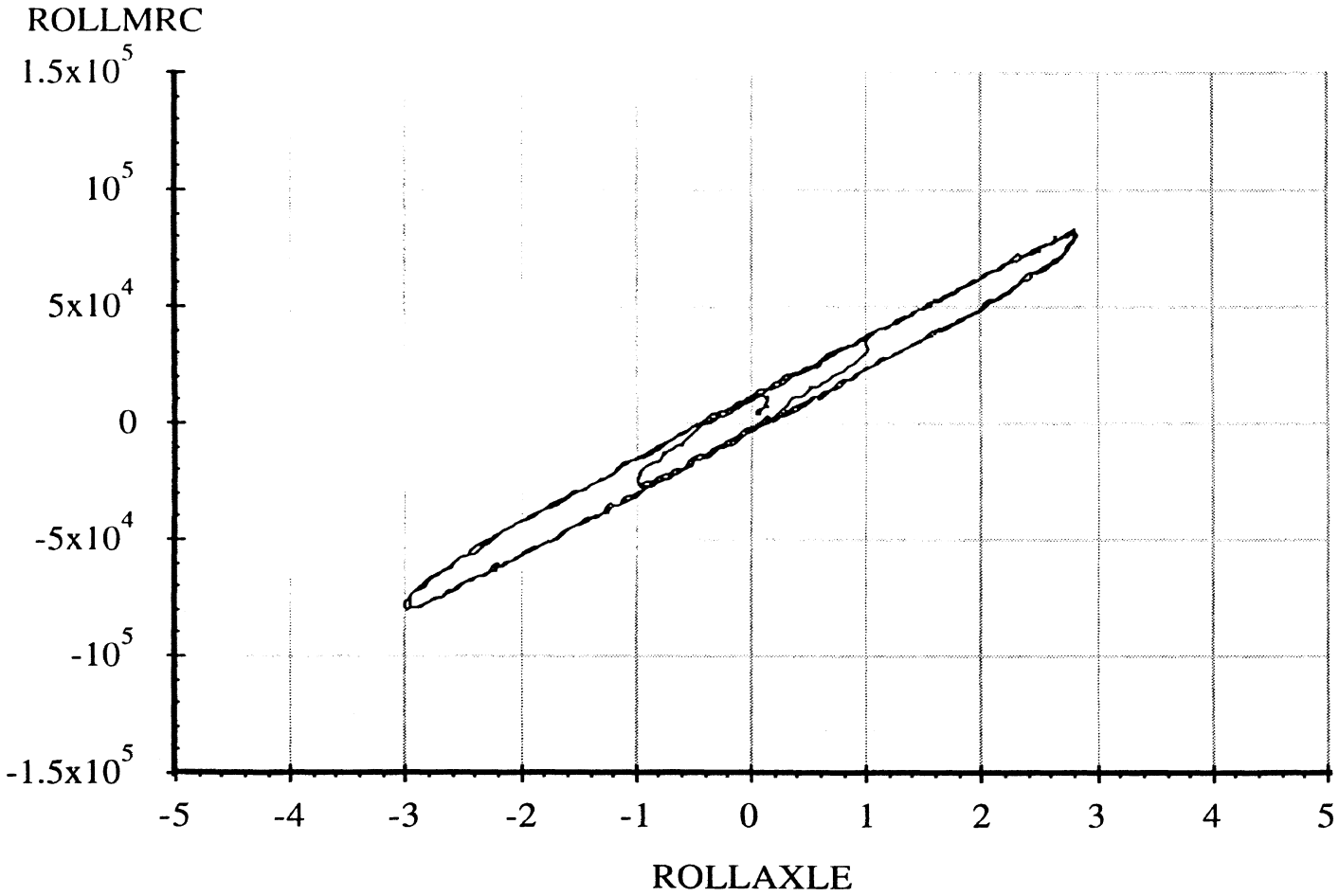

Abscissa (X): Axle roll angle (ROLLAXLE); degrees; right side compressed, positive.

Ordinate (Y): Axle roll moment about the roll center (ROLLMRC); in-lb; right side compressed, positive.

*Note: Brakes on. Force control. Pitman arm blocked.

Measured by UMTRI for Smart Truck
Freightliner Tractor

Data file: FRTLNS03.ERD

Single Steer Axle Suspension

Roll Center Height

6 April 96
Suspension: Taper-Leaf (2)

Suspension Load: 7500 lb.

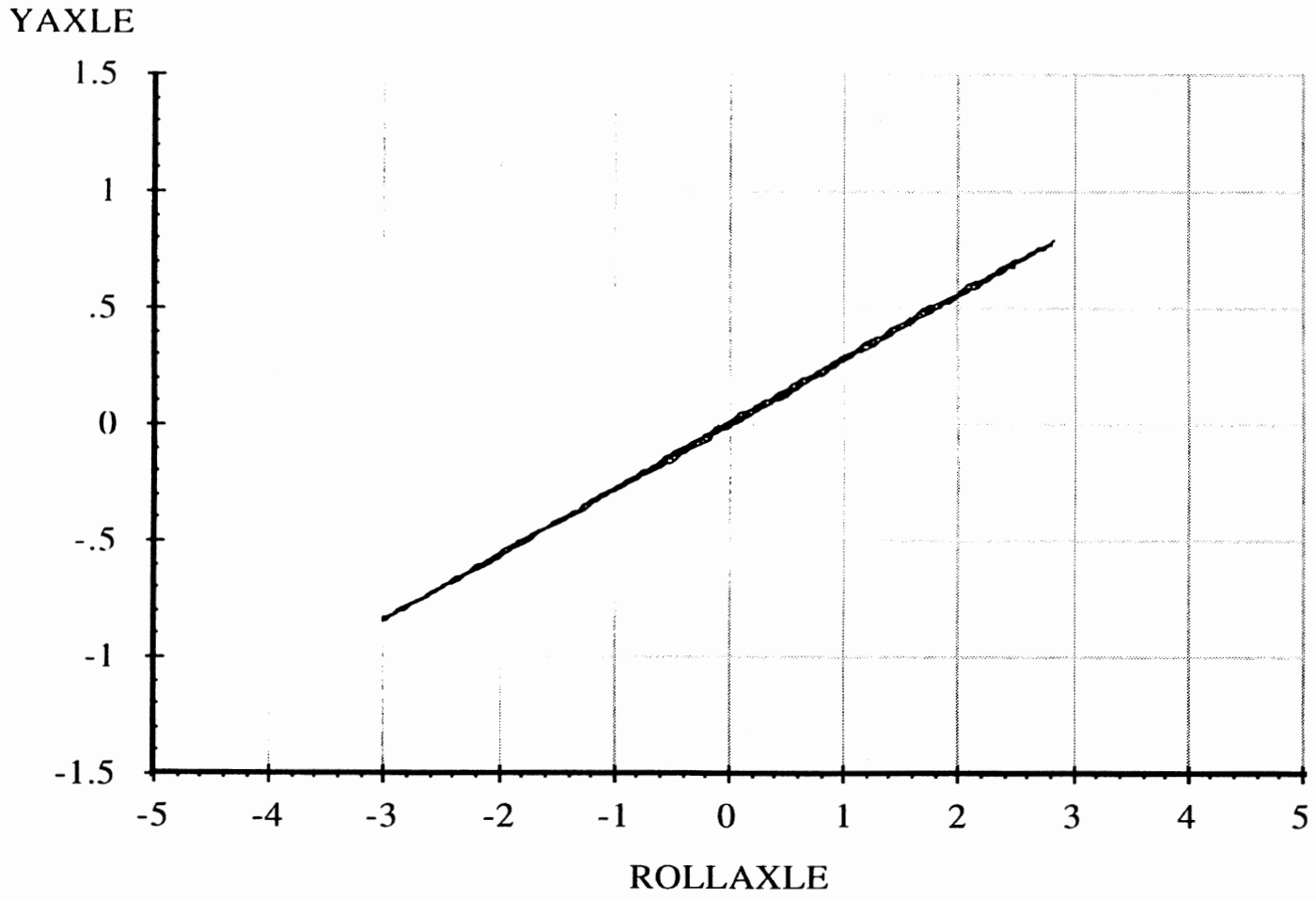

Abscissa (X): Axle roll angle (ROLLAXLE); degrees; right side compressed, positive.

Ordinate (Y): Axle reference point lateral translation (YAXLE); inches; motion toward right, positive.

*Note: Brakes on. Force control. Pitman arm blocked. Reference height of 4.00 inches.

Measured by UMTRI for Smart Truck
Freightliner Tractor

Data file: FRTLNS03.ERD

Single Steer Axle Suspension

Roll Steer

6 April 96
Suspension: Taper-Leaf (2)

Suspension Load: 7500 lb.

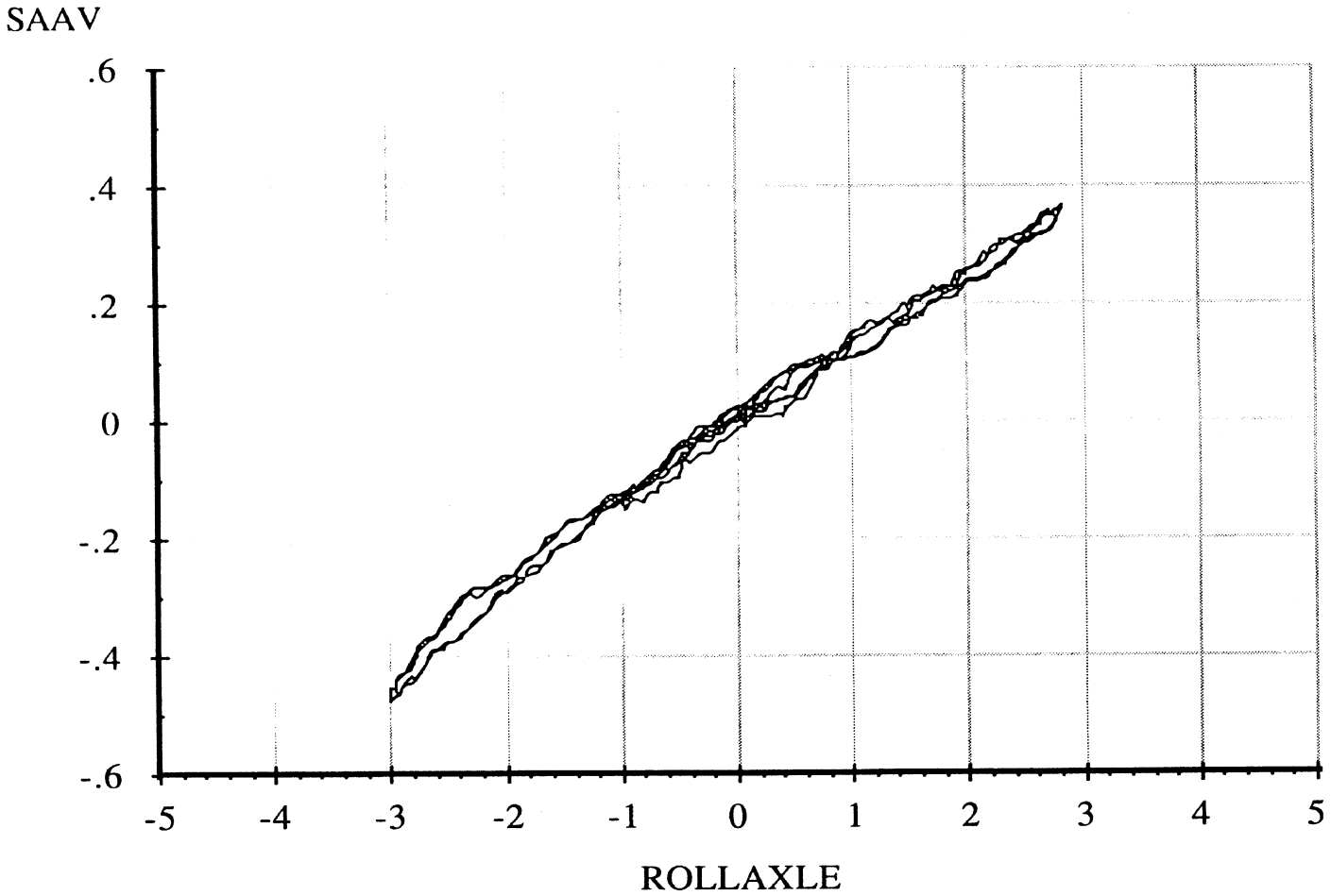

Abscissa (X): Axle roll angle (ROLLAXLE); degrees; right side compressed, positive.

Ordinate (Y): Average steer angle (SAAV); degrees; steer toward right, positive.

*Note: Brakes on. Force control. Pitman arm blocked.

Measured by UMTRI for Smart Truck
Freightliner Tractor

Data file: FRTLNS02.ERD

Single Steer Axle Suspension

Axle Roll Rate

6 April 96
Suspension: Taper-Leaf (2)

Suspension Load: 5000 lb.

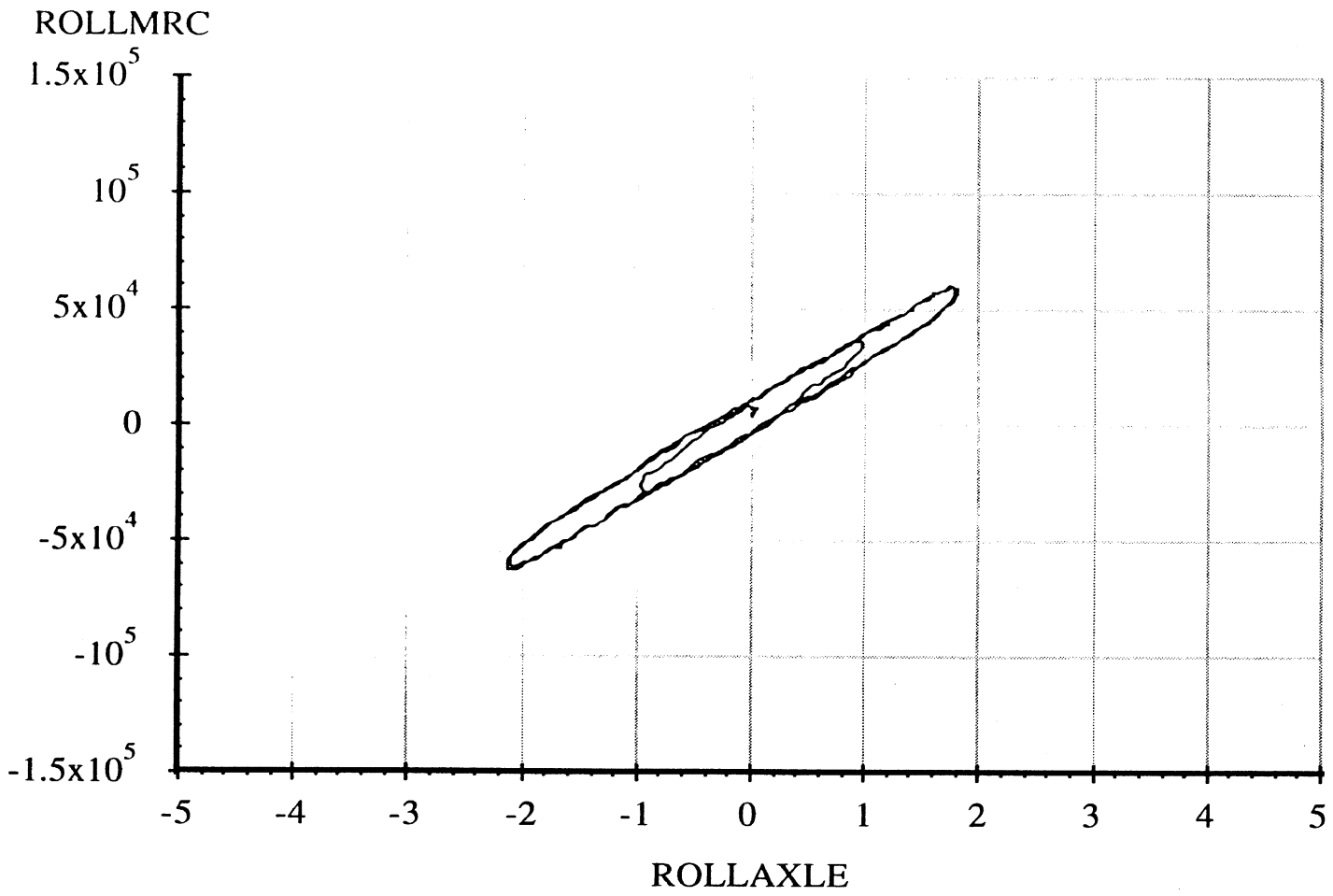

Abscissa (X): Axle roll angle (ROLLAXLE); degrees; right side compressed, positive.

Ordinate (Y): Axle roll moment about the roll center (ROLLMRC); in-lb; right side compressed, positive.

*Note: Brakes on. Force control. Pitman arm blocked.

Measured by UMTRI for Smart Truck
Freightliner Tractor

Data file: FRTLNS02.ERD

Single Steer Axle Suspension

Roll Center Height

6 April 96
Suspension: Taper-Leaf (2)

Suspension Load: 5000 lb.

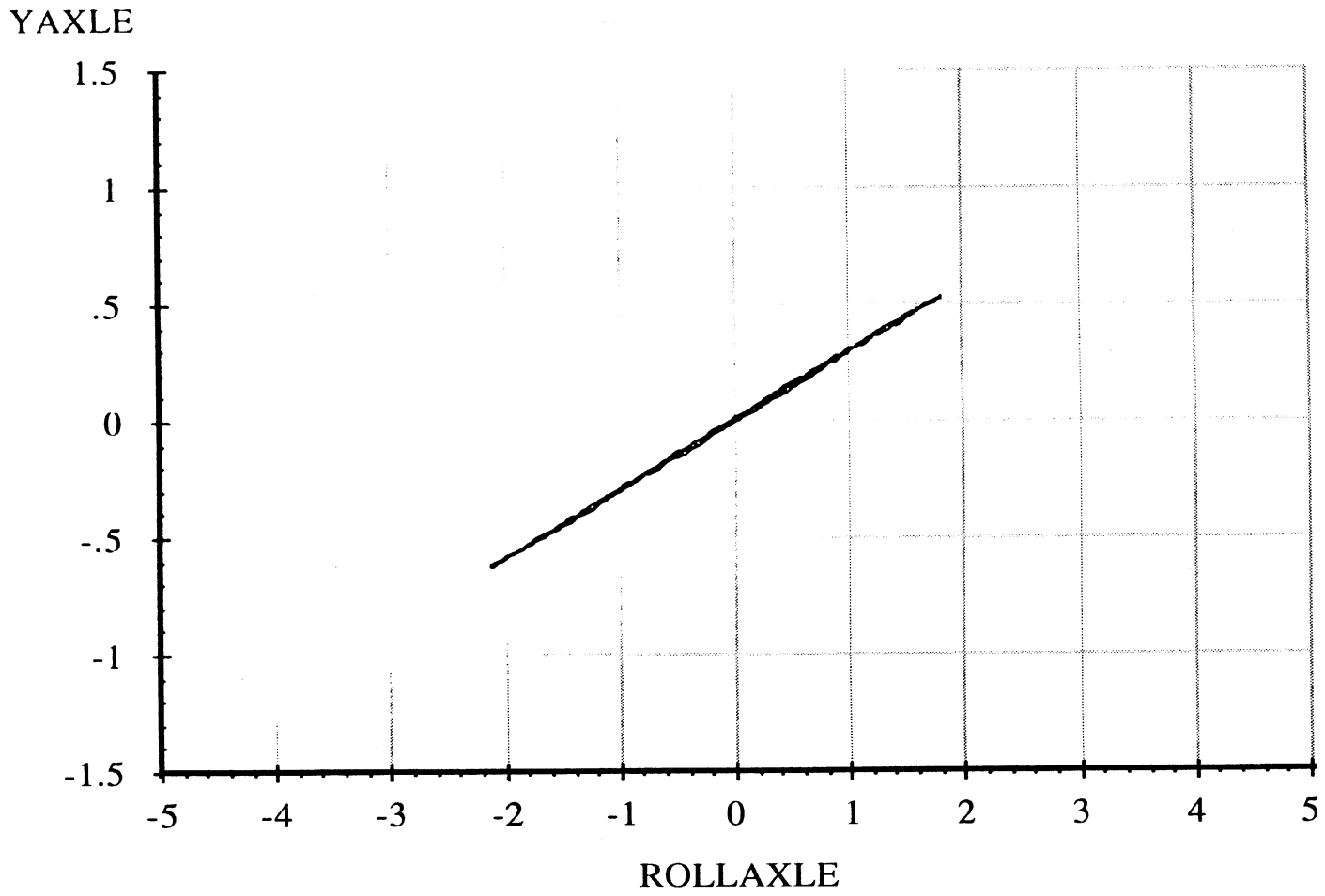

Abscissa (X): Axle roll angle (ROLLAXLE); degrees; right side compressed, positive.

Ordinate (Y): Axle reference point lateral translation (YAXLE); inches; motion toward right, positive.

*Note: Brakes on. Force control. Pitman arm blocked. Reference height of 4.25inches.

Measured by UMTRI for Smart Truck
Freightliner Tractor

Data file: FRTLNS02.ERD

Single Steer Axle Suspension

Roll Steer

6 April 96
Suspension: Taper-Leaf (2)

Suspension Load: 5000 lb.

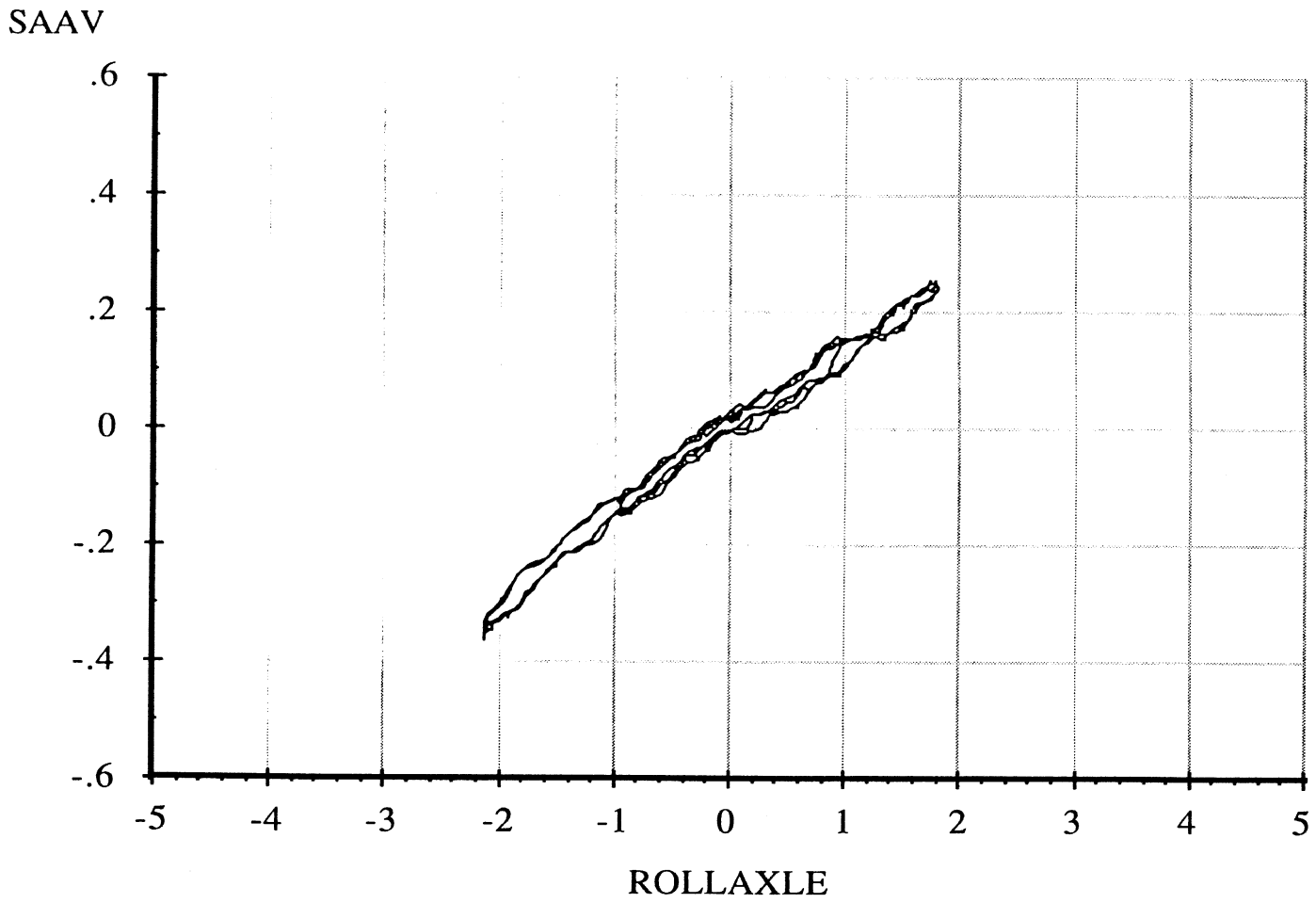

Abscissa (X): Axle roll angle (ROLLAXLE); degrees; right side compressed, positive.

Ordinate (Y): Average steer angle (SAAV); degrees; steer toward right, positive.

*Note: Brakes on. Force control. Pitman arm blocked.

Measured by UMTRI for Smart Truck
Freightliner Tractor

Data file: FRTLNS16.ERD

Single Steer Axle Suspension

Lateral Force Compliance

6 April 96
Suspension: Taper-Leaf (2)

Suspension Load: 14000 lb.

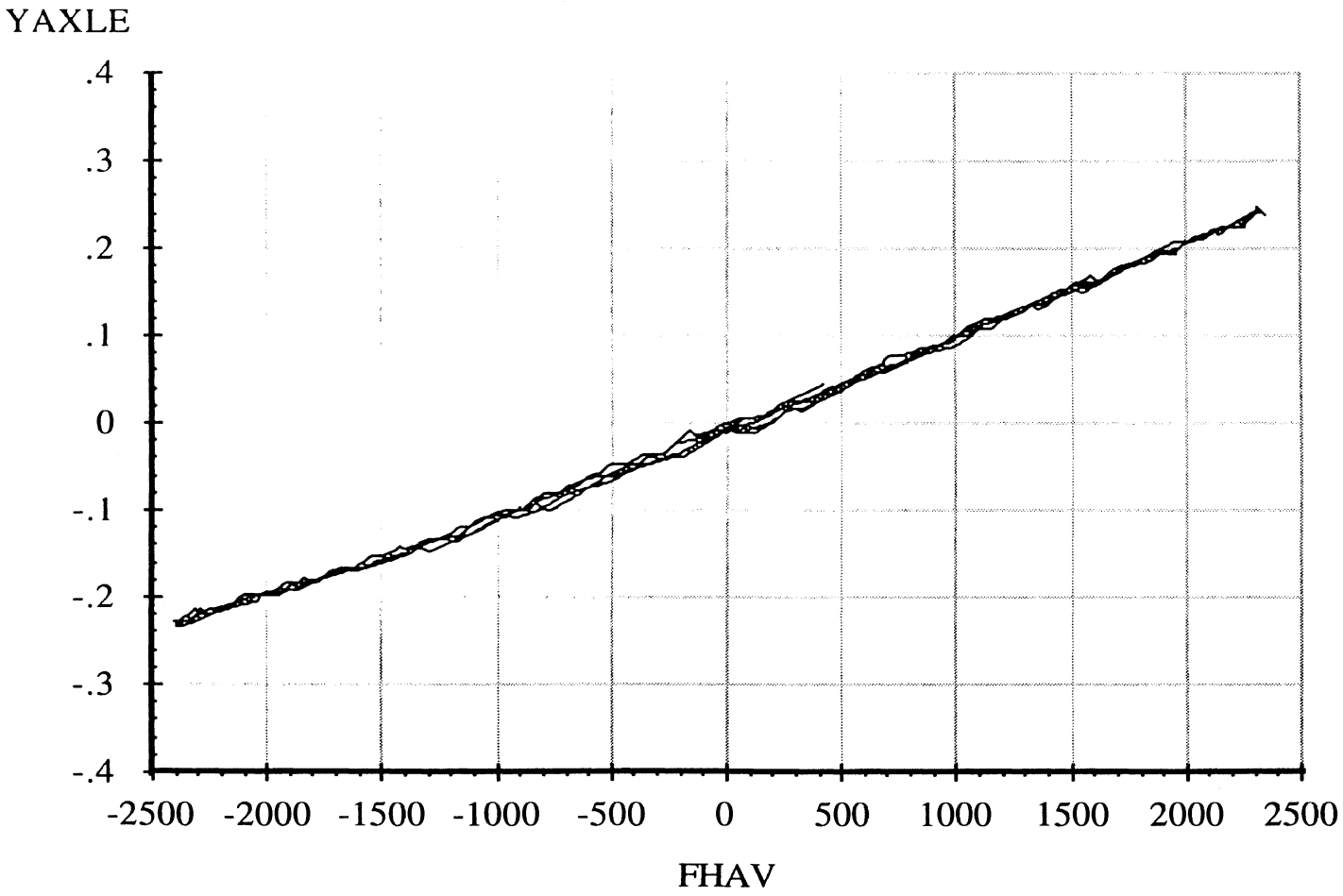

Abscissa (X): Average axle lateral force (FHAV); pounds; applied to both wheels simultaneously; force applied toward right, positive.

Ordinate (Y): Axle lateral translation (YAXLE); inches; motion toward right, positive.

*Note: Brakes on. Position control. Pitman arm blocked.

Measured by UMTRI for Smart Truck
Freightliner Tractor

Data file: FRTLNS15.ERD

Single Steer Axle Suspension

Lateral Force Compliance

6 April 96
Suspension: Taper-Leaf (2)

Suspension Load: 12000 lb.

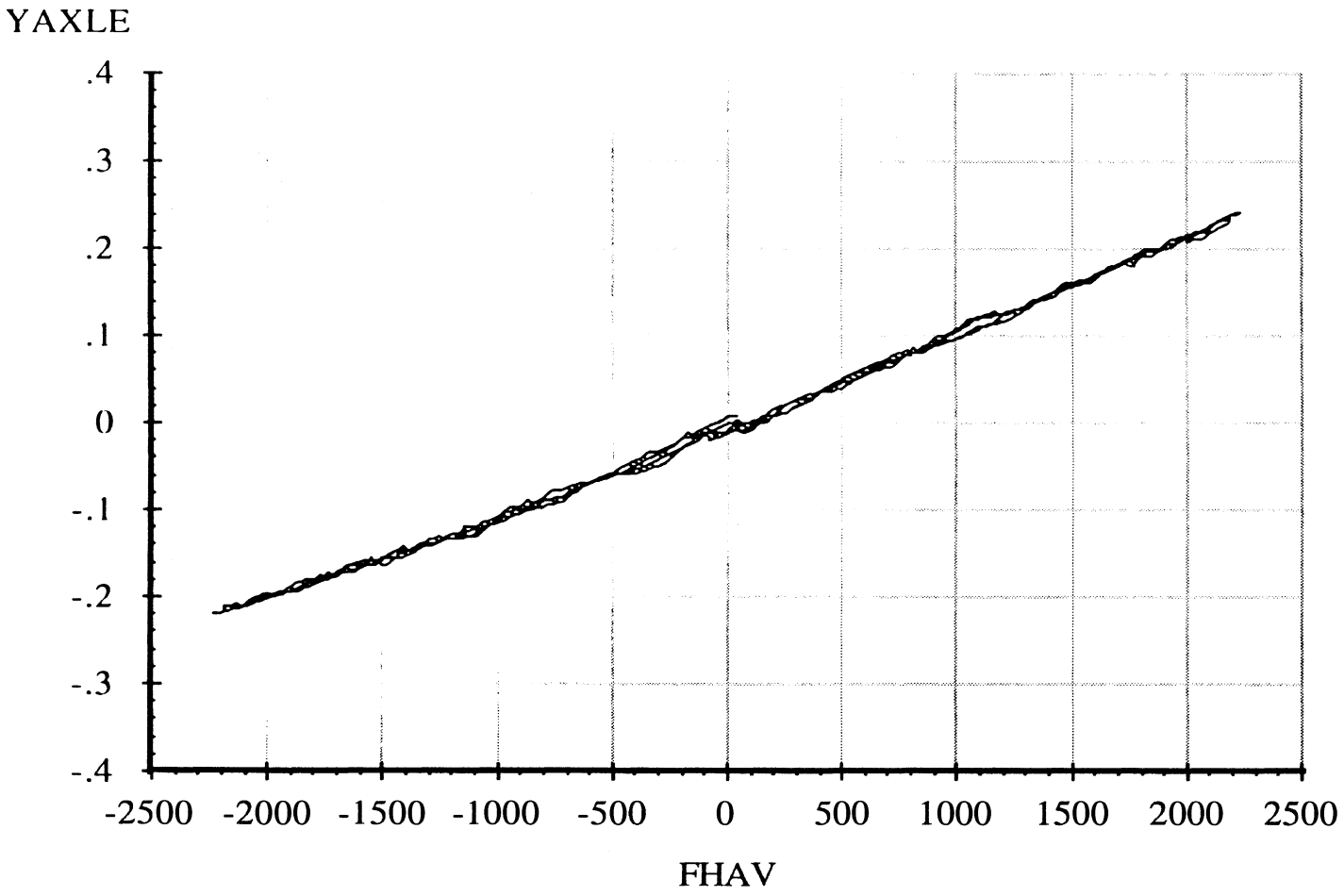

Abscissa (X): Average axle lateral force (FHAV); pounds; applied to both wheels simultaneously; force applied toward right, positive.

Ordinate (Y): Axle lateral translation (YAXLE); inches; motion toward right, positive.

*Note: Brakes on. Position control. Pitman arm blocked.

Measured by UMTRI for Smart Truck
Freightliner Tractor

Data file: FRTLNS14.ERD

Single Steer Axle Suspension

Lateral Force Compliance

6 April 96
Suspension: Taper-Leaf (2)

Suspension Load: 10000 lb.

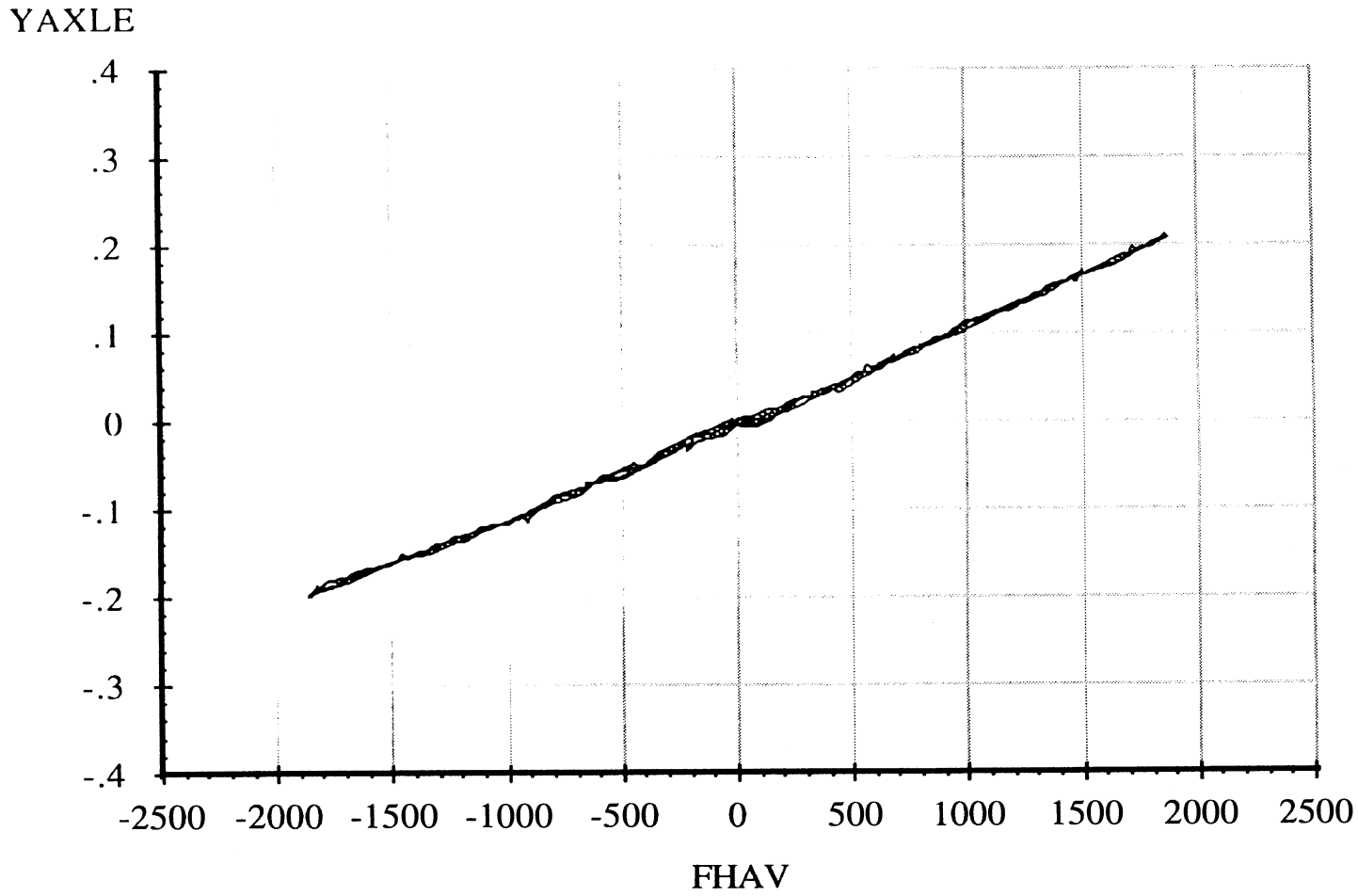

Abscissa (X): Average axle lateral force (FHAV); pounds; applied to both wheels simultaneously; force applied toward right, positive.

Ordinate (Y): Axle lateral translation (YAXLE); inches; motion toward right, positive.

*Note: Brakes on. Position control. Pitman arm blocked.

Measured by UMTRI for Smart Truck
Freightliner Tractor

Data file: FRTLNS13.ERD

Single Steer Axle Suspension

Lateral Force Compliance

6 April 96
Suspension: Taper-Leaf (2)

Suspension Load: 7500 lb.

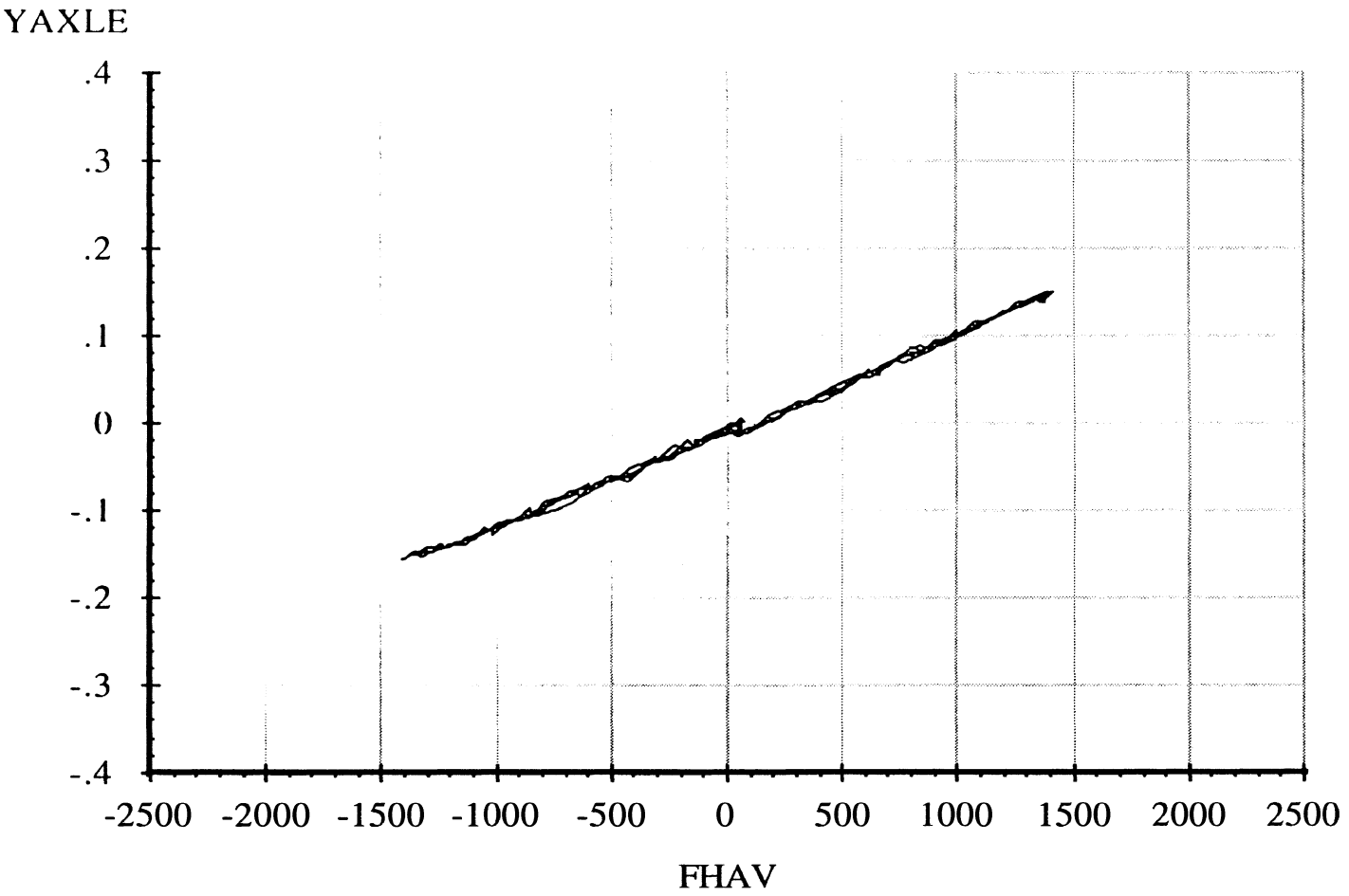

Abscissa (X): Average axle lateral force (FHAV); pounds; applied to both wheels simultaneously; force applied toward right, positive.

Ordinate (Y): Axle lateral translation (YAXLE); inches; motion toward right, positive.

*Note: Brakes on. Position control. Pitman arm blocked.

Measured by UMTRI for Smart Truck
Freightliner Tractor

Data file: FRTLNS12.ERD

Single Steer Axle Suspension

Lateral Force Compliance

6 April 96
Suspension: Taper-Leaf (2)

Suspension Load: 5000 lb.

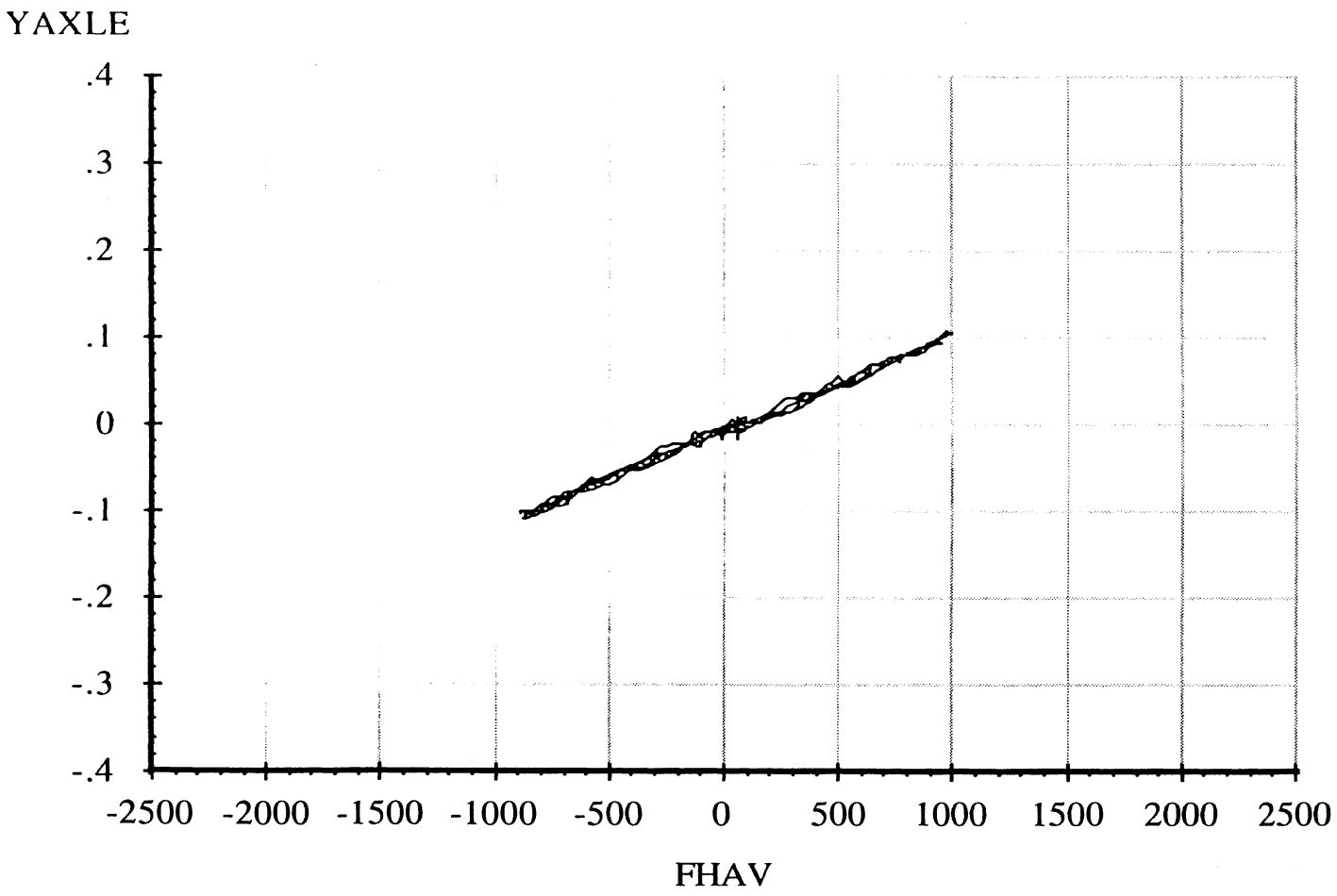

Abscissa (X): Average axle lateral force (FHAV); pounds; applied to both wheels simultaneously; force applied toward right, positive.

Ordinate (Y): Axle lateral translation (YAXLE); inches; motion toward right, positive.

*Note: Brakes on. Position control. Pitman arm blocked.

Measured by UMTRI for Smart Truck
Freightliner Tractor

Data file: FRTLNG50.ERD

Drive Axle Suspension, Trailing Only

Average Vertical Spring Rate

6 April 96
Suspension: Trailing Arm (2LU)

Nominal Suspension Load: 20000 lb.

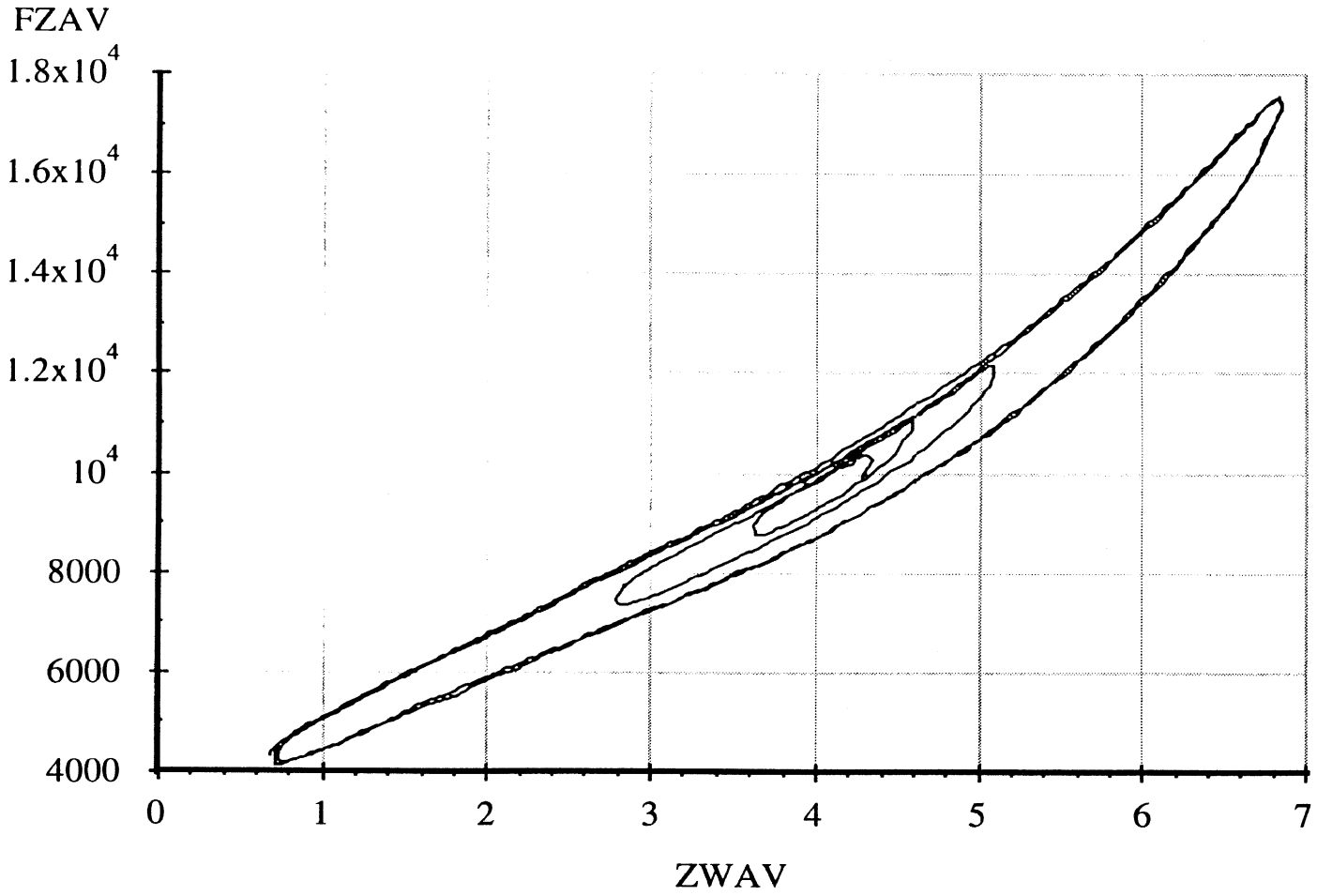

Abscissa (X): Average vertical wheel displacement (ZWAV); inches; spring compression, positive.

Ordinate (Y): Average vertical wheel load (FZAV); pounds; spring compression, positive.

*Note: Brakes on. Position control. Air bags inflated to 70.5 psi. Low side of vertical.

Measured by UMTRI for Smart Truck
Freightliner Tractor

Data file: FRTLNG54.ERD

Drive Axle Suspension, Trailing Only

Average Vertical Spring Rate

6 April 96
Suspension: Trailing Arm (2LU)

Nominal Suspension Load: 20000 lb.

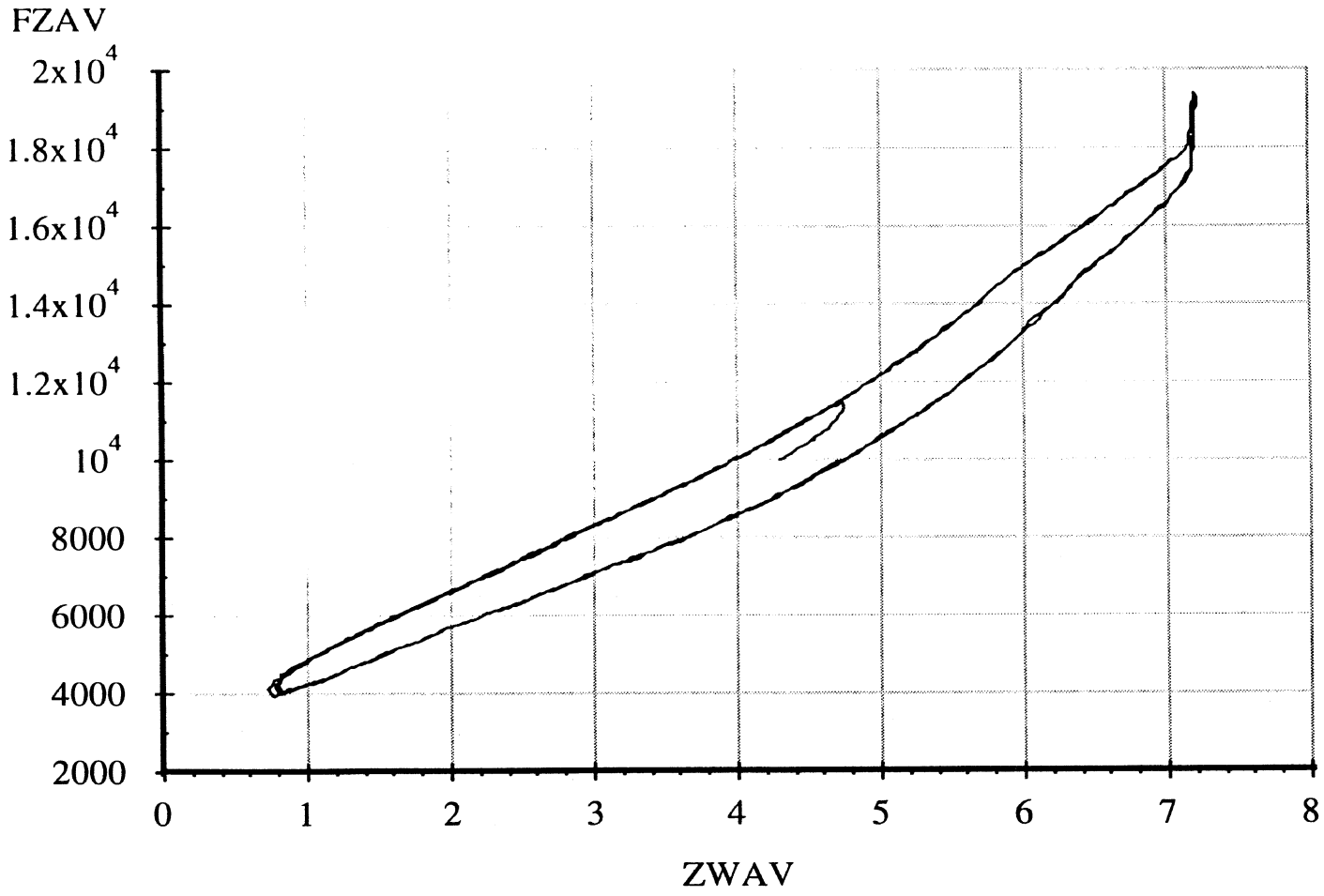

Abscissa (X): Average vertical wheel displacement (ZWAV); inches; spring compression, positive.

Ordinate (Y): Average vertical wheel load (FZAV); pounds; spring compression, positive.

*Note: Brakes on. Position control. Air bags inflated to 70.5 psi. High side of vertical.

Measured by UMTRI for Smart Truck
Freightliner Tractor

Data file: FRTLNG51.ERD

Drive Axle Suspension, Trailing Only

Axle Roll Rate

6 April 96
Suspension: Trailing Arm (2LU)

Suspension Load: 20000 lb.

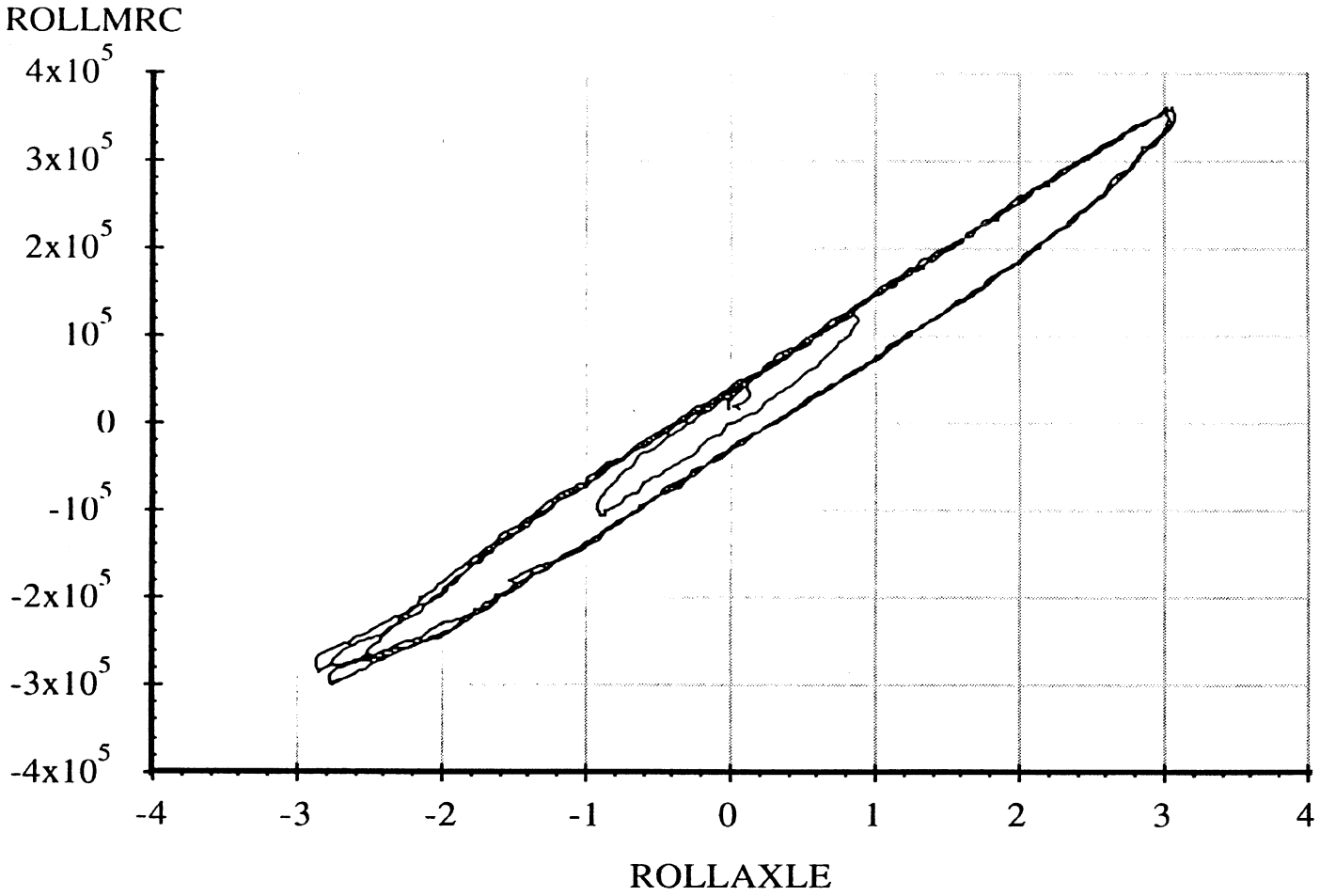

Abscissa (X): Axle roll angle (ROLLAXLE); degrees; right side compressed, positive.

Ordinate (Y): Axle roll moment about the roll center (ROLLMRC); in-lb; right side compressed, positive.

*Note: Brakes on. Force control. Air bags inflated to 70.5 psi.

Measured by UMTRI for Smart Truck
Freightliner Tractor

Data file: FRTLNG51.ERD

Drive Axle Suspension, Trailing Only

Roll Center Height

6 April 96
Suspension: Trailing Arm (2LU)

Suspension Load: 20000 lb.

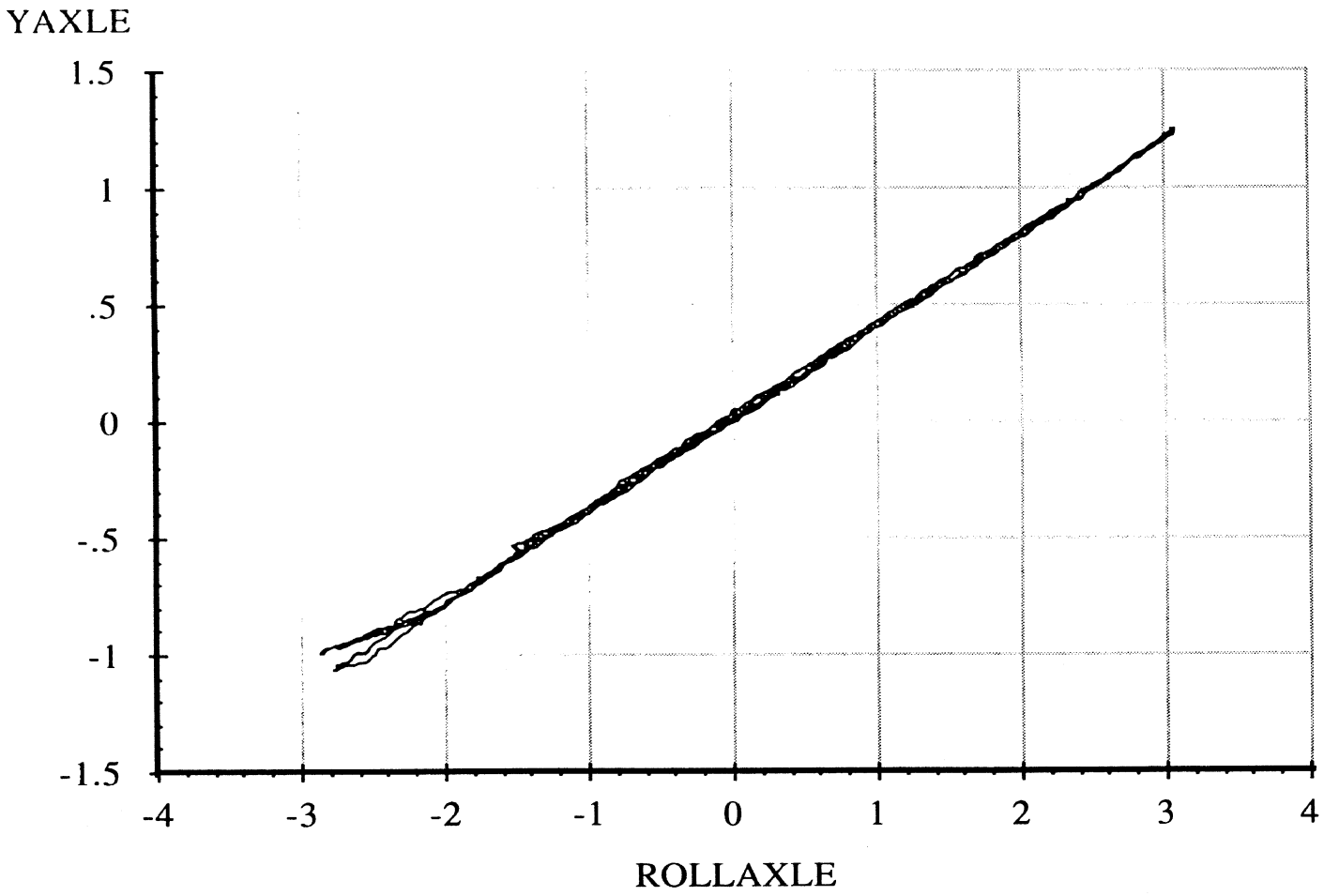

Abscissa (X): Axle roll angle (ROLLAXLE); degrees; right side compressed, positive.

Ordinate (Y): Axle reference point lateral translation (YAXLE); inches; motion toward right, positive.

*Note: Brakes on. Force control. Air bags inflated to 70.5 psi. Reference height of 7.69 inches.

Measured by UMTRI for Smart Truck
Freightliner Tractor

Data file: FRTLNG51.ERD

Drive Axle Suspension, Trailing Only

Roll Steer

6 April 96
Suspension: Trailing Arm (2LU)

Suspension Load: 20000 lb.

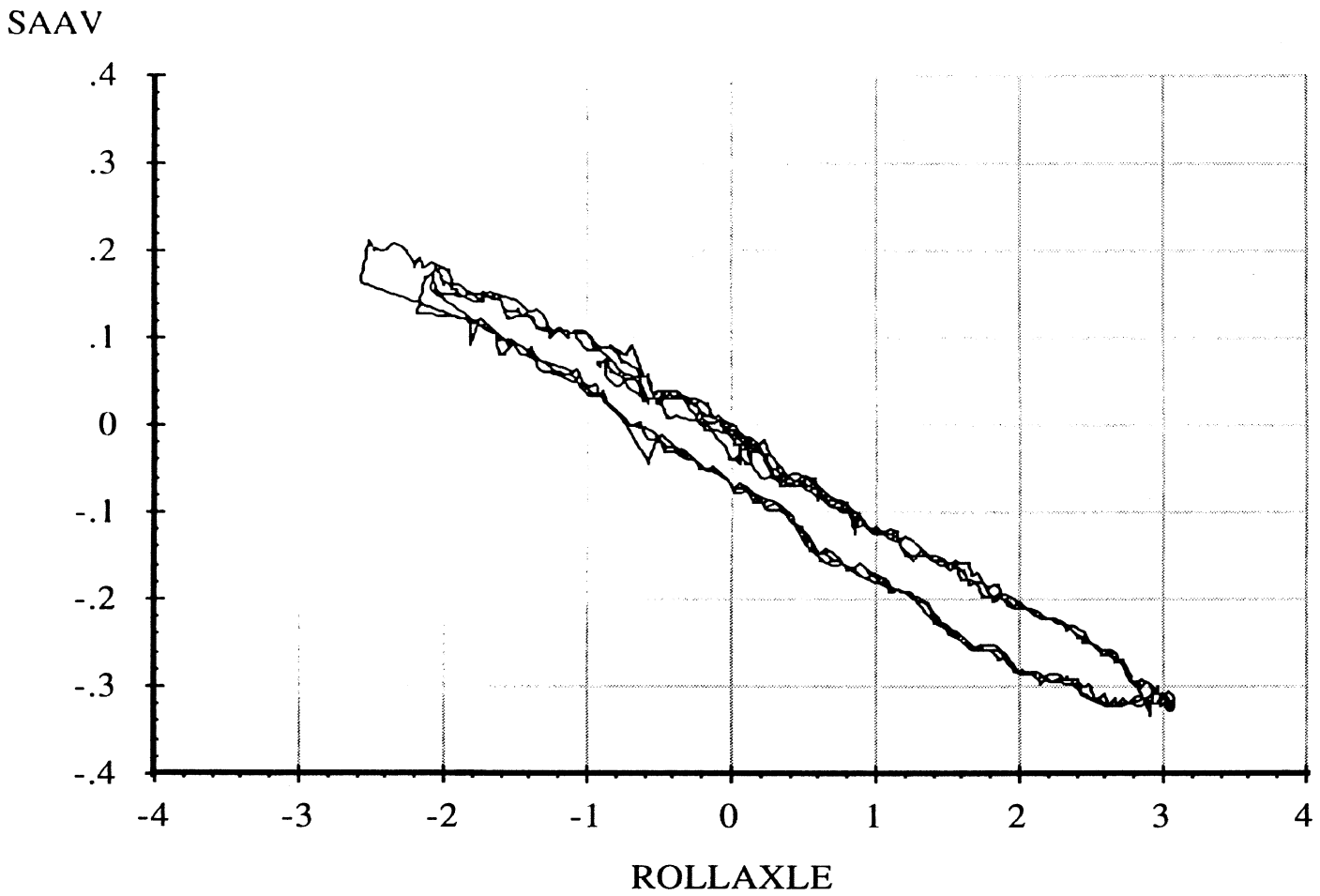

Abscissa (X): Axle roll angle (ROLLAXLE); degrees; right side compressed, positive.

Ordinate (Y): Average steer angle (SAAV); degrees; steer toward right, positive.

*Note: Brakes on. Force control. Air bags inflated to 70.5 psi.

Measured by UMTRI for Smart Truck
Freightliner Tractor

Data file: FRTLNG52.ERD

Drive Axle Suspension, Trailing Only

Lateral Force Compliance

6 April 96
Suspension: Trailing Arm (2LU)

Suspension Load: 20000 lb.

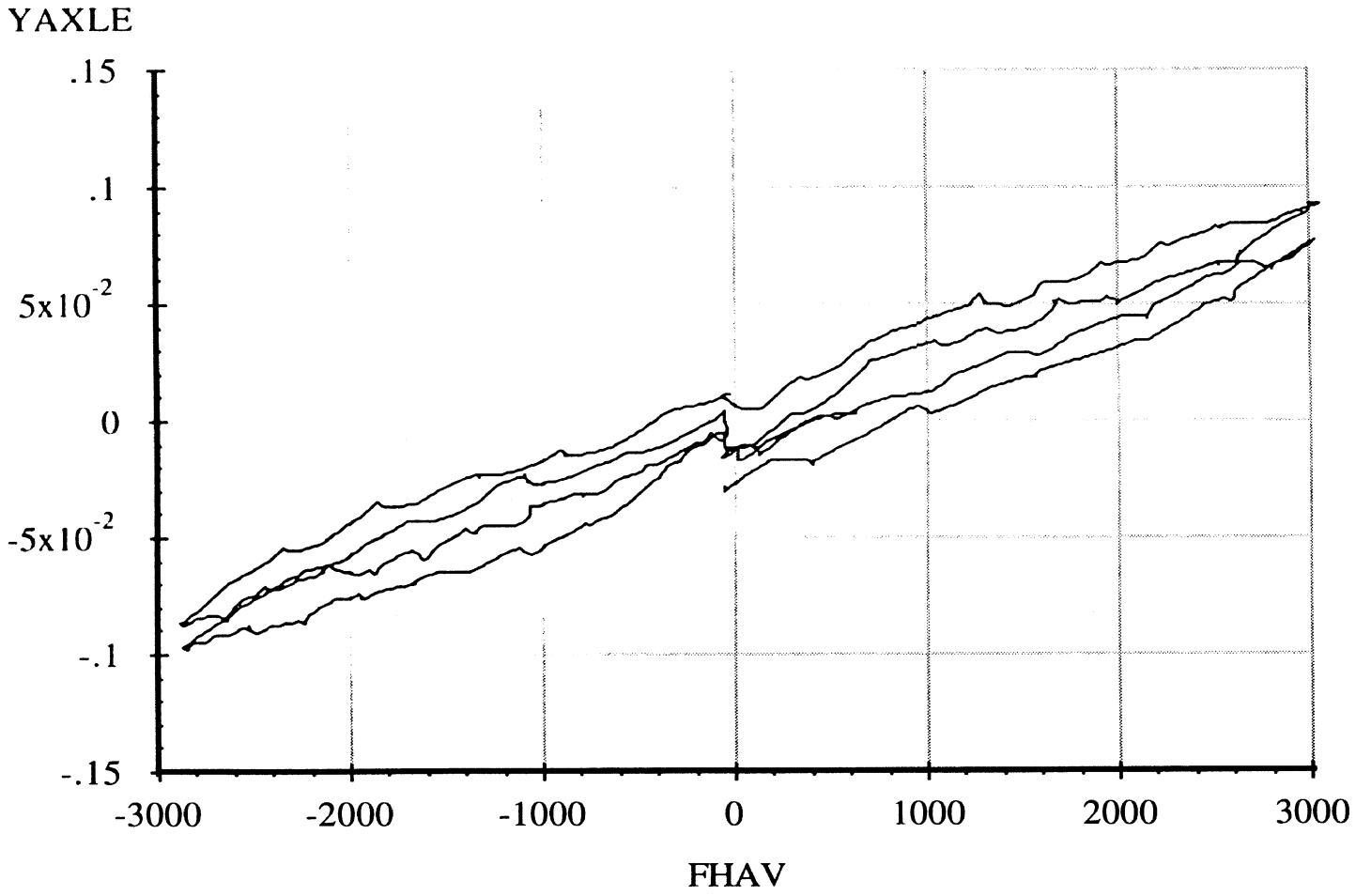

Abscissa (X): Average axle lateral force (FHAV); pounds; applied to both wheels simultaneously; force applied toward right, positive.

Ordinate (Y): Axle lateral translation (YAXLE); inches; motion toward right, positive.

*Note: Brakes on. Position control. Air bags inflated to 70.5 psi. Reference height of 7.69 inches.

Measured by UMTRI for Smart Truck
Freightliner Tractor

Data file: FRTLNG52.ERD

Drive Axle Suspension, Trailing Only

Lateral Force Steer

6 April 96
Suspension: Trailing Arm (2LU)

Suspension Load: 20000 lb.

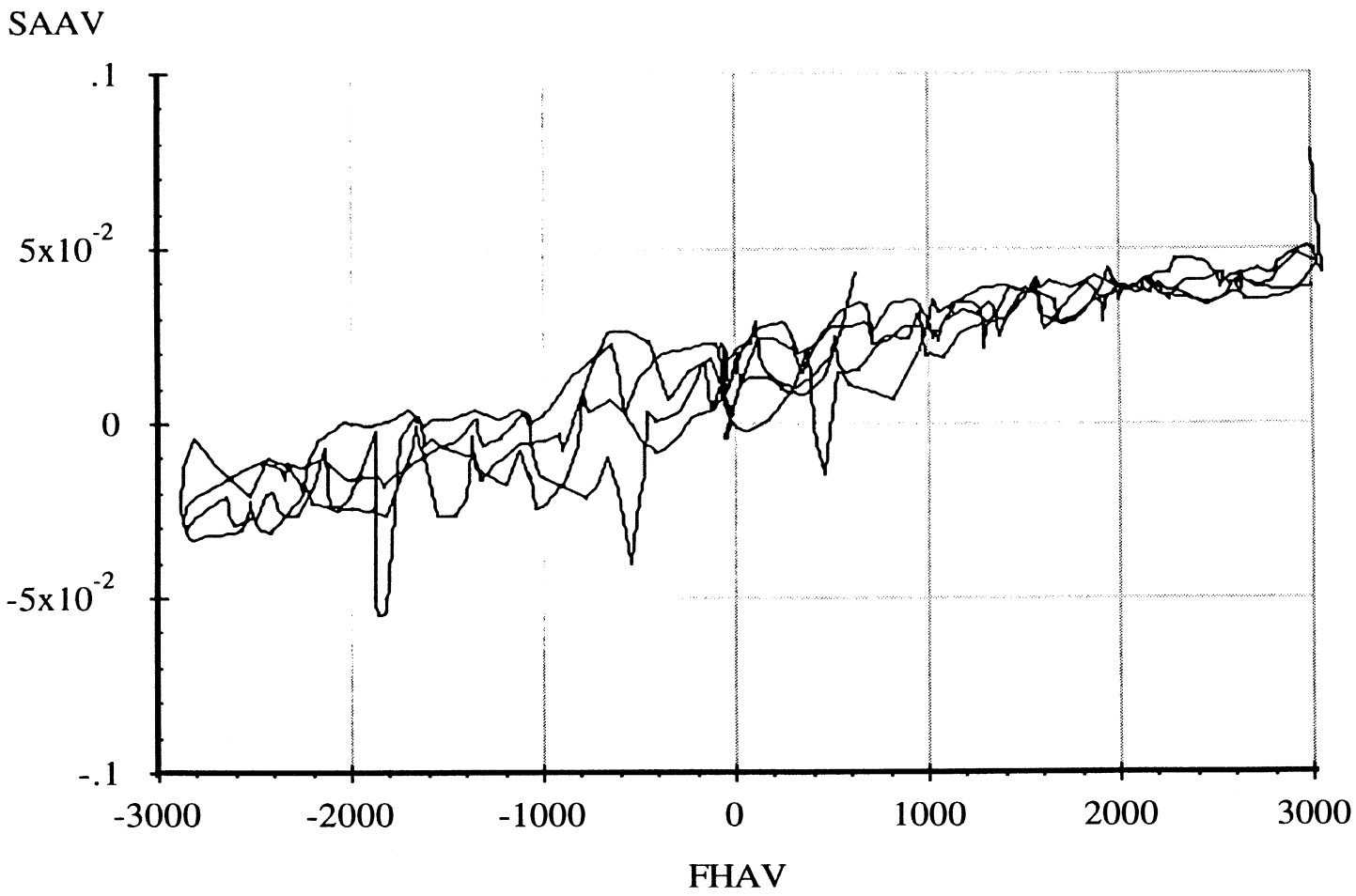

Abscissa (X): Average axle lateral force (FHAV); pounds; applied to both wheels simultaneously; force applied toward right, positive.

Ordinate (Y): Average steer angle (SAAV); degrees; steer toward right, positive.

*Note: Brakes on. Position control. Air bags inflated to 70.5 psi.

Measured by UMTRI for Smart Truck
Freightliner Tractor

Data file: FRTLNG53.ERD

Drive Axle Suspension, Trailing Only

Aligning Moment Compliance Steer

6 April 96
Suspension: Trailing Arm (2LU)
Suspension Load: 20000 lb.

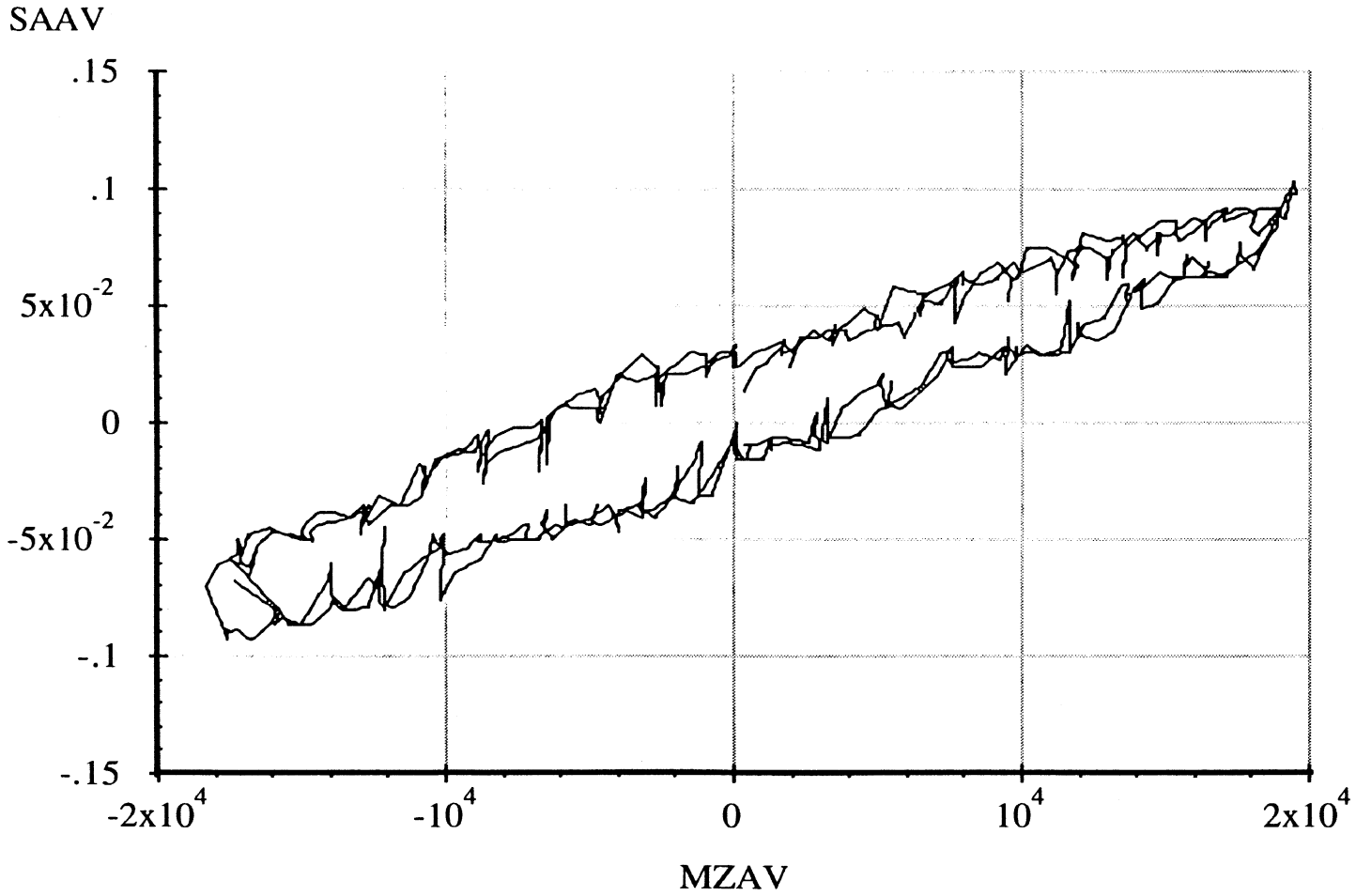

Abscissa (X): Average axle aligning moment (MZAV); in-lb per wheel; applied to both wheels simultaneously; downward (right hand rule) moment vector, positive.

Ordinate (Y): Average steer angle (SAAV); degrees; steer toward right, positive.

*Note: Brakes on. Position control. Air bags inflated to 70.5 psi.

Measured by UMTRI for Smart Truck
Freightliner Tractor

Data file: FRTLNG40.ERD

Drive Axle Suspension, Trailing Only

Average Vertical Spring Rate

6 April 96
Suspension: Trailing Arm (2LU)
Nominal Suspension Load: 18000 lb.

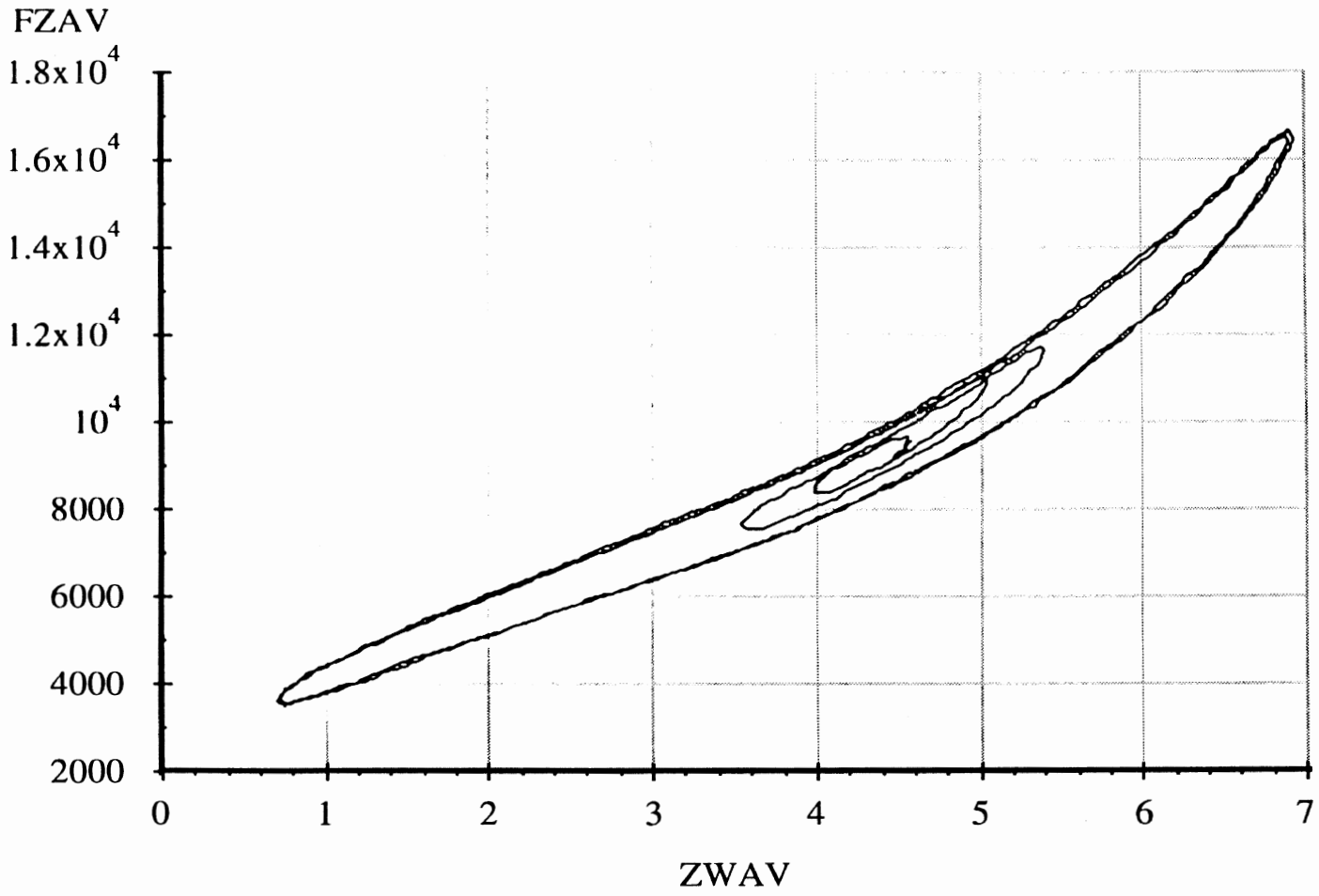

Abscissa (X): Average vertical wheel displacement (ZWAV); inches; spring compression, positive.

Ordinate (Y): Average vertical wheel load (FZAV); pounds; spring compression, positive.

*Note: Brakes on. Position control. Air bags inflated to 65 psi. Low side of vertical.

Measured by UMTRI for Smart Truck
Freightliner Tractor

Data file: FRTLNG44.ERD

Drive Axle Suspension, Trailing Only

Average Vertical Spring Rate

6 April 96
Suspension: Trailing Arm (2LU)

Nominal Suspension Load: 18000 lb.

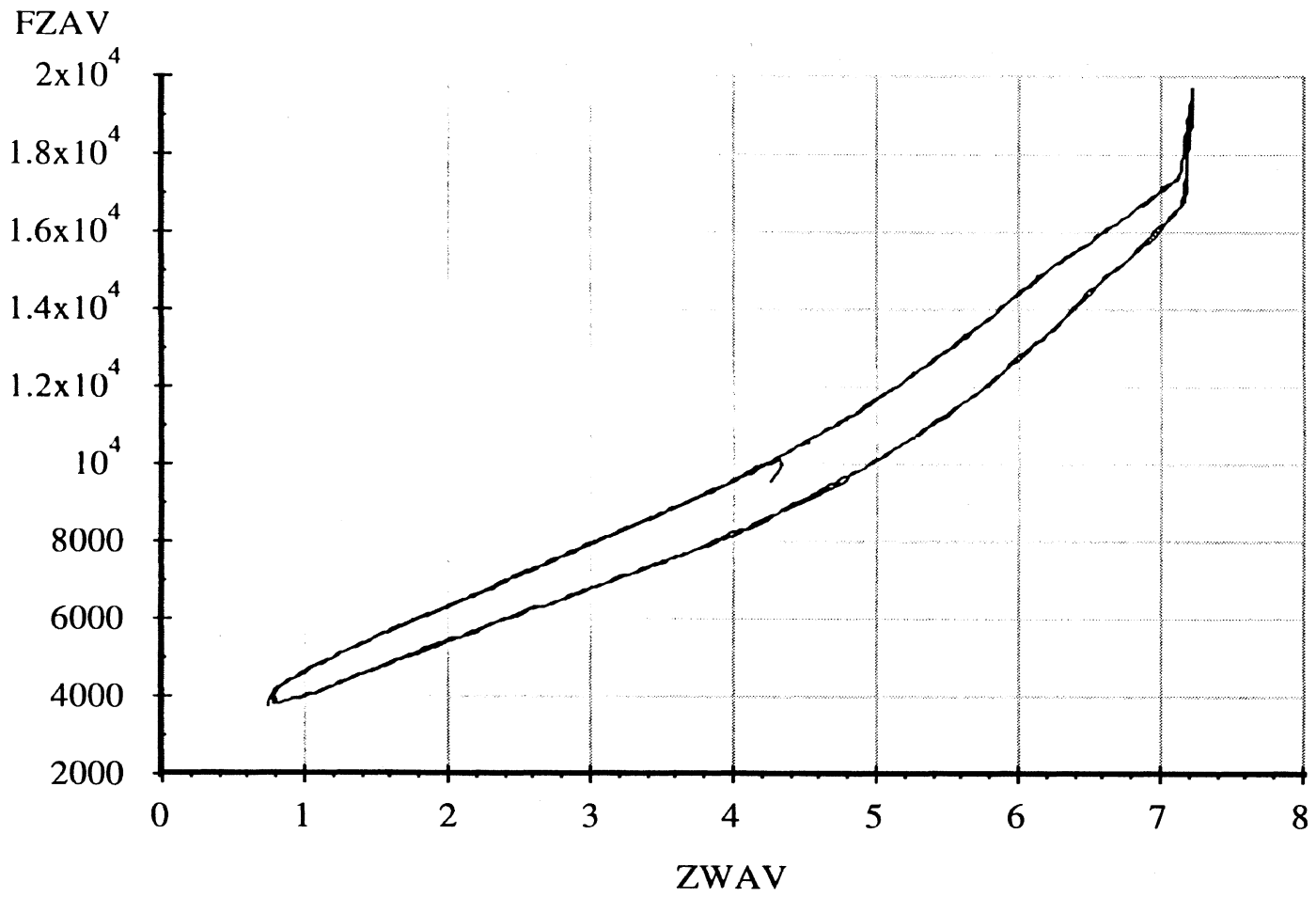

Abscissa (X): Average vertical wheel displacement (ZWAV); inches; spring compression, positive.

Ordinate (Y): Average vertical wheel load (FZAV); pounds; spring compression, positive.

*Note: Brakes on. Position control. Air bags inflated to 65 psi. High side of vertical.

Measured by UMTRI for Smart Truck
Freightliner Tractor

Data file: FRTLNG41.ERD

Drive Axle Suspension, Trailing Only

Axle Roll Rate

6 April 96
Suspension: Trailing Arm (2LU)

Suspension Load: 18000 lb.

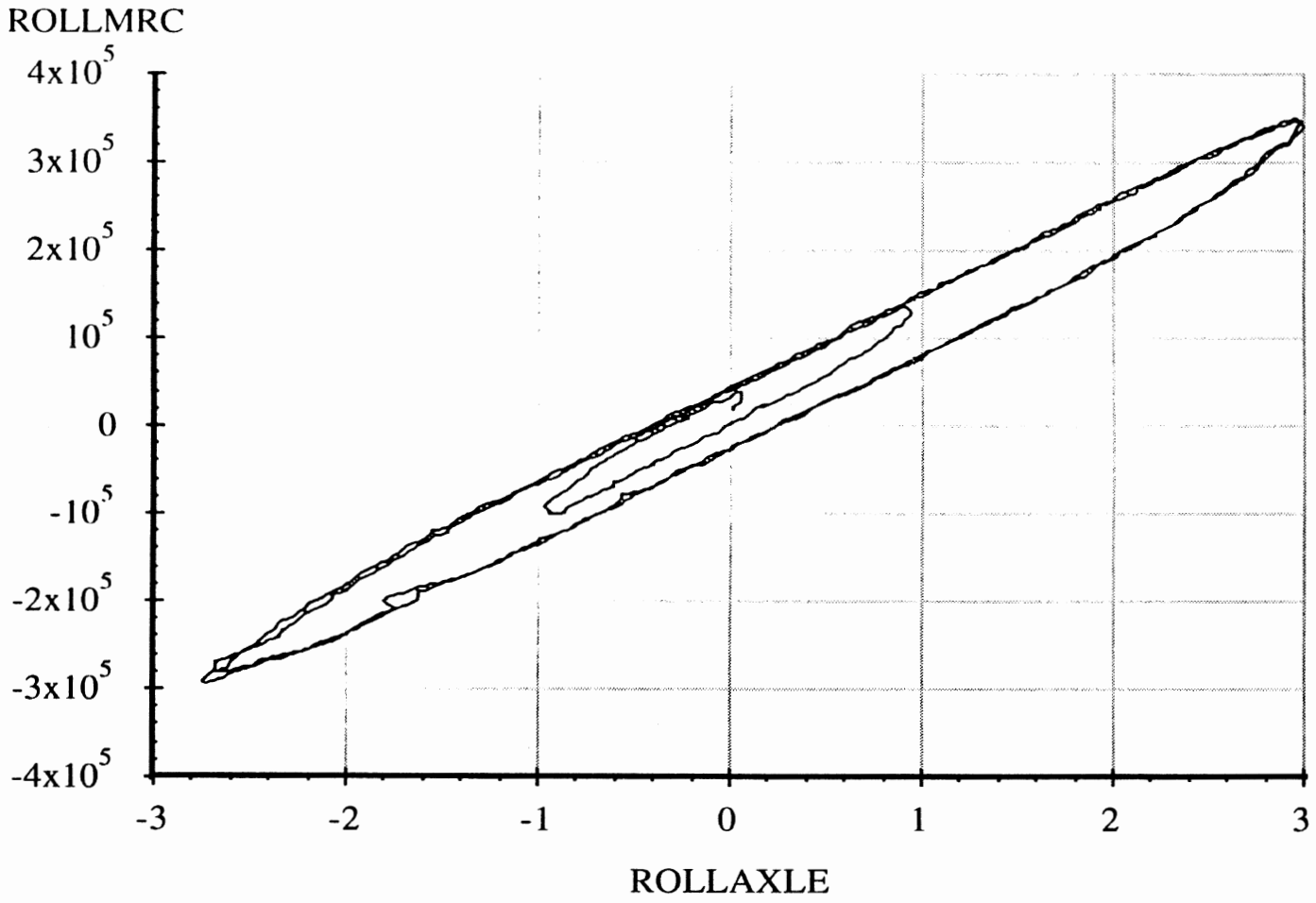

Abscissa (X): Axle roll angle (ROLLAXLE); degrees; right side compressed, positive.

Ordinate (Y): Axle roll moment about the roll center (ROLLMRC); in-lb; right side compressed, positive.

*Note: Brakes on. Force control. Air bags inflated to 65 psi.

Measured by UMTRI for Smart Truck
Freightliner Tractor

Data file: FRTLNG41.ERD

Drive Axle Suspension, Trailing Only

Roll Center Height

6 April 96
Suspension: Trailing Arm (2LU)

Suspension Load: 18000 lb.

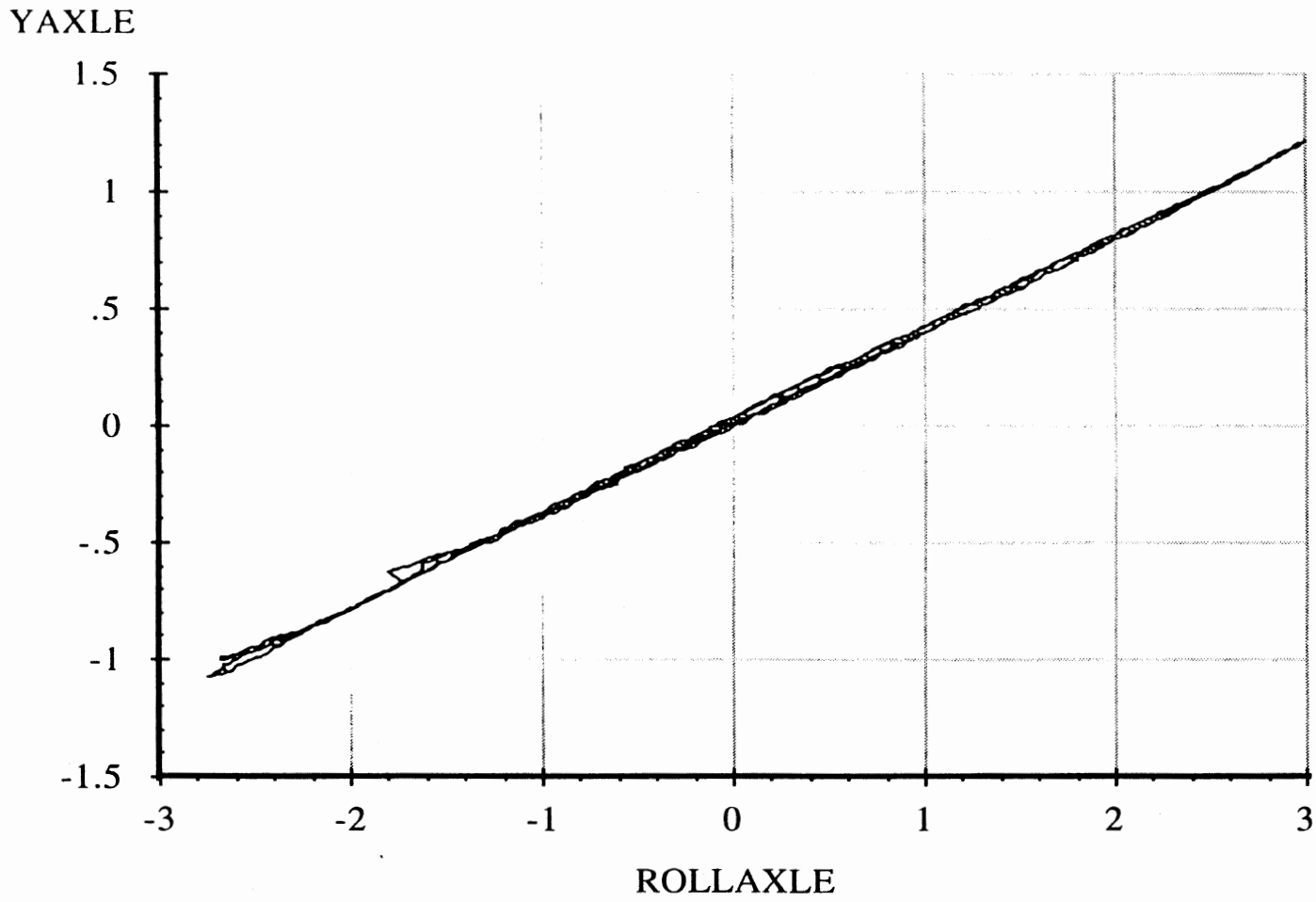

Abscissa (X): Axle roll angle (ROLLAXLE); degrees; right side compressed, positive.

Ordinate (Y): Axle reference point lateral translation (YAXLE); inches; motion toward right, positive.

*Note: Brakes on. Force control. Air bags inflated to 65 psi. Reference height of 7.81 inches.

Measured by UMTRI for Smart Truck
Freightliner Tractor

Data file: FRTLNG41.ERD

Drive Axle Suspension, Trailing Only

Roll Steer

6 April 96
Suspension: Trailing Arm (2LU)

Suspension Load: 18000 lb.

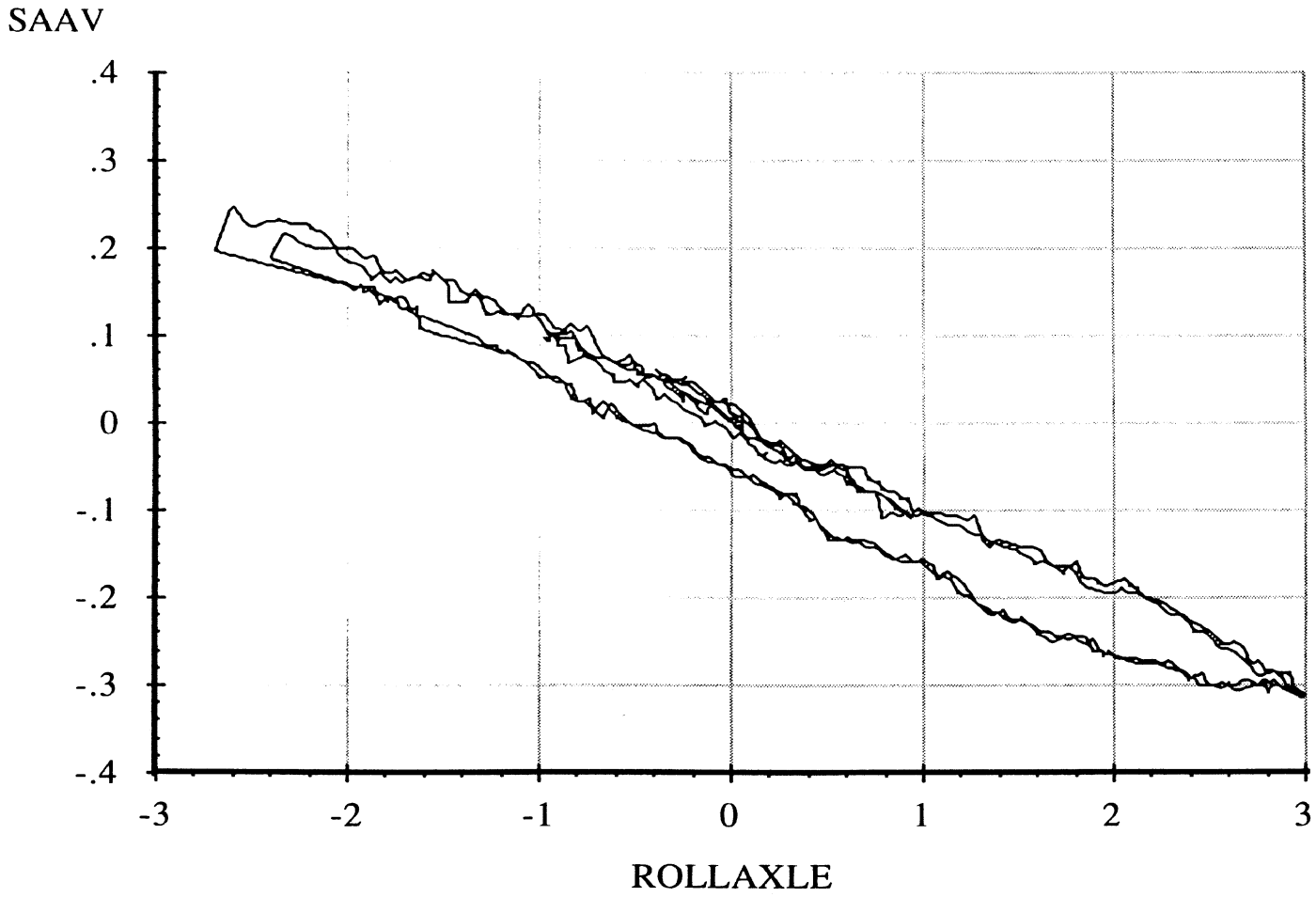

Abscissa (X): Axle roll angle (ROLLAXLE); degrees; right side compressed, positive.

Ordinate (Y): Average steer angle (SAAV); degrees; steer toward right, positive.

*Note: Brakes on. Force control. Air bags inflated to 65 psi.

Measured by UMTRI for Smart Truck
Freightliner Tractor

Data file: FRTLNG42.ERD

Drive Axle Suspension, Trailing Only

Lateral Force Compliance

6 April 96
Suspension: Trailing Arm (2LU)

Suspension Load: 18000 lb.

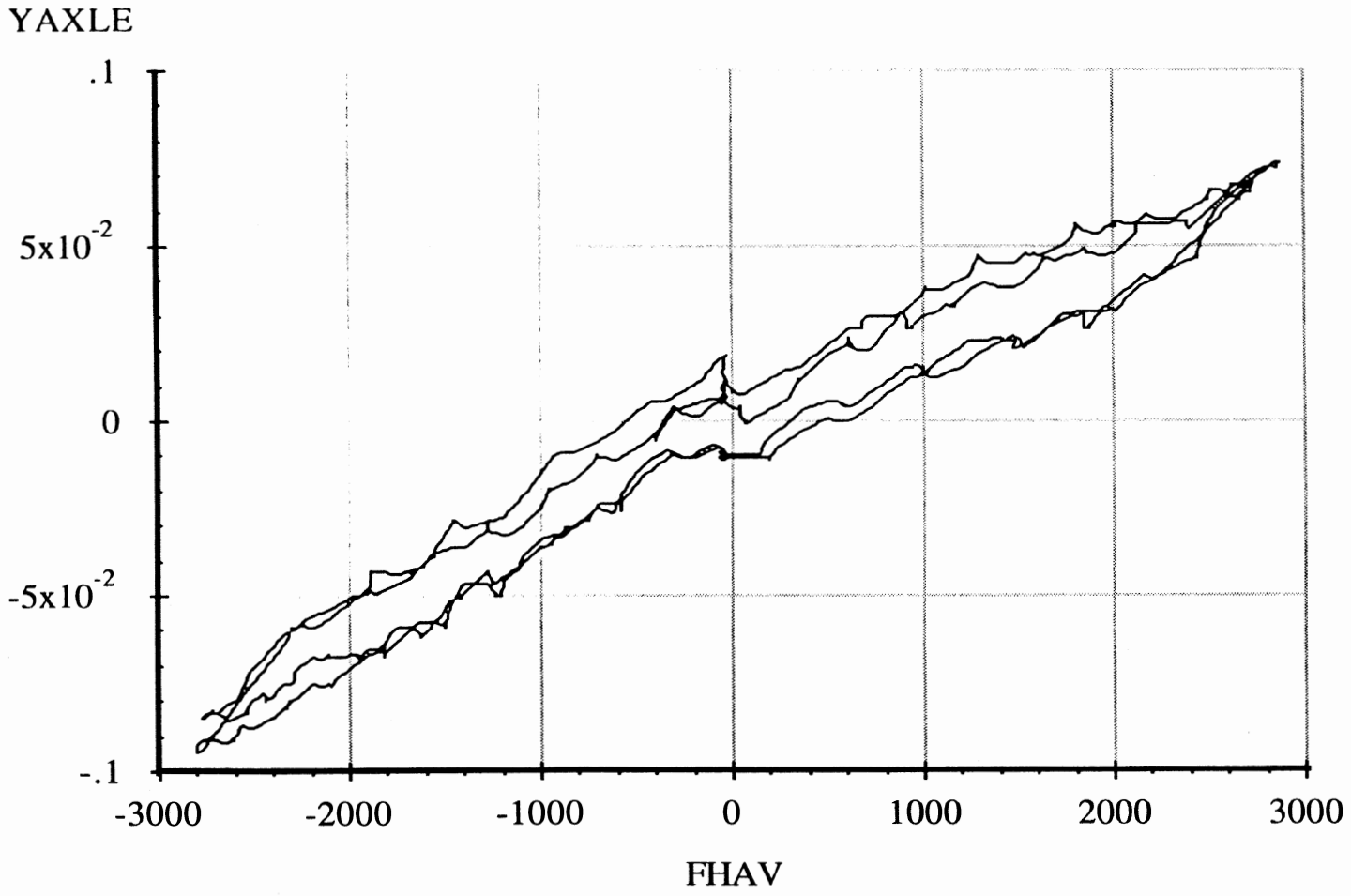

Abscissa (X): Average axle lateral force (FHAV); pounds; applied to both wheels simultaneously; force applied toward right, positive.

Ordinate (Y): Axle lateral translation (YAXLE); inches; motion toward right, positive.

*Note: Brakes on. Position control. Air bags inflated to 65 psi. Reference height of 7.81 inches.

Measured by UMTRI for Smart Truck
Freightliner Tractor

Data file: FRTLNG42.ERD

Drive Axle Suspension, Trailing Only

Lateral Force Steer

6 April 96
Suspension: Trailing Arm (2LU)

Suspension Load: 18000 lb.

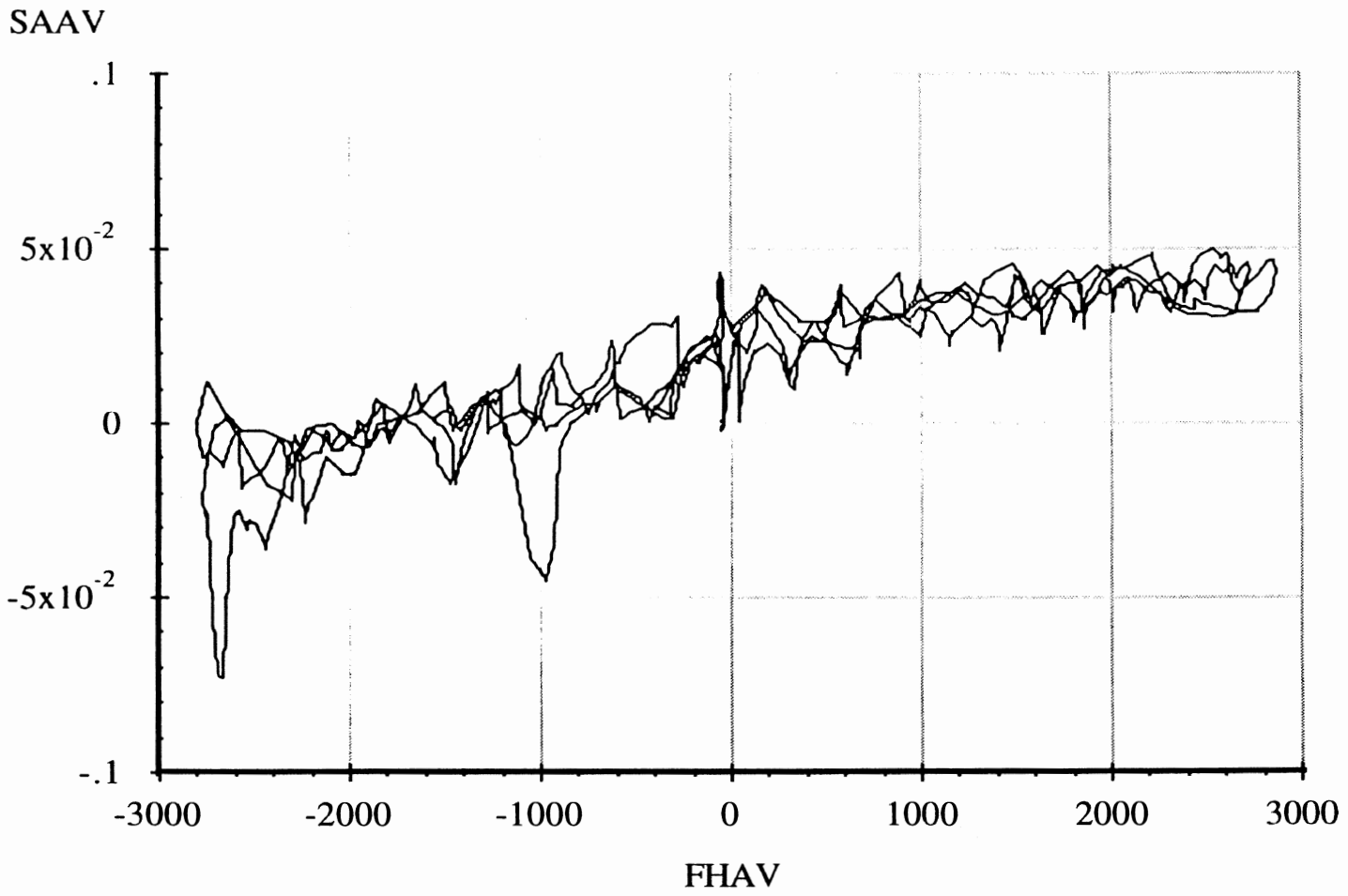

Abscissa (X): Average axle lateral force (FHAV); pounds; applied to both wheels simultaneously; force applied toward right, positive.

Ordinate (Y): Average steer angle (SAAV); degrees; steer toward right, positive.

*Note: Brakes on. Position control. Air bags inflated to 65 psi.

Measured by UMTRI for Smart Truck
Freightliner Tractor

Data file: FRTLNG43.ERD

Drive Axle Suspension, Trailing Only

Aligning Moment Compliance Steer

6 April 96
Suspension: Trailing Arm (2LU)

Suspension Load: 18000 lb.

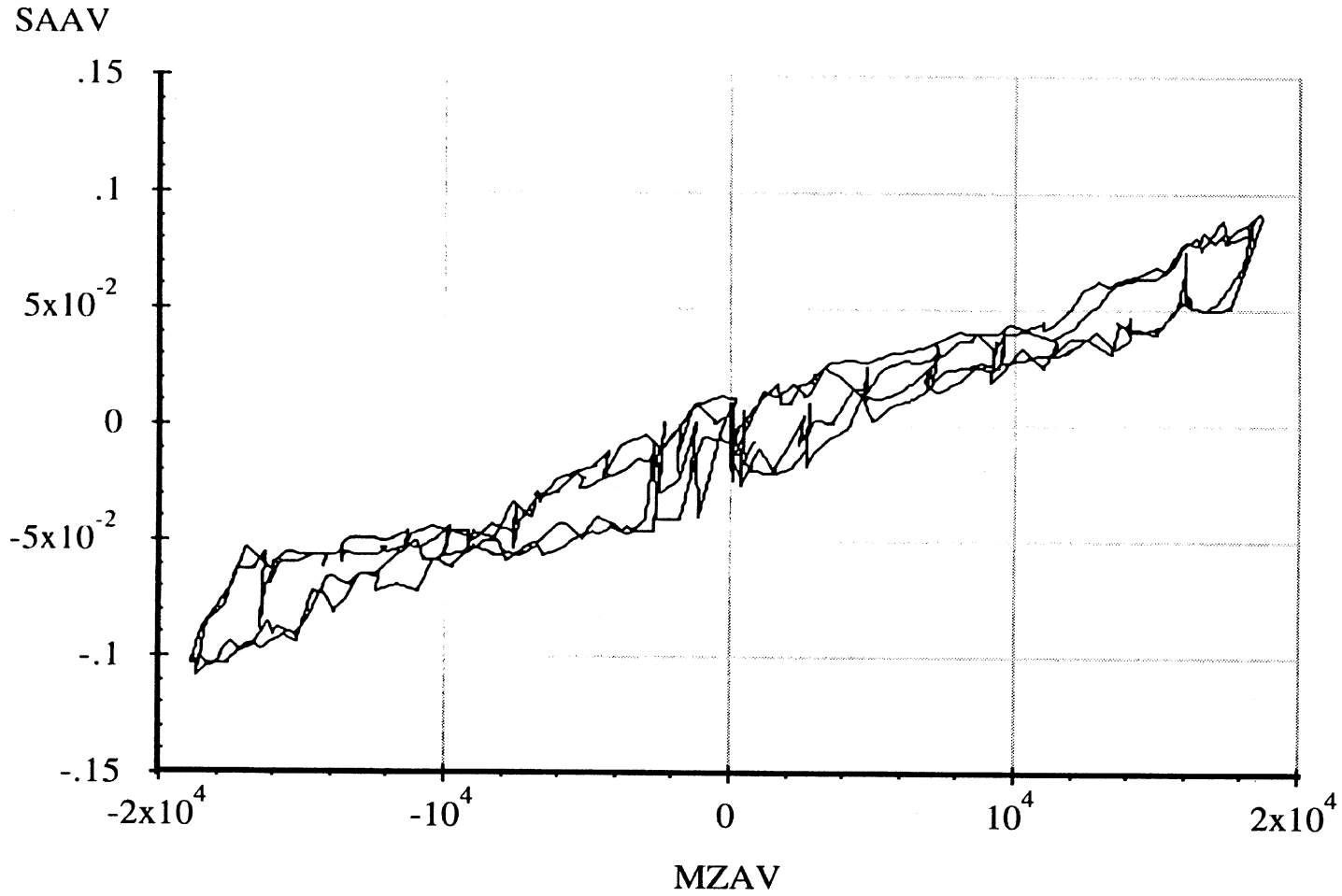

Abscissa (X): Average axle aligning moment (MZAV); in-lb per wheel; applied to both wheels simultaneously; downward (right hand rule) moment vector, positive.

Ordinate (Y): Average steer angle (SAAV); degrees; steer toward right, positive.

*Note: Brakes on. Position control. Air bags inflated to 65 psi.

Measured by UMTRI for Smart Truck
Freightliner Tractor

Data file: FRTLNG30.ERD

Drive Axle Suspension, Trailing Only

Average Vertical Spring Rate

6 April 96
Suspension: Trailing Arm (2LU)
Nominal Suspension Load: 16000 lb.

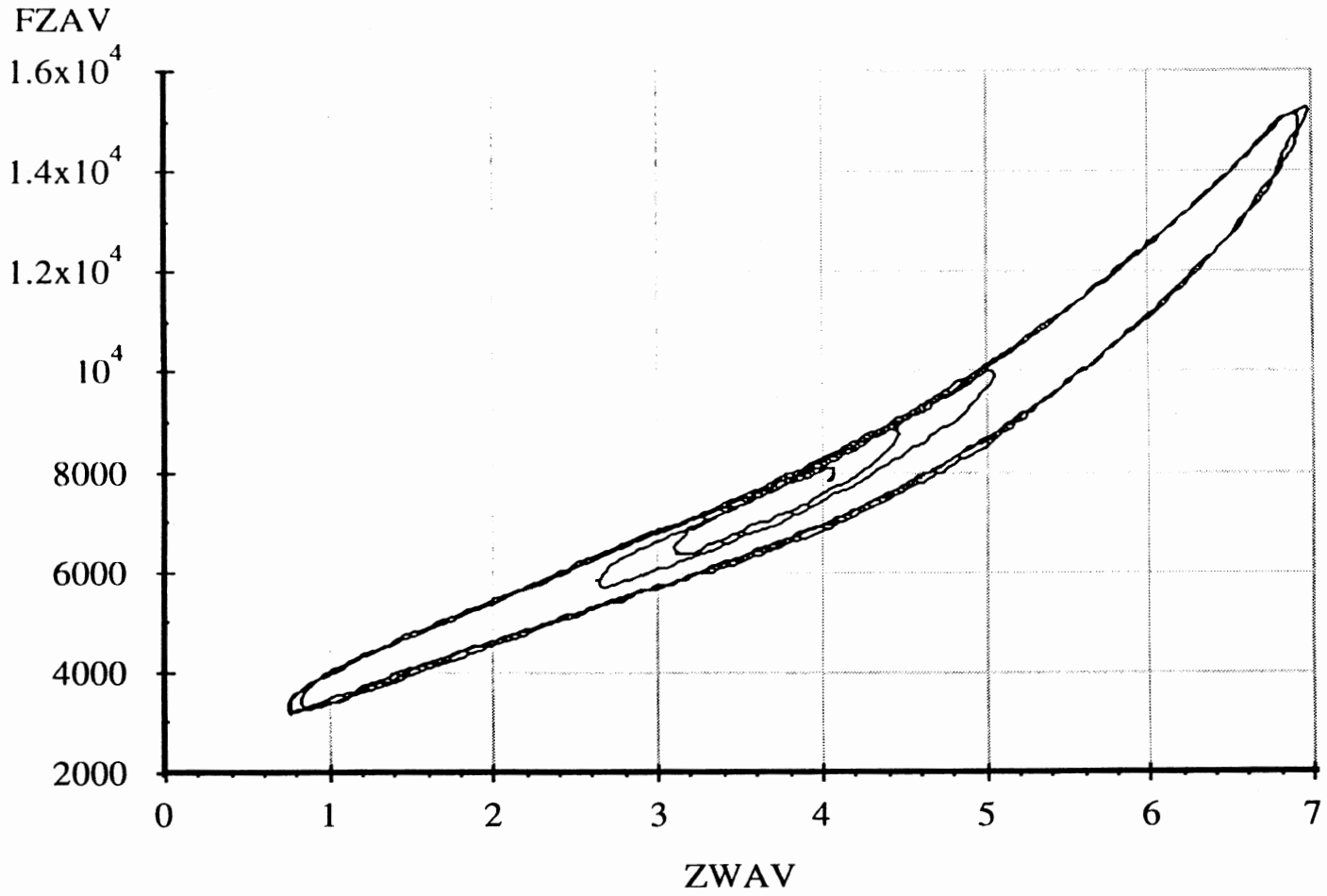

Abscissa (X): Average vertical wheel displacement (ZWAV); inches; spring compression, positive.

Ordinate (Y): Average vertical wheel load (FZAV); pounds; spring compression, positive.

*Note: Brakes on. Position control. Air bags inflated to 58 psi. Low side of vertical.

Measured by UMTRI for Smart Truck
Freightliner Tractor

Data file: FRTLNG34.ERD

Drive Axle Suspension, Trailing Only

Average Vertical Spring Rate

6 April 96
Suspension: Trailing Arm (2LU)

Nominal Suspension Load: 16000 lb.

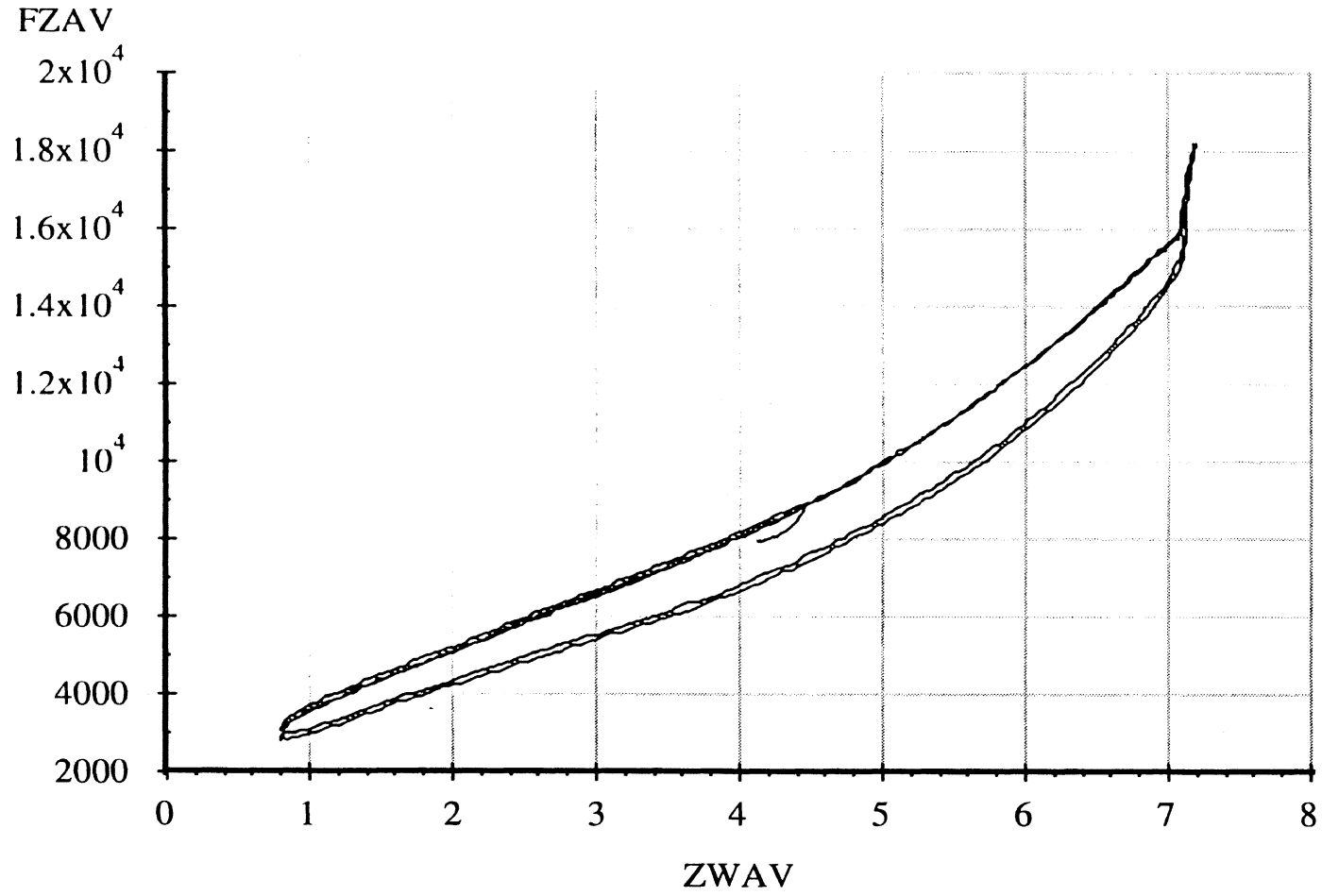

Abscissa (X): Average vertical wheel displacement (ZWAV); inches; spring compression, positive.

Ordinate (Y): Average vertical wheel load (FZAV); pounds; spring compression, positive.

*Note: Brakes on. Position control. Air bags inflated to 58 psi. High side of vertical.

Measured by UMTRI for Smart Truck
Freightliner Tractor

Drive Axle Suspension, Trailing Only

6 April 96
Suspension: Trailing Arm (2LU)

Data file: FRTLNG31.ERD

Axle Roll Rate

Suspension Load: 16000 lb.

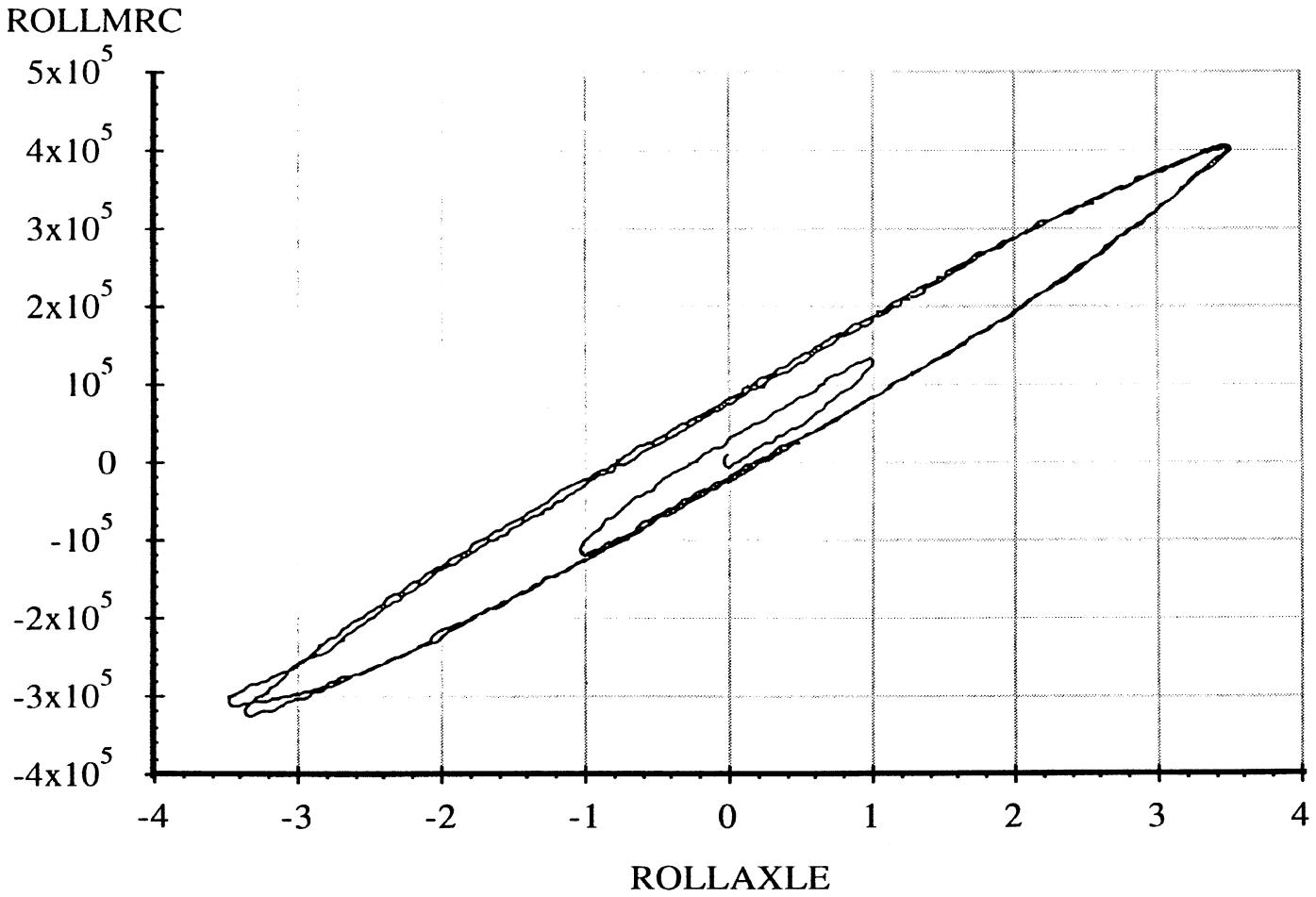

Abscissa (X): Axle roll angle (ROLLAXLE); degrees; right side compressed, positive.

Ordinate (Y): Axle roll moment about the roll center (ROLLMRC); in-lb; right side compressed, positive.

*Note: Brakes on. Force control. Air bags inflated to 58 psi.

Measured by UMTRI for Smart Truck
Freightliner Tractor

Data file: FRTLNG31.ERD

Drive Axle Suspension, Trailing Only

Roll Center Height

6 April 96
Suspension: Trailing Arm (2LU)

Suspension Load: 16000 lb.

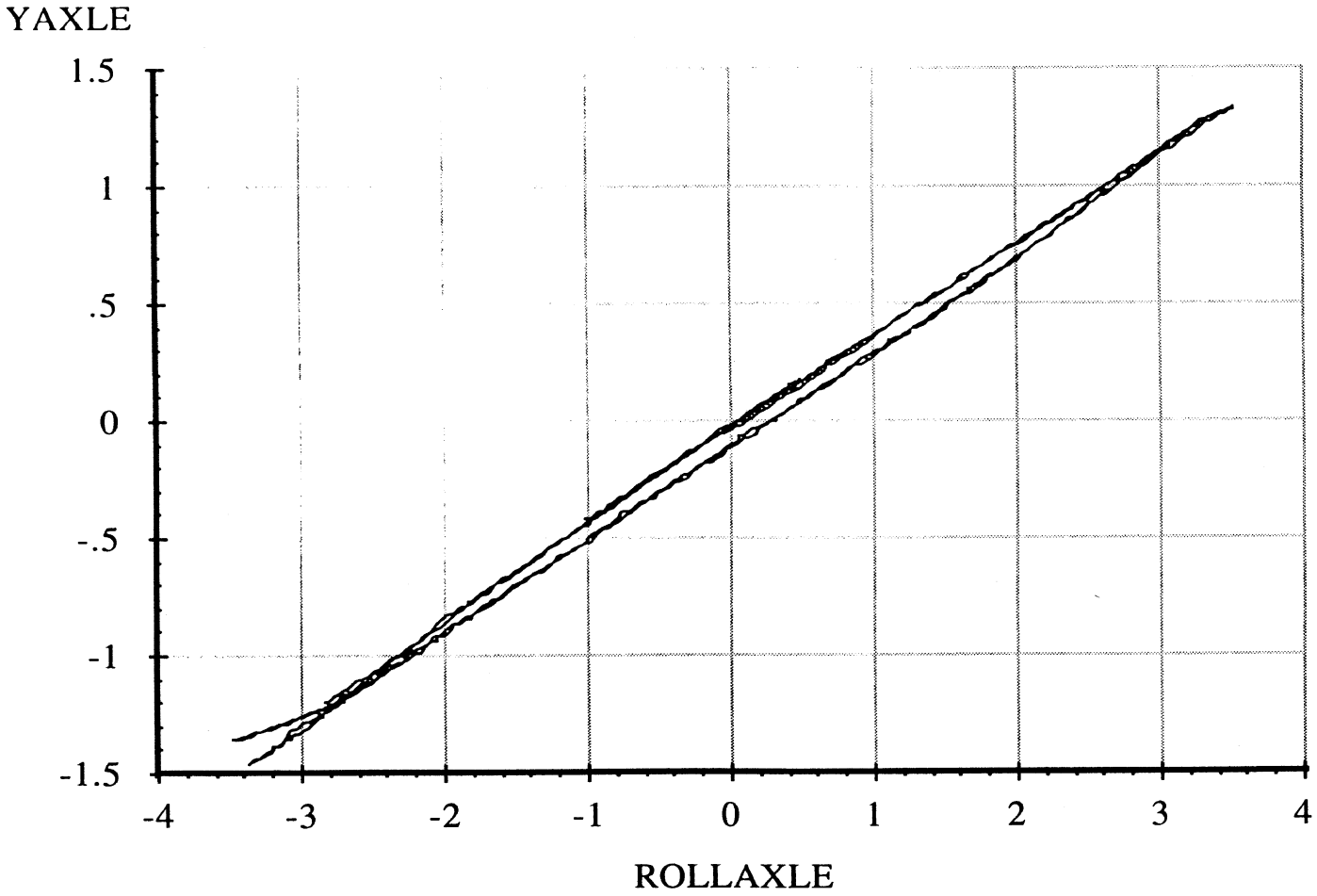

Abscissa (X): Axle roll angle (ROLLAXLE); degrees; right side compressed, positive.

Ordinate (Y): Axle reference point lateral translation (YAXLE); inches; motion toward right, positive.

*Note: Brakes on. Force control. Air bags inflated to 58 psi. Reference height of 7.88 inches.

Measured by UMTRI for Smart Truck
Freightliner Tractor

Data file: FRTLNG31.ERD

Drive Axle Suspension, Trailing Only

Roll Steer

6 April 96
Suspension: Trailing Arm (2LU)

Suspension Load: 16000 lb.

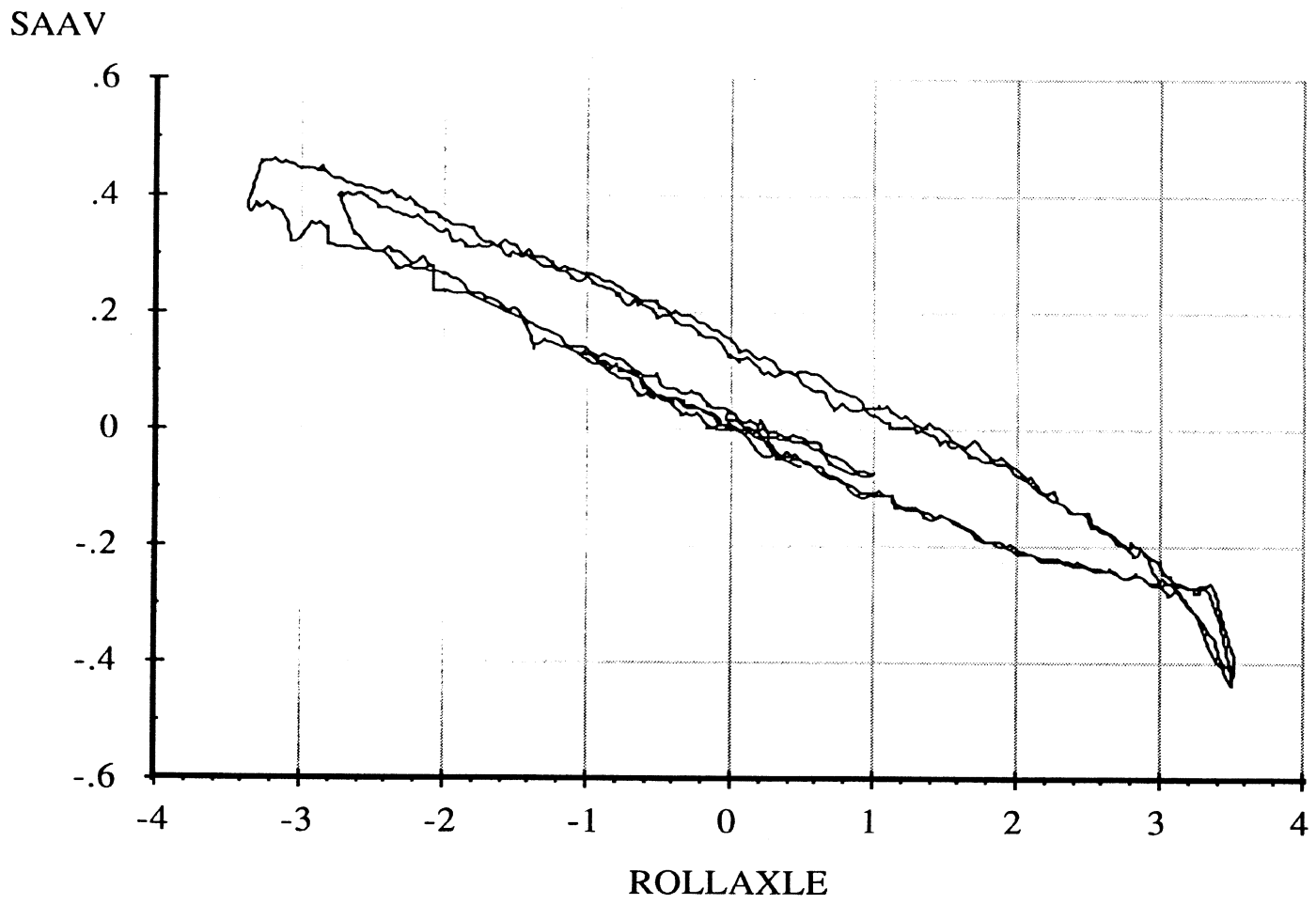

Abscissa (X): Axle roll angle (ROLLAXLE); degrees; right side compressed, positive.

Ordinate (Y): Average steer angle (SAAV); degrees; steer toward right, positive.

*Note: Brakes on. Force control. Air bags inflated to 58 psi.

Measured by UMTRI for Smart Truck
Freightliner Tractor

Drive Axle Suspension, Trailing Only

6 April 96
Suspension: Trailing Arm (2LU)

Data file: FRTLNG32.ERD

Lateral Force Compliance

Suspension Load: 16000 lb.

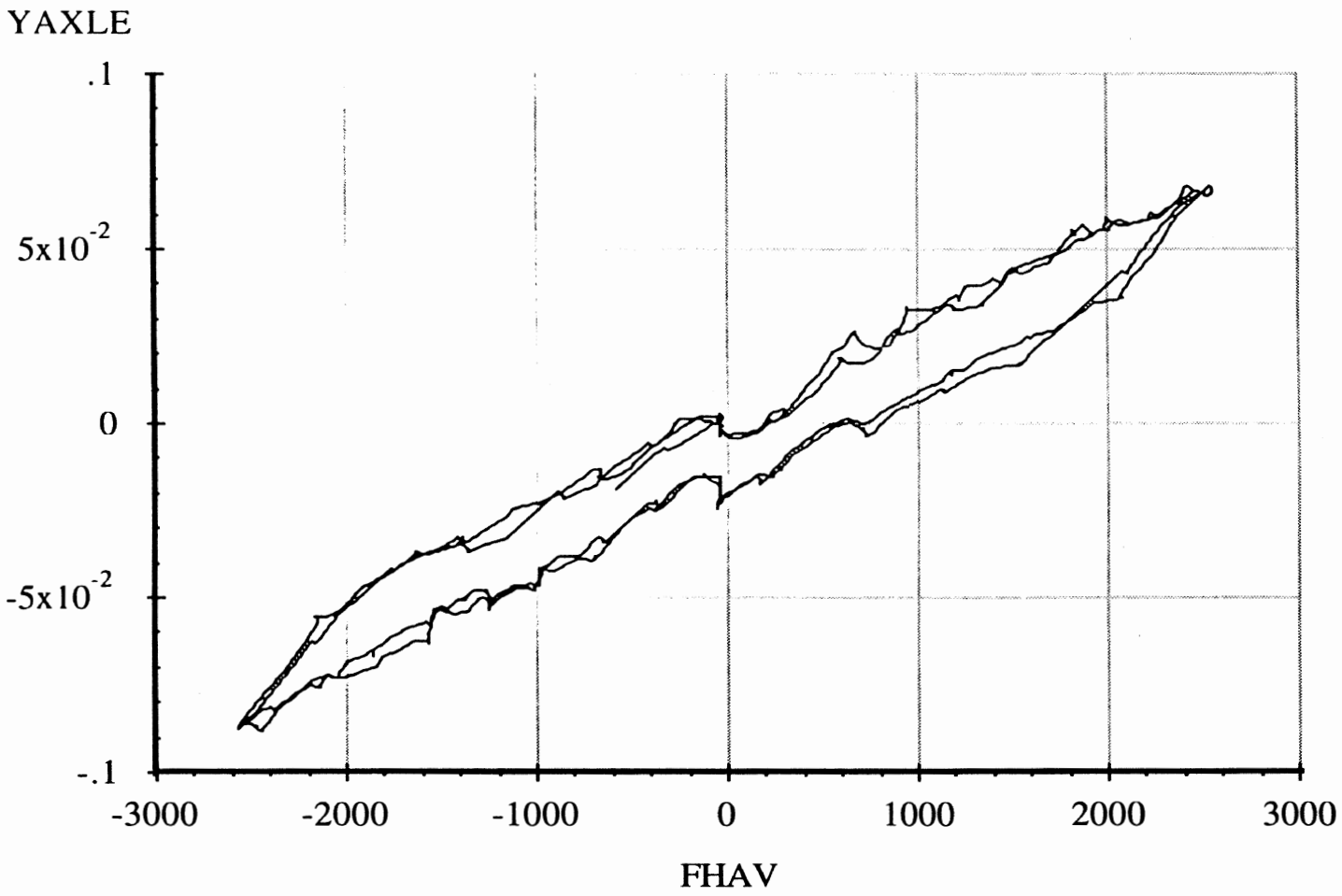

Abscissa (X): Average axle lateral force (FHAV); pounds; applied to both wheels simultaneously; force applied toward right, positive.

Ordinate (Y): Axle lateral translation (YAXLE); inches; motion toward right, positive.

*Note: Brakes on. Position control. Air bags inflated to 58 psi. Reference height of 7.88 inches.

Measured by UMTRI for Smart Truck
Freightliner Tractor

Data file: FRTLNG32.ERD

Drive Axle Suspension, Trailing Only

Lateral Force Steer

6 April 96
Suspension: Trailing Arm (2LU)

Suspension Load: 16000 lb.

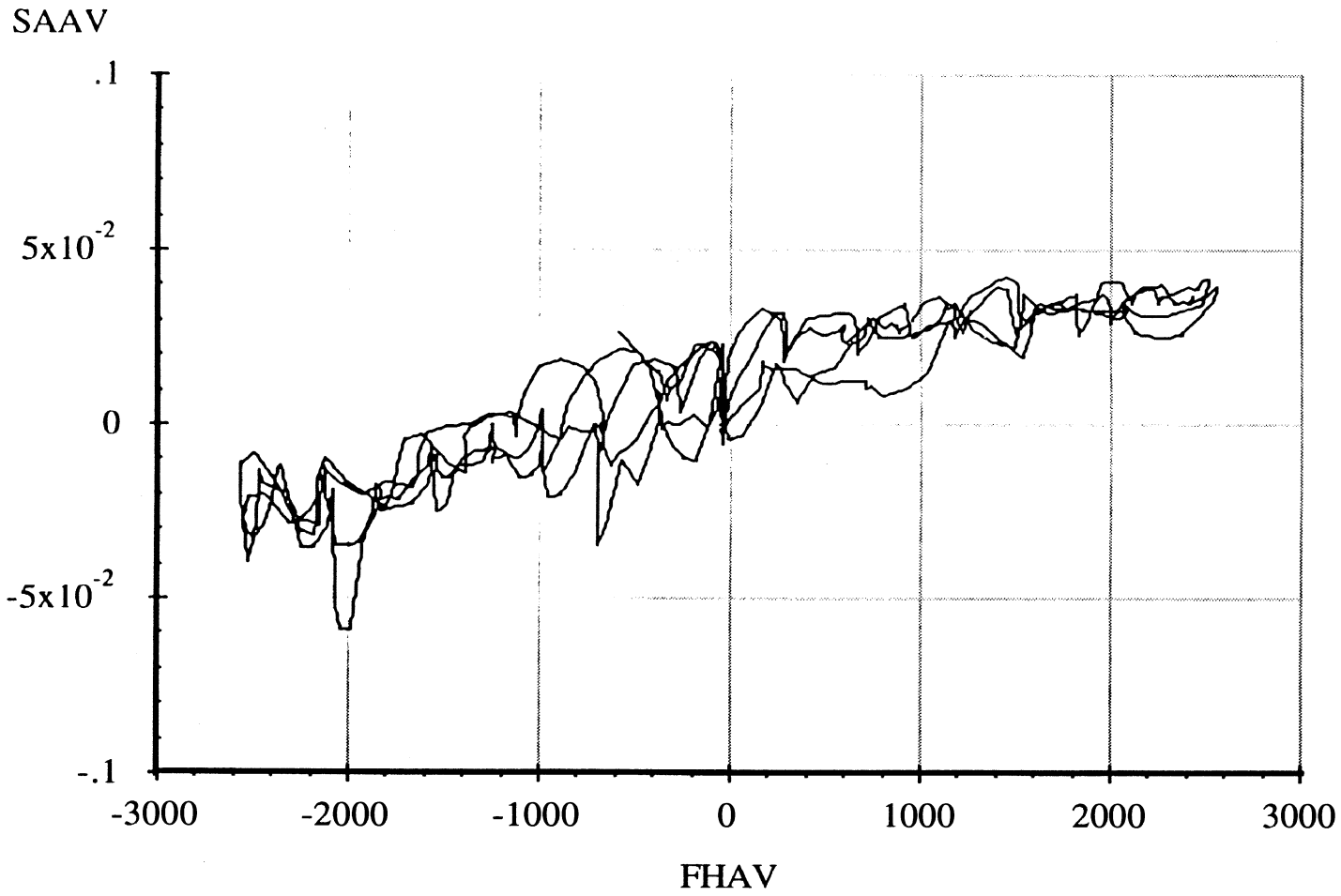

Abscissa (X): Average axle lateral force (FHAV); pounds; applied to both wheels simultaneously; force applied toward right, positive.

Ordinate (Y): Average steer angle (SAAV); degrees; steer toward right, positive.

*Note: Brakes on. Position control. Air bags inflated to 58 psi.

Measured by UMTRI for Smart Truck
Freightliner Tractor

Data file: FRTLNG33.ERD

Drive Axle Suspension, Trailing Only

Aligning Moment Compliance Steer

6 April 96
Suspension: Trailing Arm (2LU)

Suspension Load: 16000 lb.

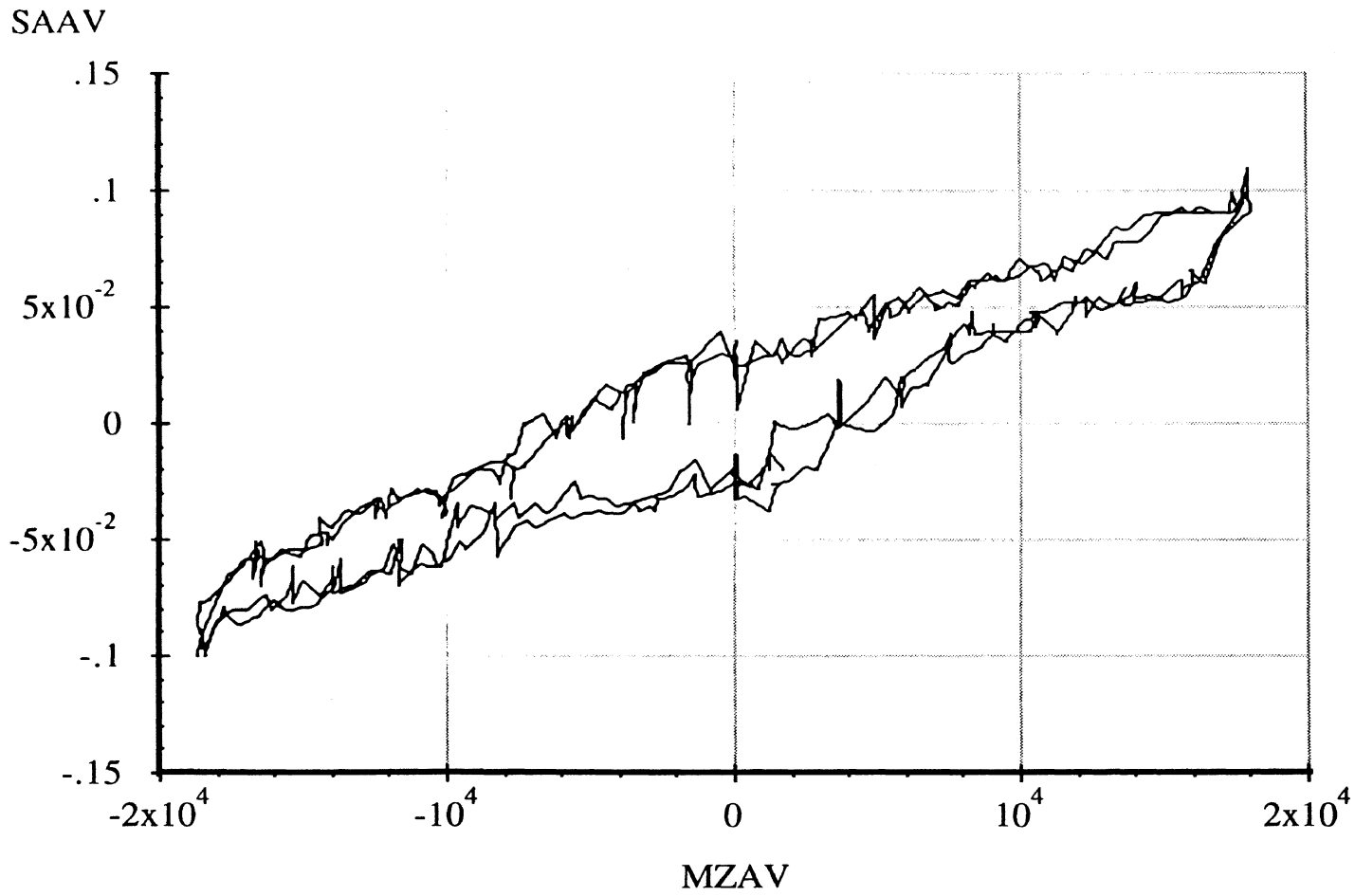

Abscissa (X): Average axle aligning moment (MZAV); in-lb per wheel; applied to both wheels simultaneously; downward (right hand rule) moment vector, positive.

Ordinate (Y): Average steer angle (SAAV); degrees; steer toward right, positive.

*Note: Brakes on. Position control. Air bags inflated to 58 psi.

Measured by UMTRI for Smart Truck
Freightliner Tractor

Data file: FRTLNG20.ERD

Drive Axle Suspension, Trailing Only

Average Vertical Spring Rate

6 April 96
Suspension: Trailing Arm (2LU)

Nominal Suspension Load: 14000 lb.

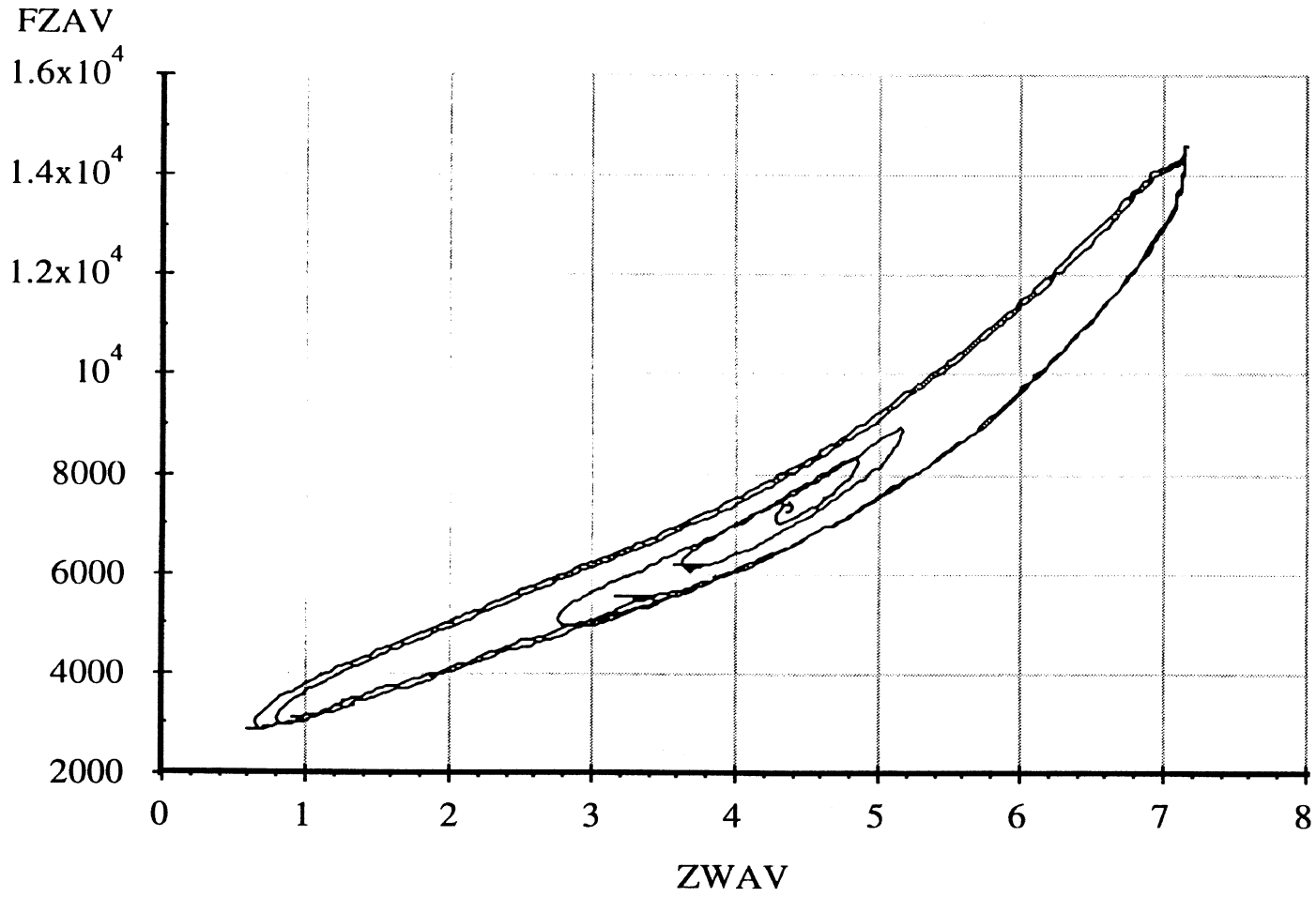

Abscissa (X): Average vertical wheel displacement (ZWAV); inches; spring compression, positive.

Ordinate (Y): Average vertical wheel load (FZAV); pounds; spring compression, positive.

*Note: Brakes on. Position control. Air bags inflated to 51 psi.

Measured by UMTRI for Smart Truck
Freightliner Tractor

Data file: FRTLNG21.ERD

Drive Axle Suspension, Trailing Only

Axle Roll Rate

6 April 96
Suspension: Trailing Arm (2LU)

Suspension Load: 14000 lb.

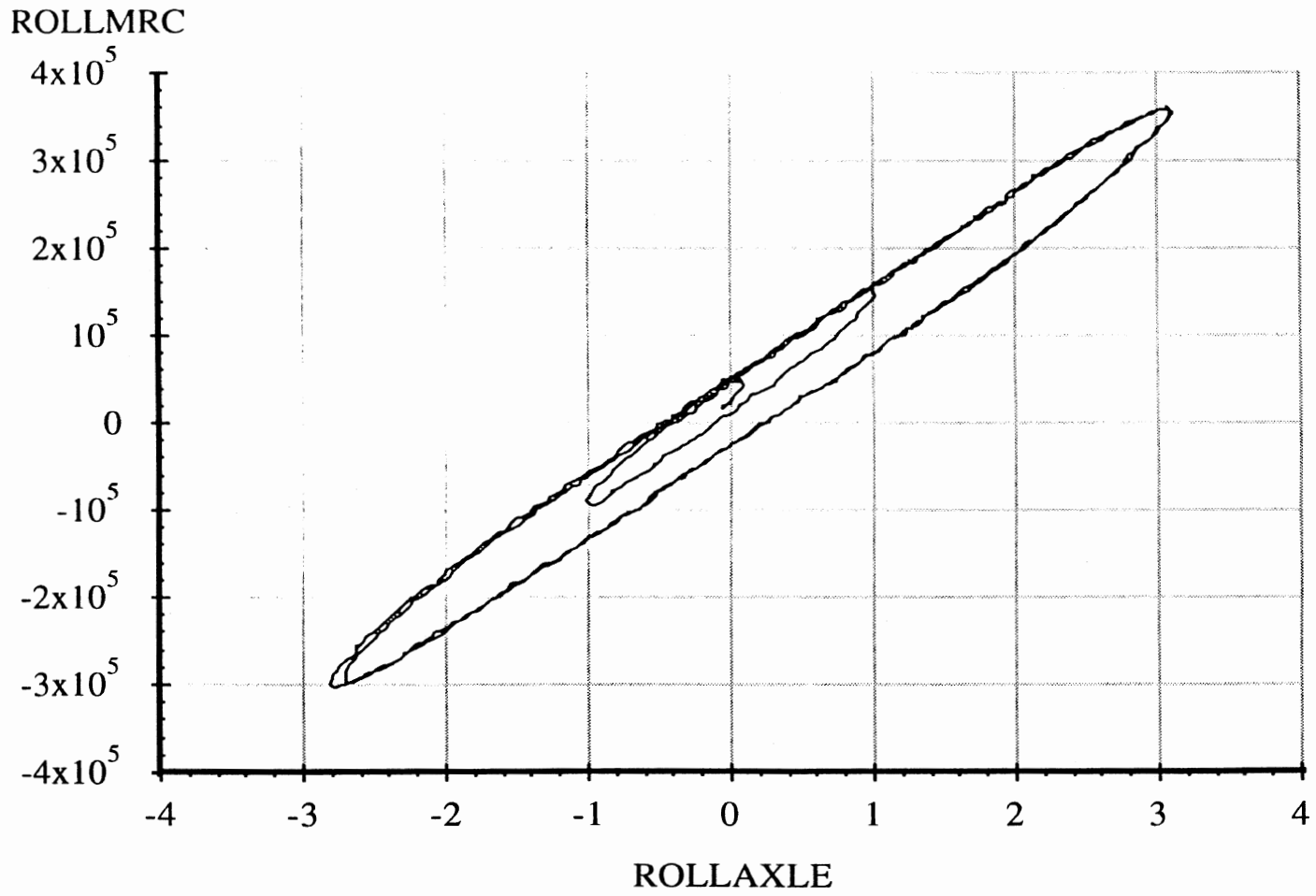

Abscissa (X): Axle roll angle (ROLLAXLE); degrees; right side compressed, positive.

Ordinate (Y): Axle roll moment about the roll center (ROLLMRC); in-lb; right side compressed, positive.

*Note: Brakes on. Force control. Air bags inflated to 51 psi.

Measured by UMTRI for Smart Truck
Freightliner Tractor

Data file: FRTLNG21.ERD

Drive Axle Suspension, Trailing Only

Roll Center Height

6 April 96
Suspension: Trailing Arm (2LU)

Suspension Load: 14000 lb.

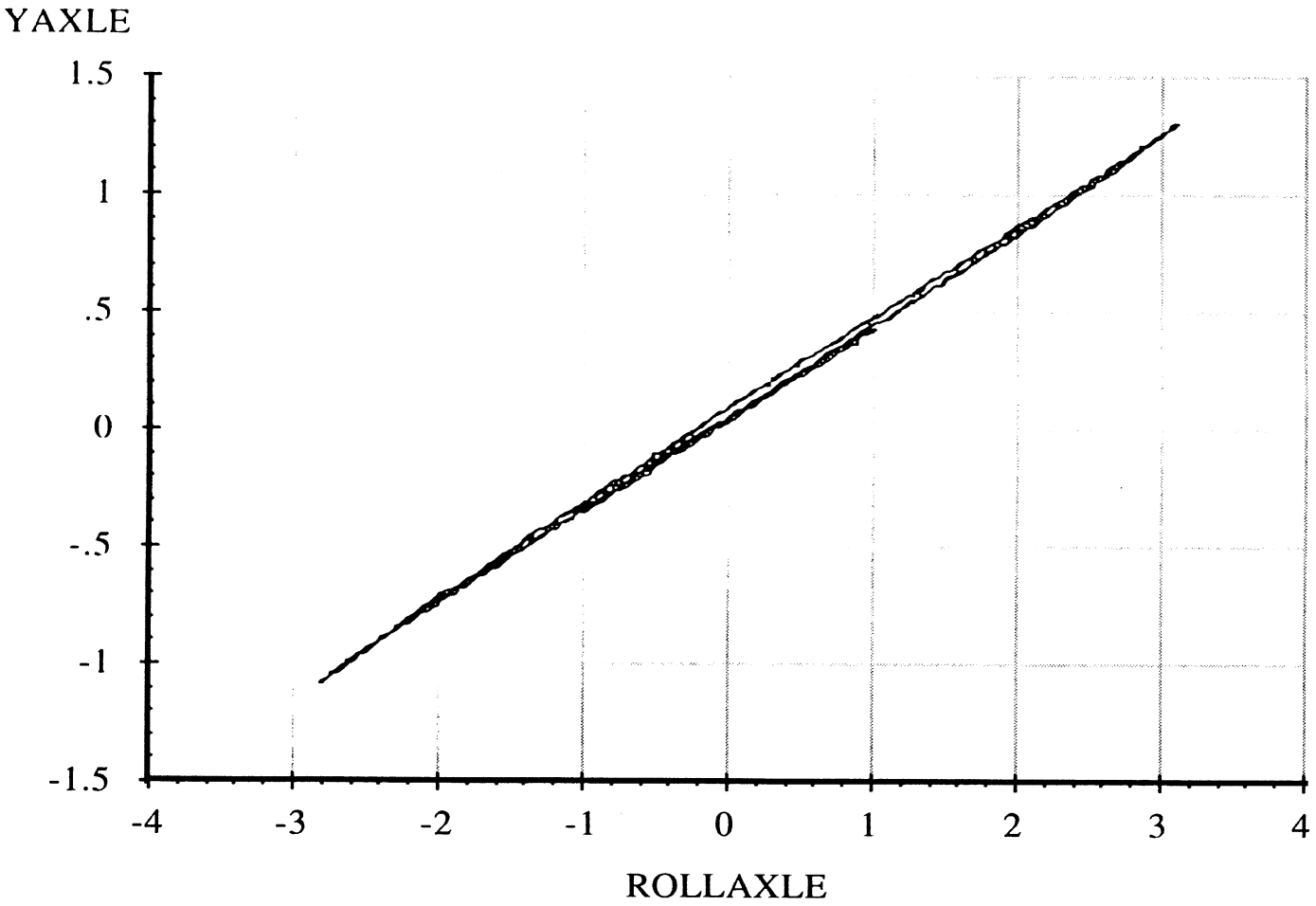

Abscissa (X): Axle roll angle (ROLLAXLE); degrees; right side compressed, positive.

Ordinate (Y): Axle reference point lateral translation (YAXLE); inches; motion toward right, positive.

*Note: Brakes on. Force control. Air bags inflated to 58 psi. Reference height of 8.00 inches.

Measured by UMTRI for Smart Truck
Freightliner Tractor

Data file: FRTLNG21.ERD

Drive Axle Suspension, Trailing Only

Roll Steer

6 April 96
Suspension: Trailing Arm (2LU)

Suspension Load: 14000 lb.

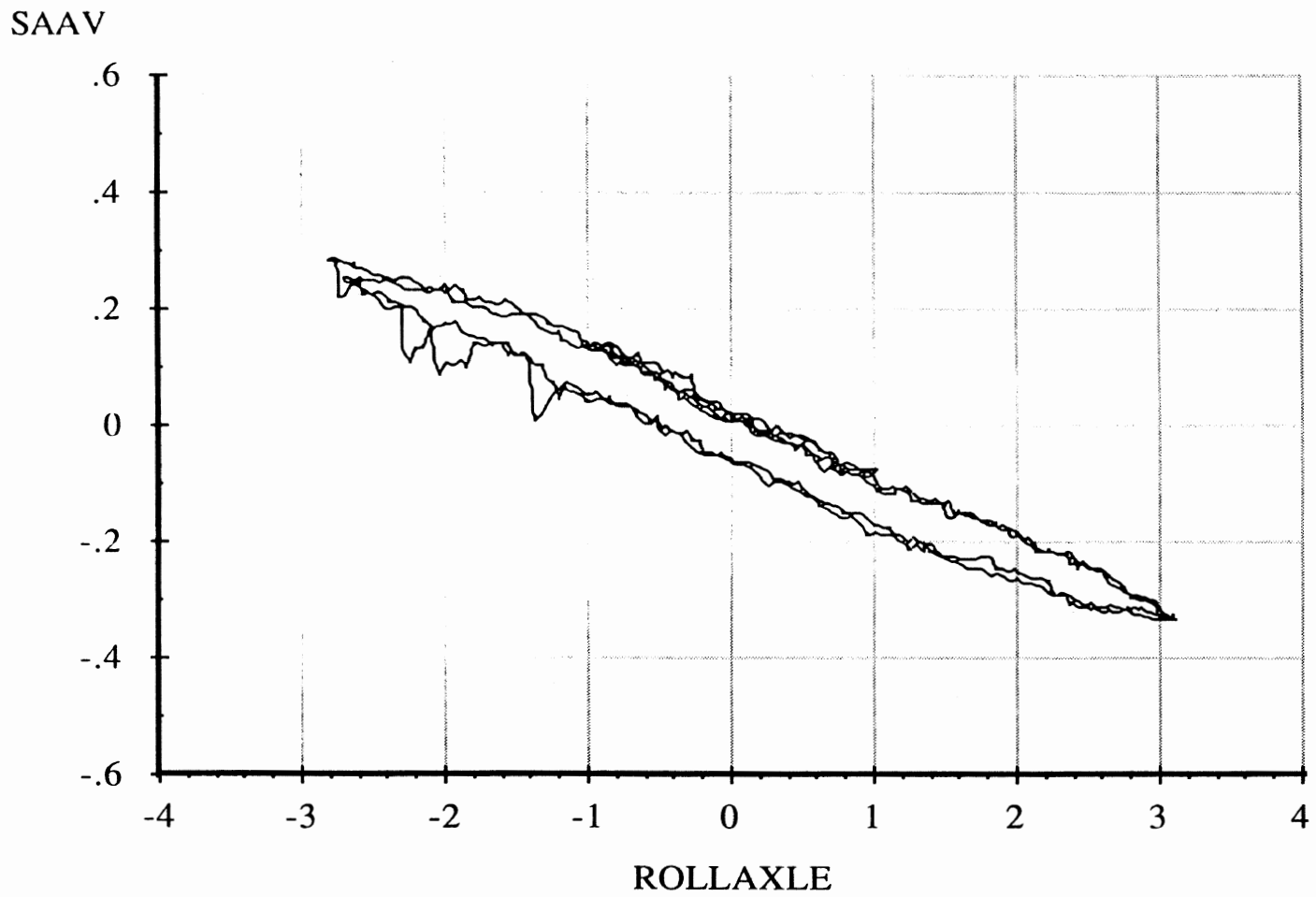

Abscissa (X): Axle roll angle (ROLLAXLE); degrees; right side compressed, positive.

Ordinate (Y): Average steer angle (SAAV); degrees; steer toward right, positive.

*Note: Brakes on. Force control. Air bags inflated to 51 psi.

Measured by UMTRI for Smart Truck
Freightliner Tractor

Data file: FRTLNG22.ERD

Drive Axle Suspension, Trailing Only

Lateral Force Compliance

6 April 96
Suspension: Trailing Arm (2LU)

Suspension Load: 14000 lb.

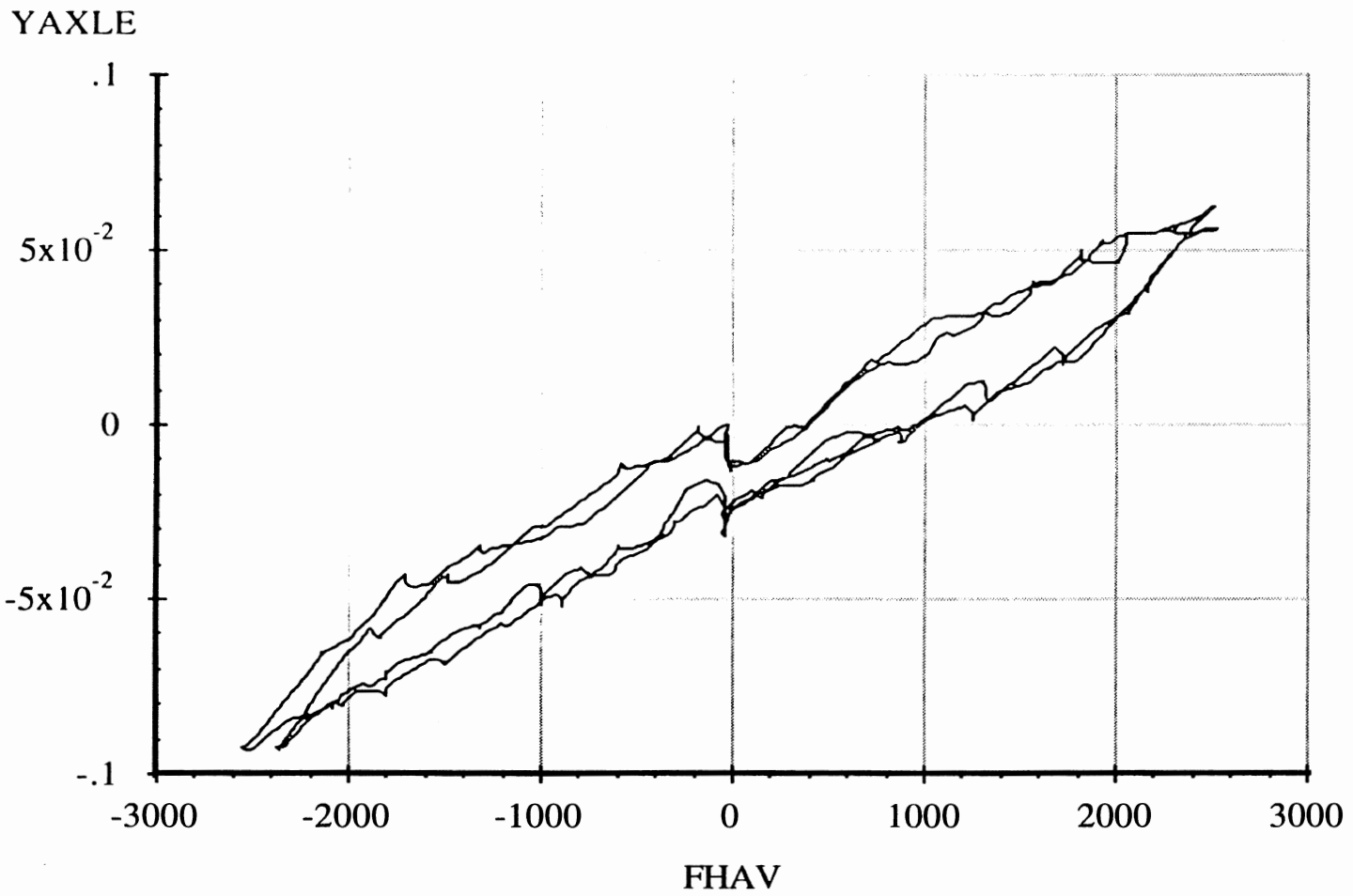

Abscissa (X): Average axle lateral force (FHAV); pounds; applied to both wheels simultaneously; force applied toward right, positive.

Ordinate (Y): Axle lateral translation (YAXLE); inches; motion toward right, positive.

*Note: Brakes on. Position control. Air bags inflated to 51 psi. Reference height of 8.00 inches.

Measured by UMTRI for Smart Truck
Freightliner Tractor

Data file: FRTLNG23.ERD

Drive Axle Suspension, Trailing Only

Aligning Moment Compliance Steer

6 April 96
Suspension: Trailing Arm (2LU)

Suspension Load: 14000 lb.

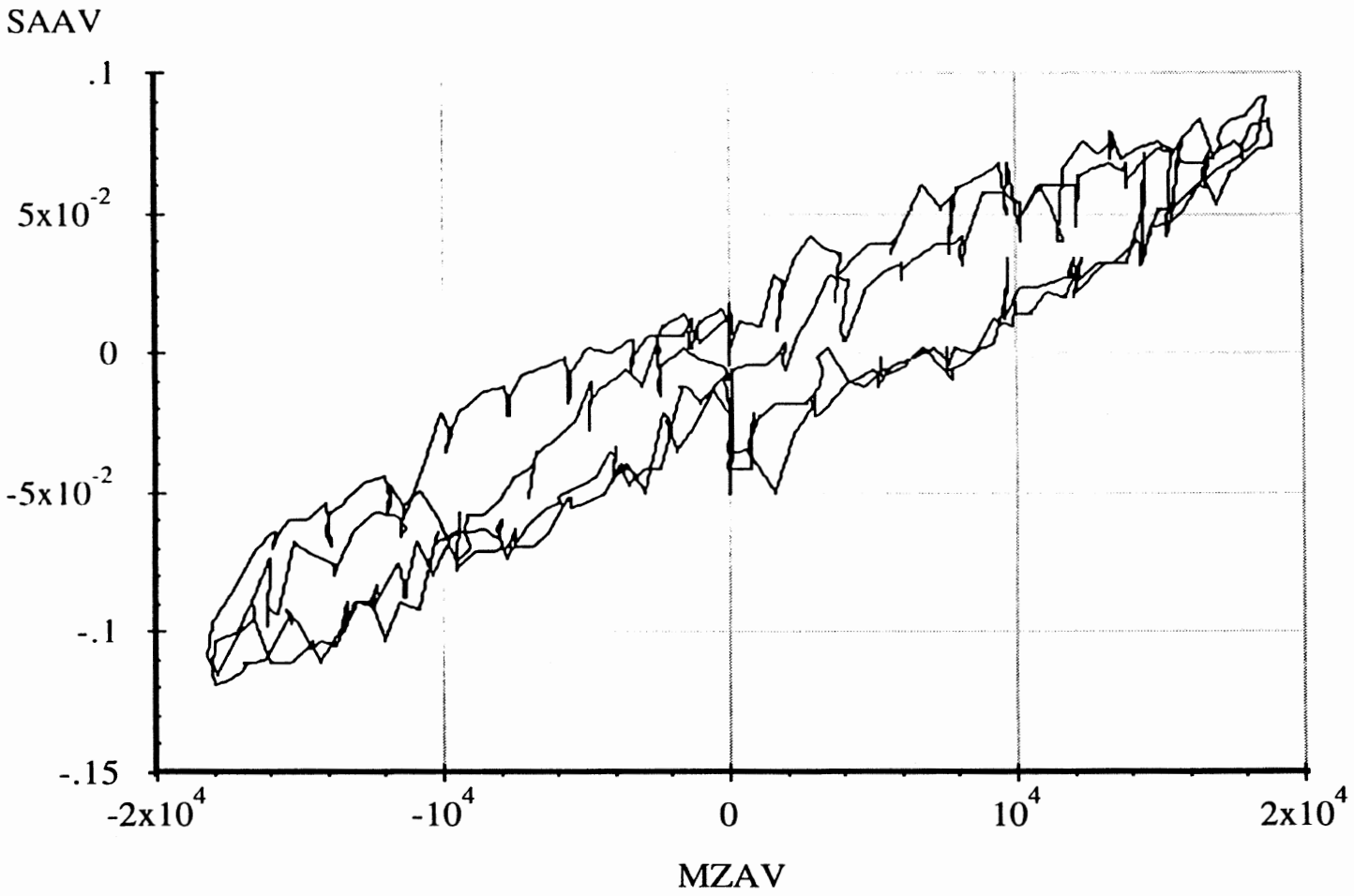

Abscissa (X): Average axle aligning moment (MZAV); in-lb per wheel; applied to both wheels simultaneously; downward (right hand rule) moment vector, positive.

Ordinate (Y): Average steer angle (SAAV); degrees; steer toward right, positive.

*Note: Brakes on. Position control. Air bags inflated to 51 psi.

Measured by UMTRI for Smart Truck
Freightliner Tractor

Data file: FRTLNG00.ERD

Drive Axle Suspension, Trailing Only

Average Vertical Spring Rate

6 April 96
Suspension: Trailing Arm (2LU)

Nominal Suspension Load: 8000 lb.

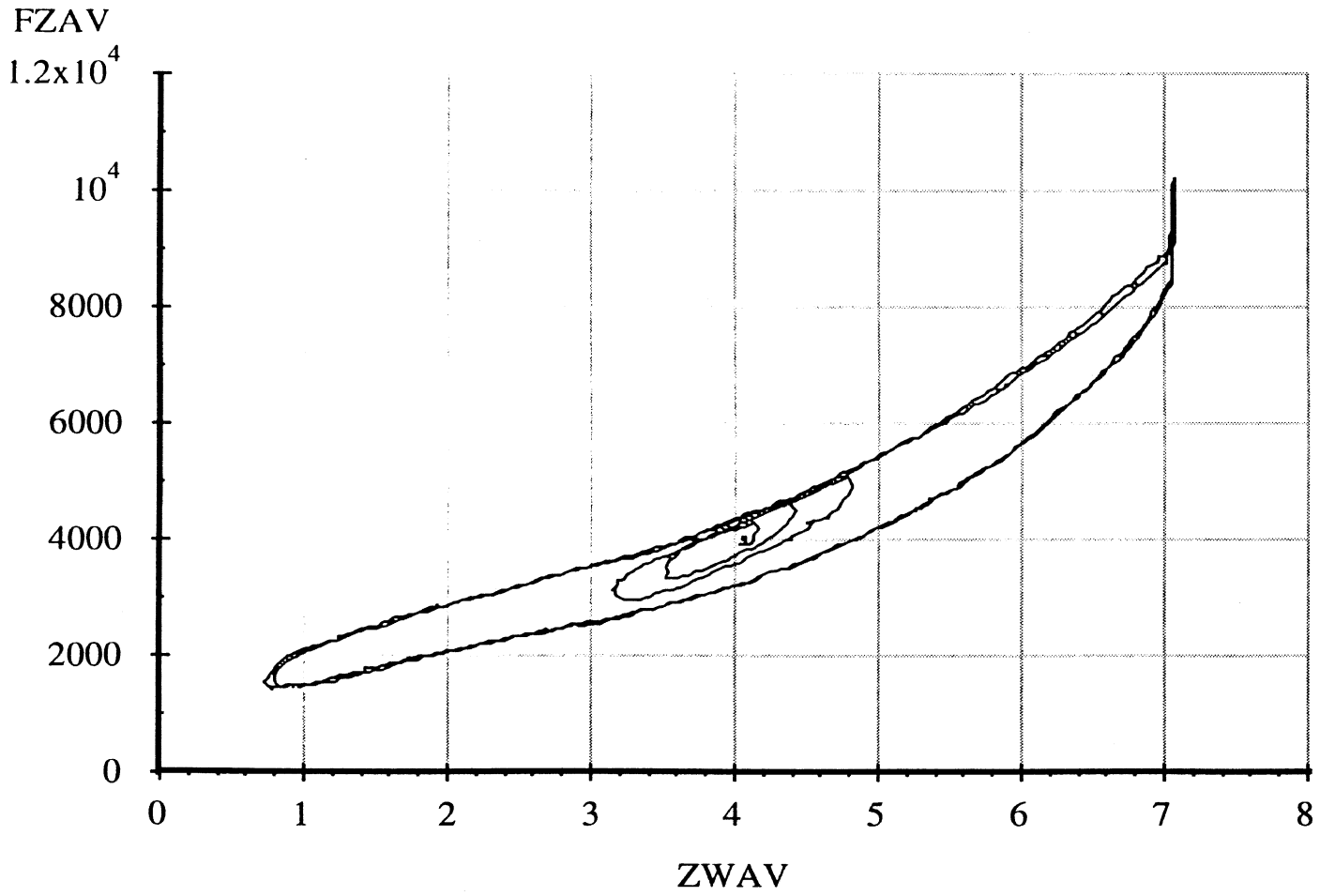

Abscissa (X): Average vertical wheel displacement (ZWAV); inches; spring compression, positive.

Ordinate (Y): Average vertical wheel load (FZAV); pounds; spring compression, positive.

*Note: Brakes on. Position control. Air bags inflated to 26 psi. Low side of vertical.

Measured by UMTRI for Smart Truck
Freightliner Tractor

Data file: FRTLNG01.ERD

Drive Axle Suspension, Trailing Only

Axle Roll Rate

6 April 96
Suspension: Trailing Arm (2LU)

Suspension Load: 8000 lb.

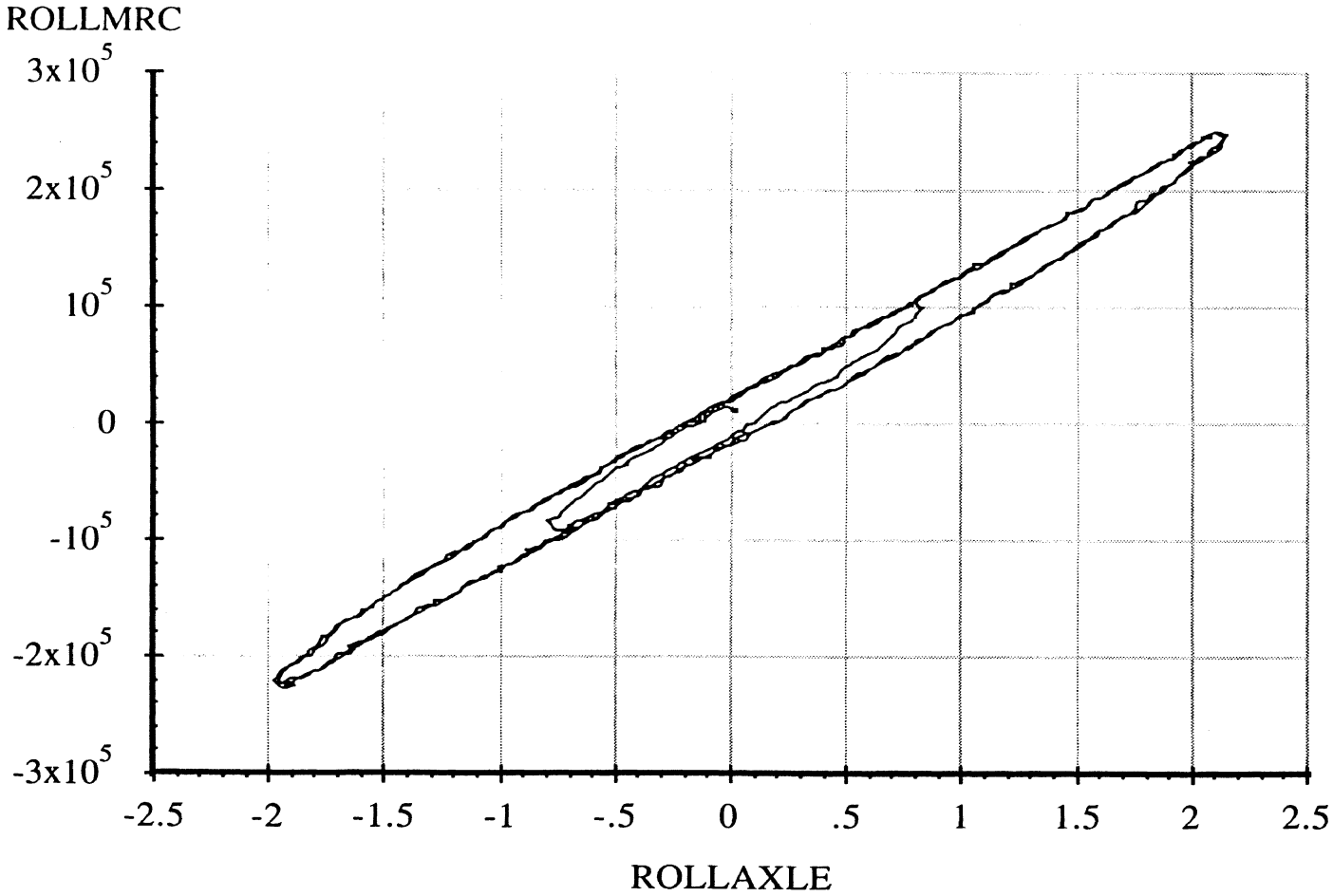

Abscissa (X): Axle roll angle (ROLLAXLE); degrees; right side compressed, positive.

Ordinate (Y): Axle roll moment about the roll center (ROLLMRC); in-lb; right side compressed, positive.

*Note: Brakes on. Force control. Air bags inflated to 26 psi.

Measured by UMTRI for Smart Truck
Freightliner Tractor

Data file: FRTLNG01.ERD

Drive Axle Suspension, Trailing Only

Roll Center Height

6 April 96
Suspension: Trailing Arm (2LU)

Suspension Load: 8000 lb.

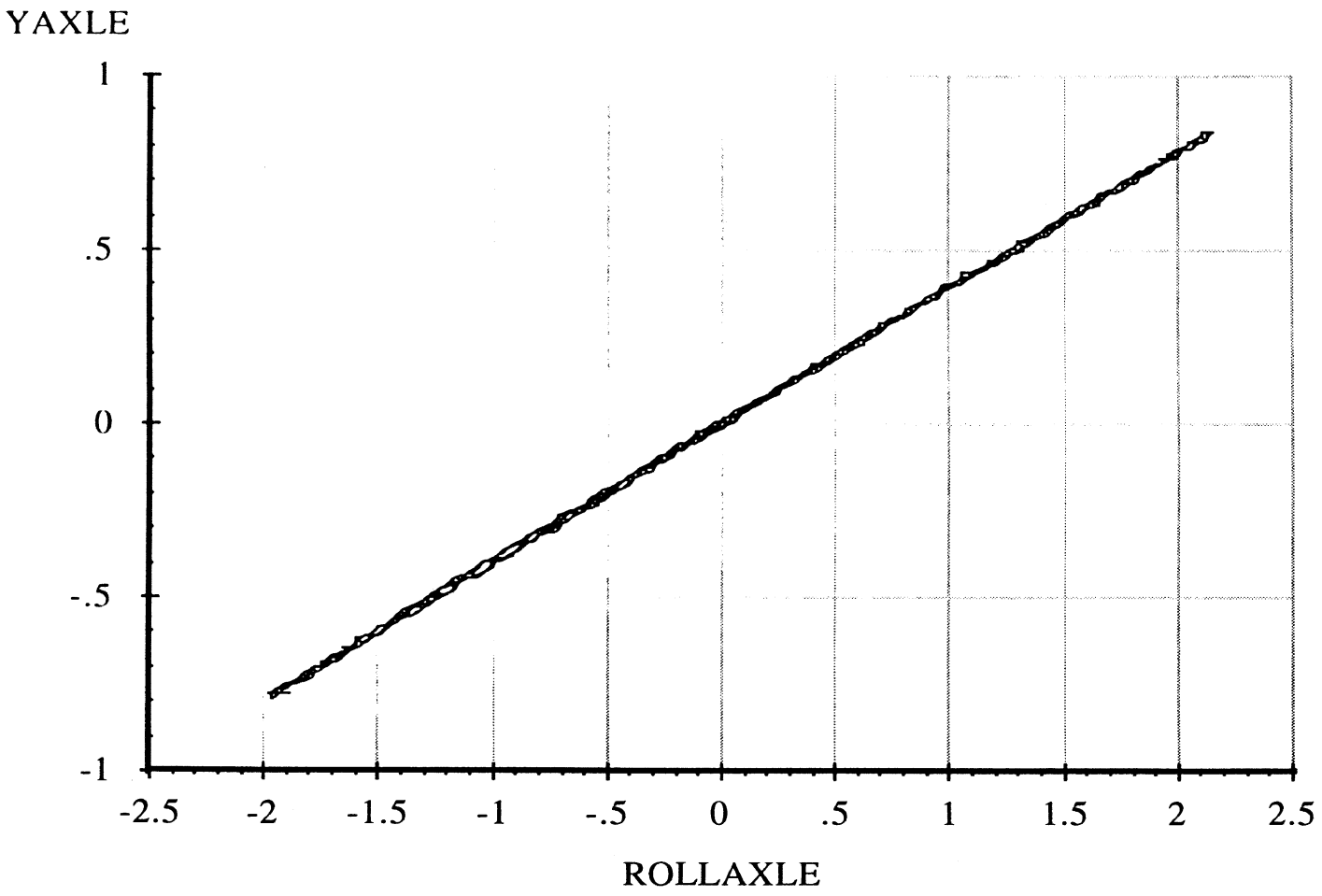

Abscissa (X): Axle roll angle (ROLLAXLE); degrees; right side compressed, positive.

Ordinate (Y): Axle reference point lateral translation (YAXLE); inches; motion toward right, positive.

*Note: Brakes on. Force control. Air bags inflated to 26 psi. Reference height of 8.31 inches.

Measured by UMTRI for Smart Truck
Freightliner Tractor

Data file: FRTLNG01.ERD

Drive Axle Suspension, Trailing Only

Roll Steer

6 April 96
Suspension: Trailing Arm (2LU)

Suspension Load: 8000 lb.

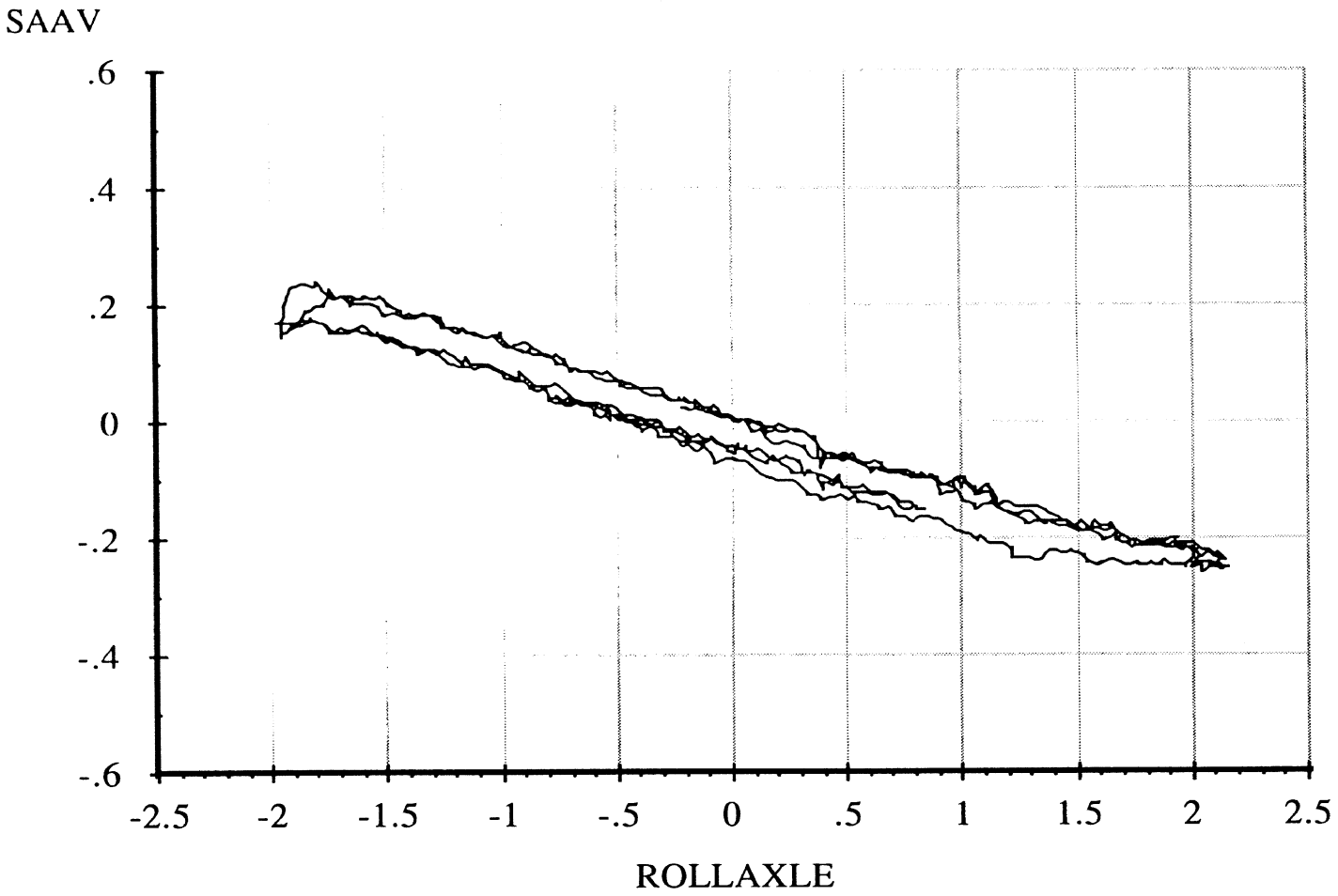

Abscissa (X): Axle roll angle (ROLLAXLE); degrees; right side compressed, positive.

Ordinate (Y): Average steer angle (SAAV); degrees; steer toward right, positive.

*Note: Brakes on. Force control. Air bags inflated to 26 psi.

Measured by UMTRI for Smart Truck
Freightliner Tractor

Data file: FRTLNG02.ERD

Drive Axle Suspension, Trailing Only

Lateral Force Compliance

6 April 96
Suspension: Trailing Arm (2LU)

Suspension Load: 8000 lb.

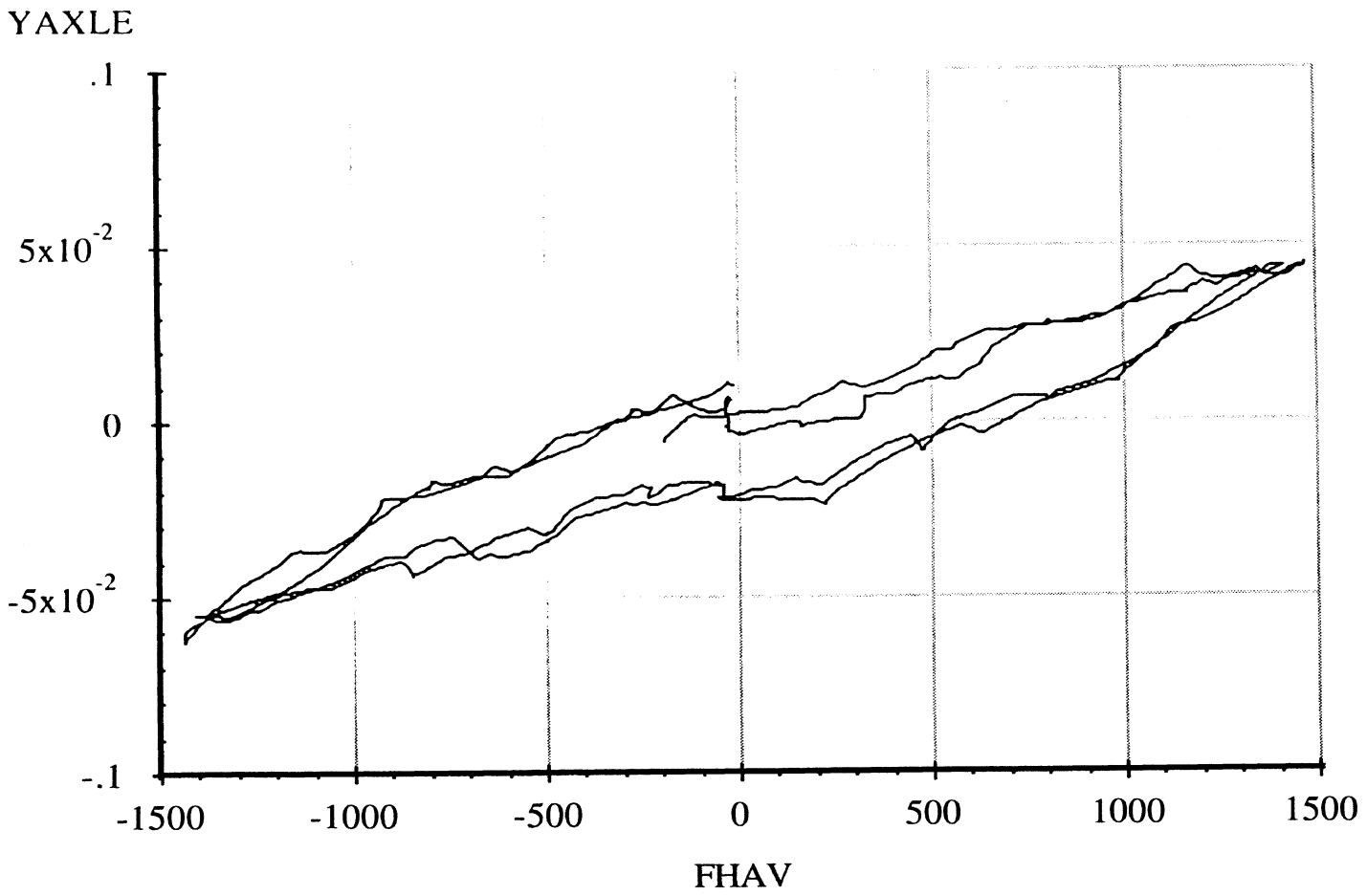

Abscissa (X): Average axle lateral force (FHAV); pounds; applied to both wheels simultaneously; force applied toward right, positive.

Ordinate (Y): Axle lateral translation (YAXLE); inches; motion toward right, positive.

*Note: Brakes on. Position control. Air bags inflated to 26 psi. Reference height of 8.31 inches.

Measured by UMTRI for Smart Truck
Freightliner Tractor

Data file: FRTLNG02.ERD

Drive Axle Suspension, Trailing Only

Lateral Force Steer

6 April 96
Suspension: Trailing Arm (2LU)

Suspension Load: 8000 lb.

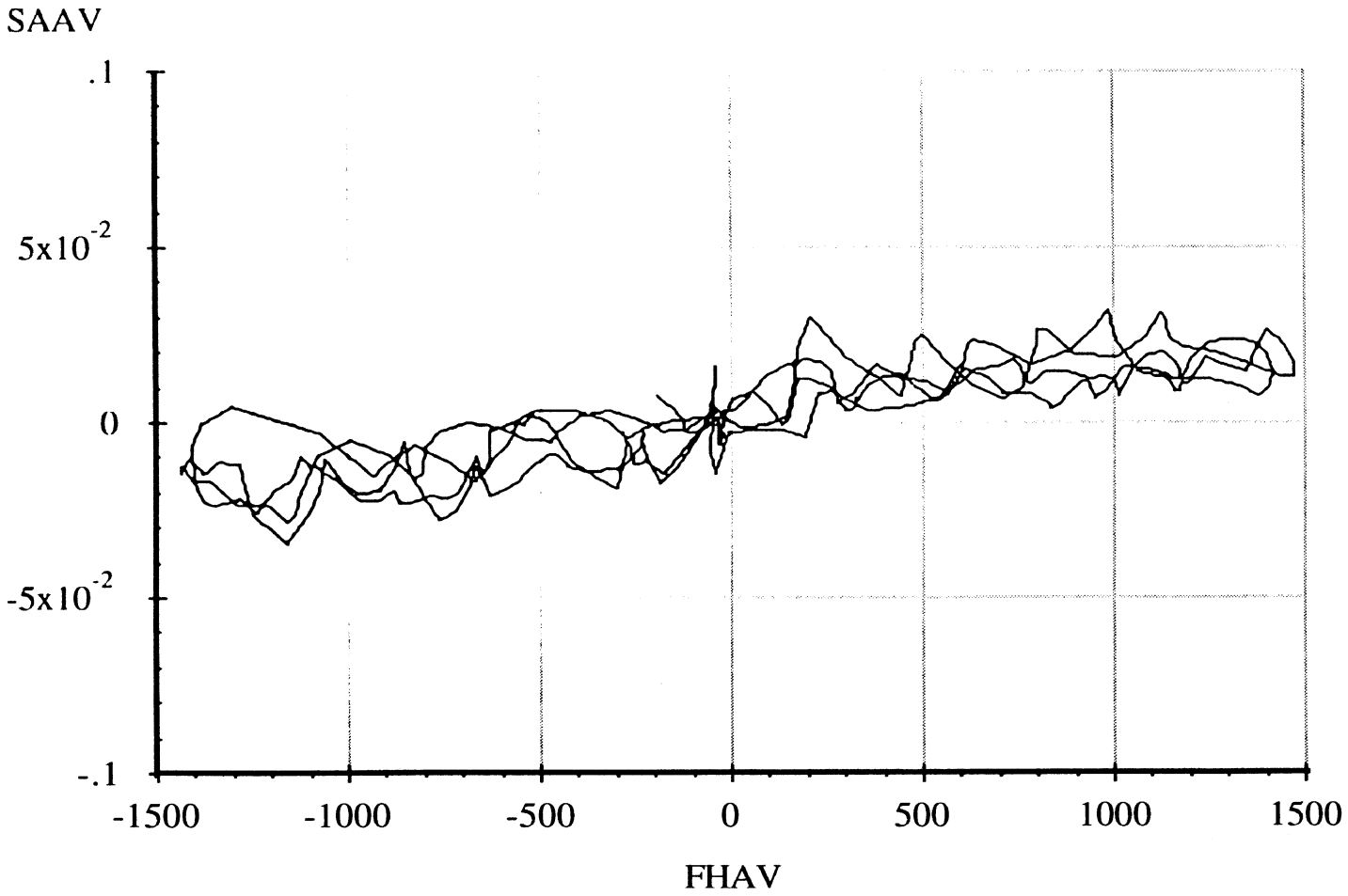

Abscissa (X): Average axle lateral force (FHAV); pounds; applied to both wheels simultaneously; force applied toward right, positive.

Ordinate (Y): Average steer angle (SAAV); degrees; steer toward right, positive.

*Note: Brakes on. Position control. Air bags inflated to 26 psi.

Measured by UMTRI for Smart Truck
Freightliner Tractor

Data file: FRTLNG03.ERD

Drive Axle Suspension, Trailing Only

Aligning Moment Compliance Steer

6 April 96
Suspension: Trailing Arm (2LU)

Suspension Load: 8000 lb.

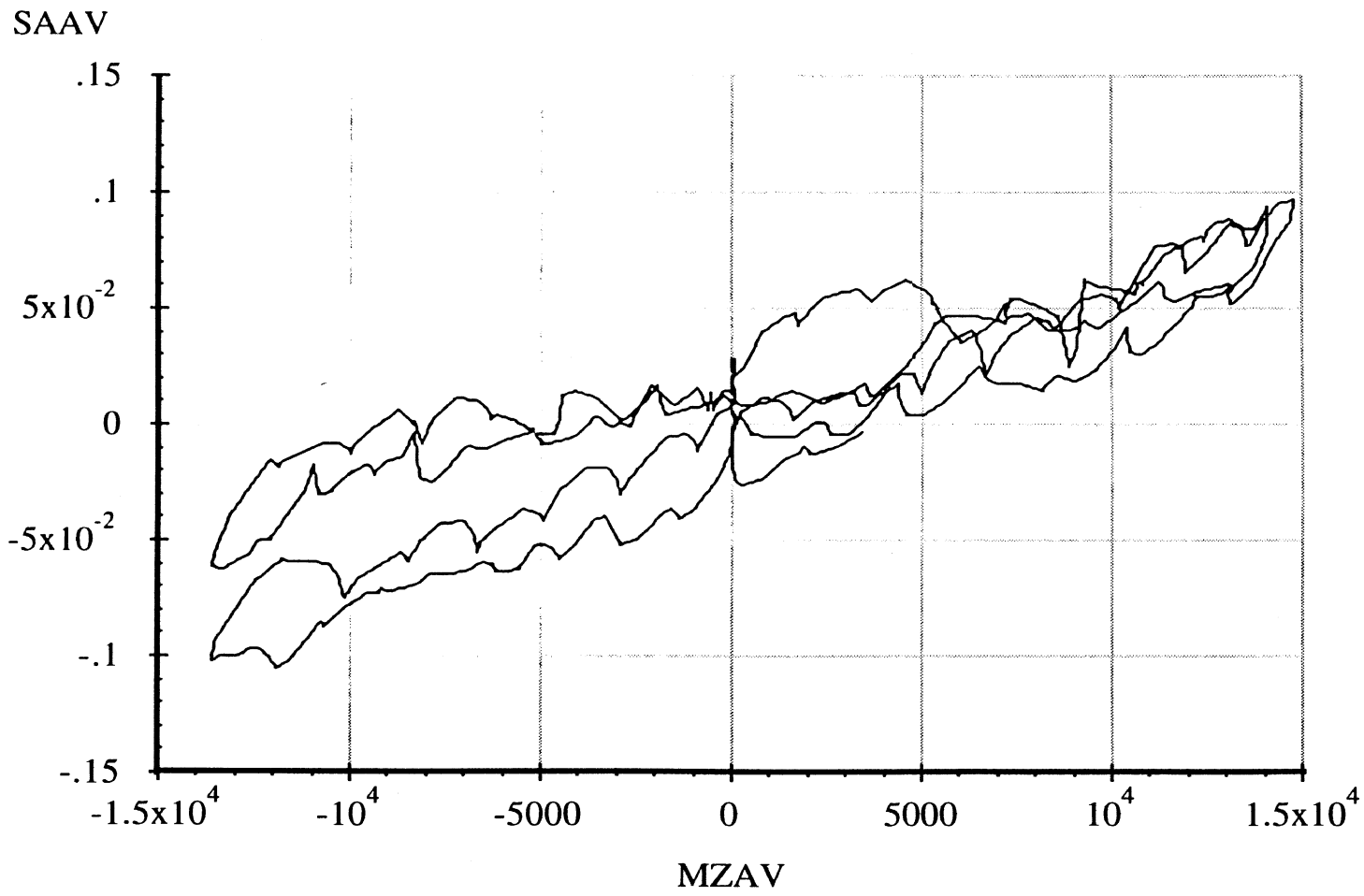

Abscissa (X): Average axle aligning moment (MZAV); in-lb per wheel; applied to both wheels simultaneously; downward (right hand rule) moment vector, positive.

Ordinate (Y): Average steer angle (SAAV); degrees; steer toward right, positive.

*Note: Brakes on. Position control. Air bags inflated to 26 psi.

Measured by UMTRI for Smart Truck
Freightliner Tractor

Data file: FRTLNG00.ERD

Drive Axle Suspension, Trailing Only

Average Vertical Spring Rate

6 April 96
Suspension: Trailing Arm (2LU)

Nominal Suspension Load: 4000 lb.

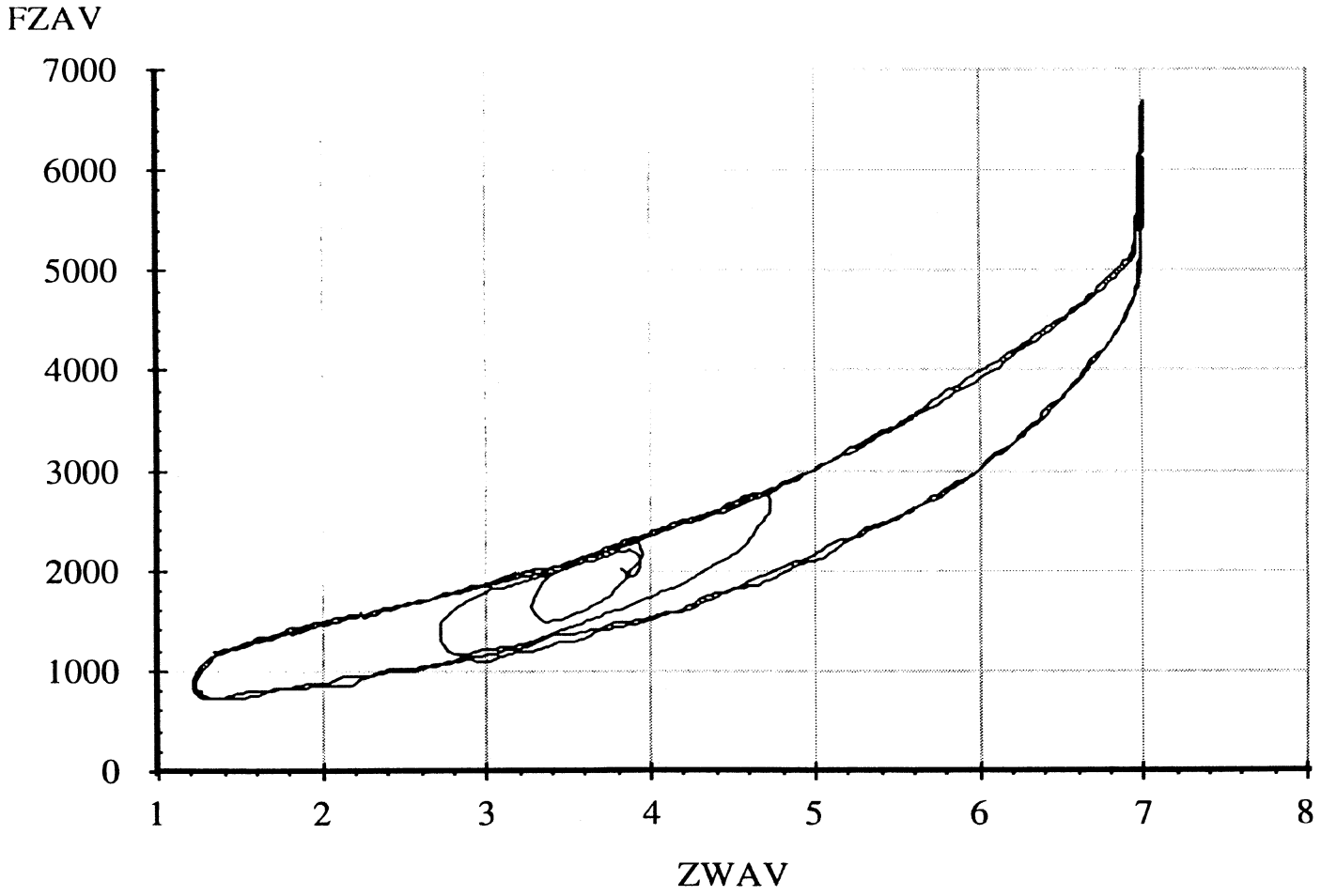

Abscissa (X): Average vertical wheel displacement (ZWAV); inches; spring compression, positive.

Ordinate (Y): Average vertical wheel load (FZAV); pounds; spring compression, positive.

*Note: Brakes on. Position control. Air bags inflated to 8 psi.

Measured by UMTRI for Smart Truck
Freightliner Tractor

Data file: FRTLNG11.ERD

Drive Axle Suspension, Trailing Only

Axle Roll Rate

6 April 96
Suspension: Trailing Arm (2LU)

Suspension Load: 4000 lb.

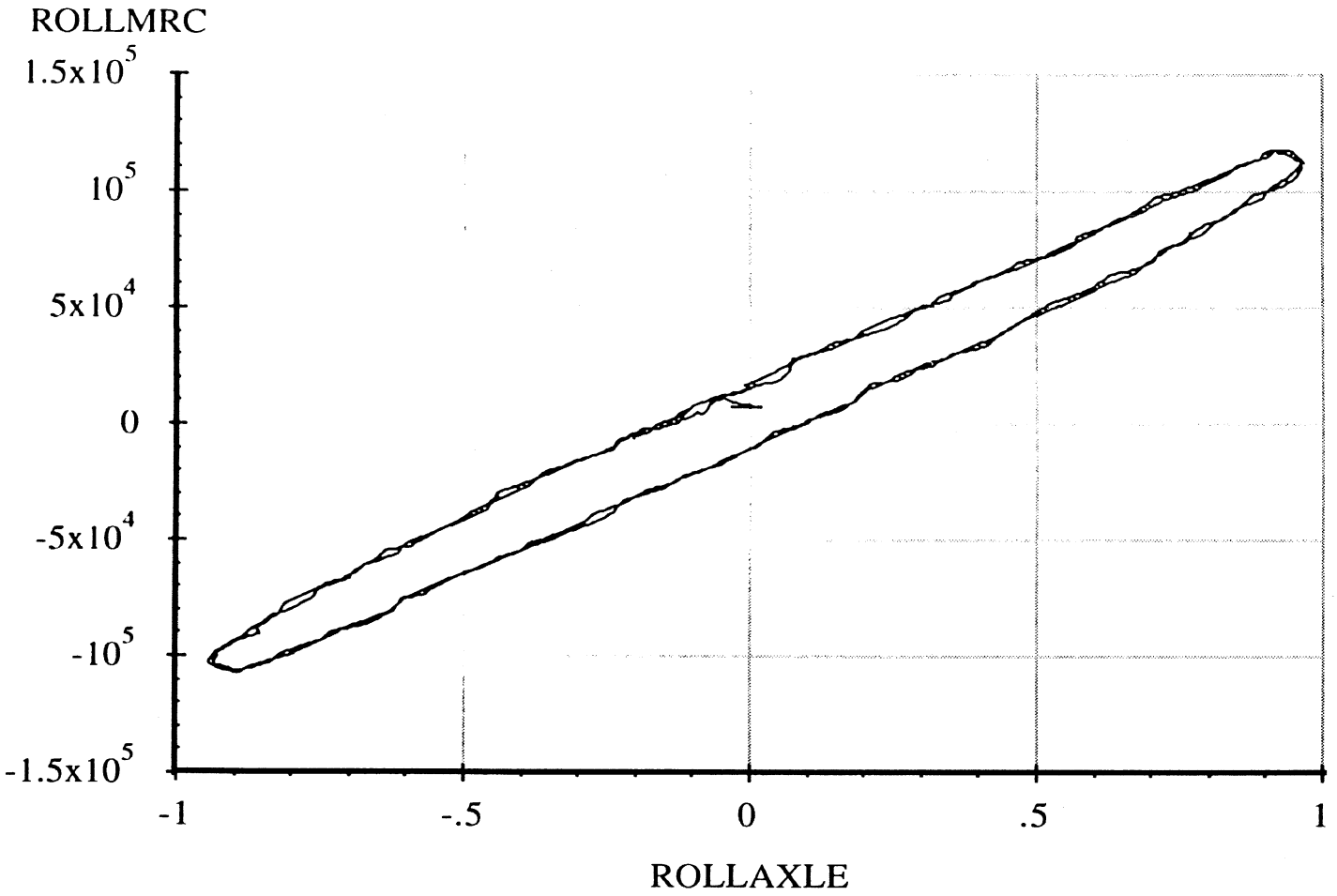

Abscissa (X): Axle roll angle (ROLLAXLE); degrees; right side compressed, positive.

Ordinate (Y): Axle roll moment about the roll center (ROLLMRC); in-lb; right side compressed, positive.

*Note: Brakes on. Force control. Air bags inflated to 8 psi.

Measured by UMTRI for Smart Truck
Freightliner Tractor

Data file: FRTLNG11.ERD

Drive Axle Suspension, Trailing Only

Roll Center Height

6 April 96
Suspension: Trailing Arm (2LU)

Suspension Load: 4000 lb.

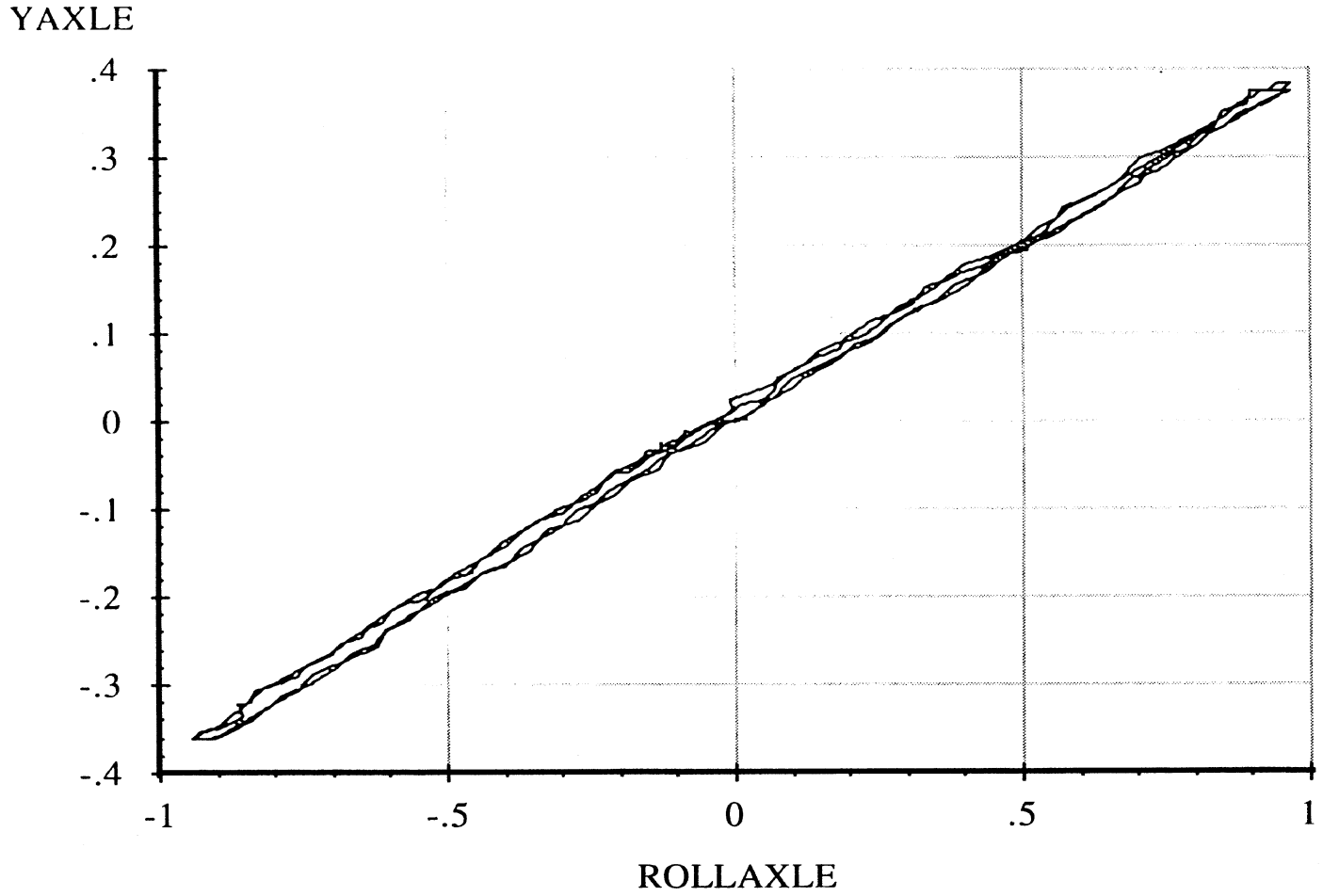

Abscissa (X): Axle roll angle (ROLLAXLE); degrees; right side compressed, positive.

Ordinate (Y): Axle reference point lateral translation (YAXLE); inches; motion toward right, positive.

*Note: Brakes on. Force control. Air bags inflated to 8 psi. Reference height of 8.56 inches.

Measured by UMTRI for Smart Truck
Freightliner Tractor

Data file: FRTLNG11.ERD

Drive Axle Suspension, Trailing Only

Roll Steer

6 April 96
Suspension: Trailing Arm (2LU)

Suspension Load: 4000 lb.

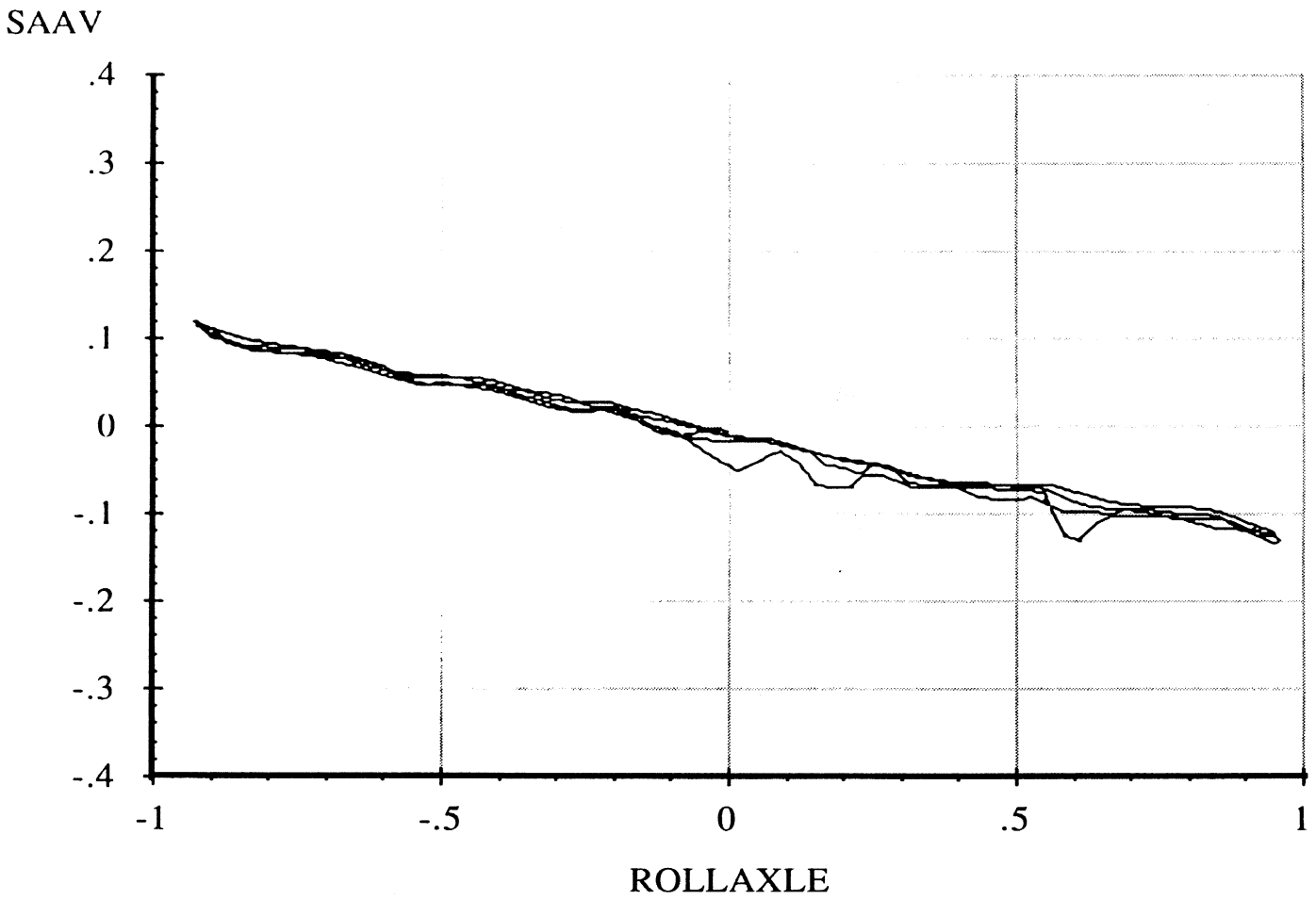

Abscissa (X): Axle roll angle (ROLLAXLE); degrees; right side compressed, positive.

Ordinate (Y): Average steer angle (SAAV); degrees; steer toward right, positive.

*Note: Brakes on. Force control. Air bags inflated to 8 psi.

Measured by UMTRI for Smart Truck
Freightliner Tractor

Data file: FRTLNG12.ERD

Drive Axle Suspension, Trailing Only

Lateral Force Compliance

6 April 96
Suspension: Trailing Arm (2LU)

Suspension Load: 4000 lb.

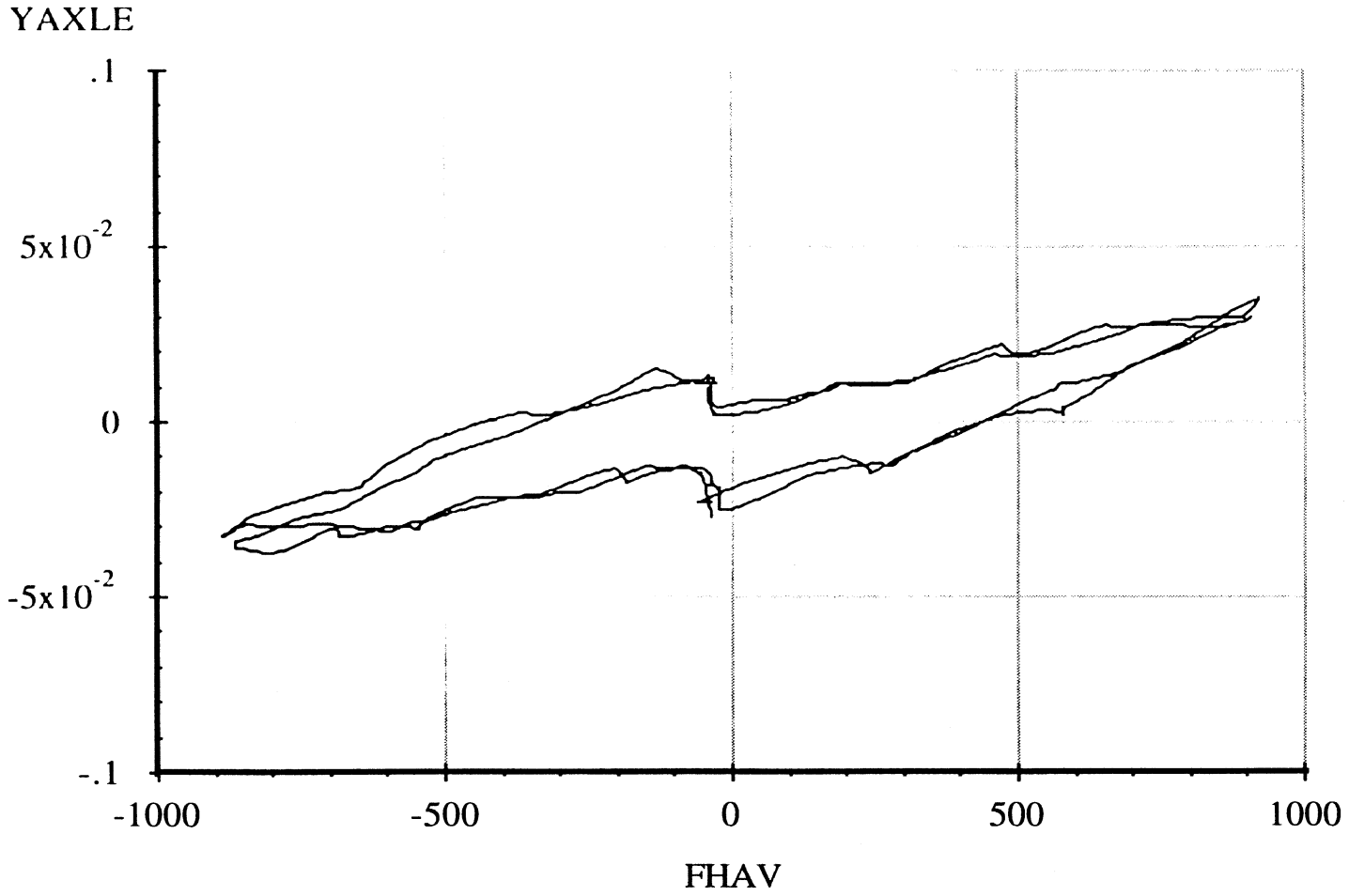

Abscissa (X): Average axle lateral force (FHAV); pounds; applied to both wheels simultaneously; force applied toward right, positive.

Ordinate (Y): Axle lateral translation (YAXLE); inches; motion toward right, positive.

*Note: Brakes on. Position control. Air bags inflated to 8 psi. Reference height of 8.56 inches.

Measured by UMTRI for Smart Truck
Freightliner Tractor

Data file: FRTLNG12.ERD

Drive Axle Suspension, Trailing Only

Lateral Force Steer

6 April 96
Suspension: Trailing Arm (2LU)

Suspension Load: 4000 lb.

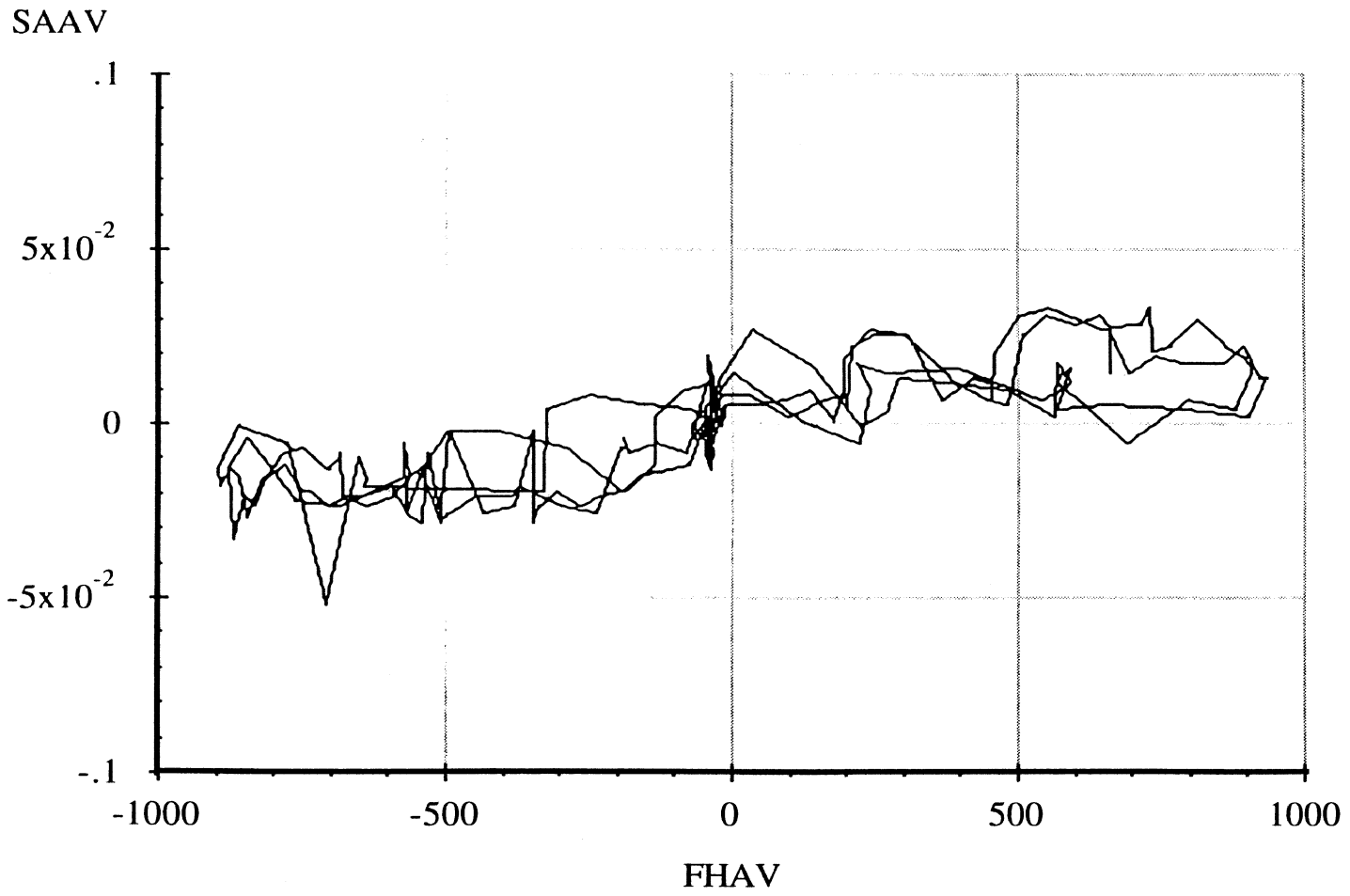

Abscissa (X): Average axle lateral force (FHAV); pounds; applied to both wheels simultaneously; force applied toward right, positive.

Ordinate (Y): Average steer angle (SAAV); degrees; steer toward right, positive.

*Note: Brakes on. Position control. Air bags inflated to 8 psi.

Measured by UMTRI for Smart Truck
Freightliner Tractor

Data file: FRTLNG13.ERD

Drive Axle Suspension, Trailing Only

Aligning Moment Compliance Steer

6 April 96
Suspension: Trailing Arm (2LU)

Suspension Load: 4000 lb.

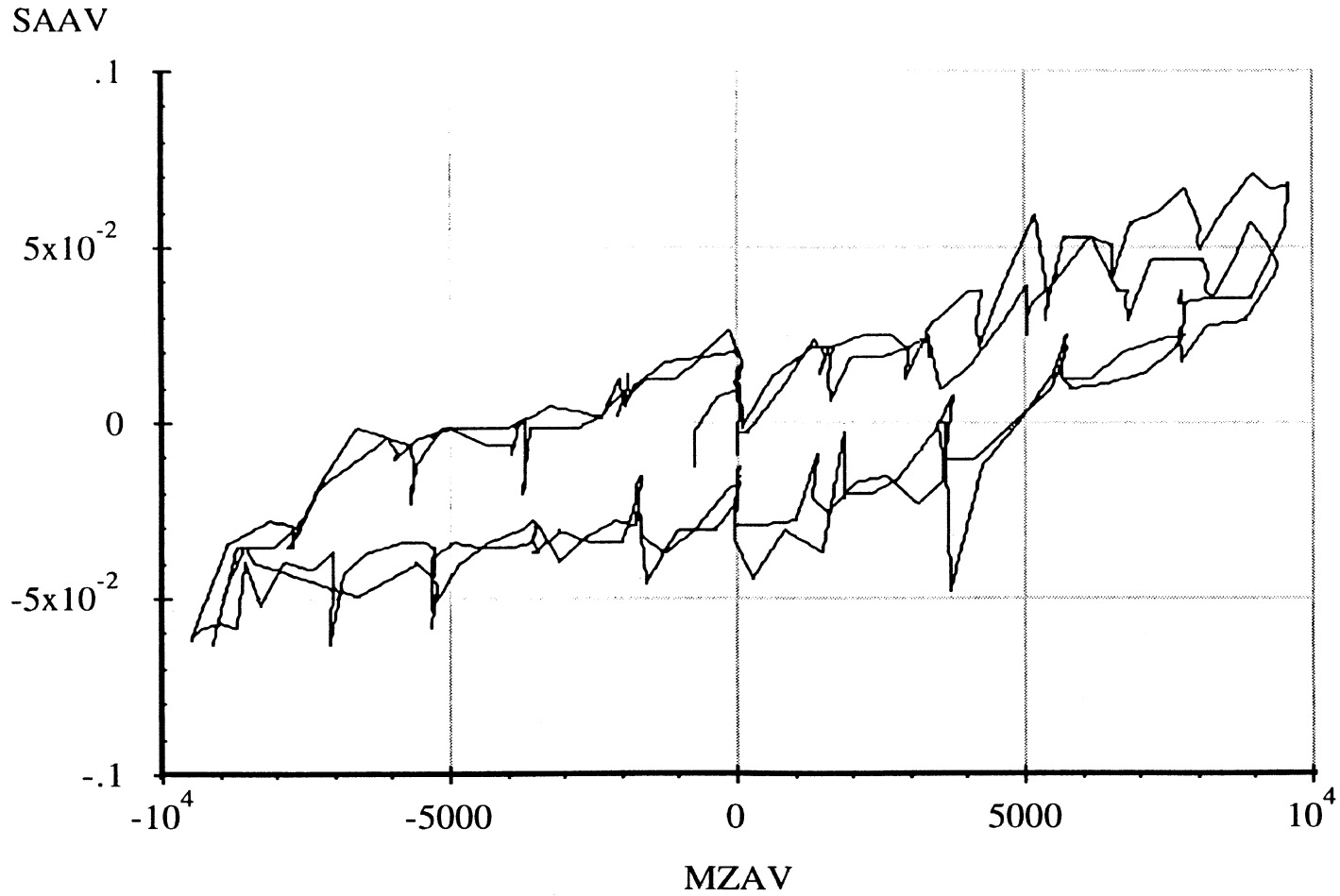

Abscissa (X): Average axle aligning moment (MZAV); in-lb per wheel; applied to both wheels simultaneously; downward (right hand rule) moment vector, positive.

Ordinate (Y): Average steer angle (SAAV); degrees; steer toward right, positive.

*Note: Brakes on. Position control. Air bags inflated to 8 psi.

Measured by UMTRI for Smart Truck
Fruehauf Model FBB9-F1-28

Data file: SMTTRL05.ERD

Single Trailer Axle Suspension

Average Vertical Spring Rate

4 Jan 98
Suspension: Trailing Arm (WT)

Nominal Suspension Load: 25800 lb.

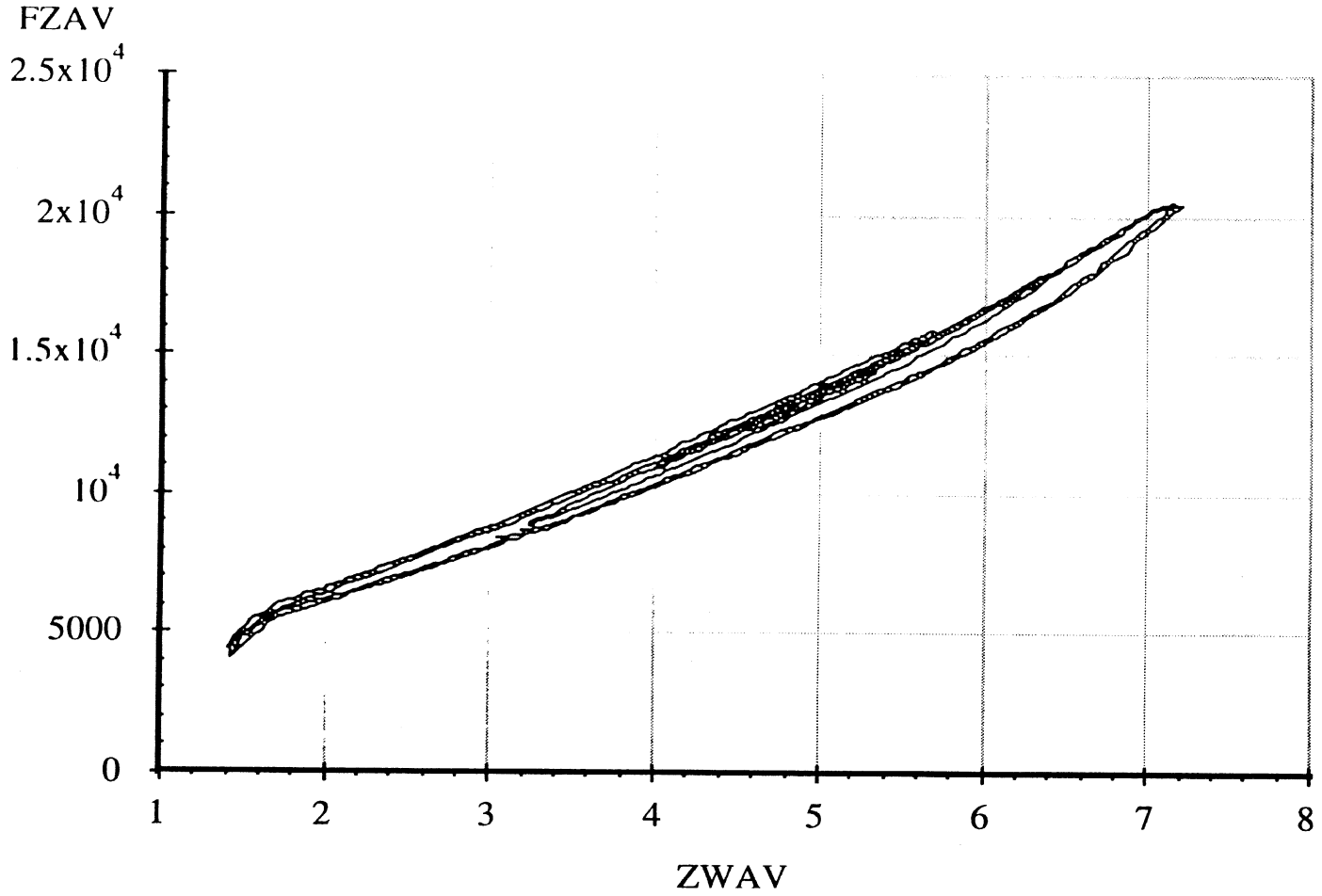

Abscissa (X): Average vertical wheel displacement (ZWAV); inches; spring compression, positive.

Ordinate (Y): Average vertical wheel load (FZAV); pounds; spring compression, positive.

*Note: Brakes on. Position control. Air bags inflated to 100 psi.

Measured by UMTRI for Smart Truck
Fruehauf Model FBB9-F1-28

Data file: SMTTRL15.ERD

Single Trailer Axle Suspension

Axle Roll Rate

4 Jan 98
Suspension: Trailing Arm (WT)

Suspension Load: 25800 lb.

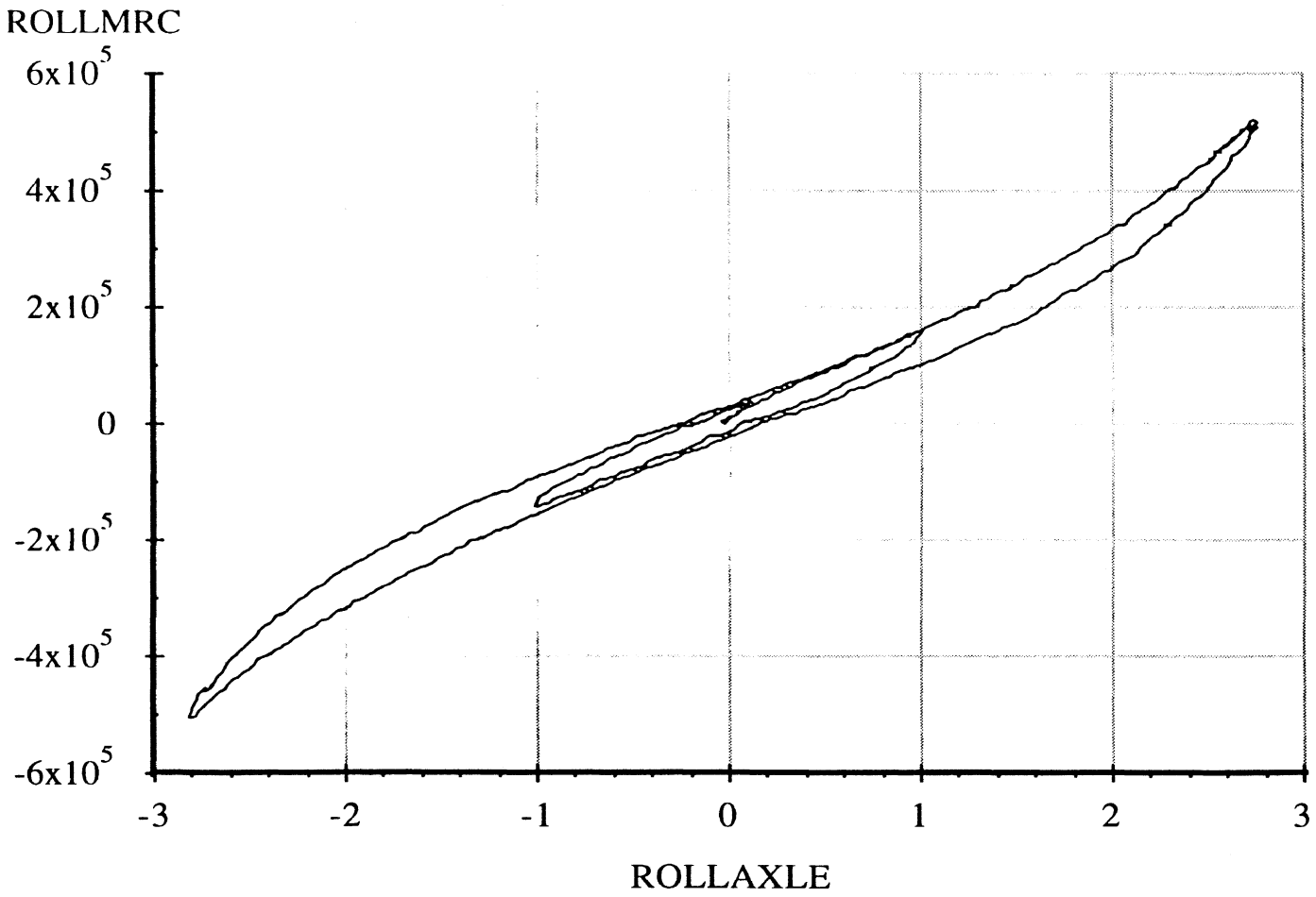

Abscissa (X): Axle roll angle (ROLLAXLE); degrees; right side compressed, positive.

Ordinate (Y): Axle roll moment about the roll center (ROLLMRC); in-lb; right side compressed, positive.

*Note: Brakes on. Force control. Air bags inflated to 100 psi.

Measured by UMTRI for Smart Truck
Fruehauf Model FBB9-F1-28

Data file: SMTTRL15.ERD

Single Trailer Axle Suspension

Roll Center Height

4 Jan 98
Suspension: Trailing Arm (WT)

Suspension Load: 25800 lb.

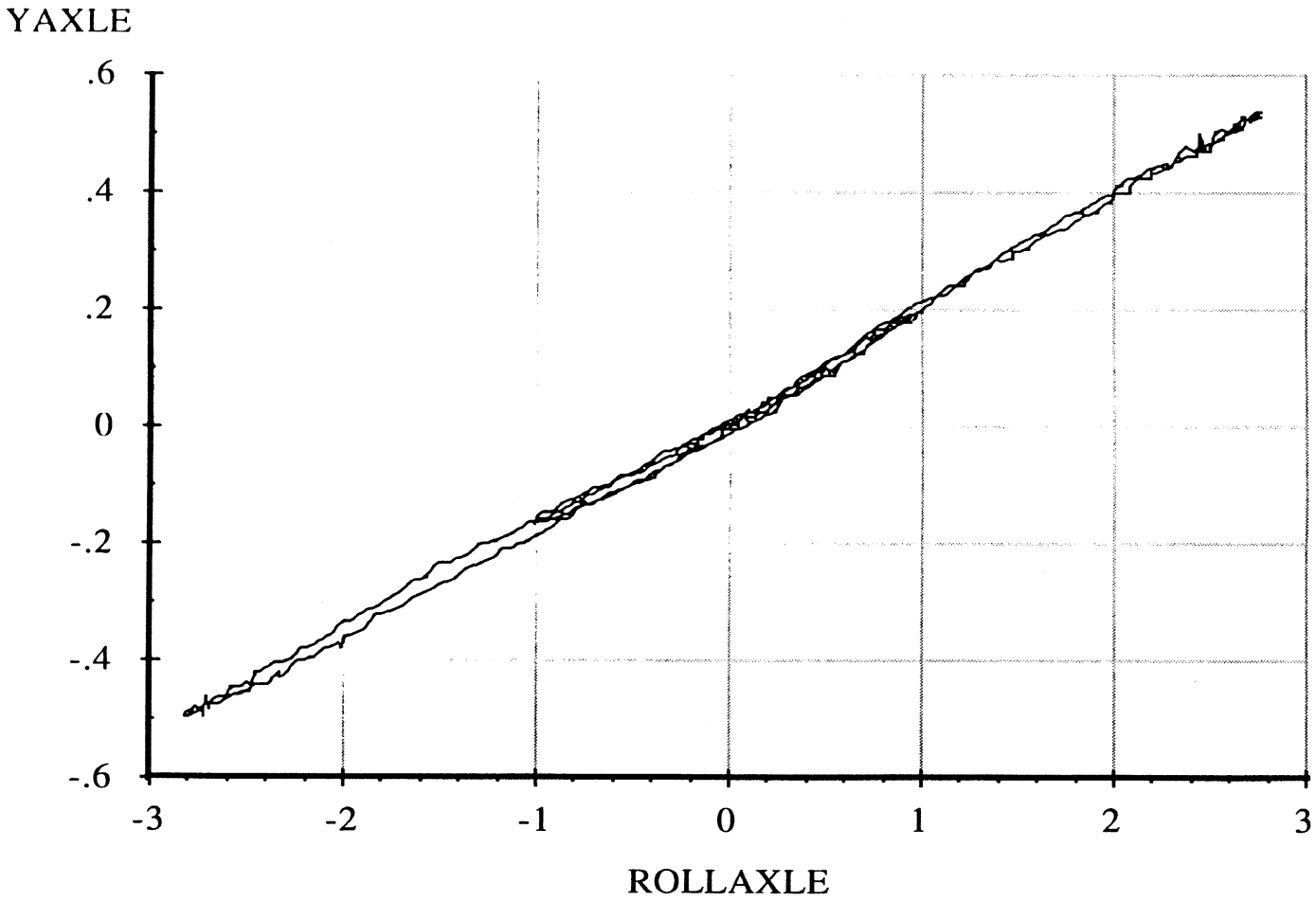

Abscissa (X): Axle roll angle (ROLLAXLE); degrees; right side compressed, positive.

Ordinate (Y): Axle reference point lateral translation (YAXLE); inches; motion toward right, positive.

*Note: Brakes on. Force control. Air bags inflated to 100 psi. Reference height of 13.69 inches.

Measured by UMTRI for Smart Truck
Fruehauf Model FBB9-F1-28

Data file: SMTTRL15.ERD

Single Trailer Axle Suspension

Roll Steer

4 Jan 98
Suspension: Trailing Arm (WT)

Suspension Load: 25800 lb.

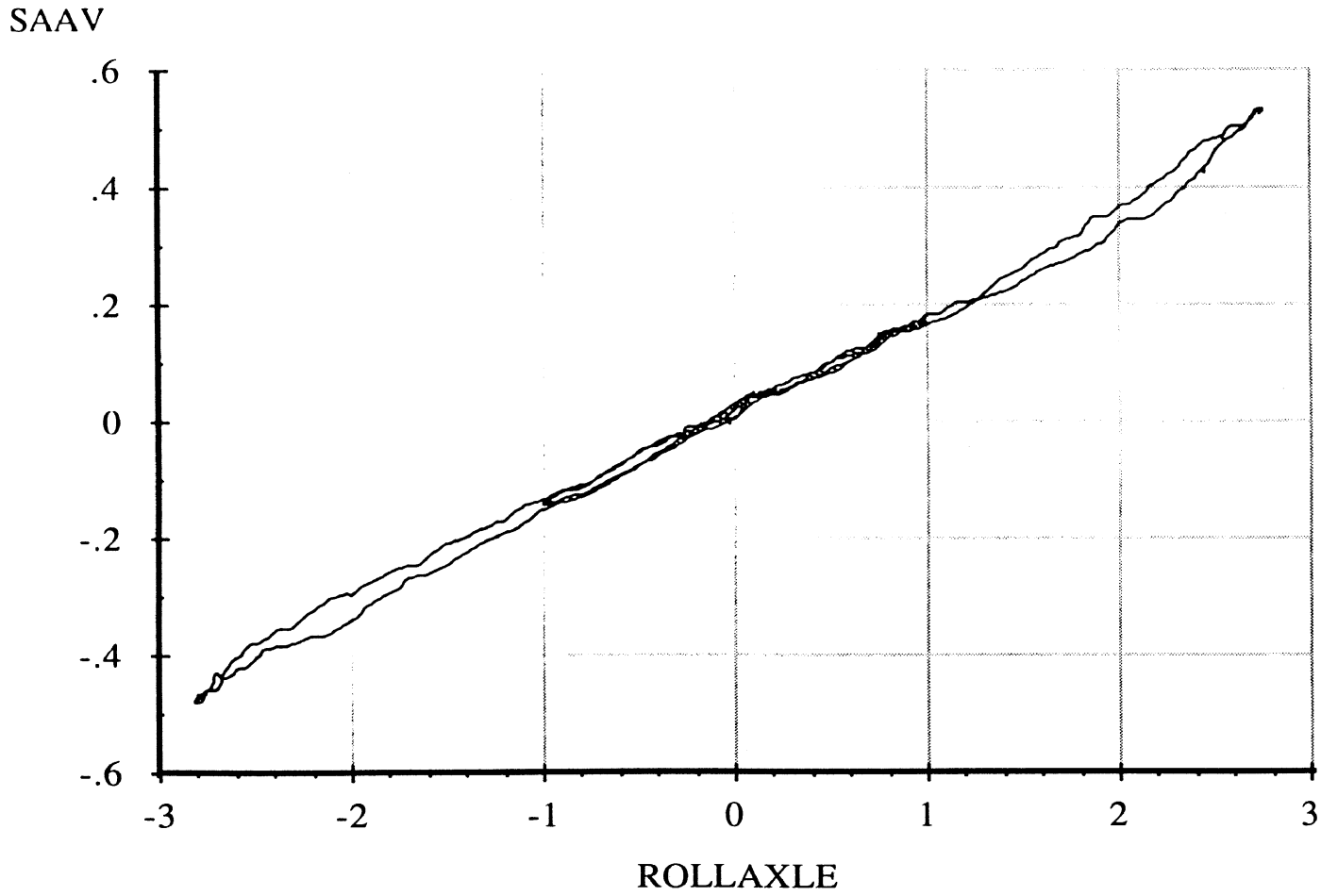

Abscissa (X): Axle roll angle (ROLLAXLE); degrees; right side compressed, positive.

Ordinate (Y): Average steer angle (SAAV); degrees; steer toward right, positive.

*Note: Brakes on. Force control. Air bags inflated to 100 psi.

Measured by UMTRI for Smart Truck
Fruehauf Model FBB9-F1-28

Data file: SMTTRL25.ERD

Single Trailer Axle Suspension

Lateral Force Compliance

4 Jan 98
Suspension: Trailing Arm (WT)

Suspension Load: 25800 lb.

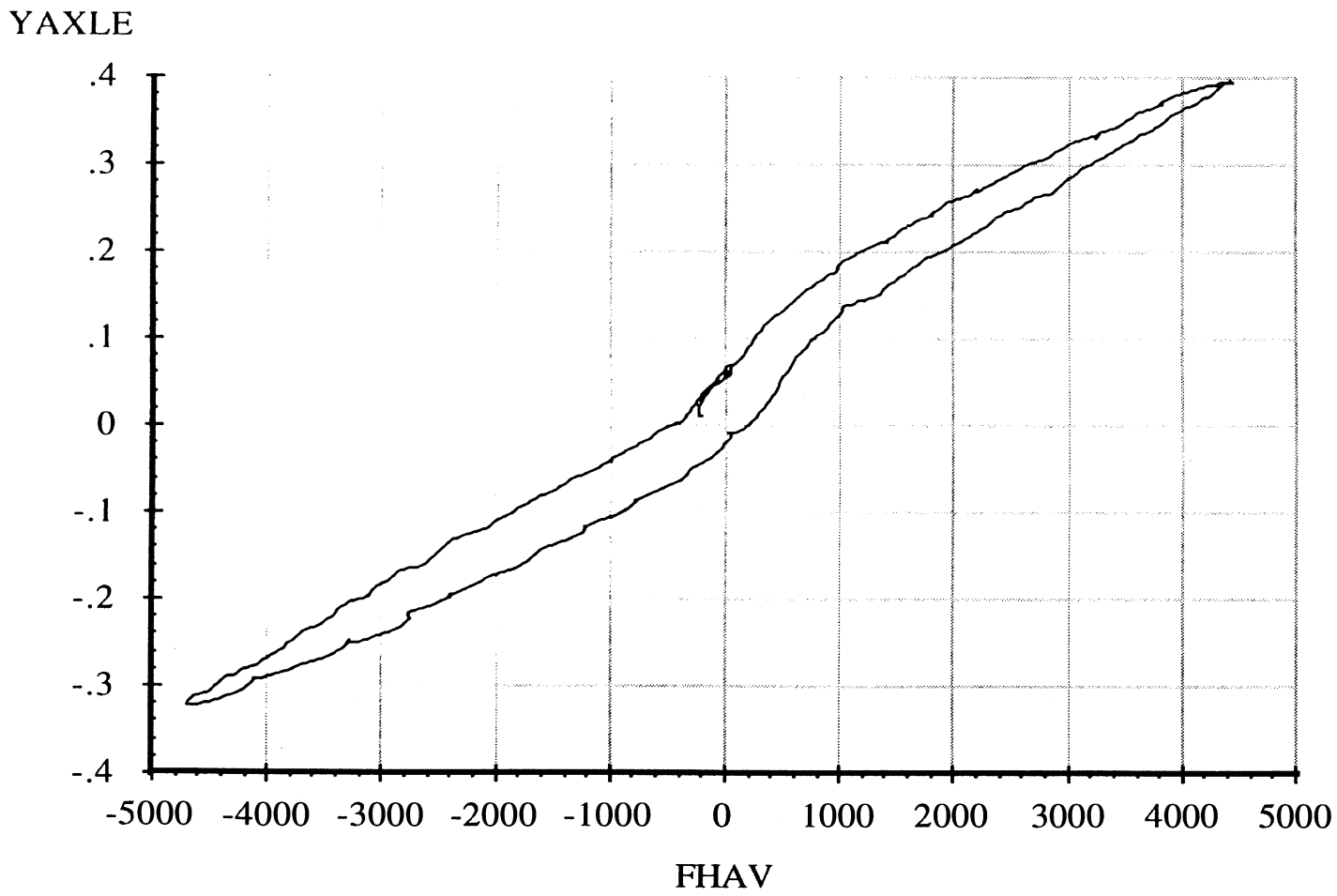

Abscissa (X): Average axle lateral force (FHAV); pounds; applied to both wheels simultaneously; force applied toward right, positive.

Ordinate (Y): Axle lateral translation (YAXLE); inches; motion toward right, positive.

*Note: Brakes on. Position control. Air bags inflated to 100 psi. Reference height of 13.69 inches.

Measured by UMTRI for Smart Truck
Fruehauf Model FBB9-F1-28

Data file: SMTTRL25.ERD

Single Trailer Axle Suspension

Lateral Force Steer

4 Jan 98
Suspension: Trailing Arm (WT)

Suspension Load: 25800 lb.

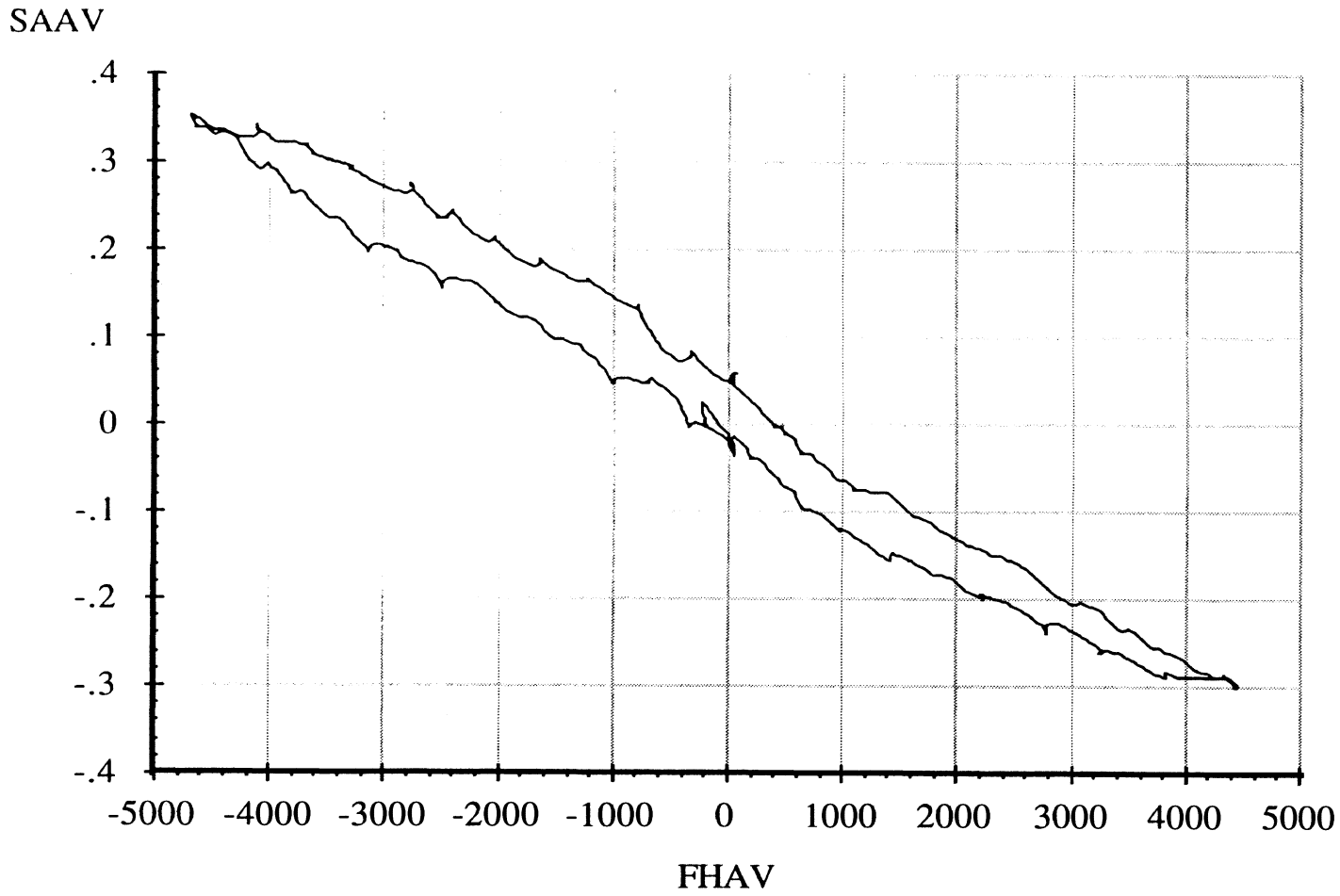

Abscissa (X): Average axle lateral force (FHAV); pounds; applied to both wheels simultaneously; force applied toward right, positive.

Ordinate (Y): Average steer angle (SAAV); degrees; steer toward right, positive.

*Note: Brakes on. Position control. Air bags inflated to 100 psi.

Measured by UMTRI for Smart Truck
Fruehauf Model FBB9-F1-28

Data file: SMTTRL04.ERD

Single Trailer Axle Suspension

Average Vertical Spring Rate

4 Jan 98
Suspension: Trailing Arm (WT)

Nominal Suspension Load: 20800 lb.

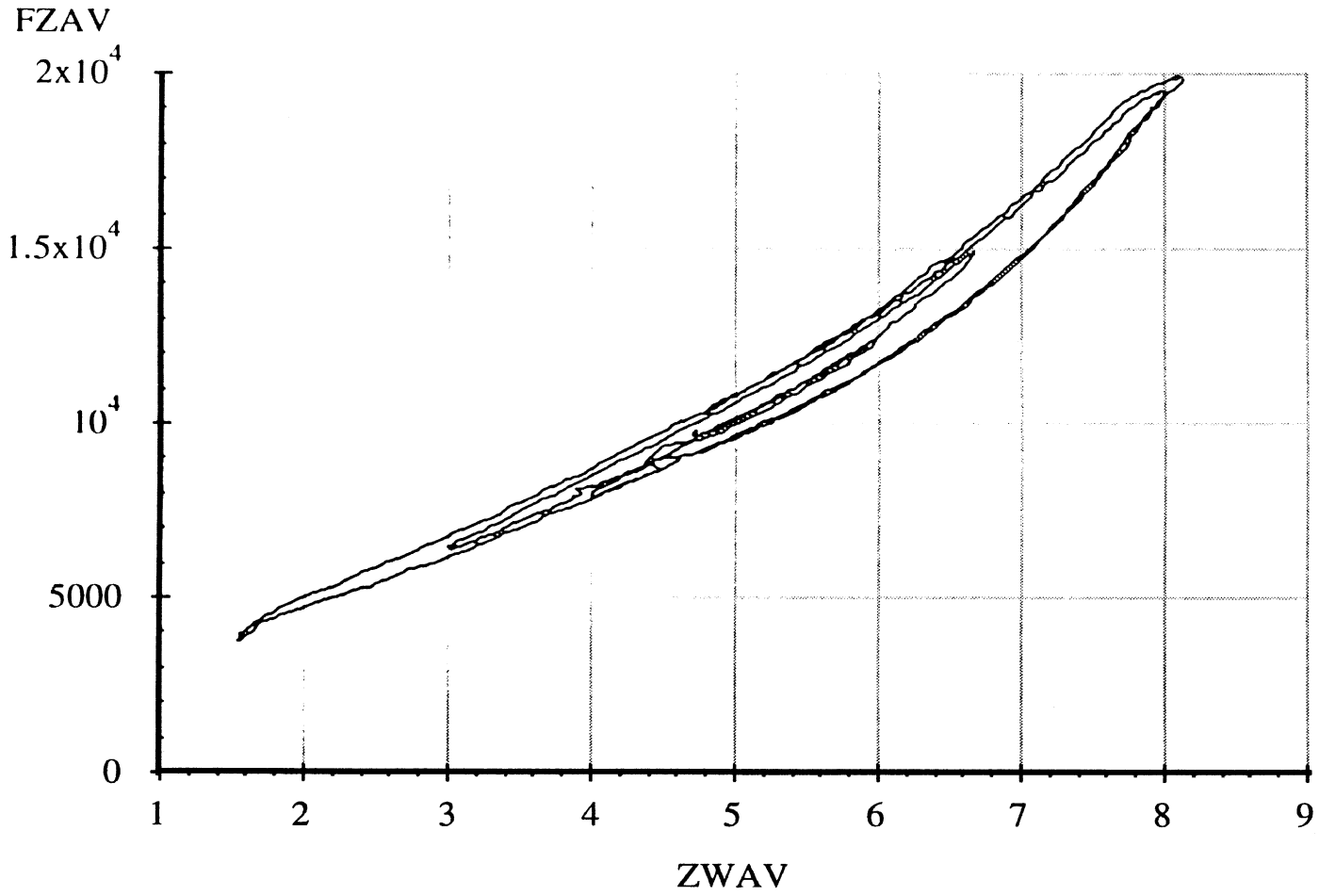

Abscissa (X): Average vertical wheel displacement (ZWAV); inches; spring compression, positive.

Ordinate (Y): Average vertical wheel load (FZAV); pounds; spring compression, positive.

*Note: Brakes on. Position control. Air bags inflated to 80 psi.

Measured by UMTRI for Smart Truck
Fruehauf Model FBB9-F1-28

Data file: SMTTRL14.ERD

Single Trailer Axle Suspension

Axle Roll Rate

4 Jan 98
Suspension: Trailing Arm (WT)

Suspension Load: 20800 lb.

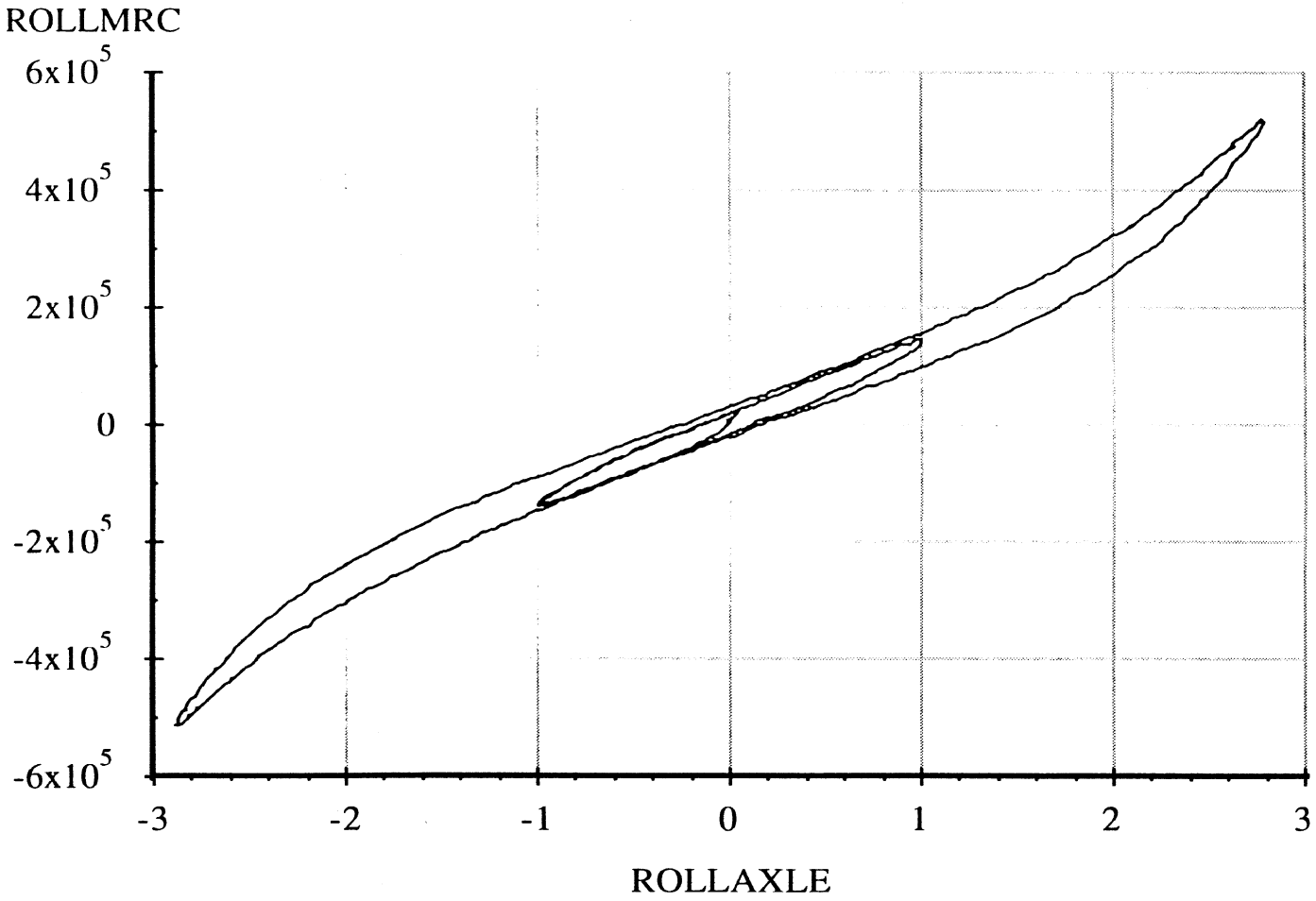

Abscissa (X): Axle roll angle (ROLLAXLE); degrees; right side compressed, positive.

Ordinate (Y): Axle roll moment about the roll center (ROLLMRC); in-lb; right side compressed, positive.

*Note: Brakes on. Force control. Air bags inflated to 80 psi.

Measured by UMTRI for Smart Truck
Fruehauf Model FBB9-F1-28

Data file: SMTTRL14.ERD

Single Trailer Axle Suspension

Roll Center Height

4 Jan 98
Suspension: Trailing Arm (WT)

Suspension Load: 20800 lb.

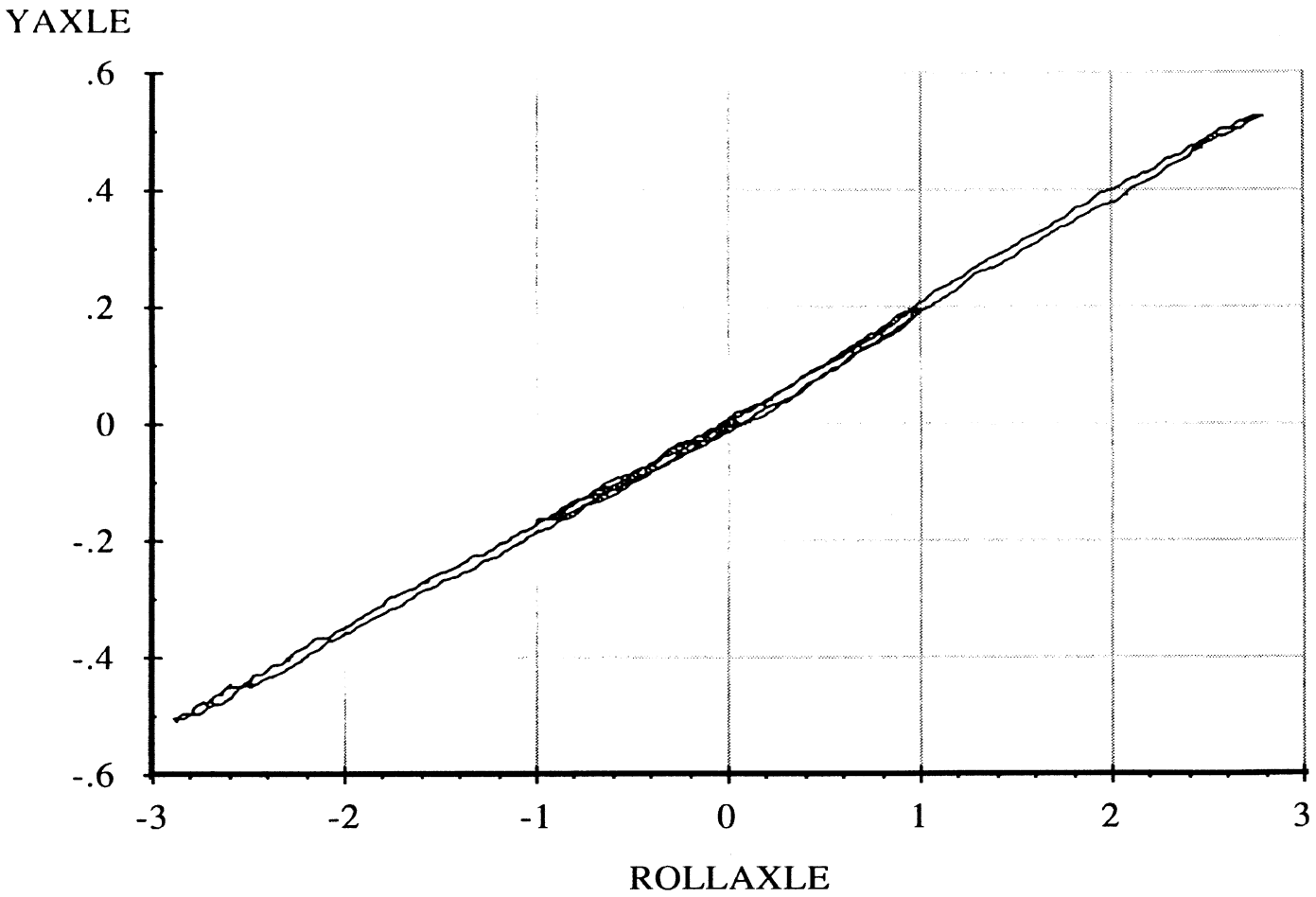

Abscissa (X): Axle roll angle (ROLLAXLE); degrees; right side compressed, positive.

Ordinate (Y): Axle reference point lateral translation (YAXLE); inches; motion toward right, positive.

*Note: Brakes on. Force control. Air bags inflated to 80 psi. Reference height of 13.94 inches.

Measured by UMTRI for Smart Truck
Fruehauf Model FBB9-F1-28

Data file: SMTTRL14.ERD

Single Trailer Axle Suspension

Roll Steer

4 Jan 98
Suspension: Trailing Arm (WT)

Suspension Load: 20800 lb.

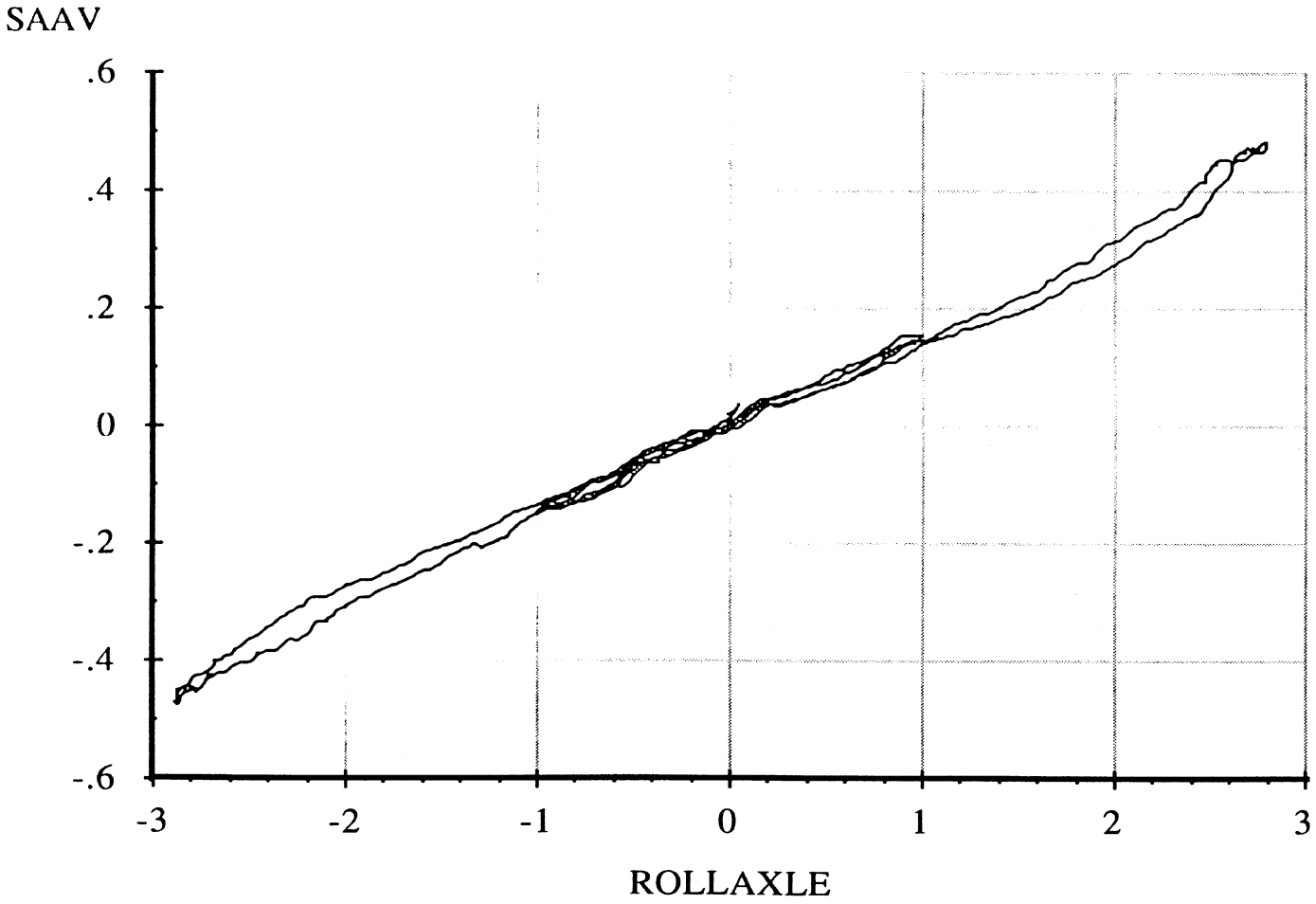

Abscissa (X): Axle roll angle (ROLLAXLE); degrees; right side compressed, positive.

Ordinate (Y): Average steer angle (SAAV); degrees; steer toward right, positive.

*Note: Brakes on. Force control. Air bags inflated to 80 psi.

Measured by UMTRI for Smart Truck
Fruehauf Model FBB9-F1-28

Data file: SMTTRL24.ERD

Single Trailer Axle Suspension

Lateral Force Compliance

4 Jan 98
Suspension: Trailing Arm (WT)

Suspension Load: 20800 lb.

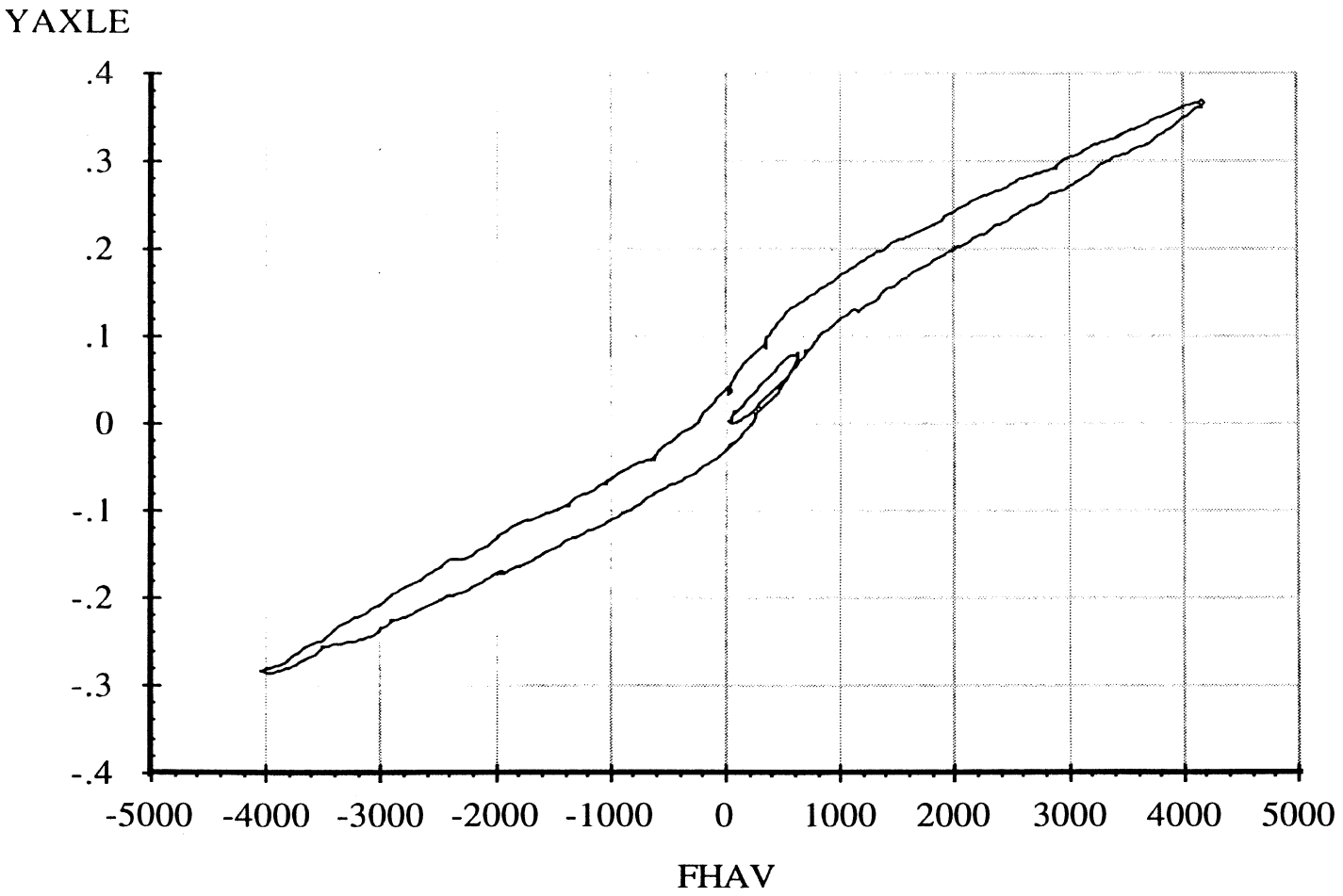

Abscissa (X): Average axle lateral force (FHAV); pounds; applied to both wheels simultaneously; force applied toward right, positive.

Ordinate (Y): Axle lateral translation (YAXLE); inches; motion toward right, positive.

*Note: Brakes on. Position control. Air bags inflated to 80 psi. Reference height of 13.94 inches.

Measured by UMTRI for Smart Truck
Fruehauf Model FBB9-F1-28

Data file: SMTTRL24.ERD

Single Trailer Axle Suspension

Lateral Force Steer

4 Jan 98
Suspension: Trailing Arm (WT)

Suspension Load: 20800 lb.

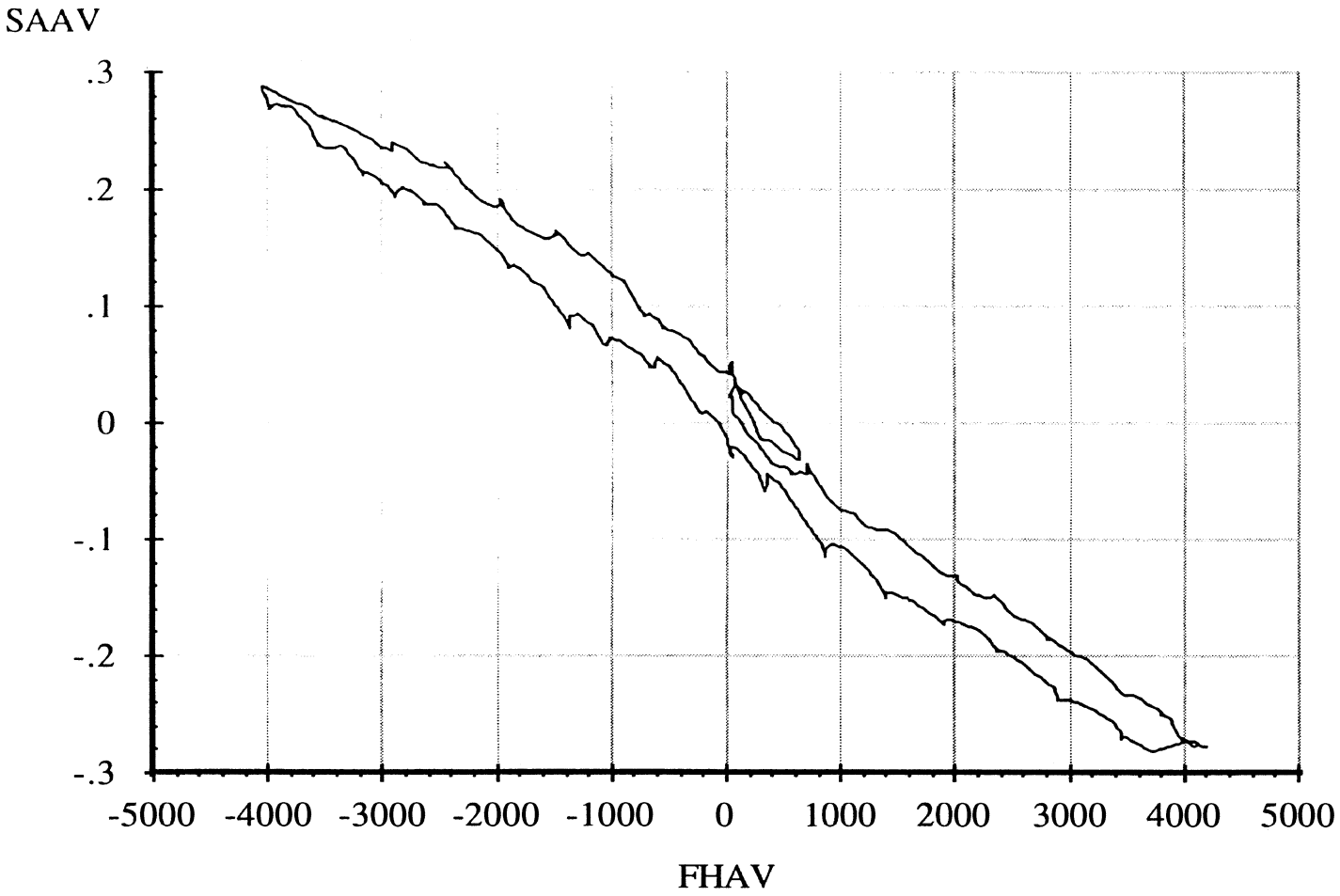

Abscissa (X): Average axle lateral force (FHAV); pounds; applied to both wheels simultaneously; force applied toward right, positive.

Ordinate (Y): Average steer angle (SAAV); degrees; steer toward right, positive.

*Note: Brakes on. Position control. Air bags inflated to 80 psi.

Measured by UMTRI for Smart Truck
Fruehauf Model FBB9-F1-28

Data file: SMTTRL34.ERD

Single Trailer Axle Suspension

Aligning Moment Compliance Steer

4 Jan 98
Suspension: Trailing Arm (WT)
Suspension Load: 20800 lb.

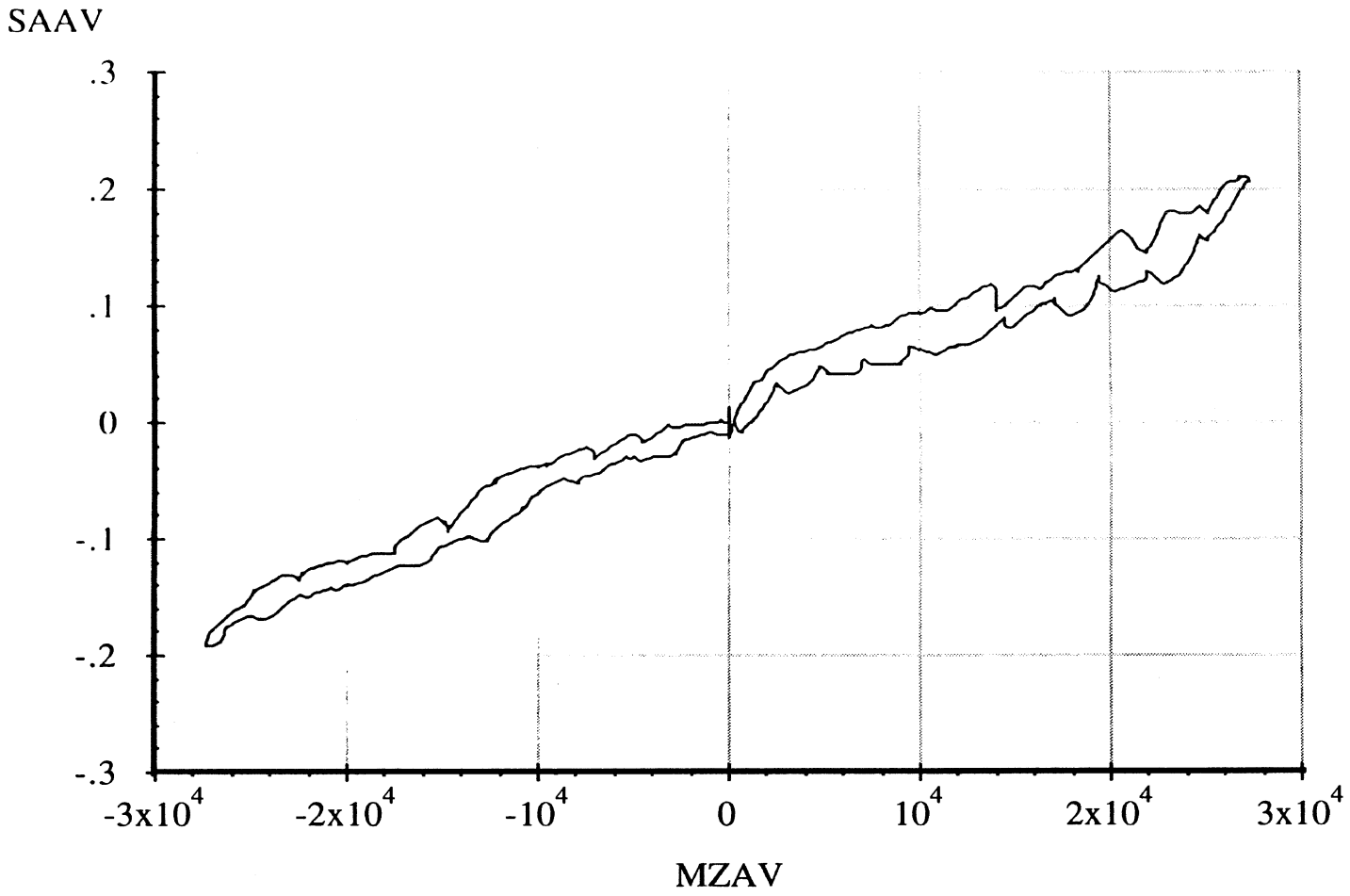

Abscissa (X): Average axle aligning moment (MZAV); in-lb per wheel; applied to both wheels simultaneously; downward (right hand rule) moment vector, positive.

Ordinate (Y): Average steer angle (SAAV); degrees; steer toward right, positive.

*Note: Brakes on. Position control. Air bags inflated to 80 psi.

Measured by UMTRI for Smart Truck
Fruehauf Model FBB9-F1-28

Data file: SMTTRL03.ERD

Single Trailer Axle Suspension

Average Vertical Spring Rate

4 Jan 98
Suspension: Trailing Arm (WT)

Nominal Suspension Load: 15300 lb.

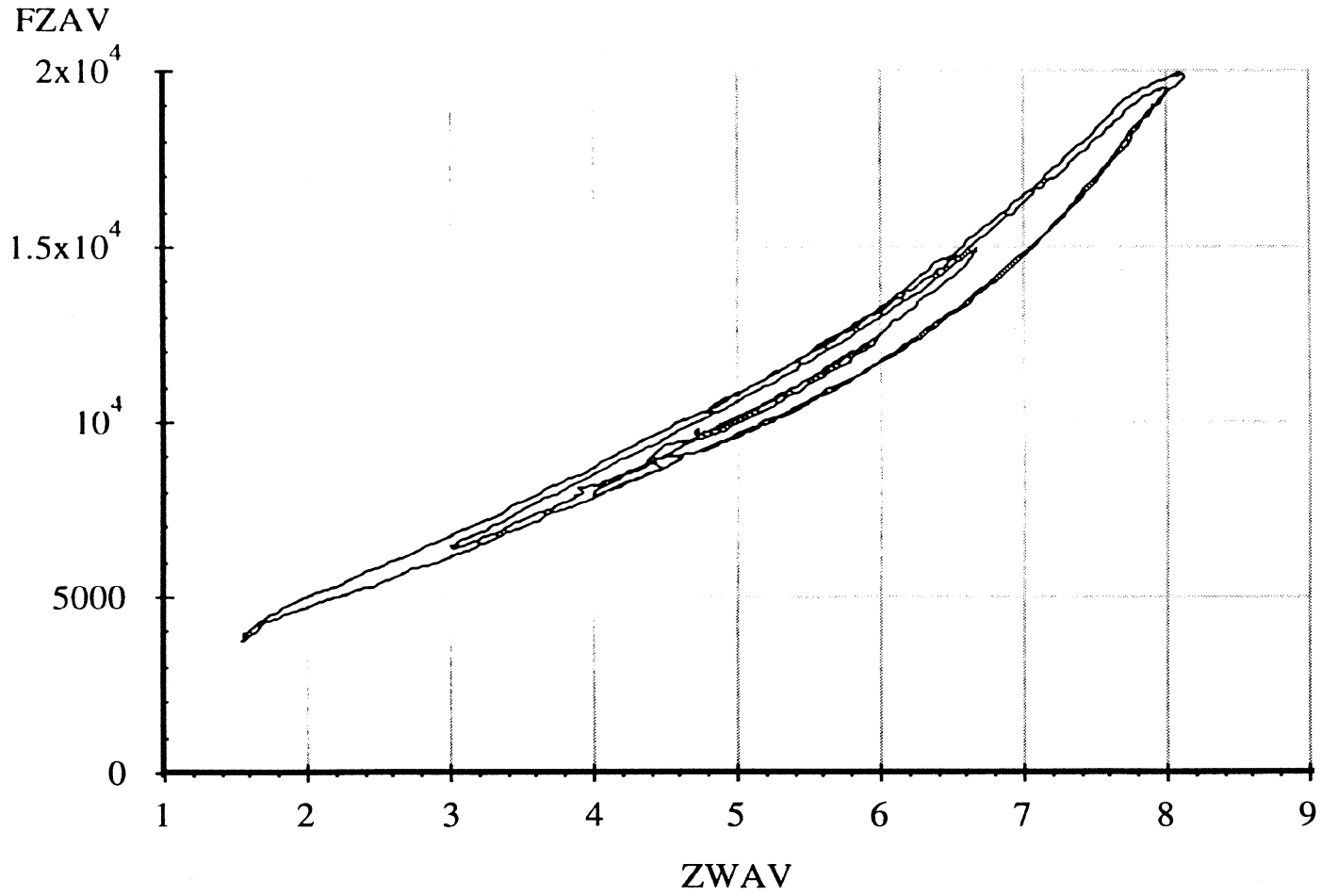

Abscissa (X): Average vertical wheel displacement (ZWAV); inches; spring compression, positive.

Ordinate (Y): Average vertical wheel load (FZAV); pounds; spring compression, positive.

*Note: Brakes on. Position control. Air bags inflated to 60 psi.

Measured by UMTRI for Smart Truck
Fruehauf Model FBB9-F1-28

Data file: SMTTRL13.ERD

Single Trailer Axle Suspension

Axle Roll Rate

4 Jan 98
Suspension: Trailing Arm (WT)

Suspension Load: 15300 lb.

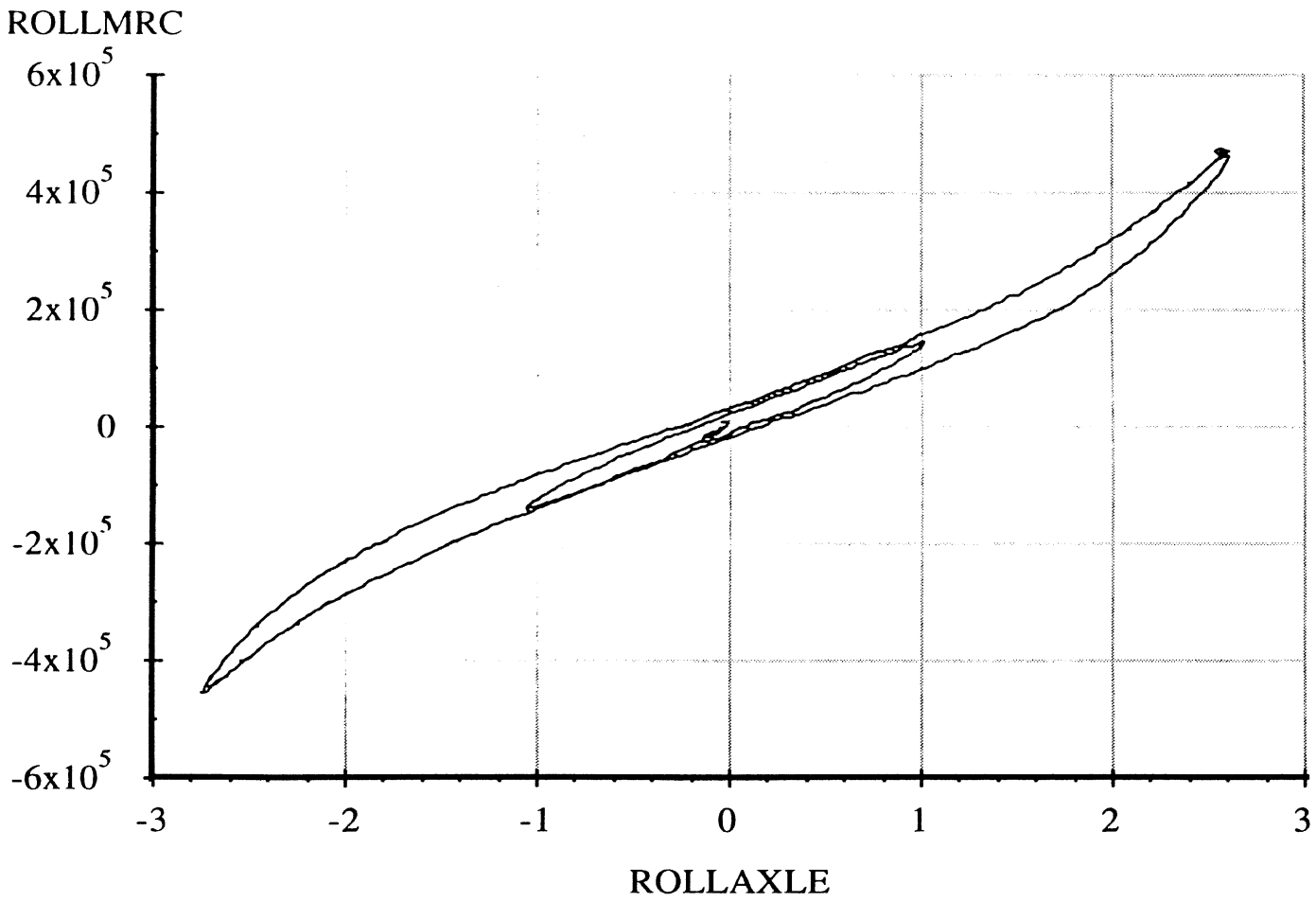

Abscissa (X): Axle roll angle (ROLLAXLE); degrees; right side compressed, positive.

Ordinate (Y): Axle roll moment about the roll center (ROLLMRC); in-lb; right side compressed, positive.

*Note: Brakes on. Force control. Air bags inflated to 60 psi.

Measured by UMTRI for Smart Truck
Fruehauf Model FBB9-F1-28

Data file: SMTTRL13.ERD

Single Trailer Axle Suspension

Roll Center Height

4 Jan 98
Suspension: Trailing Arm (WT)

Suspension Load: 15300 lb.

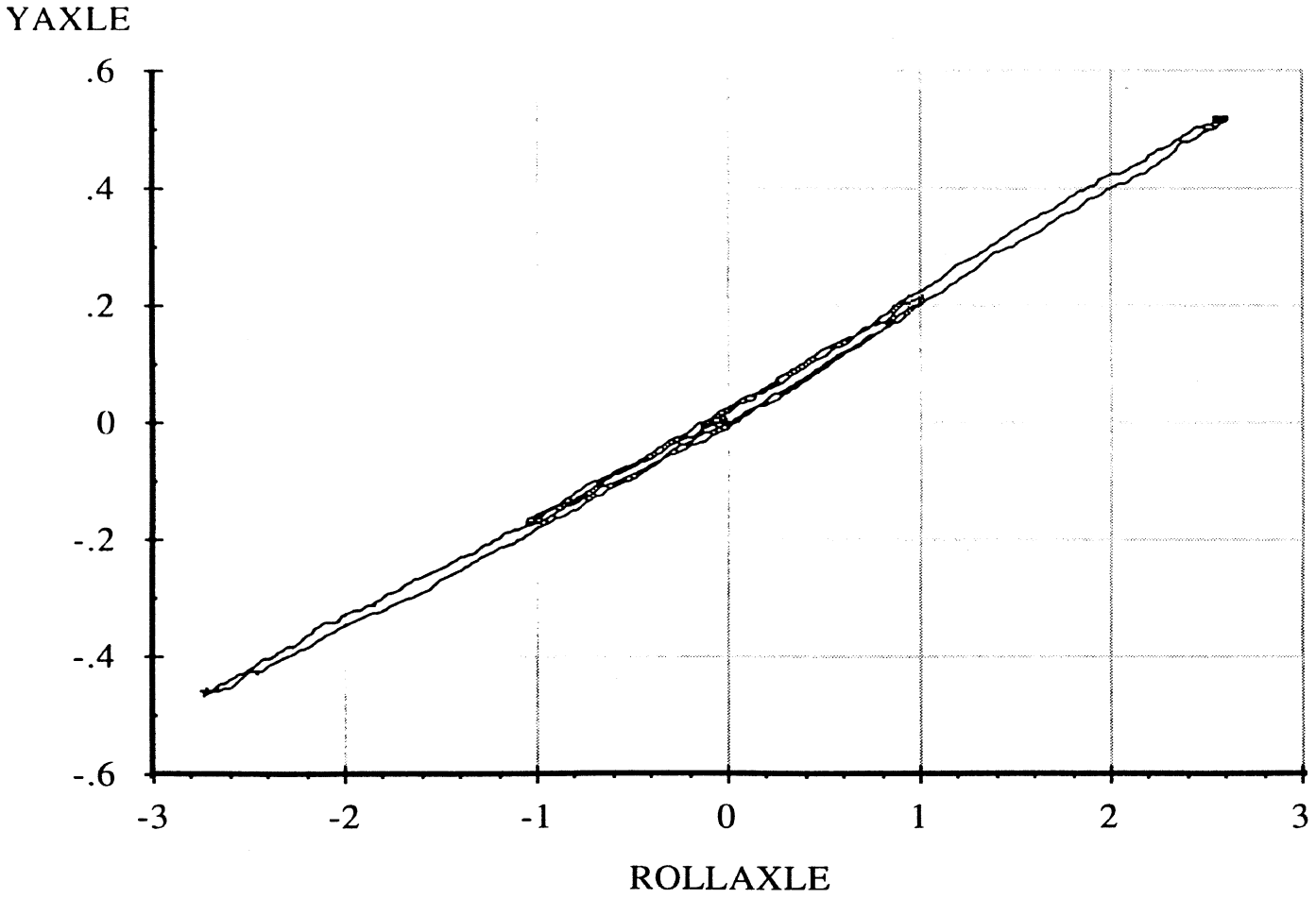

Abscissa (X): Axle roll angle (ROLLAXLE); degrees; right side compressed, positive.

Ordinate (Y): Axle reference point lateral translation (YAXLE); inches; motion toward right, positive.

*Note: Brakes on. Force control. Air bags inflated to 60 psi. Reference height of 14.19 inches.

Measured by UMTRI for Smart Truck
Fruehauf Model FBB9-F1-28

Data file: SMTTRL13.ERD

Single Trailer Axle Suspension

Roll Steer

4 Jan 98
Suspension: Trailing Arm (WT)

Suspension Load: 15300 lb.

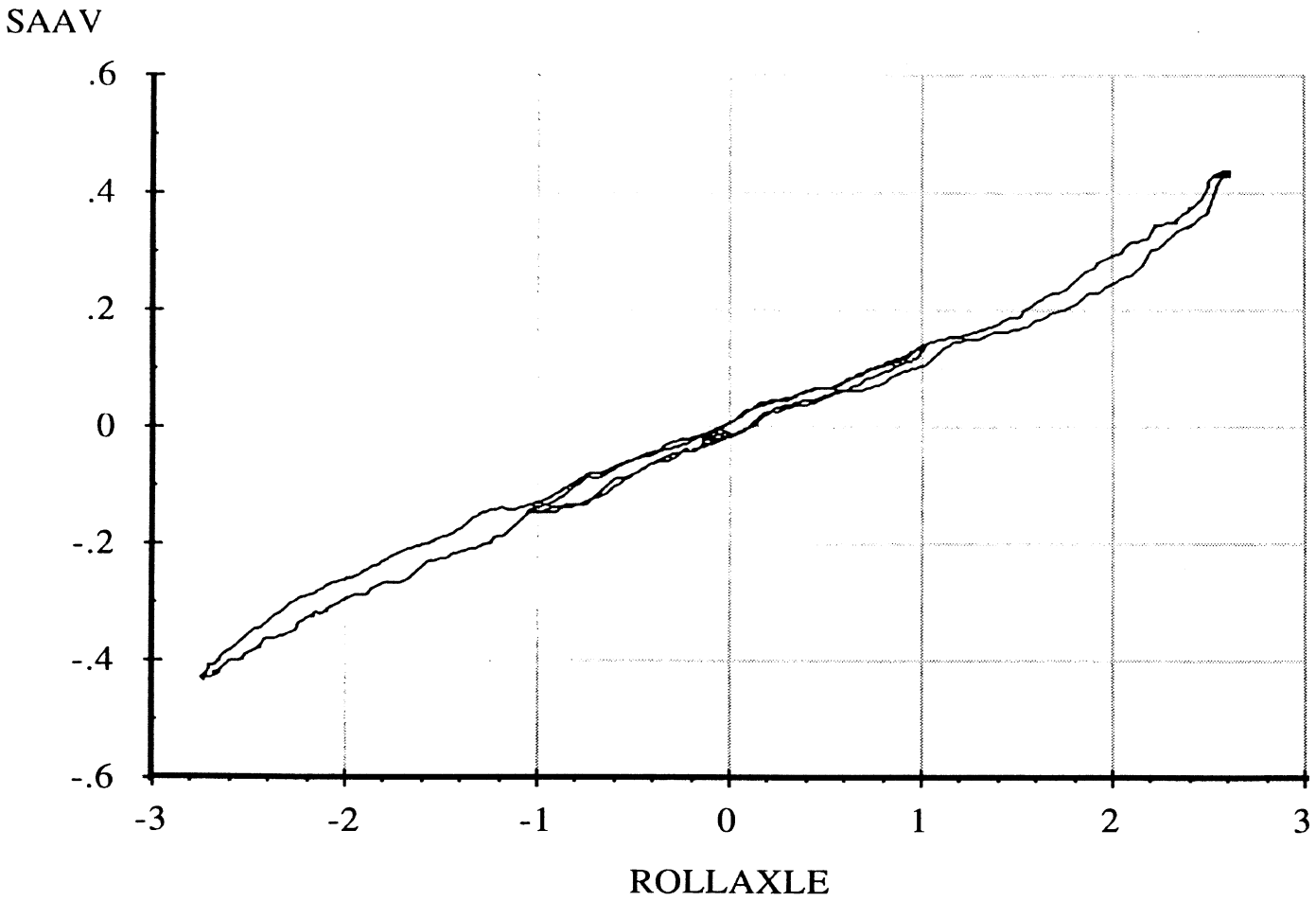

Abscissa (X): Axle roll angle (ROLLAXLE); degrees; right side compressed, positive.

Ordinate (Y): Average steer angle (SAAV); degrees; steer toward right, positive.

*Note: Brakes on. Force control. Air bags inflated to 60 psi.

Measured by UMTRI for Smart Truck
Fruehauf Model FBB9-F1-28

Data file: SMTTRL23.ERD

Single Trailer Axle Suspension

Lateral Force Compliance

4 Jan 98
Suspension: Trailing Arm (WT)

Suspension Load: 15300 lb.

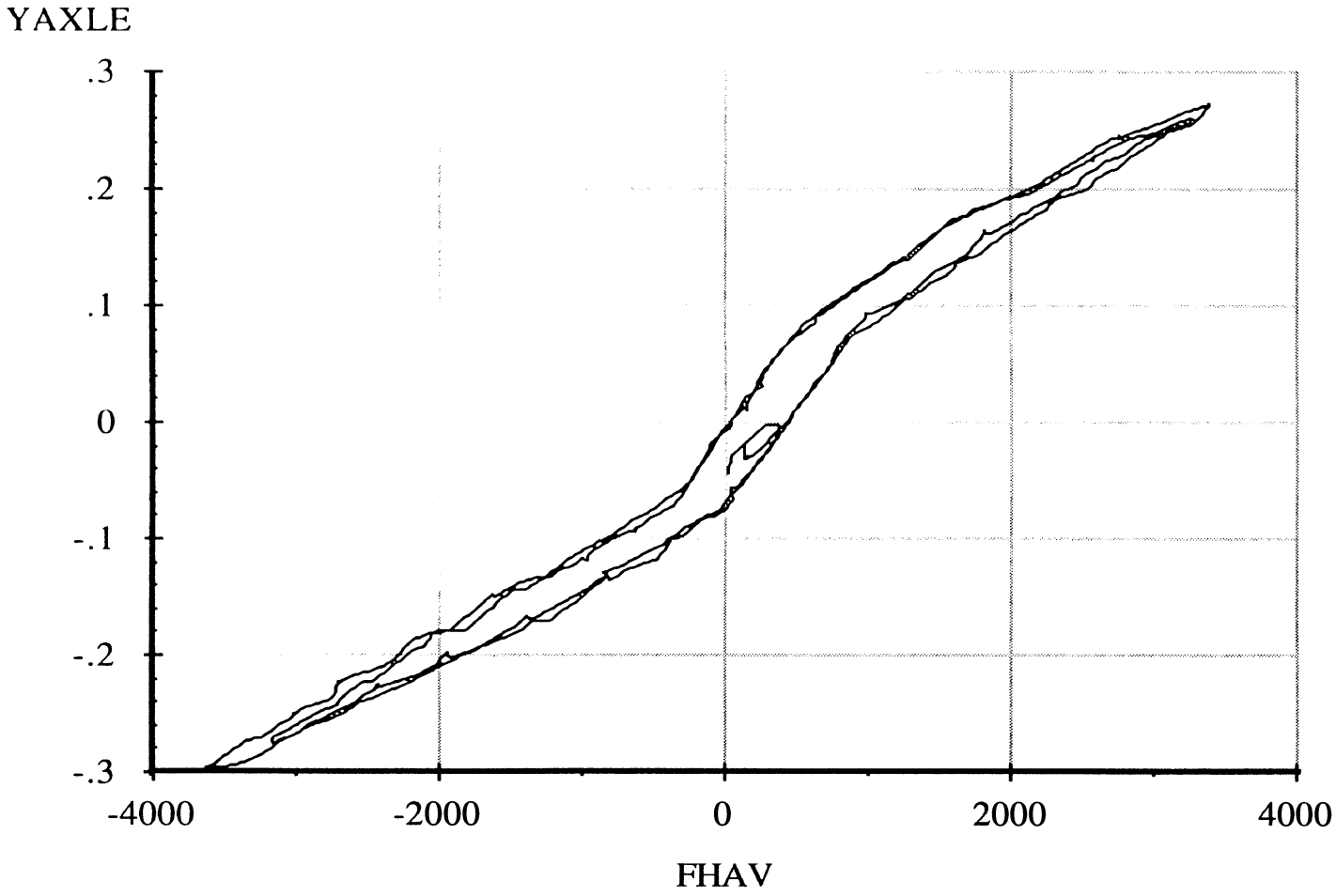

Abscissa (X): Average axle lateral force (FHAV); pounds; applied to both wheels simultaneously; force applied toward right, positive.

Ordinate (Y): Axle lateral translation (YAXLE); inches; motion toward right, positive.

*Note: Brakes on. Position control. Air bags inflated to 60 psi. Reference height of 14.19 inches.

Measured by UMTRI for Smart Truck
Fruehauf Model FBB9-F1-28

Data file: SMTTRL23.ERD

Single Trailer Axle Suspension

Lateral Force Steer

4 Jan 98
Suspension: Trailing Arm (WT)

Suspension Load: 15300 lb.

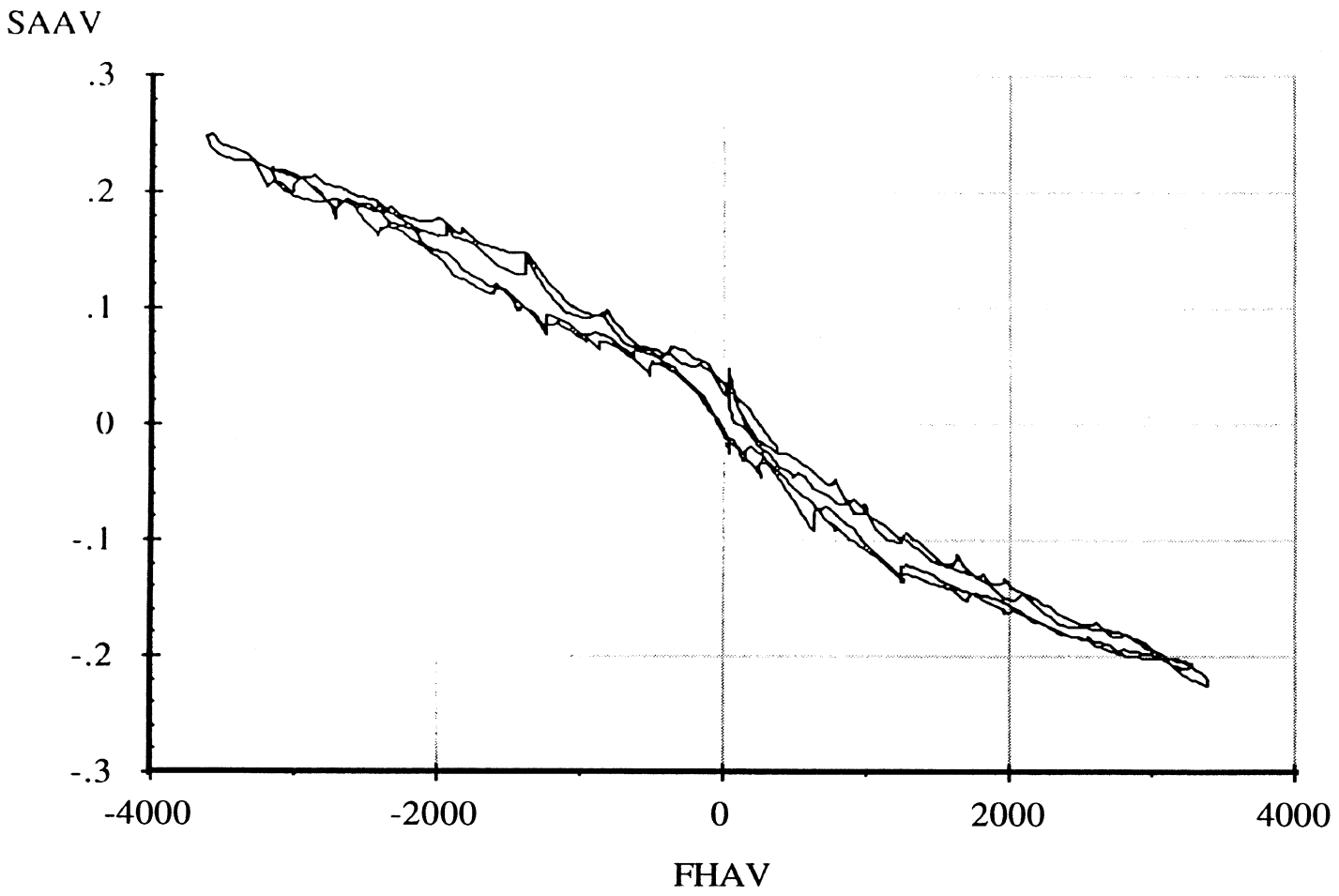

Abscissa (X): Average axle lateral force (FHAV); pounds; applied to both wheels simultaneously; force applied toward right, positive.

Ordinate (Y): Average steer angle (SAAV); degrees; steer toward right, positive.

*Note: Brakes on. Position control. Air bags inflated to 60 psi.

Measured by UMTRI for Smart Truck
Fruehauf Model FBB9-F1-28

Data file: SMTTRL02.ERD

Single Trailer Axle Suspension

Average Vertical Spring Rate

4 Jan 98
Suspension: Trailing Arm (WT)

Nominal Suspension Load: 10400 lb.

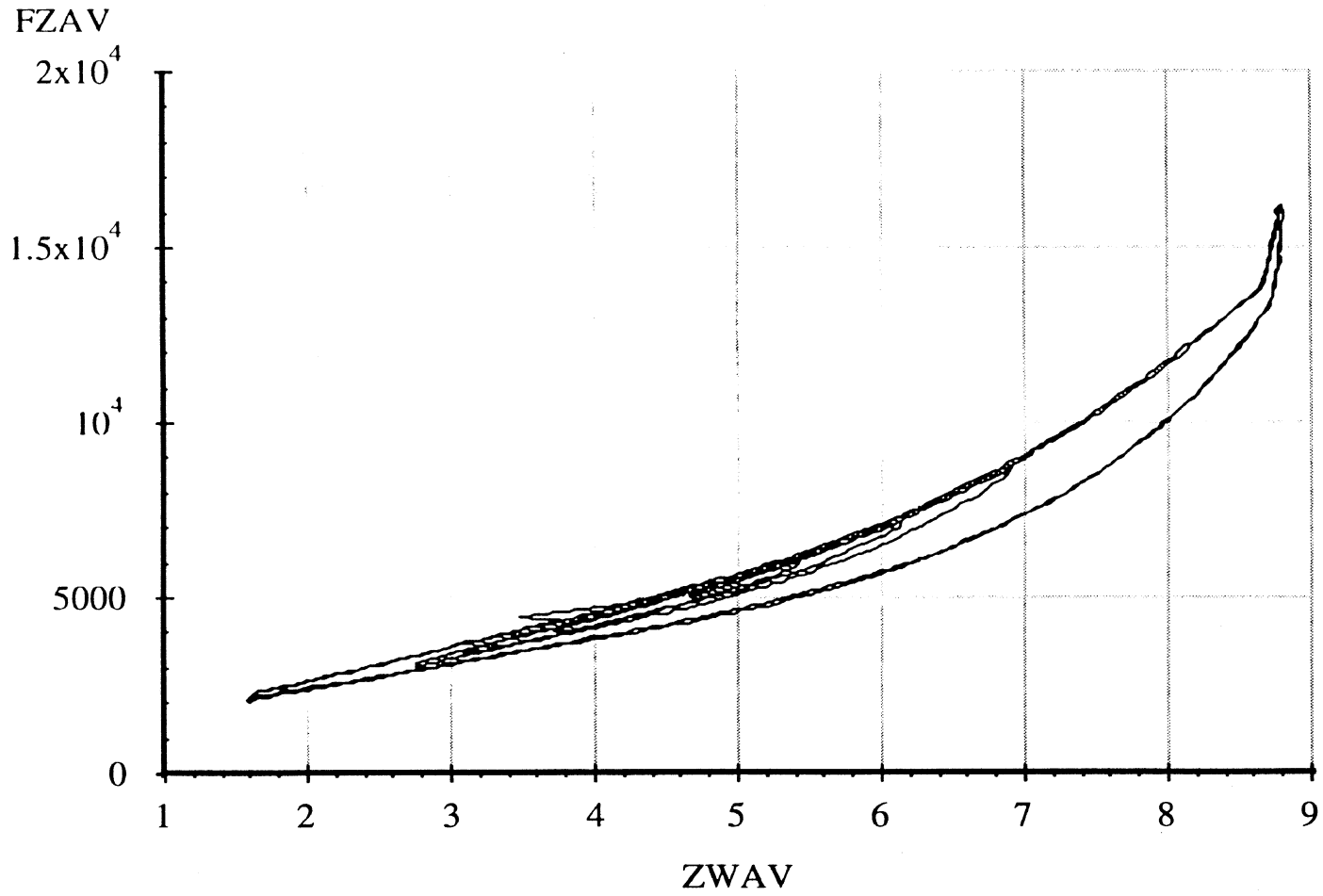

Abscissa (X): Average vertical wheel displacement (ZWAV); inches; spring compression, positive.

Ordinate (Y): Average vertical wheel load (FZAV); pounds; spring compression, positive.

*Note: Brakes on. Position control. Air bags inflated to 40 psi.

Measured by UMTRI for Smart Truck
Fruehauf Model FBB9-F1-28

Data file: SMTTRL12.ERD

Single Trailer Axle Suspension

Axle Roll Rate

4 Jan 98
Suspension: Trailing Arm (WT)

Suspension Load: 10400 lb.

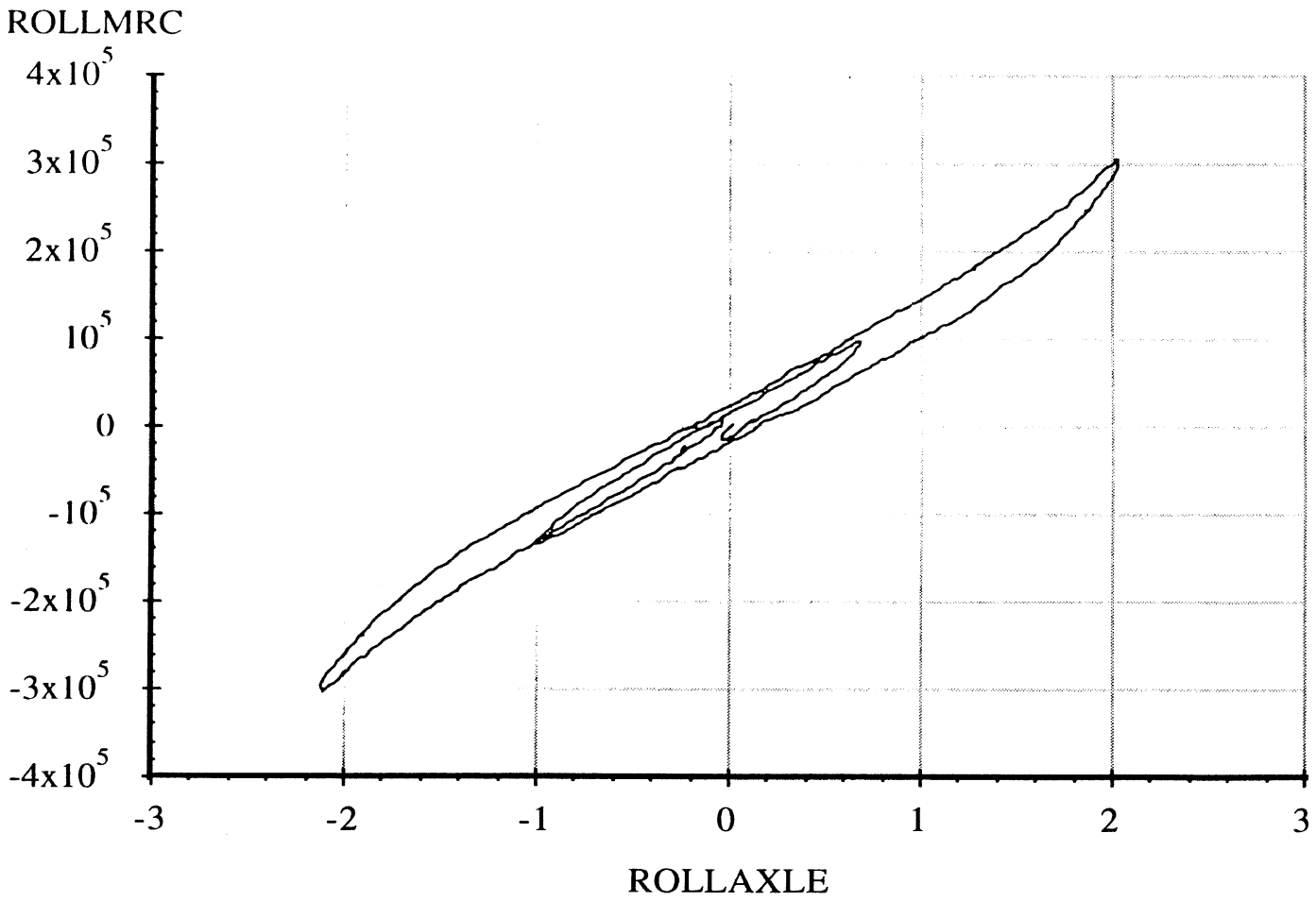

Abscissa (X): Axle roll angle (ROLLAXLE); degrees; right side compressed, positive.

Ordinate (Y): Axle roll moment about the roll center (ROLLMRC); in-lb; right side compressed, positive.

*Note: Brakes on. Force control. Air bags inflated to 40 psi.

Measured by UMTRI for Smart Truck
Fruehauf Model FBB9-F1-28

Data file: SMTTRL12.ERD

Single Trailer Axle Suspension

Roll Center Height

4 Jan 98
Suspension: Trailing Arm (WT)

Suspension Load: 10400 lb.

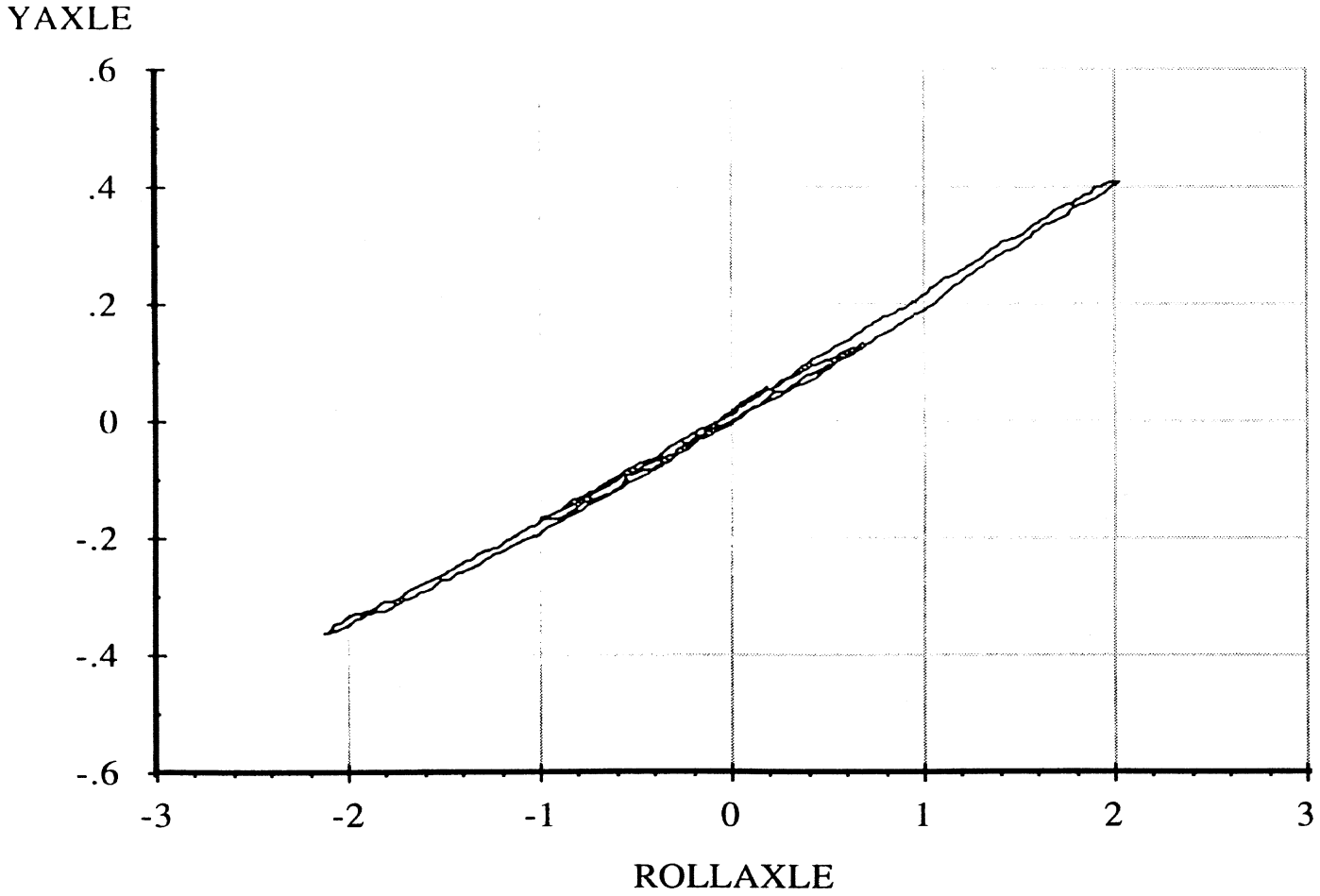

Abscissa (X): Axle roll angle (ROLLAXLE); degrees; right side compressed, positive.

Ordinate (Y): Axle reference point lateral translation (YAXLE); inches; motion toward right, positive.

*Note: Brakes on. Force control. Air bags inflated to 40 psi. Reference height of 14.50 inches.

Measured by UMTRI for Smart Truck
Fruehauf Model FBB9-F1-28

Data file: SMTTRL12.ERD

Single Trailer Axle Suspension

Roll Steer

4 Jan 98
Suspension: Trailing Arm (WT)

Suspension Load: 10400 lb.

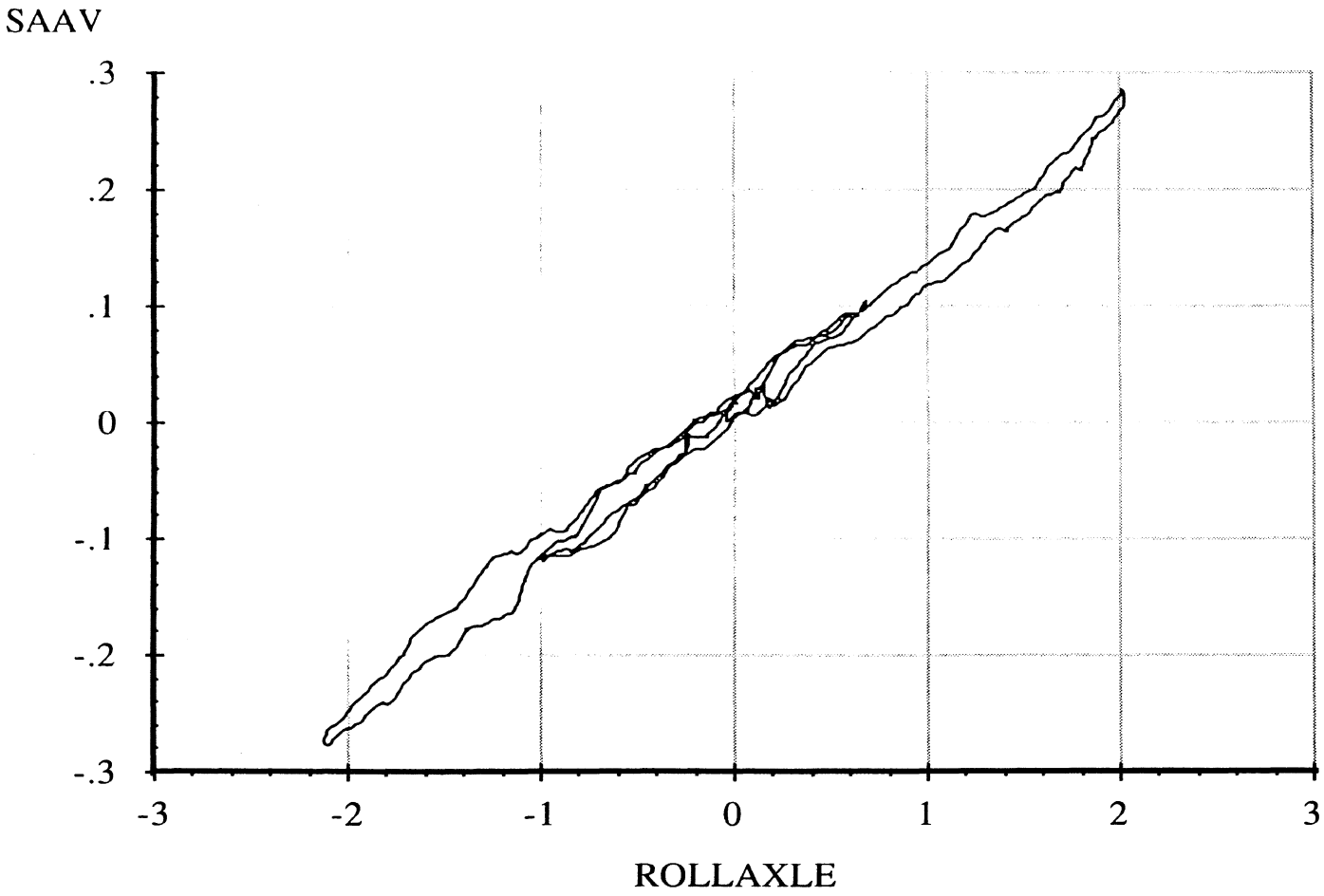

Abscissa (X): Axle roll angle (ROLLAXLE); degrees; right side compressed, positive.

Ordinate (Y): Average steer angle (SAAV); degrees; steer toward right, positive.

*Note: Brakes on. Force control. Air bags inflated to 40 psi.

Measured by UMTRI for Smart Truck
Fruehauf Model FBB9-F1-28

Data file: SMTTRL22.ERD

Single Trailer Axle Suspension

Lateral Force Compliance

4 Jan 98
Suspension: Trailing Arm (WT)

Suspension Load: 10400 lb.

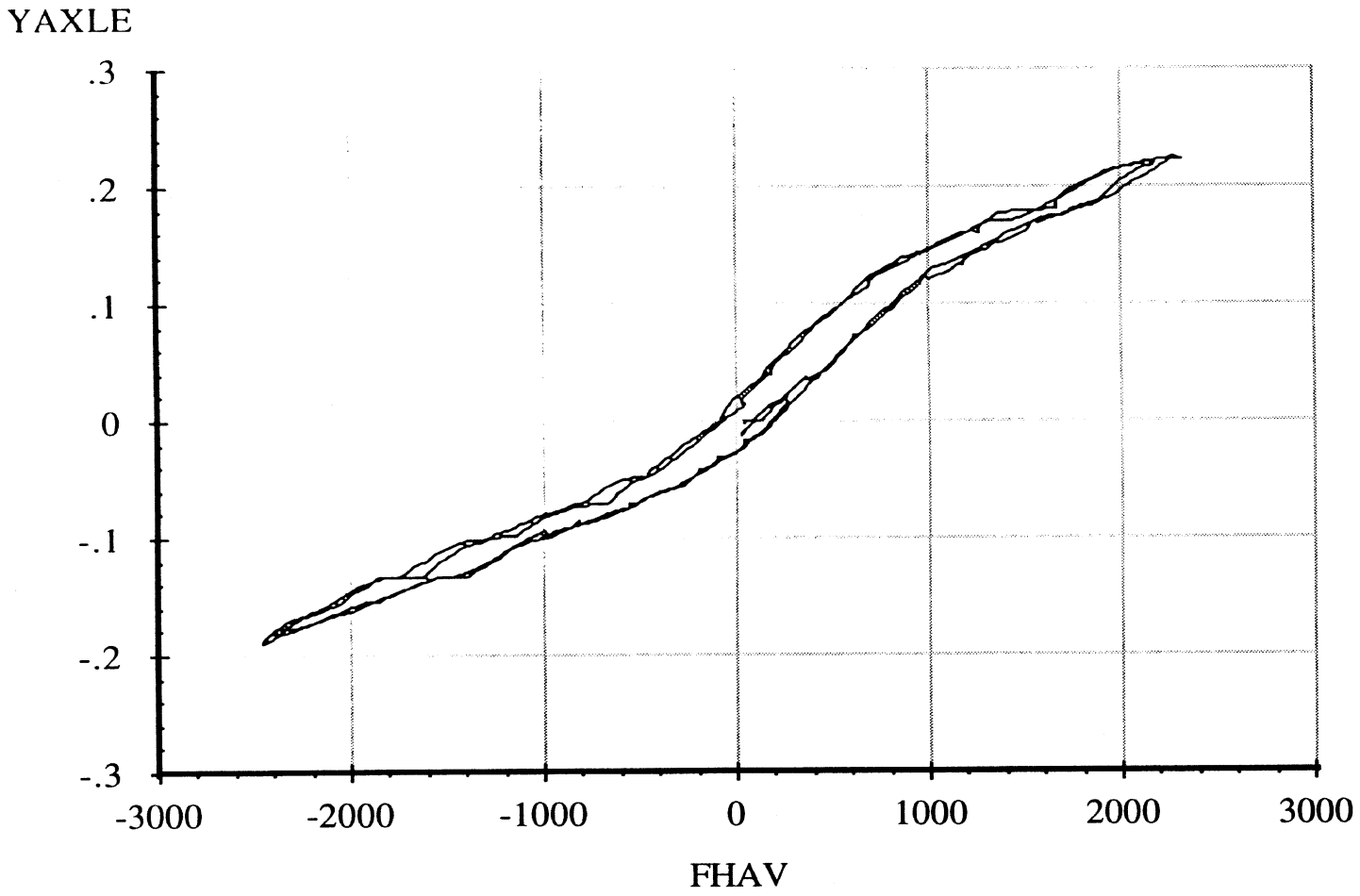

Abscissa (X): Average axle lateral force (FHAV); pounds; applied to both wheels simultaneously; force applied toward right, positive.

Ordinate (Y): Axle lateral translation (YAXLE); inches; motion toward right, positive.

*Note: Brakes on. Position control. Air bags inflated to 40 psi. Reference height of 14.50 inches.

Measured by UMTRI for Smart Truck
Fruehauf Model FBB9-F1-28

Data file: SMTTRL22.ERD

Single Trailer Axle Suspension

Lateral Force Steer

4 Jan 98
Suspension: Trailing Arm (WT)

Suspension Load: 10400 lb.

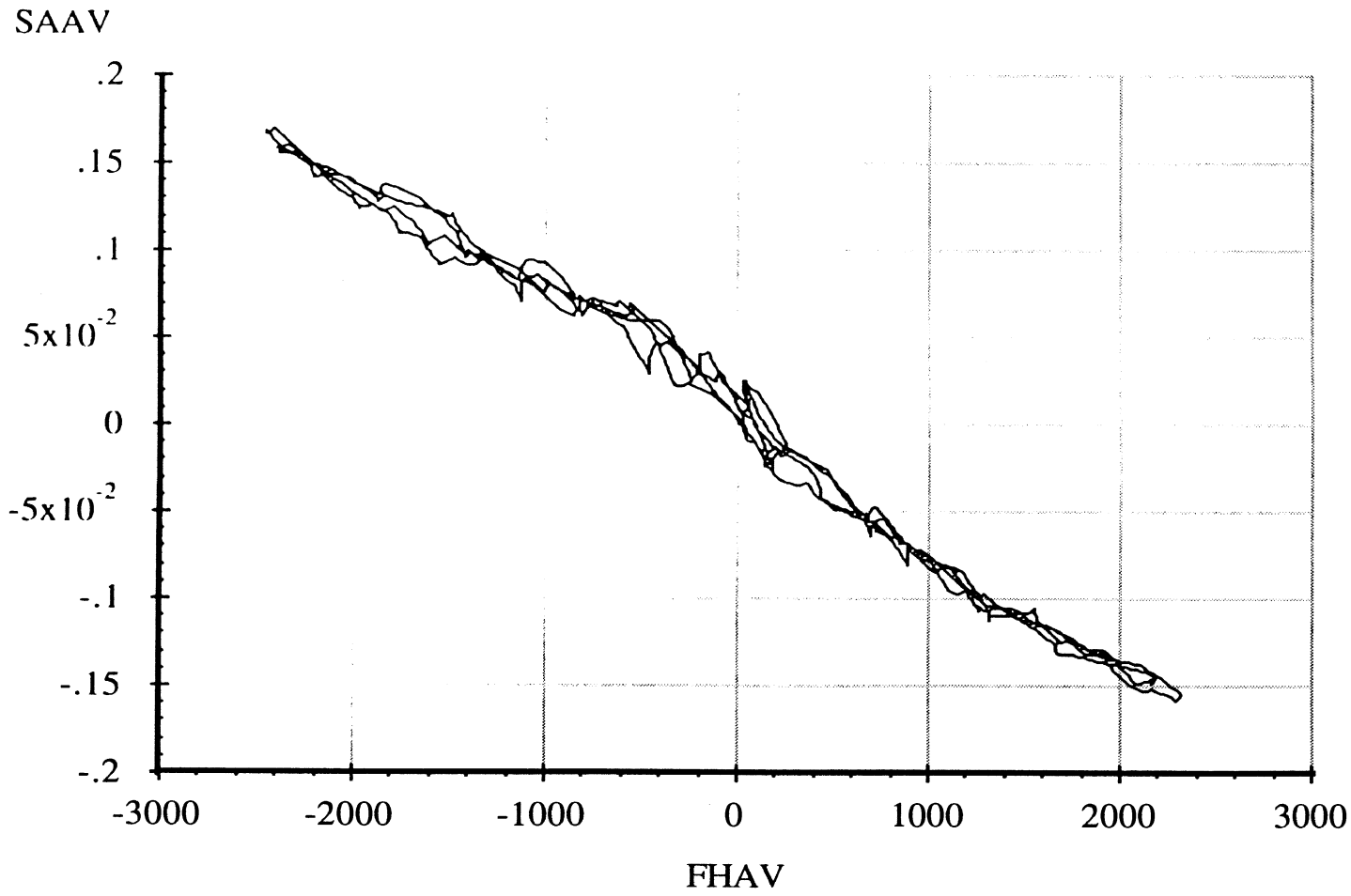

Abscissa (X): Average axle lateral force (FHAV); pounds; applied to both wheels simultaneously; force applied toward right, positive.

Ordinate (Y): Average steer angle (SAAV); degrees; steer toward right, positive.

*Note: Brakes on. Position control. Air bags inflated to 40 psi.

Measured by UMTRI for Smart Truck
Fruehauf Model FBB9-F1-28

Data file: SMTTRL01.ERD

Single Trailer Axle Suspension

Average Vertical Spring Rate

4 Jan 98
Suspension: Trailing Arm (WT)

Nominal Suspension Load: 5900 lb.

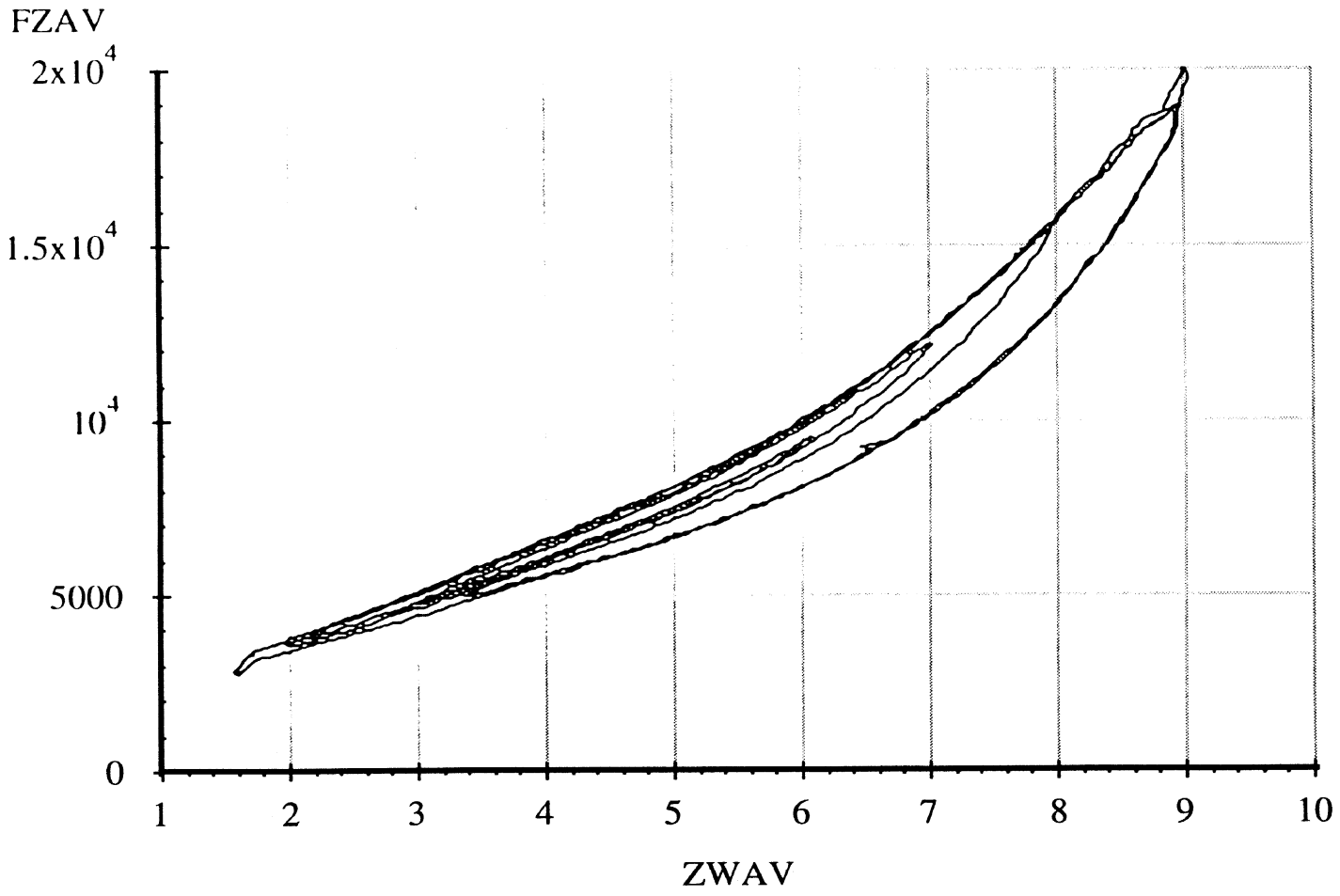

Abscissa (X): Average vertical wheel displacement (ZWAV); inches; spring compression, positive.

Ordinate (Y): Average vertical wheel load (FZAV); pounds; spring compression, positive.

*Note: Brakes on. Position control. Air bags inflated to 20 psi.

Measured by UMTRI for Smart Truck
Fruehauf Model FBB9-F1-28

Data file: SMTTRL11.ERD

Single Trailer Axle Suspension

Axle Roll Rate

4 Jan 98
Suspension: Trailing Arm (WT)

Suspension Load: 5900 lb.

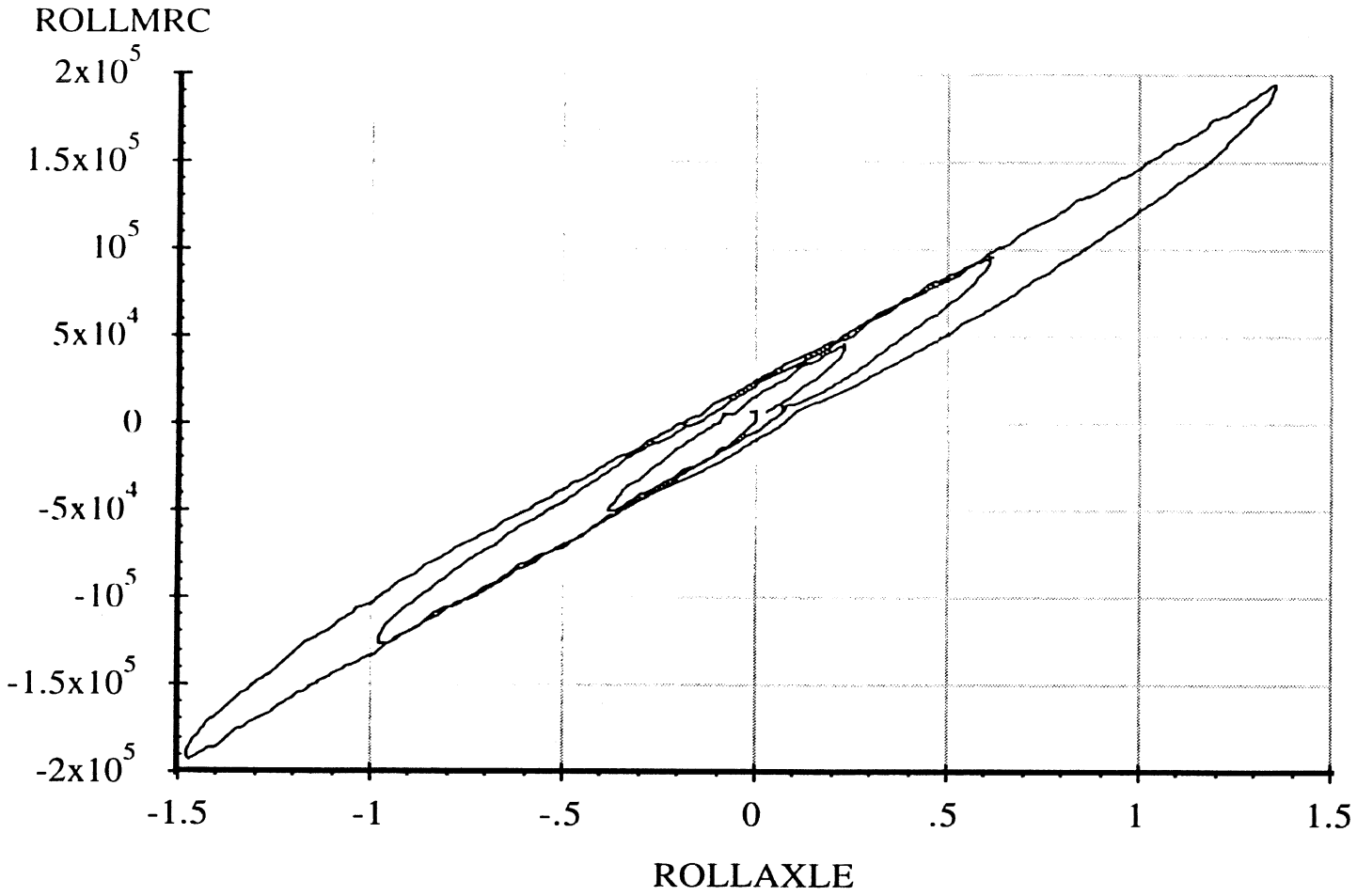

Abscissa (X): Axle roll angle (ROLLAXLE); degrees; right side compressed, positive.

Ordinate (Y): Axle roll moment about the roll center (ROLLMRC); in-lb; right side compressed, positive.

*Note: Brakes on. Force control. Air bags inflated to 20 psi.

Measured by UMTRI for Smart Truck
Fruehauf Model FBB9-F1-28

Data file: SMTTRL11.ERD

Single Trailer Axle Suspension

Roll Center Height

4 Jan 98
Suspension: Trailing Arm (WT)

Suspension Load: 5900 lb.

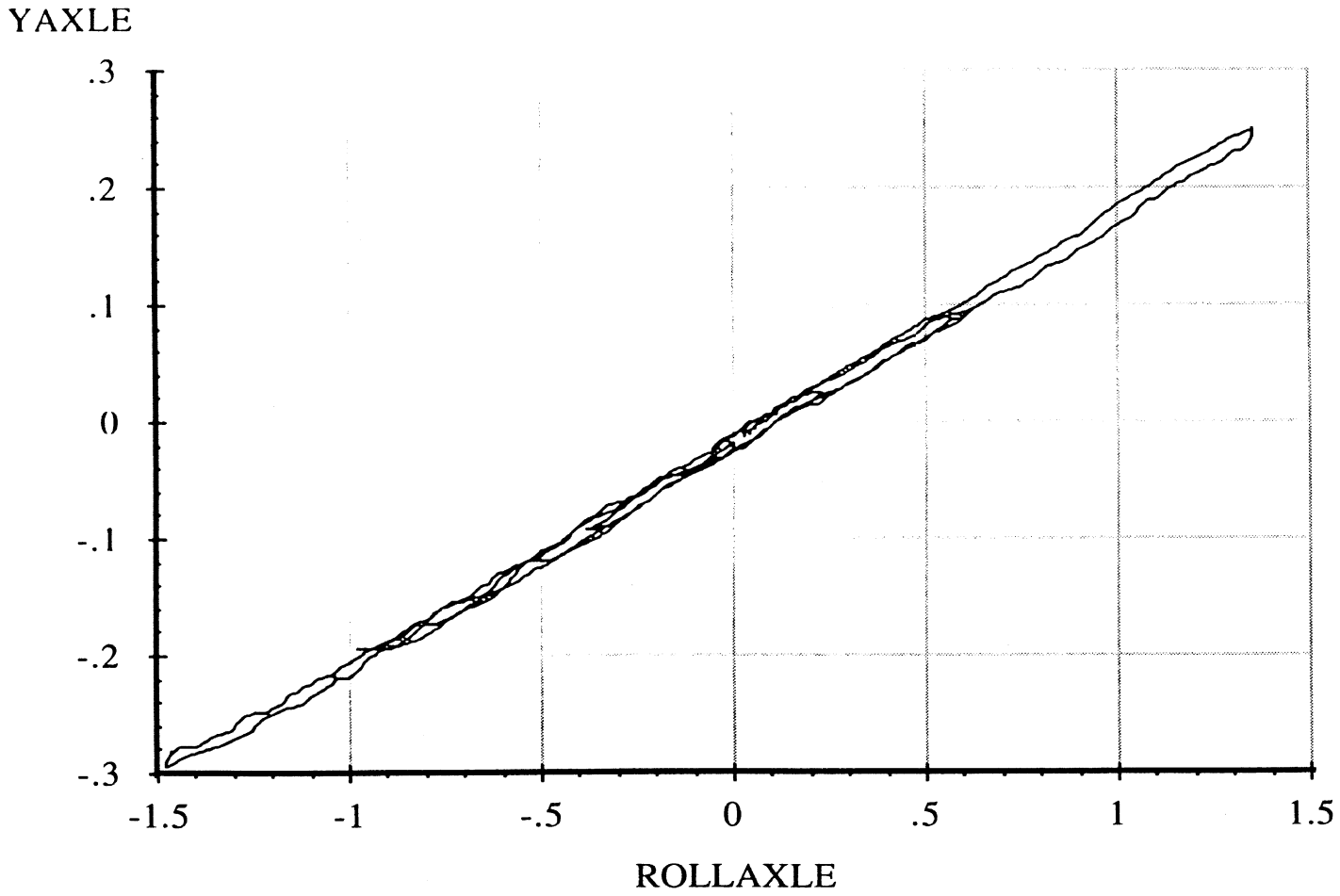

Abscissa (X): Axle roll angle (ROLLAXLE); degrees; right side compressed, positive.

Ordinate (Y): Axle reference point lateral translation (YAXLE); inches; motion toward right, positive.

*Note: Brakes on. Force control. Air bags inflated to 20 psi. Reference height of 14.75 inches.

Measured by UMTRI for Smart Truck
Fruehauf Model FBB9-F1-28

Data file: SMTTRL11.ERD

Single Trailer Axle Suspension

Roll Steer

4 Jan 98
Suspension: Trailing Arm (WT)

Suspension Load: 5900 lb.

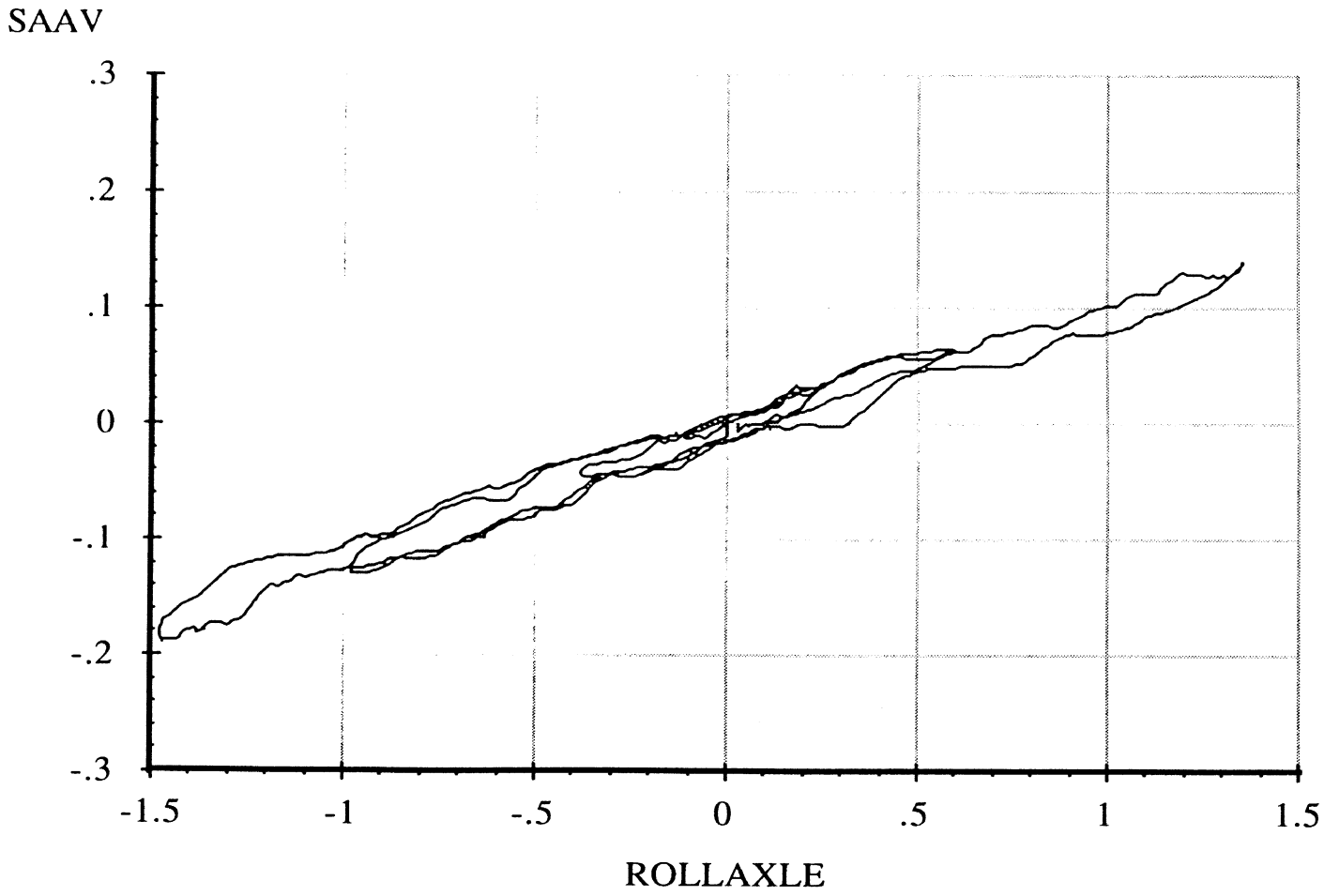

Abscissa (X): Axle roll angle (ROLLAXLE); degrees; right side compressed, positive.

Ordinate (Y): Average steer angle (SAAV); degrees; steer toward right, positive.

*Note: Brakes on. Force control. Air bags inflated to 20 psi.

Measured by UMTRI for Smart Truck
Fruehauf Model FBB9-F1-28

Data file: SMTTRL22.ERD

Single Trailer Axle Suspension

Lateral Force Compliance

4 Jan 98
Suspension: Trailing Arm (WT)

Suspension Load: 5900 lb.

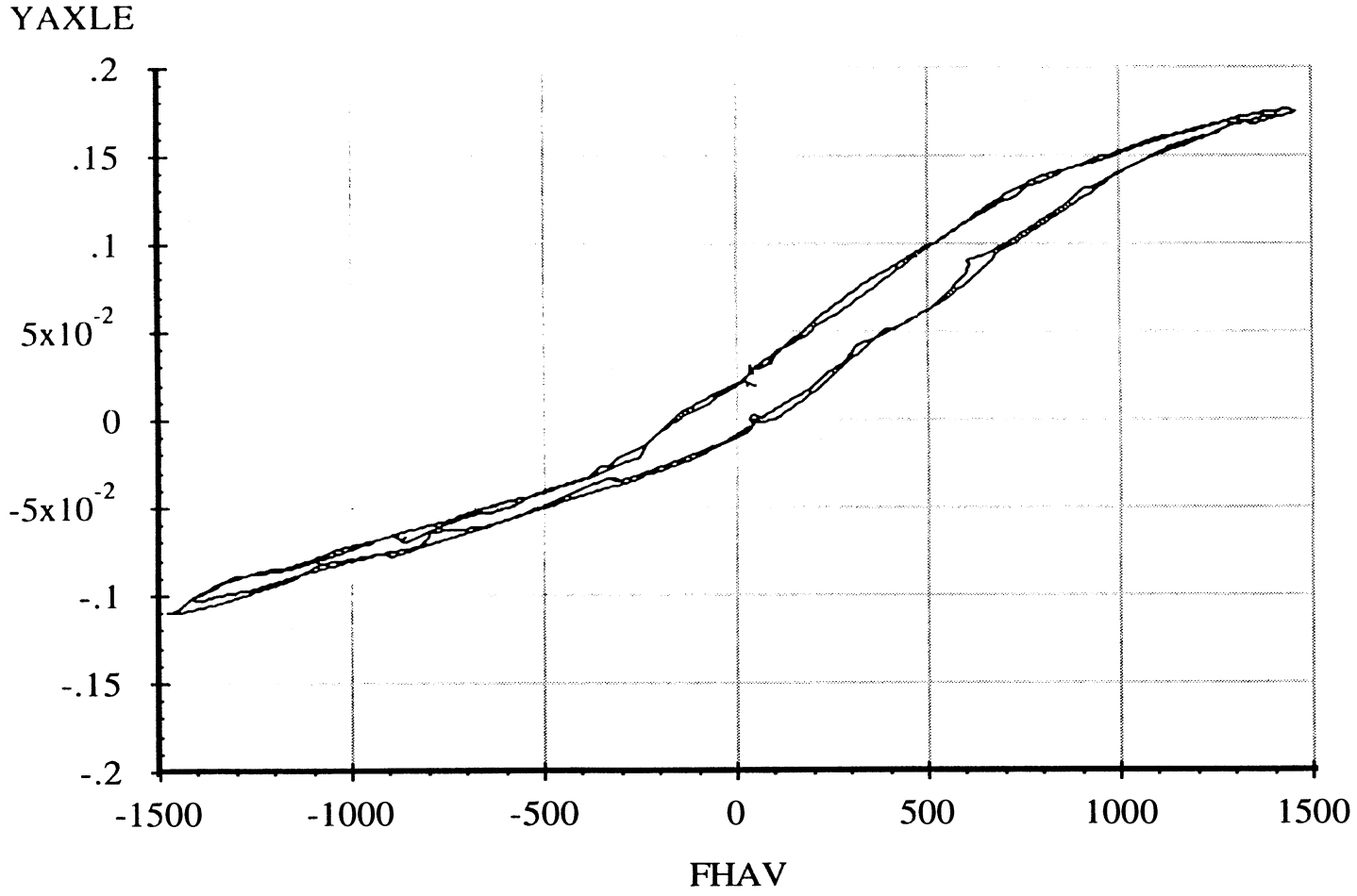

Abscissa (X): Average axle lateral force (FHAV); pounds; applied to both wheels simultaneously; force applied toward right, positive.

Ordinate (Y): Axle lateral translation (YAXLE); inches; motion toward right, positive.

*Note: Brakes on. Position control. Air bags inflated to 20 psi. Reference height of 14.75 inches.

Measured by UMTRI for Smart Truck
Fruehauf Model FBB9-F1-28

Data file: SMTTRL22.ERD

Single Trailer Axle Suspension

Lateral Force Steer

4 Jan 98
Suspension: Trailing Arm (WT)

Suspension Load: 5900 lb.

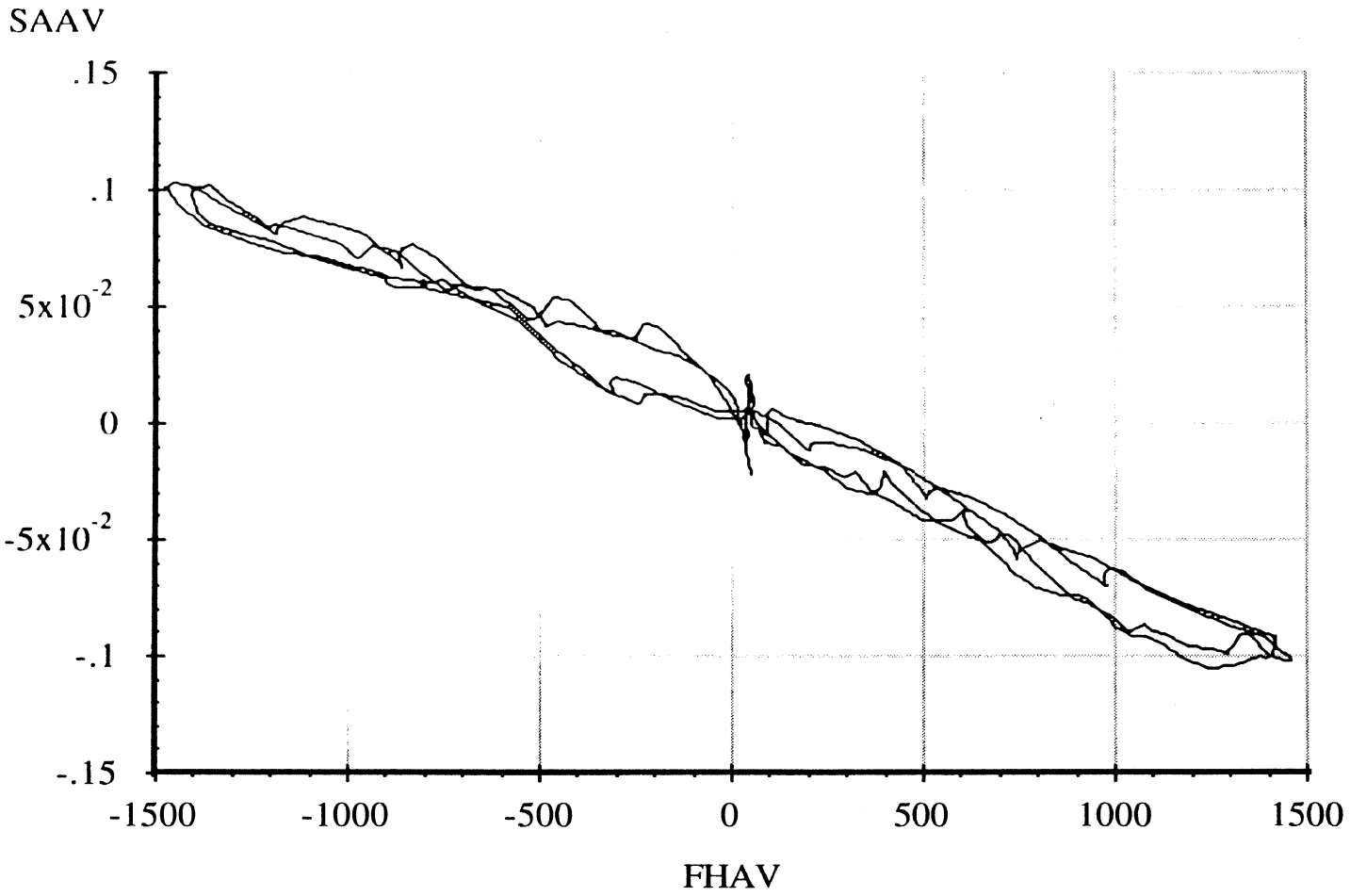

Abscissa (X): Average axle lateral force (FHAV); pounds; applied to both wheels simultaneously; force applied toward right, positive.

Ordinate (Y): Average steer angle (SAAV); degrees; steer toward right, positive.

*Note: Brakes on. Position control. Air bags inflated to 20 psi.

APPENDIX B. MAP OF THE RSA TEST COURSE

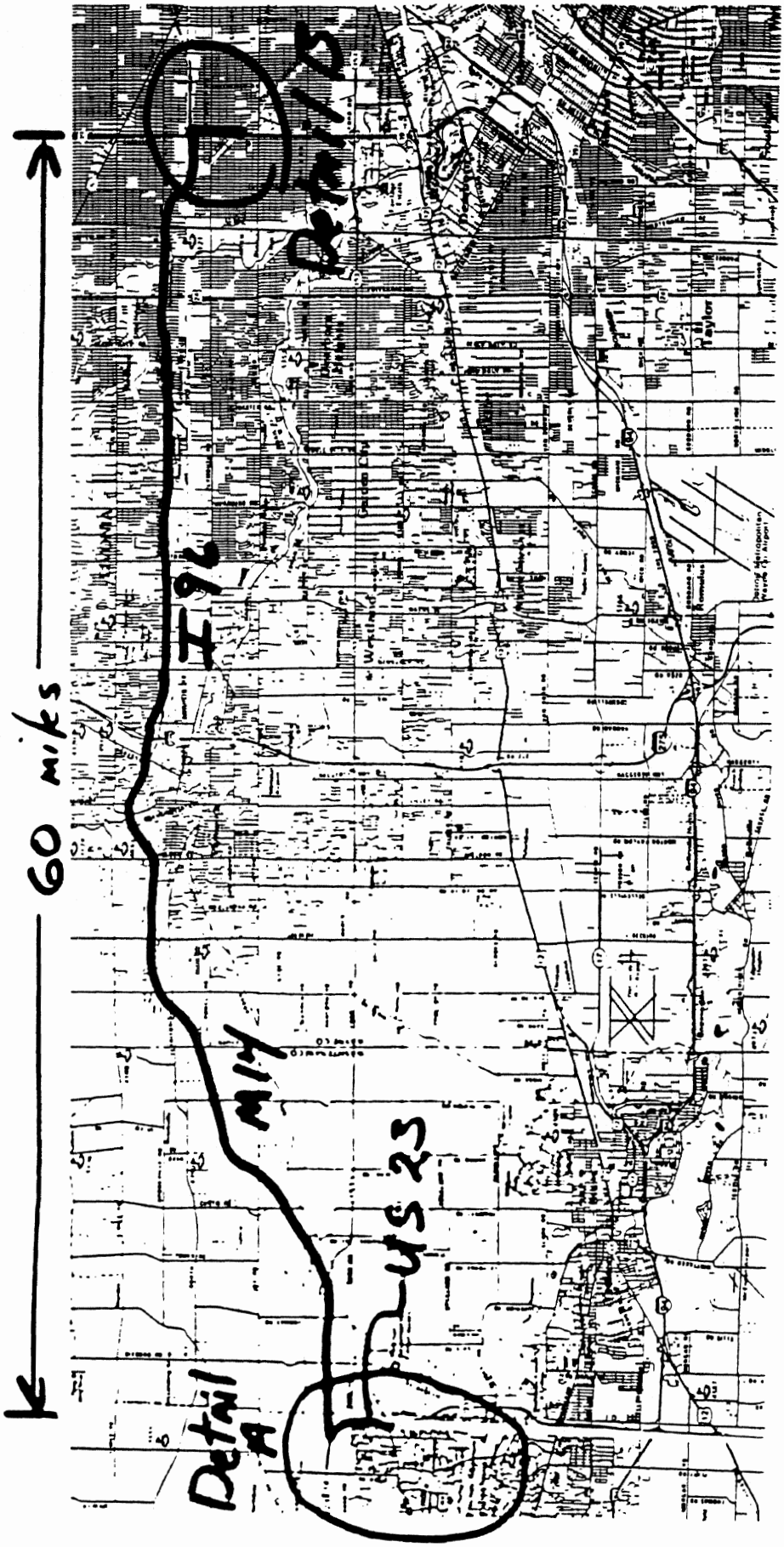

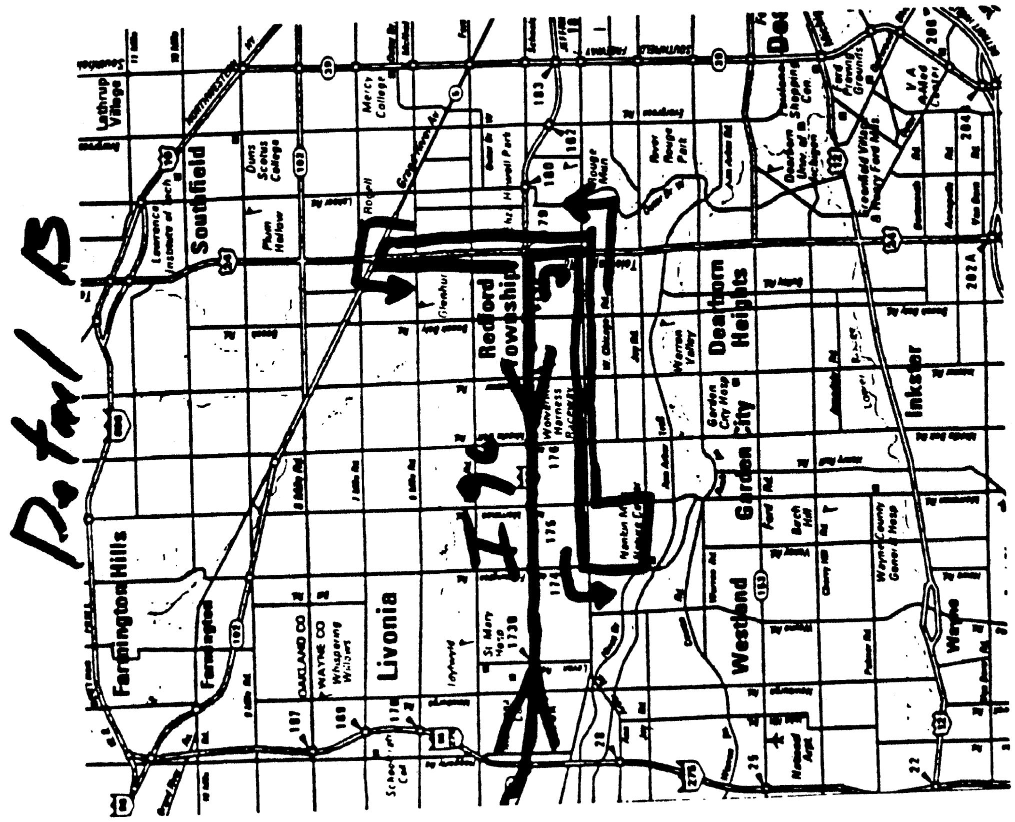
Detail B
I 96
Farmington Hills
Farmington
Livonia
Southfield
Redford Township
Dearborn Heights
Garden City
Westland
Inkster
Wayne

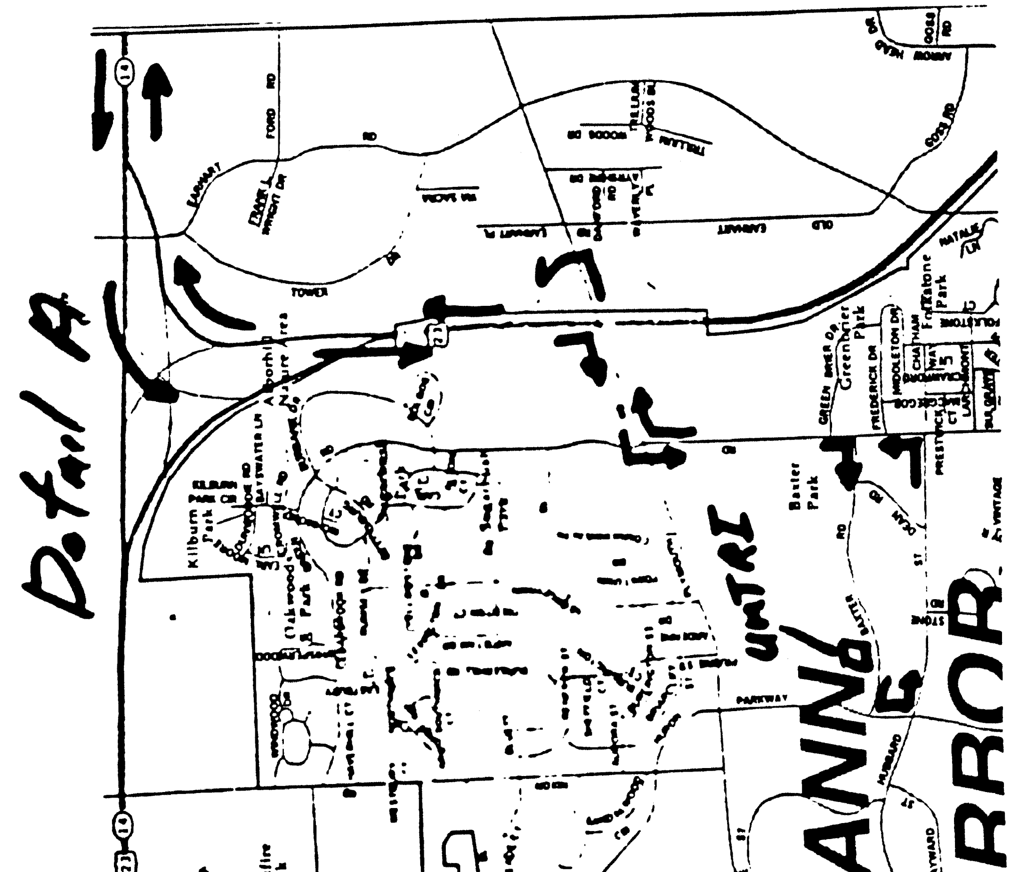
Detail A
UMTRI
ANN ARBOR
Kilburn Park
Foxfire Park
Baxter Park
Greenbrier Park

APPENDIX C

INTRODUCTION

This appendix presents analyses underlying the RSA concept and exploring alternative approaches for computing vehicle properties using sensory data. Two alternative concepts were pursued: one of which addressed an exclusively tractor-mounted system (referred to here as "RSA for dummy trailer"); the other addressed trailer-borne elements to further enhance RSA performance (referred to here as "RSA for smart trailer"). Taking real-world market factors into consideration, the first concept is generally more attractive as a potential product.

The key issue to develop a RSA system either for the smart trailer or the dummy trailer case is to estimate the critical lateral acceleration for truck rollover. In the RSA for smart trailer case, we analyzed the truck rollover process. According to the mechanism of truck rollover, the process was classified into three categories: 1) full load transfer occurs across the fifth wheel first, 2)the tires of axle 2 lift off the ground, and 3) the tires of axle 3 lift off the ground. The appropriate methods of estimating the critical lateral acceleration for truck rollover were developed for each of these categories. Exercises using simulated data show that there is a fair agreement between the estimated critical lateral acceleration and the simulated one. However, it is worthwhile to note that these estimations were conducted on the simulated data in steady state. Dynamic effects will pose a big impact on the critical lateral acceleration for truck rollover. Up to this point in the study the dynamic effects have not been incorporated into a stability prediction algorithm.

In the RSA for dummy trailer, the biggest issue is to obtain the estimations of basic trailer parameters such as: CG (center of gravity) height of trailer, trailer wheelbase, and trailer mass. After the required trailer parameters are determined, the trailer can be regarded as a smart trailer, and the critical lateral acceleration for truck rollover can be estimated. In order to determine the trailer parameters, different methods are used. At first, we developed dynamic equilibrium equations of the trailer, and used these equations to fit the measured dynamic signals from force and moment sensors. From the coefficients of the equations obtained by linear regression, trailer parameters were estimated. Practices show that adequate estimations of trailer parameters could not be obtained except for the trailer mass. Then, a spatial spectrum analysis was used to identify trailer wheelbase, and

analysis of the freebody of the sprung mass of the tractor over axle 2 was used to identify CG height of trailer. Fair estimation for trailer wheelbase and CG height can be obtained using these two methods. It should be noted that a specific parameter is estimated by a specific method under the assumption that other parameters are known. It remains to be tested if the above various methods can be integrated. Also, current research is based on the simulated data. In the real world, environment and instrumental noises may significantly degrade these methods. With these concerns and the ignorance of dynamic effects, the feasibility of an RSA for dummy trailer system is questionable.

In Section 2, the research for the feasibility of the RSA for smart trailer approach was reported. The section starts with the definition of a smart trailer. Then the truck rollover processes are presented. Based on the mechanism of truck rollover, methods to estimate the critical lateral acceleration for truck rollover are introduced and detailed implementation procedures are also given. The methods and procedures are then demonstrated for various cases.

Section 3 reports the research for the feasibility of the RSA for dummy trailer approach. Similarly, the section starts with the definition of a smart trailer. A research strategy was then established. The spatial spectrum analysis to identify trailer wheelbase, the analysis of the freebody of the sprung mass of tractor over axle 2 to identify the CG height of the trailer, and the linear regression methods of pitch and roll plane models are introduced. Case studies were given for these methods.

2 RSA FOR SMART TRAILER

2.1 Definition for Smart Trailer

By a smart trailer, we mean that we know the trailer's basic parameters, such as:

T_3	track of axle 3
W_{3US}	unsprung mass of axle 3
h_{3USCG}	CG height of the unsprung mass of axle 3
h_{3r}	height of roll center of axle 3

and we will measure the suspension loads and roll moments of axle 3. Certainly, we also know the tractor's basic parameters, such as:

$W_{2STractor}$	sprung mass of axle 2 when tractor is not connected to a trailer
$h_{2STractor}$	CG height of $W_{2STractor}$
W_{2US}	unsprung mass of axle 2
h_{2USCG}	CG height of the unsprung mass of axle 2
h_{2r}	height of roll center of axle 2
T_2	track of axle 2
h_5	height of the fifth wheel
Y_5	width of the fifth wheel

and we will measure forces and moments at the fifth wheel, such as:

F_{x5}	longitudinal force at the fifth wheel
F_{y5}	lateral force at the fifth wheel
F_{z5}	vertical force at the fifth wheel
M_{x5}	roll moment at the fifth wheel

and the accelerations of the tractor

a_x	longitudinal acceleration of tractor
a_y	lateral acceleration of tractor

2.2 TRUCK ROLLOVER PROCESSES

Rollover processes of the truck will depend on the trailer structure and load distribution. In other words, the trailer structure and load distribution will determine the sequence of rollover at either the fifth wheel or via tire lift off at axle 2 or axle 3. If the load is aligned at the center line of trailer, for the fifth wheel to rollover, the lateral acceleration of trailer must satisfy

$$a_y^5 \geq \frac{\frac{Y_5}{2} F_{Z5}}{K_5}, \tag{2.1}$$

for the tires of axle 2 to lift off the ground, the lateral acceleration of trailer must be,

$$a_y^2 \geq \frac{\frac{(W_{2S} + W_{2US})T_2}{2}}{K_2 + W_{2S}h_{2r} + W_{2US}h_{2USCG}}, \tag{2.2}$$

and for the tire of axle 3 to lift off the ground, the lateral acceleration of trailer must be,

$$a_y^3 \geq \frac{\frac{(W_{3S} + W_{3US})T_3}{2}}{K_3 + W_{3S}h_{3r} + W_{3US}h_{3USCG}} \tag{2.3}$$

where K_5, K_2 and K_3 are respectively the coefficients of the roll moments at the fifth wheel, the roll center of axle 2, and the roll center of axle 3 with the lateral acceleration of the trailer. The deduction of equation (2.1), (2.2) and (2.3) will be given later in this report. For a specific truck, when $a_y^5 = a_y^2$, the fifth wheel will start to rollover at the same time as the tires of axle 2 lift off the ground; when $a_y^5 < a_y^2$, the fifth wheel will start to rollover before the tires of axle 2 start to lift off the ground; when $a_y^5 > a_y^2$, the tires of axle 2 will start to lift off the ground before the fifth wheel starts to rollover. The similar conclusions exist for a_y^3 and a_y^5, a_y^2 and a_y^3. Therefore, the rollover processes of truck can be classified into three categories upon a_y^2, a_y^3 and a_y^5: the fifth wheel rollover first, the tires of axle 2 lift off ground first and the tires of axle 3 lift off ground first.

2.3 CRITICAL LATERAL ACCELERATION FOR TRAILER ROLLOVER

Based on the above analyses, we develop an estimation procedure of critical lateral acceleration for trailer rollover. Figure 2.1 is a flowchart of estimating the critical lateral

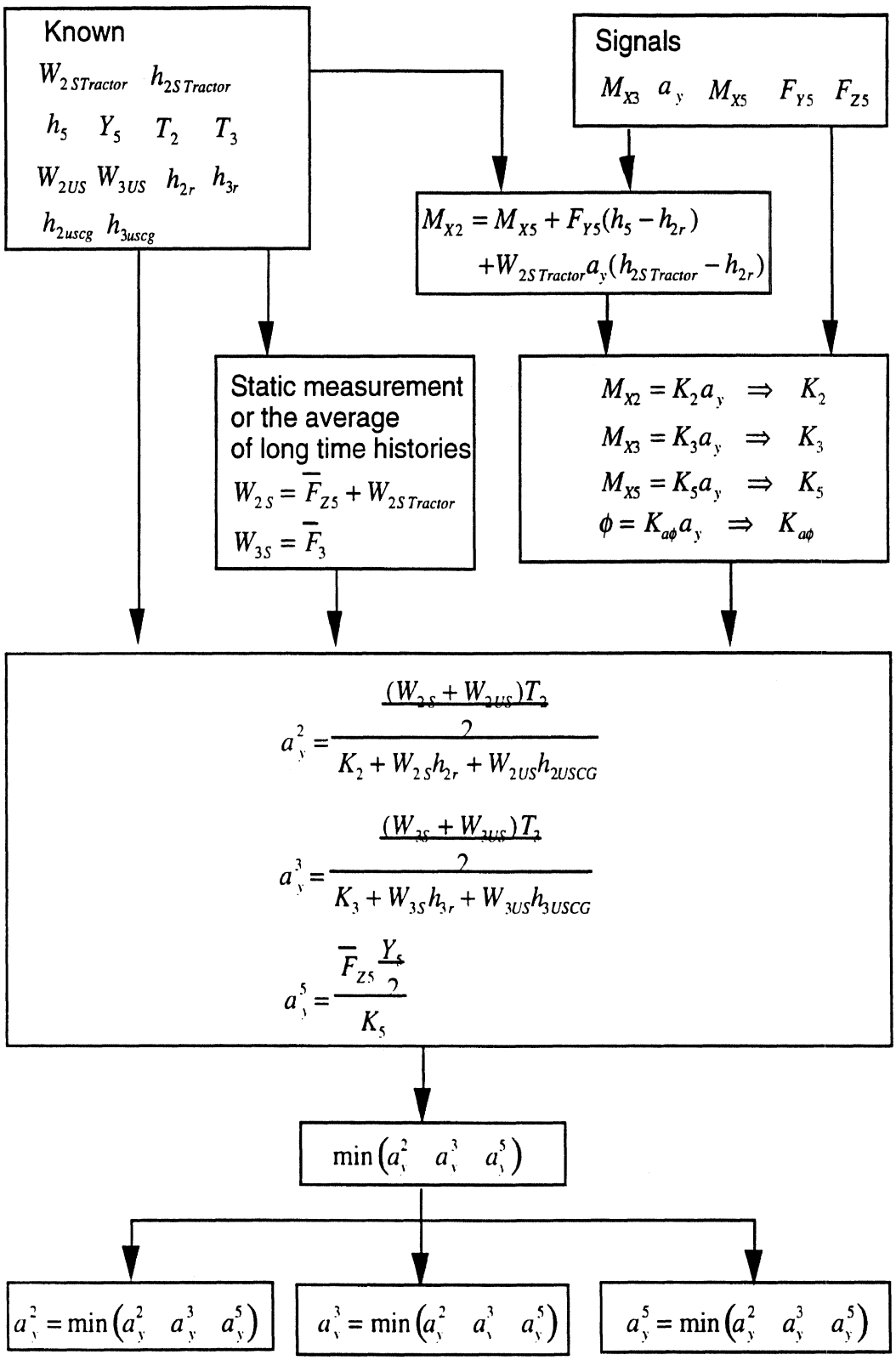

Figure 2.1(a) A flowchart of estimating critical lateral acceleration for rollover of smart trailer

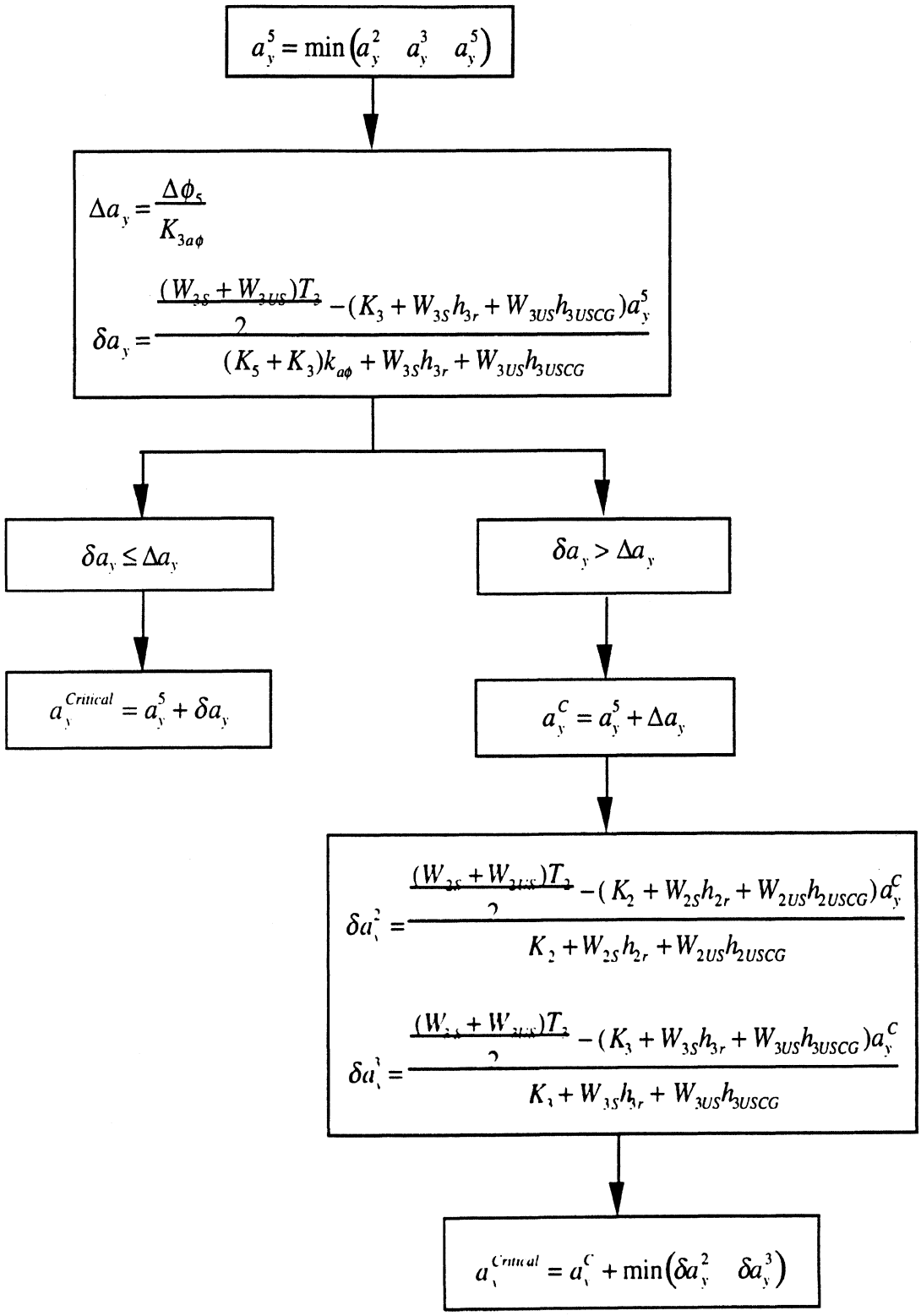

Figure 2.1(b) A flowchart of estimating critical lateral acceleration rollover of smart trailer

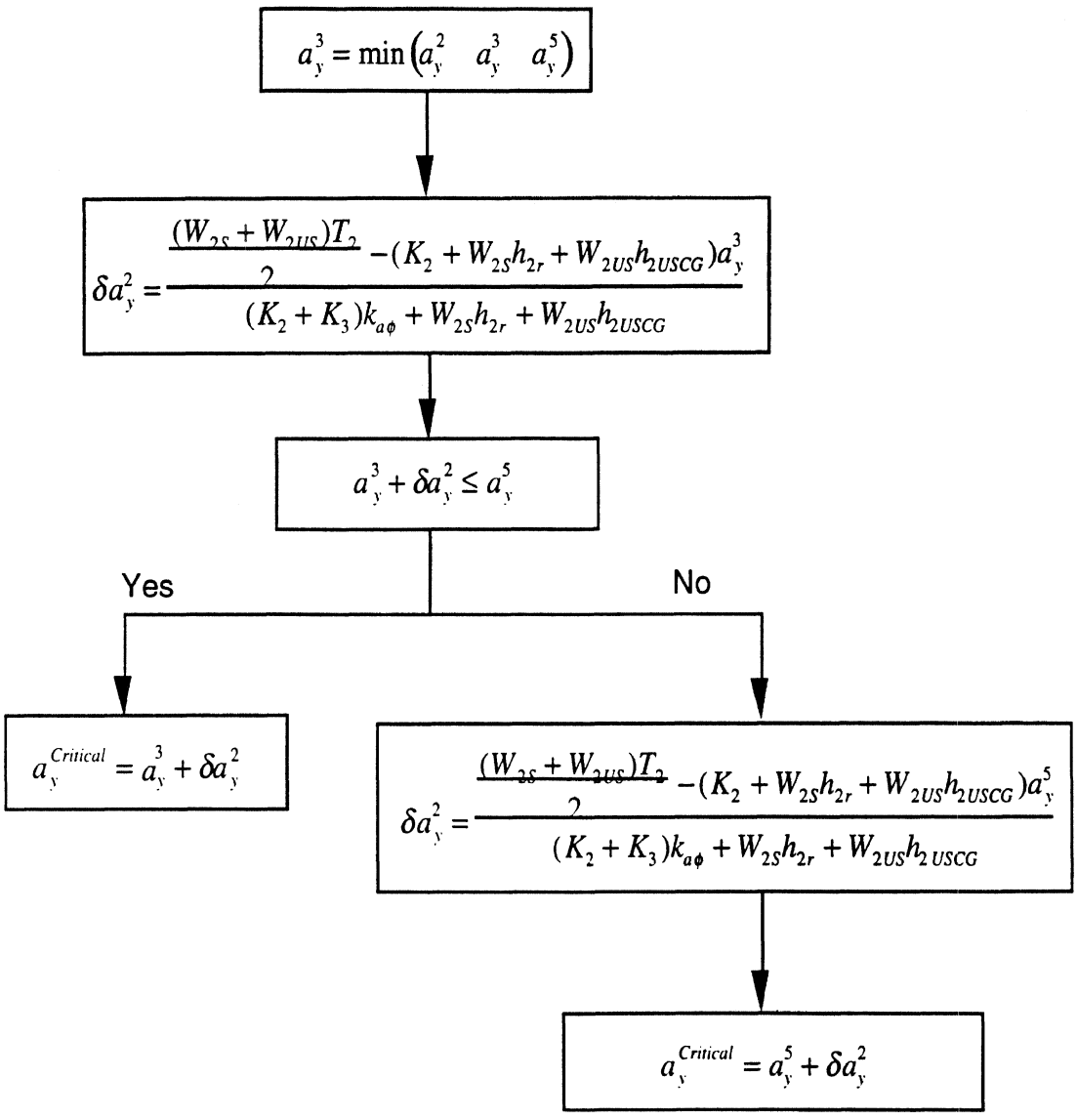

Figure 2.1(c) A flowchart of estimating critical lateral acceleration for rollover of smart trailer

acceleration for smart trailer. Since we are currently dealing with smart trailer, we know tractor and trailer structural parameters, such as: $W_{2STractor}$, $h_{2STractor}$, h_5, Y_5, T_2, T_3, W_{2US}, W_{3US}, h_{2r}, h_{3r}, h_{2USCG}, h_{3USCG}. We can also obtain the sprung masses over axle 2 and 3 by static measurement or the average of dynamic measurement over long time

$$W_{2S} = \overline{F}_{Z5} + W_{2STractor} \tag{2.4}$$

$$W_{3S} = \overline{F}_3 \tag{2.5}$$

where $\overline{F}_{Z5}$ is static measurement or the average of vertical force at the fifth wheel over long time, and $\overline{F}_3$ static measurement or the average of suspension forces of axle 3 over long time.

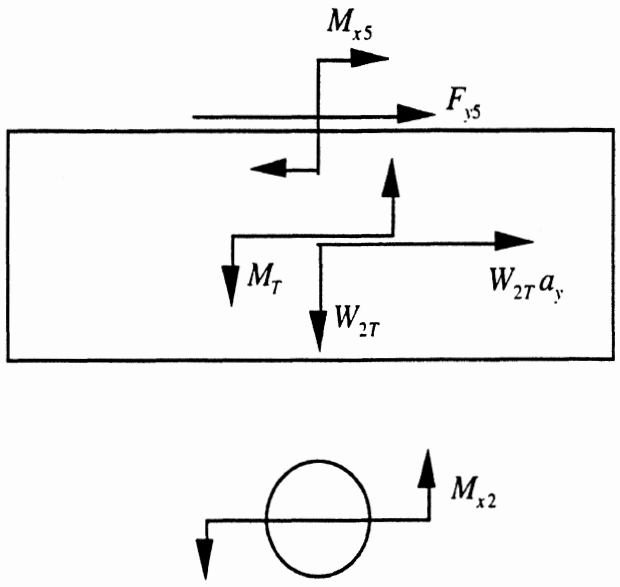

Figure 2.2 A diagram of the freebody of sprung mass of tractor over axle 2

Figure 2.2 is a free-body diagram of the sprung mass of axle 2 when tractor is not connected to a trailer. For the dynamic equilibrium of roll moment , there is

$$M_{x2} = M_{x5} + F_{y5}(h_5 - h_{2r}) + W_{2STractor}a_y(h_{2STractor} - h_{2r}) - M_T \tag{2.6}$$

where M_T is the roll moment sustained by tractor frame. Because of low stiffness of tractor, M_T can be ignored comparing to other terms in equation (2.6). In this case, equation (2.6) is reduced into

$$M_{x2} = M_{x5} + F_{y5}(h_5 - h_{2r}) + W_{2STractor}a_y(h_{2STractor} - h_{2r}) \tag{2.7}$$

Since we will measure dynamic signals of M_{x3}, M_{x5}, F_{y5} and a_y, equation (2.7) can be used to calculate the roll moments at the roll center of axle 2 M_{x2}. If we are going to consider the effect of M_T, equation (2.6) should be used. M_T can be measured by setting sensors on the tractor frame.

When roll angle is small, M_{x2}, M_{x3} and M_{x5} will linearly change with a_y, the following linear equation can be used to fit measured data or calculated data:

$$M_{x2} = K_2 a_y \tag{2.8}$$

$$M_{x3} = K_3 a_y \tag{2.9}$$

$$M_{x5} = K_5 a_y \tag{2.10}$$

The coefficients of equation (2.8), (2.9) and (2.10) can be obtained using linear regression analyses.

In the following, we assume that the load is aligned at the center line of trailer. For the fifth wheel to start rollover, the roll moment and vertical force sustained by the fifth wheel must satisfy

$$M_{x5} \geq F_{z5}\frac{Y_5}{2}, \tag{2.11}$$

or

$$K_5 a_y \geq F_{z5}\frac{Y_5}{2}. \tag{2.12}$$

Therefore

$$a_y^5 \geq \frac{\frac{Y_5}{2}F_{Z5}}{K_5}. \tag{2.13}$$

In order to develop the condition for the tire to lift off the ground, we study the free body of axle shown in Figure 2.3. From the dynamic equilibrium of roll moment , we have

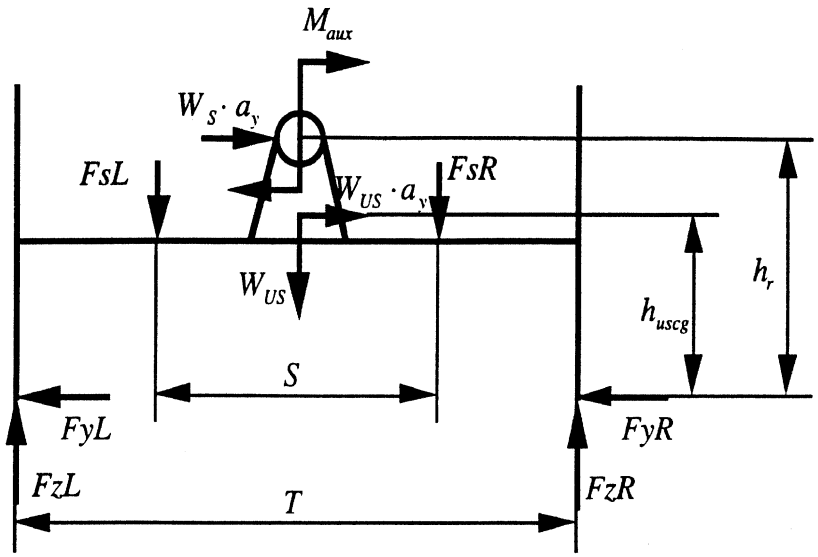

Figure 2.3 A free-body diagram of axle

$$FsL\frac{T+S}{2} - FzL \cdot T + W_{US}\frac{T}{2} - W_S a_y h_r - W_{US} a_y h_{USCG} + FsR\frac{T-S}{2} + M_{aux} = 0, \quad (2.14)$$

or

$$FzL \cdot T = \frac{FsL+FsR}{2}T + W_{US}\frac{T}{2} - W_S a_y h_r - W_{US} a_y h_{USCG} + \frac{FsL-FsR}{2}S + M_{aux}. \quad (2.15)$$

Since

$$W_S = \frac{FsL+FsR}{2}, \quad (2.16)$$

and

$$M_x = \frac{FsL-FsR}{2}S + M_{aux}, \quad (2.17)$$

equation (2.15) can be rewritten into

$$FzL \cdot T = W_S\frac{T}{2} + W_{US}\frac{T}{2} - W_S a_y h_r - W_{US} a_y h_{USCG} + M_x. \quad (2.18)$$

For the tires to lift off the ground, $FzL \cdot T = 0$. Therefore

$$W_S\frac{T}{2} + W_{US}\frac{T}{2} - W_S a_y h_r - W_{US} a_y h_{USCG} + M_x = 0. \quad (2.19)$$

For specifying the analysis for a specific axle, say axle 2, we affix subscript 2 into signs of equation (2.19)

$$W_{2S}\frac{T_2}{2}+W_{2US}\frac{T_2}{2}-W_{2S}a_y h_{2r}-W_{2US}a_y h_{2USCG}+M_{2x}=0. \tag{2.20}$$

Substituting equation (2.8) into (2.20) produces

$$W_{2S}\frac{T_2}{2}+W_{2US}\frac{T_2}{2}-W_{2S}a_y h_{2r}-W_{2US}a_y h_{2USCG}+K_2 a_y=0. \tag{2.21}$$

Therefore, the critical lateral acceleration for the tires of axle 2 to lift off the ground is

$$a_y^2=\frac{\frac{(W_{2S}+W_{2US})T_2}{2}}{K_2+W_{2S}h_{2r}+W_{2US}h_{2USCG}}. \tag{2.22}$$

Similarly, we can obtain the critical lateral acceleration for the tires of axle 3 to lift off the ground

$$a_y^3=\frac{\frac{(W_{3S}+W_{3US})T_3}{2}}{K_3+W_{3S}h_{3r}+W_{3US}h_{3USCG}}. \tag{2.23}$$

When the lateral acceleration of trailer reaches the minimum of a_y^5, a_y^2 and a_y^3, the rollover mechanism corresponding to the minimum of a_y^5, a_y^2 and a_y^3 will come into play.

Figure 2.1(b) is the continuation to the flowchart of estimating critical lateral acceleration for rollover of smart trailer when the fifth wheel comes into rollover first. Since lash exists in the fifth wheel, the restoring roll moment provided by the fifth wheel will no longer increase when the fifth wheel comes into rollover process until the trailer completes lash journey of the fifth wheel. During this process, the tire of axle 2 will obviously keep contact with ground. Now, we need to know if the tire of axle 3 will lift off ground during this process.

For trailer to get an increment of roll angle $\Delta\phi$, the lateral acceleration of trailer should increase

$$\Delta a_y=\frac{\Delta\phi}{K_{a\phi}}. \tag{2.24}$$

where $K_{a\phi}$ is the coefficient of trailer roll angle and trailer lateral acceleration. Therefore, for trailer to finish the lash journey of the fifth wheel, the lateral acceleration of trailer should have an increment

$$\Delta a_y^5 = \frac{\Delta\phi_5}{K_{a\phi}}. \tag{2.25}$$

When the lateral acceleration of trailer reaches a_y^5, the destabilizing moment sustained by axle 3 due to lateral acceleration is

$$M_{destabilizing} = (K_3 + W_{3S}h_{3r} + W_{3US}h_{3USCG})a_y. \tag{2.26}$$

Since the residual restoring moment which axle 3 is able to provide is

$$M_{restoring} = \frac{(W_{3S} + W_{3US})T_3}{2} - (K_3 + W_{3S}h_{3r} + W_{3US}h_{3USCG})a_y^5, \tag{2.27}$$

the increment of trailer lateral acceleration for the tires of axle 3 to lift off ground is

$$\delta a_y = \frac{\frac{(W_{3S} + W_{3US})T_3}{2} - (K_3 + W_{3S}h_{3r} + W_{3US}h_{3USCG})a_y^5}{K_3 + W_{3S}h_{3r} + W_{3US}h_{3USCG}}. \tag{2.28}$$

If $\delta a_y \le \Delta a_y^5$, the tires of axle 3 will lift off ground before the fifth wheel finishes the lash journey. In this case, the critical lateral acceleration for trailer to rollover is

$$a_y^{Critical} = a_y^5 + \delta a_y. \tag{2.29}$$

If $\delta a_y > \Delta a_y^5$, the fifth wheel will finish the lash journey before the tires of axle 3 lift off ground. For the fifth wheel to finish the lash journey, the lateral acceleration will increase to

$$a_y^C = a_y^5 + \delta a_y. \tag{2.30}$$

After the fifth wheel finishes the lash journey, the fifth wheel regain the roll restoring capability. The next task is to figure out whether the tires of axle 2 will lift off ground before the tires of axle 3 lift off ground. When the lateral acceleration of trailer reaches a_y^C, the destabilizing moment sustained by axle 3 due to lateral acceleration is

$$M_{destabilizing} = (K_3 + W_{3S}h_{3r} + W_{3US}h_{3USCG})a_y. \tag{2.31}$$

Since the residual restoring moment which axle 3 is able to provide is

$$M_{restoring} = \frac{(W_{3S} + W_{3US})T_3}{2} - (K_3 + W_{3S}h_{3r} + W_{3US}h_{3USCG})a_y^C, \tag{2.32}$$

the increment of trailer lateral acceleration for the tires of axle 3 to lift off ground is

$$\delta a_y^3 = \frac{\frac{(W_{3S} + W_{3US})T_3}{2} - (K_3 + W_{3S}h_{3r} + W_{3US}h_{3USCG})a_y^C}{K_3 + W_{3S}h_{3r} + W_{3US}h_{3USCG}}. \tag{2.33}$$

Similarly, the increment of trailer lateral acceleration for the tires of axle 2 to lift off ground is

$$\delta a_y^2 = \frac{\frac{(W_{2S}+W_{2US})T_2}{2} - (K_2 + W_{2S}h_{2r} + W_{2US}h_{2USCG})a_y^C}{K_2 + W_{2S}h_{2r} + W_{2US}h_{2USCG}}. \tag{2.34}$$

The final critical lateral acceleration for trailer to rollover is

$$a_y^{Critical} = a_y^C + \min\left(\delta a_y^2, \delta a_y^3\right). \tag{2.35}$$

Figure 2.1(c) is the continuation to the flowchart of estimating critical lateral acceleration for rollover of smart trailer when the tires of axle 3 lift off ground first. The reasoning processes are the same as the above.

2.4 CASE STUDY

2.4.1 Case 1 Fifth Wheel_Axle 3_Axle 2

Figure 2.4 is a schematic representation of the vehicle dynamics simulation model for case 1. From simulation results, the fifth wheel rollover (i.e., complete load transfer) occurs first. The lateral acceleration for the initiation of the fifth wheel rollover is 0.294. During the process of the fifth wheel rollover, the left side tires of axle 3 start to lift off the ground at a lateral acceleration of 0.338. Once the left side tires of axle 3 start to lift off the ground, axle 2 loses its stability immediately. Figure 2.5, 2.6, 2.7 and 2.8 show these results clearly.

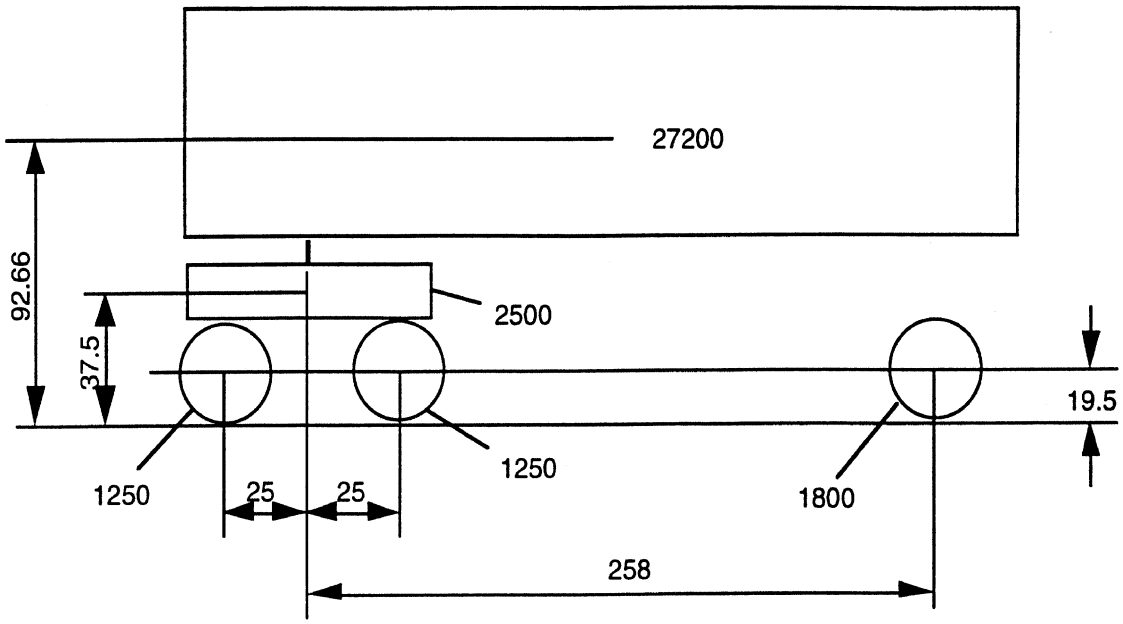

Figure 2.4 A schematic representation of the vehicle dynamics simulation model

According to the procedure shown in Figure 2.1, the calculation processes are explained in the following. The known parameters are

$$W_{2STractor} = 2500 \quad Lb$$
$$h_{2STractor} = 37.5 \quad in$$
$$h_5 = 48 \quad in$$
$$Y_5 = 36 \quad in$$
$$T_2 = 72 \quad in$$
$$T_3 = 72 \quad in$$
$$W_{2US} = 2500 \quad Lb$$
$$W_{3US} = 1800 \quad Lb$$
$$h_{2r} = 23 \quad in$$
$$h_{3r} = 21 \quad in$$
$$h_{2USCG} = 19.5 \quad in$$
$$h_{3USCG} = 19.5 \quad in.$$

In the above parameters and the following analyses, the axle 1 and 2 are lumped into a equivalent axle 2.

Since the roll moment, vertical force and lateral force will be measured during truck operating, we consider the simulated data shown in Figure 2.5, 2.6 and 2.7 as the measured signals. The difference is the measured signals include a heavy noise. For smart

trailer system, the roll moment at the roll center of axle 3 will be measured. Similarly, we consider the simulated data shown in Figure 2.8 as the measured signal.

Because of the tractor frame is very soft, there is a slight effect of the tractor on the roll behavior of trailer. If we ignore this effect, the roll moment at the roll center of axle 2 can be calculated by equation (2.36) when the lateral acceleration of trailer, the roll moment and lateral force at the fifth wheel are available

$$M_{X2} = M_{X5} + F_{Y5}(h_5 - h_{2r}) + W_{2STractor}a_y(h_{2STractor} - h_{2r}). \tag{2.36}$$

Figure 2.9 shows a comparison of the estimated roll moment by equation (2.36) and the simulated roll moment at the roll center of axle 2. It can be seen that there is a very good agreement between the estimated data and simulated data. This give us the confidence to use equation (2.36) to calculate the roll moment at the roll center of axle 2 instead of measuring it. However, equation (2.36) should be verified by using the data from the real world before it is applied in the real world.

From the principles of dynamics, the roll moments at the fifth wheel, the roll center of axle 2 and 3, and the roll angle of trailer should increase with the lateral acceleration of trailer linearly when the roll angle of trailer is small enough, for example, 5 degrees.

$$M_{x2} = K_2 a_y \tag{2.36}$$

$$M_{x3} = K_3 a_y \tag{2.37}$$

$$M_{x5} = K_5 a_y \tag{2.38}$$

$$\phi = K_{a\phi} a_y \tag{2.39}$$

Figure 2.5, 2.9 and 2.10 show this kind of linear relationship. The coefficients in equation (2.36), (2.37), (2.38) and (2.39) can be obtained by regression analysis. For this case,

$K_2 = 1109185$ LB-in/g

$K_3 = 1307143$ LB-in/g

$K_5 = 704083$ LB-in/g

$K_{a\phi} = 12.536$ deg/g.

From the static measurement, we obtained the vertical force at the fifth wheel of 12000 LB and the support force at the rear suspension of trailer of 15200 lb. Therefore, the sprung masses for the front and rear suspensions of trailer are respectively

$$W_{2S} = F_{Z5}^{Static} + W_{2STractor} = 12000 + 2500 = 14500 \text{ LB},$$

and

$$W_{3S} = F_{3S}^{Static} = 15200 \text{ LB}.$$

Also, the average of long time histories can be used in lieu of the static measurements.

When all of these data is available, we can estimate the critical lateral accelerations for the fifth wheel, axle 2 and 3

$$a_y^2 = \frac{\frac{(W_{2S} + W_{2US})T_2}{2}}{K_2 + W_{2S}h_{2r} + W_{2US}h_{2USCG}} = \frac{\frac{(14500 + 2500)\cdot 72}{2}}{1109185 + 14500\cdot 23 + 2500\cdot 19.5} = 0.4103 \text{ g}$$

$$a_y^3 = \frac{\frac{(W_{3S} + W_{3US})T_3}{2}}{K_3 + W_{3S}h_{3r} + W_{3US}h_{3USCG}} = \frac{\frac{(15200 + 1800)\cdot 72}{2}}{1307143 + 15200\cdot 21 + 1800\cdot 19.5} = 0.3684 \text{ g}$$

$$a_y^5 = \frac{\frac{Y_5}{2}\overline{F}_{Z5}}{K_5} = \frac{\frac{36}{2}\cdot 11500}{704083} = 0.294 \text{ g}.$$

From the above results, we conclude that the fifth wheel will rollover first. Since there is a lash of 1.7 degree at the fifth wheel, the lateral acceleration of trailer will increase for the fifth wheel to finish the lash travel

$$\Delta a_y = \frac{\Delta\phi_5}{K_{a\phi}} = \frac{1.7}{12.536} = 0.1356 \text{ g}.$$

However, for axle 3 to lift off the ground, the lateral acceleration of trailer will only increase

$$\delta a_y = \frac{\frac{(W_{3S}+W_{3US})T_3}{2} - (K_3 + W_{3S}h_{3r} + W_{3US}h_{3USCG})a_y^5}{(K_5+K_3)K_{\phi a} + W_{3S}h_{3r} + W_{3US}h_{3USCG}}$$

$$= \frac{\frac{(15200+1800)\cdot 72}{2} - (1307143 + 15200\cdot 21 + 1800\cdot 19.5)\cdot 0.294}{(704083+1307143)\cdot 1.2327 + 15200\cdot 21 + 1800\cdot 19.5}$$

$$= 0.0422 \text{ g.}$$

Since δa_y is smaller than Δa_y, axle 3 will lift off the ground before the fifth wheel finishes its lash travel. Therefore, the critical lateral acceleration for trailer stability is

$$a_y^{Critical} = a_y^5 + \delta a_y = 0.294 + 0.0442 = 0.3382 \text{ g.}$$

Comparing to the simulated results, this is a very good estimation for the trailer rollover.

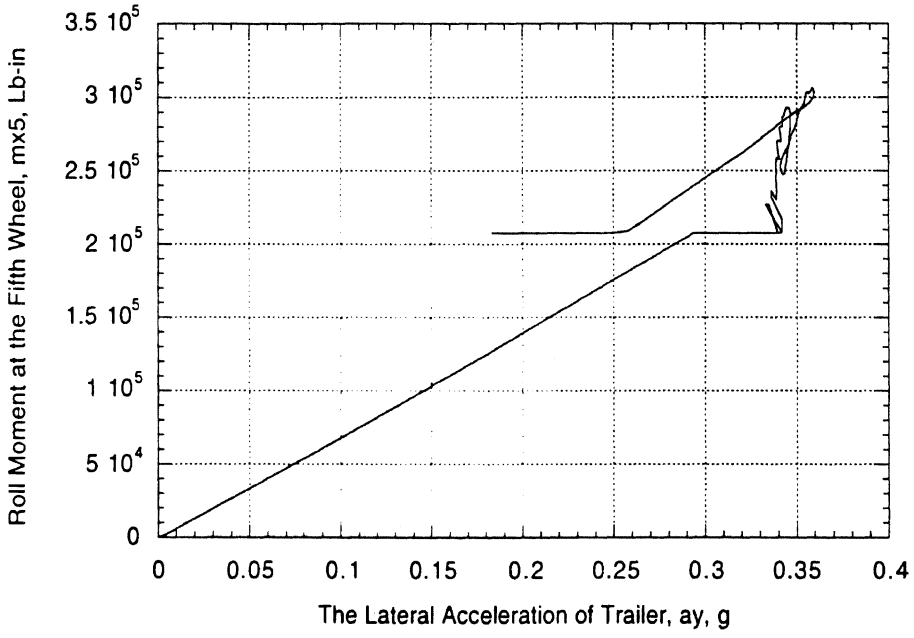

Figure 2.5 Simulation results: roll moment at the fifth wheel vs. lateral acceleration

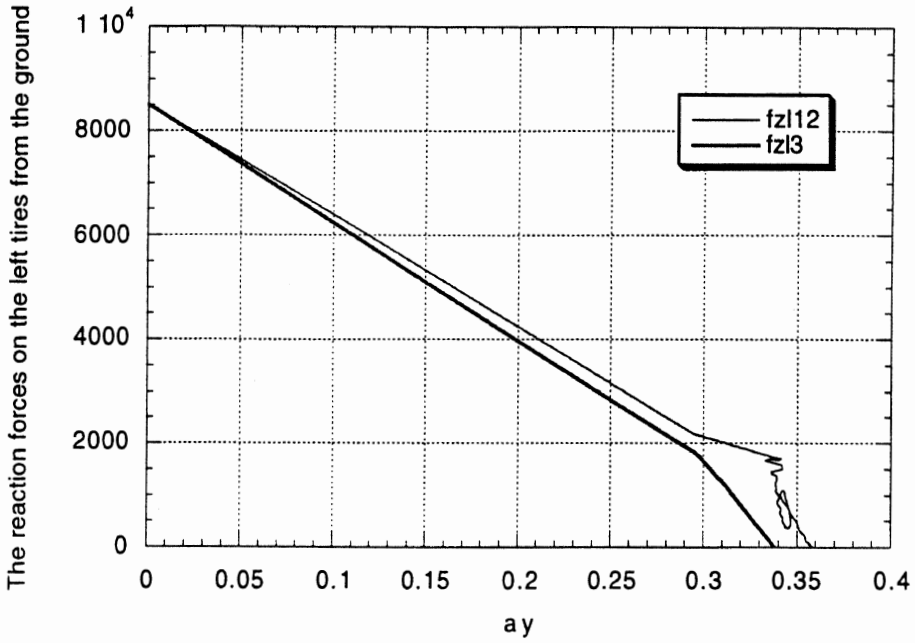

Figure 2.6 Simulation results: reaction forces vs. lateral acceleration

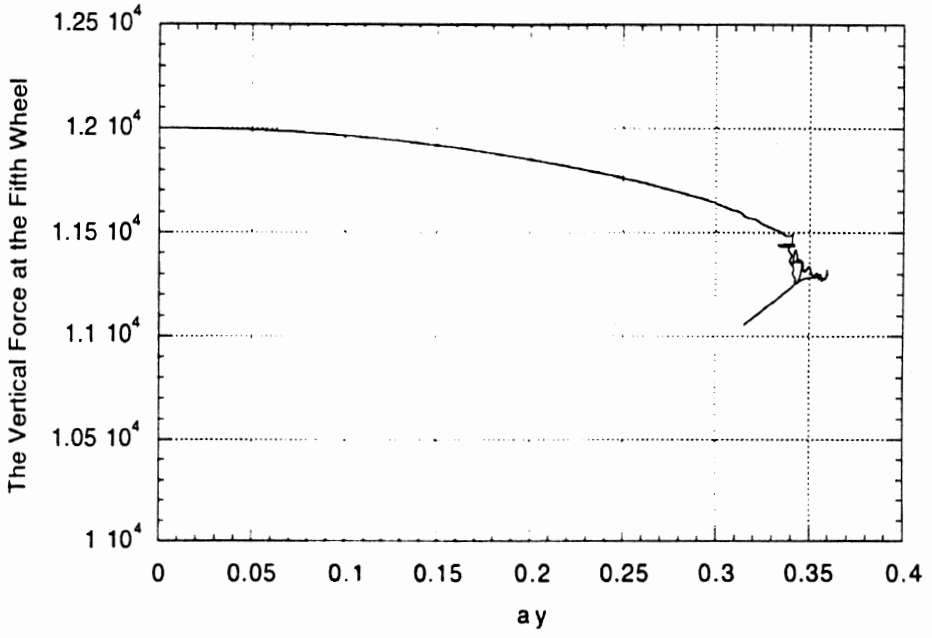

Figure 2.7 Simulation results: vertical force at the fifth wheel vs. lateral acceleration

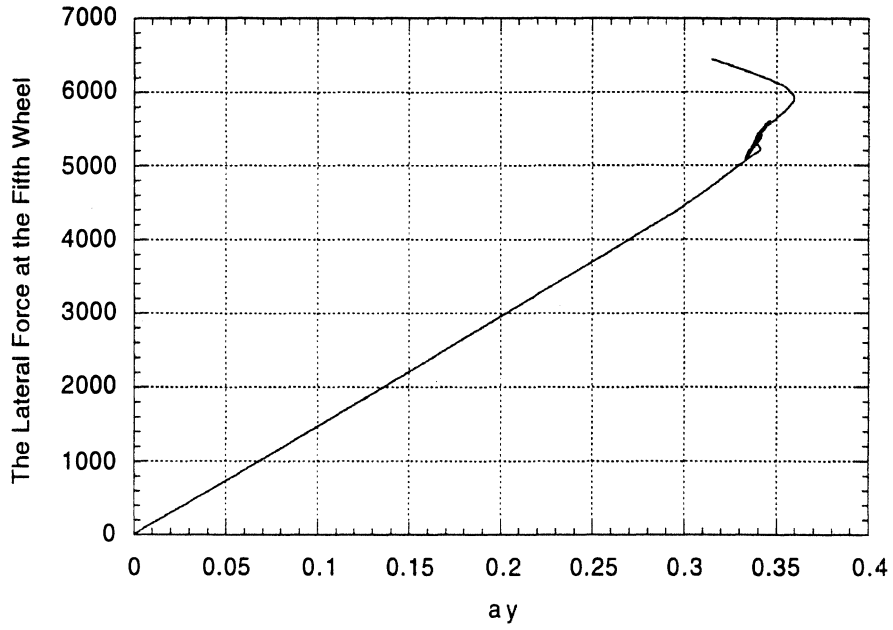

Figure 2.8 Simulation results: lateral force at the fifth wheel vs. lateral acceleration

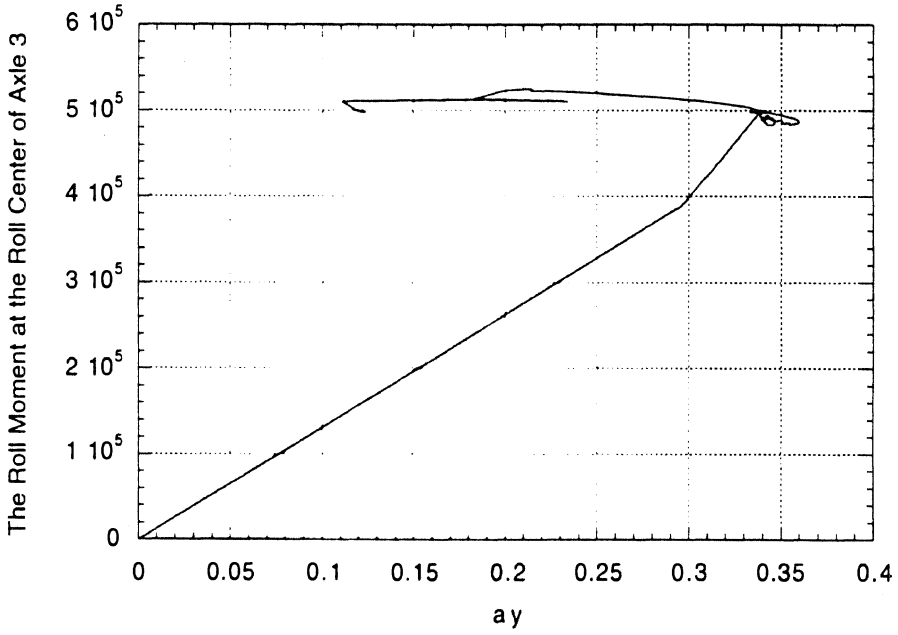

Figure 2.9 Simulation results: roll moment at the roll center of axle 3 vs. lateral acceleration

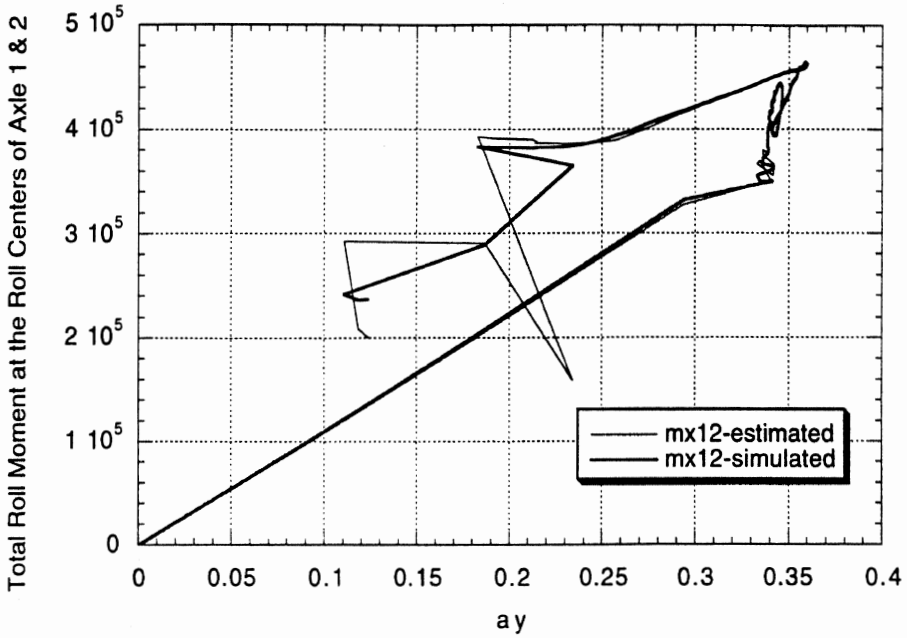

Figure 2.10 Simulation results: reaction forces vs. lateral acceleration

3 RSA FOR DUMMY TRAILER

3.1 Definition for Dummy Trailer

By dummy trailer, we mean that we do not have information about the trailer's basic parameters and load distribution. Certainly, we know tractor structure parameters, such as:

$W_{2STractor}$	sprung mass of axle 2 when tractor is not connected to a trailer
$h_{2STractor}$	CG height of $W_{2STractor}$
W_{2US}	unsprung mass of axle 2
h_{2USCG}	CG height of the unsprung mass of axle 2
h_{2r}	height of roll center of axle 2
T_2	track of axle 2
h_5	height of the fifth wheel
Y_5	width of the fifth wheel

and we will measure forces and moments at the fifth wheel, such as:

F_{x5}	longitudinal force at the fifth wheel
F_{y5}	lateral force at the fifth wheel
F_{z5}	vertical force at the fifth wheel
M_{x5}	roll moment at the fifth wheel

and the accelerations of tractor, such as:

a_x	longitudinal acceleration of tractor
a_y	lateral acceleration of tractor

3.2 Research Strategy

Since we do not have information about trailer parameters and load distribution, the system must itself, identify the trailer parameters and load distribution, such as: trailer mass, CG height, wheelbase, the distance from the fifth-wheel hitch to the trailer CG, and

roll stiffness of the trailer rear suspension. When the required parameters are available, we can estimate the critical lateral acceleration for truck rollover.

Taking market factors into consideration, we exclude traditional system identification approaches in which the system is excited by a typical input, and the responses are analyzed to obtain the information of system structure. System complexity prohibits us to use state-space identification. What we can do is to develop simple vehicle dynamic models, measure dynamic forces and moments at the fifth wheel and some dynamic signals at the tractor, and estimate trailer parameters and load distribution using proposed vehicle dynamic models to fit measured data.

Figure 3.1 is a flowchart for the identification of trailer structural parameters. From the normal driving motions of vehicle, some specific driving motions are picked out to be analyzed by appropriate methods. For example, straight forward movements of the vehicle will be picked out, and signals F_{z5} for this situation will be analyzed in frequency domain

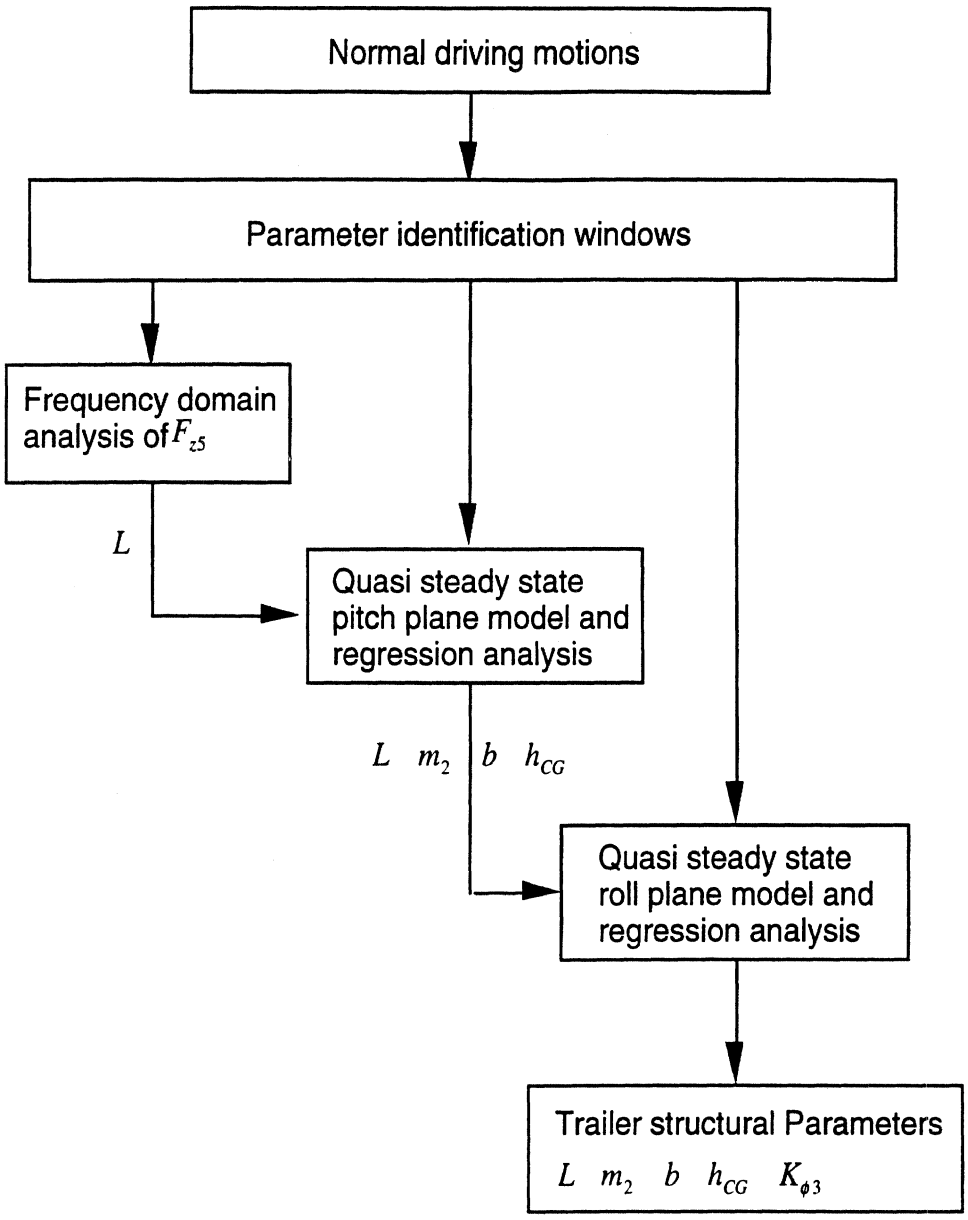

Figure 3.1 A flowchart for the identification of trailer parameters

to obtain trailer wheelbase L. Signals from the straight forward movements of the vehicle can also be analyzed according to pitch plane model to estimate trailer mass m_2, CG height h_{CG}, and the distance from hitch to trailer CG in X direction b. When L, m_2, h_{CG} and b are available, we can import them into roll plane model, and use roll plane model to analyze the signals from the steady turning movements of the vehicle to obtain the estimation of the roll stiffness of trailer rear suspension $K_{\phi 3}$.

3.3 Identification of Trailer Wheelbase

The wheelbase of trailer can be estimated by conducting frequency domain analysis on the signals of F_{z5}. When the truck moves in straight forward direction, road irregularity will be sequentially experienced by the tires of axle 2 and axle 3. Ordinarily, axle 2 is located directly under the fifth wheel, and axle 3 is located apart from the fifth wheel by a distance of wheelbase. In other words, there are two contributions to the vertical forces at the fifth wheel. One is the response of axle 2 to the road irregularity, and another is the response of axle 3 to the road irregularity. Both of them are separated by a spatial distance of wheelbase. If the vertical forces at the fifth wheel are analyzed by spatial spectral analysis, their auto correlation function will show two peaks: one peak will be at original, and another at the position with abscissa of wheelbase. By spatial spectral analysis, we mean that the signals with equal time intervals (typical sampled signals) are first converted into the signals with distance intervals. The converted signals are then analyzed by spectral analysis. In our case, the signals with equal time intervals should be converted into the signals with distance intervals by multiplying the forward velocity of vehicle with the time intervals.

To investigate the feasibility of the above method, several of vehicle dynamic simulations were conducted. The simulated vehicle moves in straight forward direction started at different initial vehicle speeds. The thrusts used in simulations were derived from engine map and transmission properties. The road profile was generated using the software **Road Make.**

From simulation results, the load histories of the vertical forces at the fifth wheel were extracted out to be analyzed by spectral analyses. Figure 3.2 to 3.10 show some results of this kind of spectral analyses. Figure 3.2 shows the auto correlations of the vertical forces at the fifth wheel for different vehicle speeds. For each vehicle speed, simulation lasted 100 seconds, and simulation time step is 0.001 seconds. The simulation results were picked out once every 20 time steps. So the signals obtained form simulations can be regarded as the signals sampled from measured signals by 50 Hz. Since the signals were from simulations, and no filter was used to pre-process the signals. For trailer wheelbase of 258 in, axle 3 should lag behind axle 2 by 1.47 seconds at the vehicle speed of 10 mph. According to the above analyses, there are two peaks for the auto correlations of F_{z5}. One is at the original, and another at time of 1.47 seconds. When the vehicle moves at the speed of 20 mph, there are two peaks for the auto correlations of F_{z5} too. One is at the original, and another at time of o.73 seconds. Similar phenomena exist for other vehicle speeds. These were clearly shown in Figure 3.2. It should be noted that some auto

correlations were vertically moved by certain distances for clarity. Actually, the auto correlations at the original are unity for different vehicle speed.

After signals F_{z5} with equal time intervals are converted into the signals with distance intervals by multiplying the instantaneous forward velocity of vehicle with the time interval, they can be analyzed by spatial spectral analysis. Figure 3.3 shows the results of this kind of analysis. All auto correlations have two peaks. One is at the original, and another at the distance of 240 inches. Since the fifth wheel locates 13 inches ahead of axle 2, the estimation for trailer wheelbase is 253 inches. Comparing to the wheelbase of 258 inches used in simulations, this is a very good estimation.

To investigate the effects of different thrust histories, four types of thrust were used in different simulations. The results of spatial spectral analyses of F_{z5} are shown in Figure 3.4. It can be seen from Figure 3.4 that there are about same peak points of spatial auto correlations for different simulations. Figure 3.5 shows the slight effects of the lengths of simulation. When the first 20 seconds of signals were cut off, the remained signals F_{z5} can be analyzed to see if the first 20 seconds of transient responses have a heavy impact to the auto correlation. Figure 3.6 shows that the effect of transient responses on auto correlation can be ignored. Figure 3.7 shows the effect of sampling rate on auto correlations. Sampling rate does change the peak amplitudes of auto correlation, but has slight effect on the locations of peak points of auto correlation. Fortunately, we only need the location information of peak points of auto correlation. Figure 3.8 shows there is a slight effect of filter on auto correlation of F_{z5} even the filter frequency is 10 Hz. In summary, spatial auto correlation of F_{z5} show two significant peaks: one is at the original, and another at the distance of wheelbase.

Figure 3.9 and 3.10 are the results of another case study. They are similar with Figure 3.2 and 3.3. The difference is that the wheelbase of 258 inches used in simulations for Figure 3.2 and 3.3 were changed to 358 inches used in simulations for Figure 3.9 and 3.10. Figure 3.9 and 3.10 show the auto correlations of F_{z5} for different vehicle speeds respectively from temporal point of view and from spatial point of view. It can be seen from Figure 3.10 that two peaks exist: one is at the original, and another at the distance of 340 inches. Since the fifth wheel is located 13 inches ahead of axle 2, the estimation for trailer wheelbase is 353 inches is a good estimation of the actual wheelbase of 358 inches.

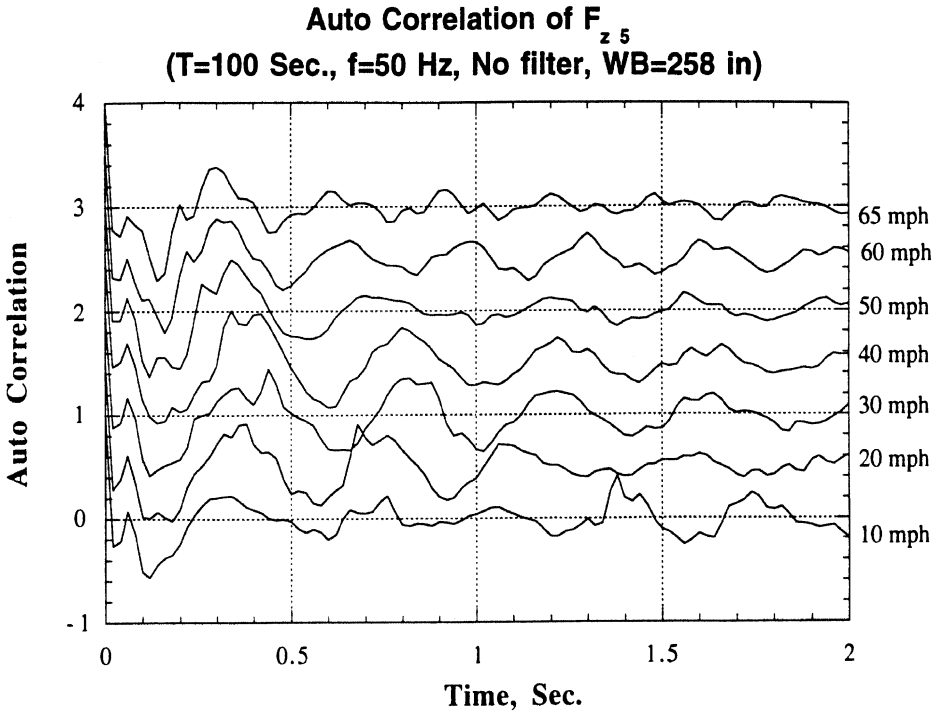

Figure 3.2 Auto correlation of the vertical forces at the fifth wheel for different vehicle initial speeds

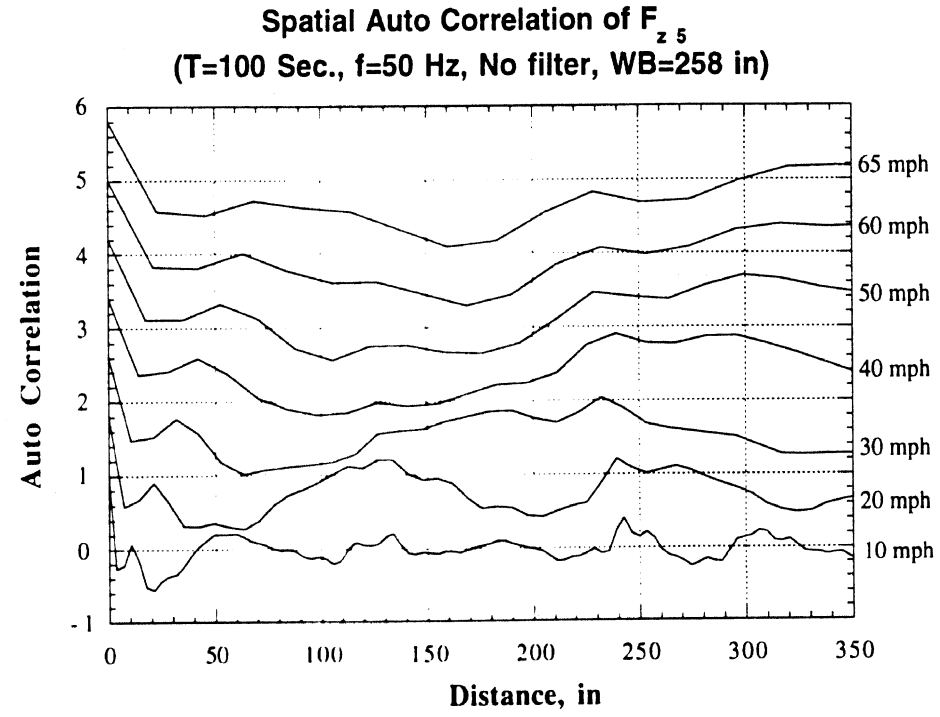

Figure 3.3 Spatial auto correlation of the vertical forces at the fifth wheel for different vehicle initial speeds

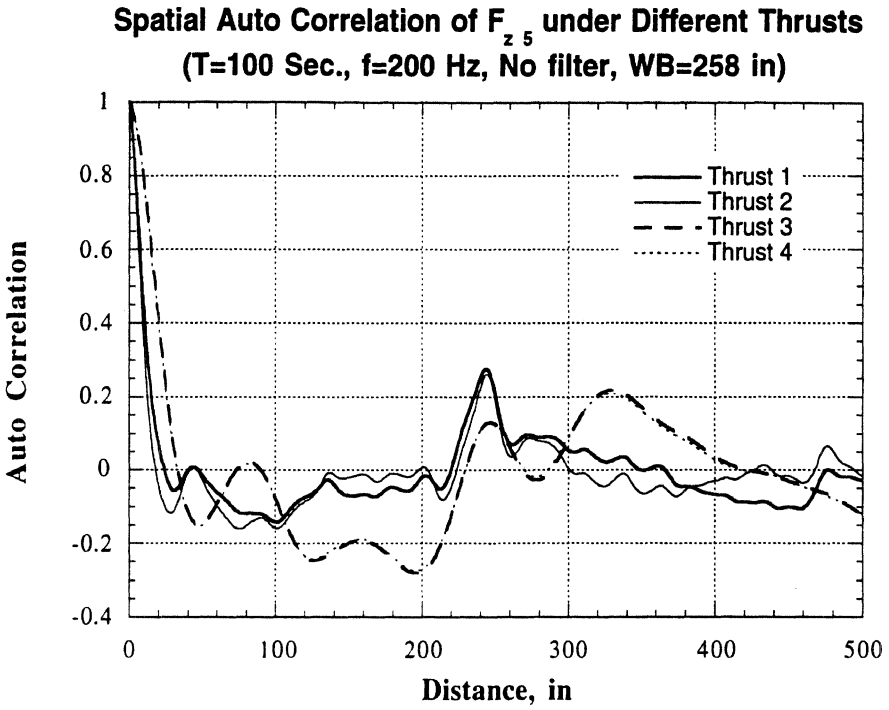

Figure 3.4 Spatial auto correlation of the vertical forces at the fifth wheel for different thrusts

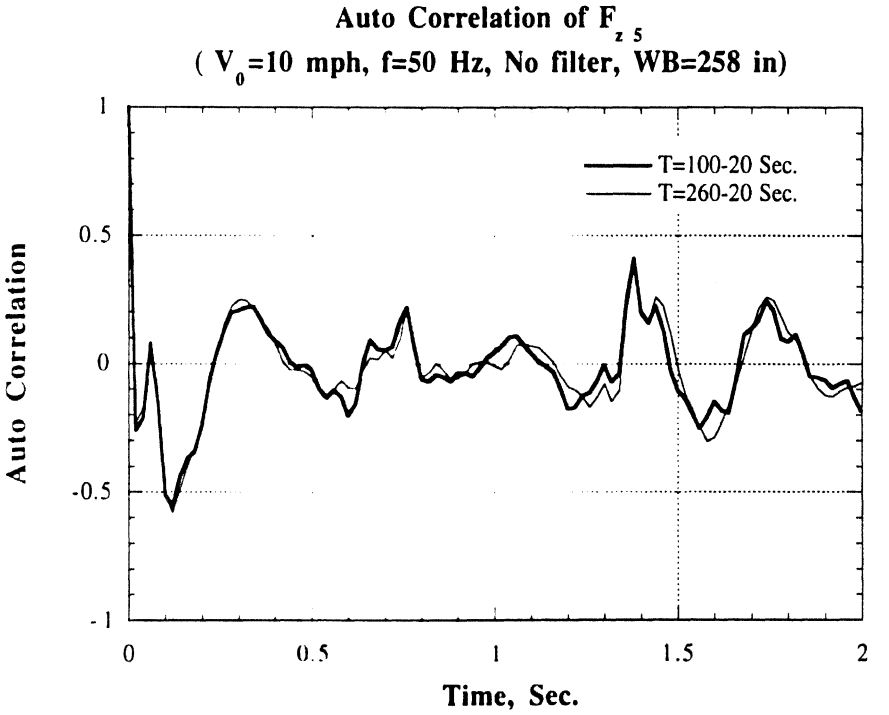

Figure 3.5 Auto correlation of the vertical forces at the fifth wheel with different time lengths

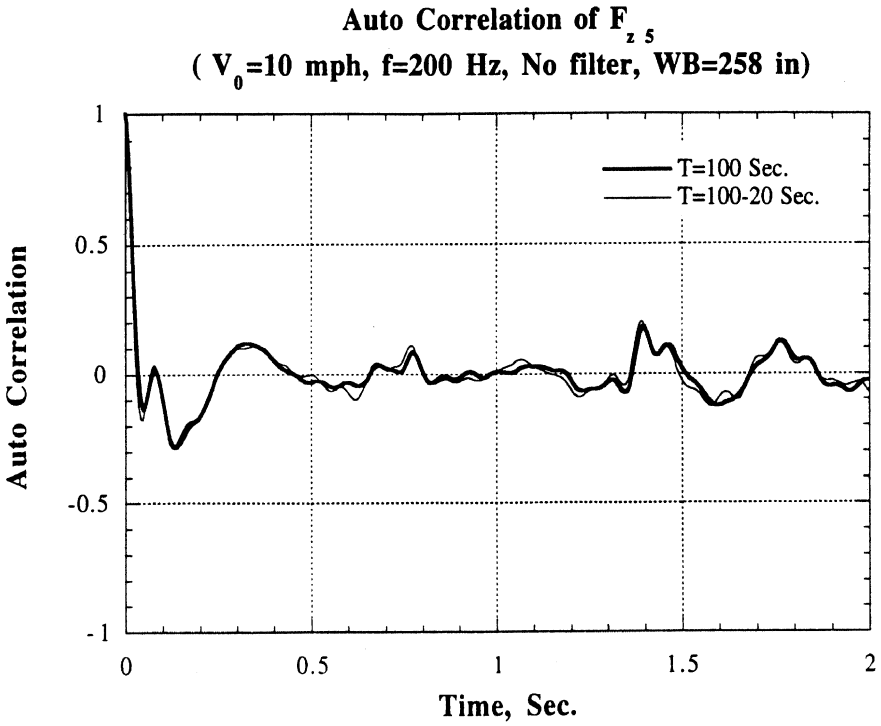

Figure 3.6 Auto correlation of the vertical forces at the fifth wheel with or without transient responses

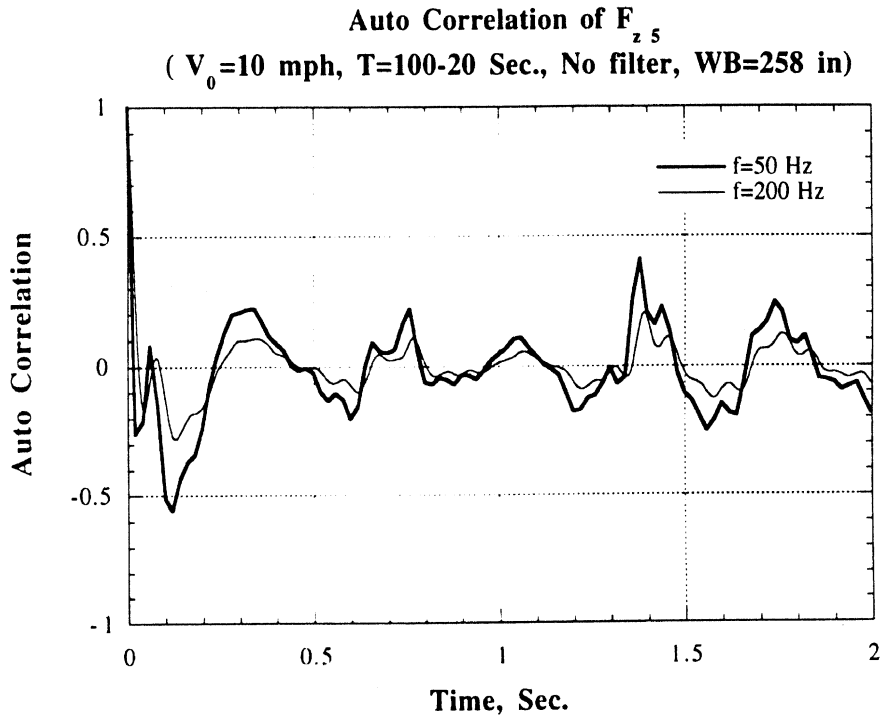

Figure 3.7 Auto correlation of the vertical forces at the fifth wheel for different sample rates

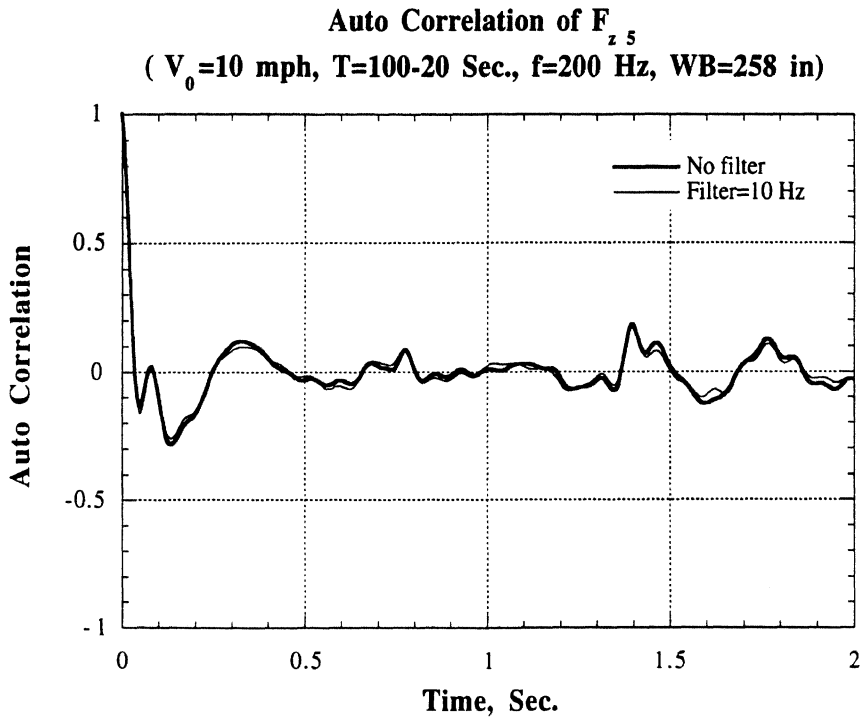

Figure 3.8 Auto correlation of the non filtered and filtered vertical forces at the fifth wheel

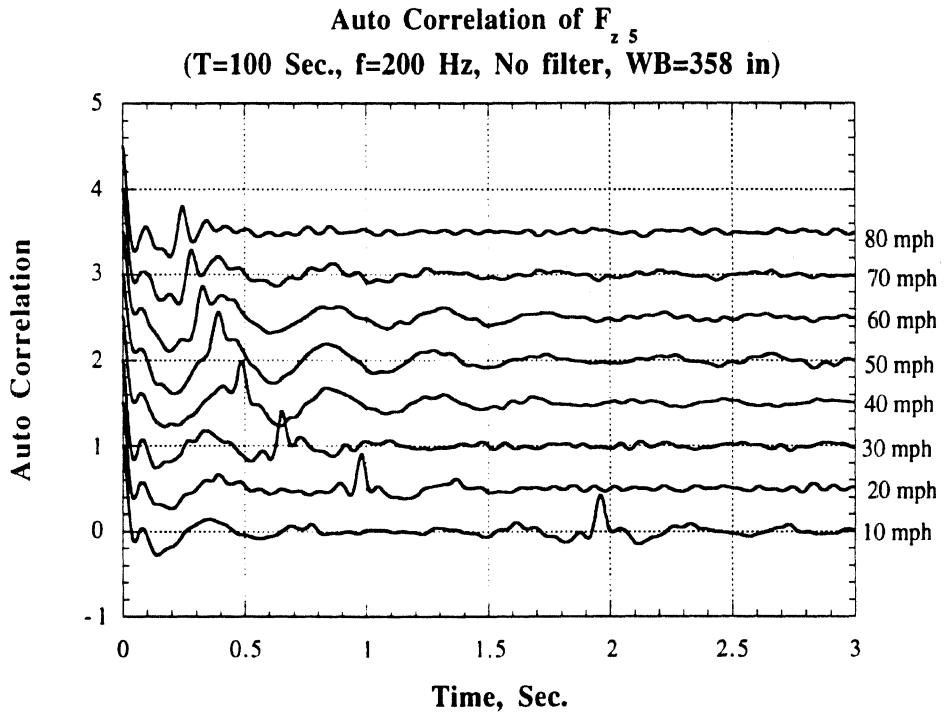

Figure 3.9 Auto correlation of the vertical forces at the fifth wheel for different vehicle initial speed (long wheelbase)

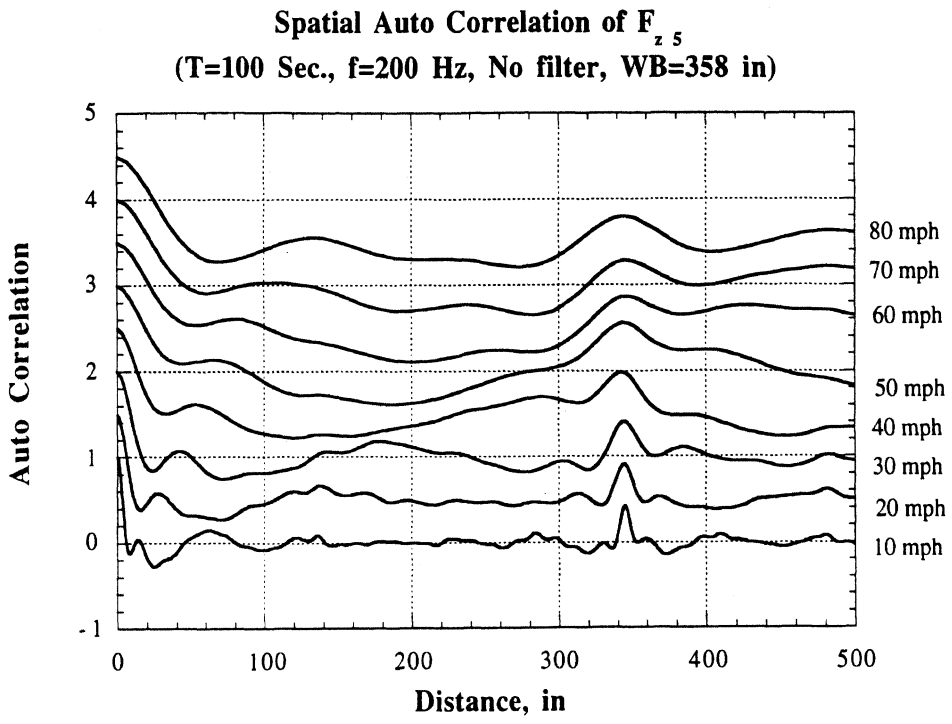

Figure 3.10 Spatial auto correlation of the vertical forces at the fifth wheel for different vehicle initial speed (long wheelbase)

3.4 IDENTIFICATION OF TRAILER STRUCTURAL PARAMETERS

3.4.1 Pitch Plane Model

Theoretically speaking, when measured signals

F_{x5}	longitudinal force at the fifth wheel
F_{y5}	lateral force at the fifth wheel
F_{z5}	vertical force at the fifth wheel
M_{x5}	roll moment at the fifth wheel
a_x	longitudinal acceleration of tractor
V_x	longitudinal velocity of tractor or trailer

are available, we can determine the coefficients of the pitch plane using the models to fit the measured data. From these coefficients of the pitch plane models, the trailer structural

parameters, such as: trailer mass m_2, wheelbase L, CG height h_{CG}, and the distance from hitch to trailer CG in X direction b, can be calculated by simple algebraic manipulations.

For the simplified trailer pitch plane models

$$F_{z5} = \frac{m_2 g b}{L} + \frac{h_5}{L} F_{x5} - \frac{m_2 h_{CG}}{L} a_{x2} - \frac{h_a}{L} f_{v2} V_{x2}^2 \tag{A.1.13}$$

and

$$F_{x5} = f_0 m_2 g + m_2 a_{x2} - f_0 F_{z5} + f_v m_2 g V_{x2} - f_v V_{x2} F_{z5} + f_{v2} V_{x2}^2 \tag{A.1.14}$$

we can rewrite them into the multiple regression format

$$F_{z5} = \beta_{A0} + \beta_{A1} F_{x5} + \beta_{A2} a_{x2} + \beta_{A3} V_{x2}^2 \tag{3.1}$$

$$F_{x5} = \beta_{B0} + \beta_{B1} a_{x2} + \beta_{B2} F_{z5} + \beta_{B3} V_{x2} + \beta_{B4} V_{x2} F_{z5} + \beta_{B5} V_{x2}^2 \tag{3.2}$$

where $\beta_{A0} = \frac{m_2 g b}{L}$ (3.3)

$$\beta_{A1} = \frac{h_5}{L} \tag{3.4}$$

$$\beta_{A2} = -\frac{m_2 h}{L} \tag{3.5}$$

$$\beta_{A3} = -\frac{h_a}{L} f_{v2} \tag{3.6}$$

$$\beta_{B0} = f_0 m_2 g \tag{3.7}$$

$$\beta_{B1} = m_2 \tag{3.8}$$

$$\beta_{B2} = -f_0 \tag{3.9}$$

$$\beta_{B3} = f_v m_2 g \tag{3.10}$$

$$\beta_{B4} = -f_v \tag{3.11}$$

$$\beta_{B5} = f_{v2} \tag{3.12}$$

The coefficients β_{A0}, β_{A1}, β_{A2}, β_{A3}, β_{B0}, β_{B1}, β_{B2}, β_{B3}, β_{B4} and β_{B5} can be obtained by fitting equation (3.1) and (3.2) to measured data using linear regression.

From equation (3.8), we can get $m_2 = \beta_{B1}$. Alternatively, we can get $m_2 = -\frac{\beta_{B0}}{\beta_{B2} g}$ from equations (3.7) and (3.9), or $m_2 = -\frac{\beta_{B3}}{\beta_{B4} g}$ from equations (3.10) and (3.11). If these three

values are adequately close, it is one of the evidences that the above model is valid. Since we have parameter h_5 (49 inches or 1245 mm), when m_2 is available, parameters L, b, h can be calculated as follows:

From equation (3.4) $$L = \frac{h_5}{\beta_{A1}} \tag{3.13}$$

From equation (3.3) $$b = \frac{\beta_{A0} L}{m_2 g} = \frac{\beta_{A0} h_5}{m_2 g \beta_{A1}} \tag{3.14}$$

From equation (3.5) $$h = -\frac{\beta_{A2} L}{m_2} = -\frac{\beta_{A2} h_5}{m_2 \beta_{A1}} \tag{3.15}$$

The same process can be applied to the full trailer pitch plane models.

To investigate the feasibility of the above approach, the following case studies were conducted. The acceleration processes of three axle tractor and semi-trailer combination in straight forward direction were simulated using **TRUCKSIM**. The road profiles used in simulations were generated using software **Make Road**. The power spectral density of road profiles is

$$G_z = 1.6E-07\frac{1}{n^2} \tag{3.16}$$

where n is wave number. The thrust supplied by driving axle was calculated from the engine map and transmission properties. From the simulation results, F_{x5}, F_{y5}, F_{z5}, M_{x5}, a_x, and V_x are extracted out to conduct the above analyses, the trailer structural parameters, such as: trailer mass m_2, wheelbase L, CG height h_{CG}, and the distance from hitch to trailer CG in X direction b, can be obtained.

Table 3.1, 3.2 and 3.3 list the calculation results. In Tables, n is the number of data points that are used in parameter identification. $\sum \Delta F_{x5}^2$ is the sums of differences between F_{x5} calculated and F_{x5} from the simulations. $\sum \Delta F_{z5}^2$ is the sums of differences between F_{z5} calculated from and F_{z5} from the simulations. $\sum \Delta F_{x5}^2$ and $\sum \Delta F_{z5}^2$ can be thought as the measures of the appropriateness of trailer pitch plane models. For repeatability study, seven simulations were made.

The full trailer pitch plane models were used to develop Table 3.1, and parameter identification windows are longitudinal acceleration of trailer $a_{x2} > 0.01\,g$. It can be seen from Table 3.1 that excellent estimation for trailer mass m_2, fair estimations for wheelbase L, CG height h_{CG}, and the distance from hitch to trailer CG in X direction can be

obtained. However, the formidable tasks of measuring trailer pitch and vertical accelerations prohibit the full trailer pitch plane models from being used in real world.

Table 3.1 Parameter identification of trailer

Parameter	m_2	L	b	h_{CG}	n	$\sum \Delta F_{z5}^2$	$\sum \Delta F_{x5}^2$
Par. used in simulation	**22821**	**258.0**	**117.8**	**74.9**			
Simulation 1	22761	303.5	139.0	75.6	3872	2.7E+06	119.2
Simulation 2	22763	286.7	131.2	77.5	3876	1.1E+05	954.3
Simulation 3	22761	266.6	122.1	75.9	3873	9.4E+03	65.4
Simulation 4	22763	278.5	127.5	76.9	3879	3.9E+04	354.2
Simulation 5	22770	316.7	144.9	80.7	3875	1.0E+05	1950.0
Simulation 6	22763	286.7	131.2	77.4	3876	1.1E+05	955.6
Simulation 7	22761	332.6	152.3	82.9	3872	2.3E+04	118.7
Mean	22763	295.9	135.5	78.1			
Std. Dev.	3.2	23.0	10.5	2.7			

* The models used in parameter identification are full trailer pitch plane. There is no restriction for trailer vertical and pitch accelerations. The limitation for trailer longitudinal acceleration is $a_{x2} > 0.01\,g$.

Table 3.2 Parameter identification of trailer

Parameter	m_2	L	b	h_{CG}	n	$\sum \Delta F_{z5}^2$	$\sum \Delta F_{x5}^2$
Par. used in simulation	**22821**	**258.0**	**117.8**	**74.9**			
Simulation 1	22838	255.9	116.8	74.4	1471	137.1	0.38
Simulation 2	22840	254.4	116.0	74.2	1471	136.2	0.36
Simulation 3	22843	232.7	106.1	71.9	1472	136.3	0.37
Simulation 4	22845	257.7	117.5	74.5	1473	137.1	0.44
Simulation 5	22840	254.6	116.1	74.2	1471	136.2	0.37
Simulation 6	22841	254.3	116.0	74.2	1471	136.2	0.37
Simulation 7	22837	255.4	116.5	74.3	1471	136.3	0.36
Mean	22841	252.1	115.0	74.0			
Std. Dev.	2.8	8.7	4.0	0.91			

* The models used in parameter identification are simplified trailer pitch plane models. The restrictions for trailer longitudinal, vertical and pitch accelerations are respectively $a_{x2} > 0.01\,g$, $a_{z2} < 0.0001\,g$ and $\dot{P} < 0.0005\,rad/s^2$.

The simplified trailer pitch plane models were used to develop Table 3.2, and parameter identification windows are longitudinal acceleration of trailer $a_{x2} > 0.01\,g$, vertical acceleration of trailer $a_{z2} < 0.0001\,g$, and pitch acceleration of trailer $\dot{P} < 0.0005\,rad/s^2$. Table 3.2 shows that excellent estimation for trailer mass m_2, wheelbase L, CG height h_{CG}, and the distance from hitch to trailer CG in X direction were obtained. Unfortunately, unrealistic parameter identification windows for trailer pitch and vertical accelerations can not be implemented in real world.

Table 3.3 Parameter identification of trailer

Parameter	m_2	L	b	h_{CG}	n	$\sum \Delta F_{z5}^2$	$\sum \Delta F_{x5}^2$
Par. used in simulation	**22821**	**258.0**	**117.8**	**74.9**			
Simulation 1	22845	2.80	0.98	48.2	3872	1.9E+08	3.0E+08
Simulation 2	22828	0.96	0.15	48.1	3876	5.7E+08	1.2E+04
Simulation 3	22832	4.60	1.80	48.4	3873	1.0E+08	4.3E+03
Simulation 4	22844	1.46	0.38	48.1	3879	3.9E+08	4.2E+03
Simulation 5	22851	0.78	0.08	48.1	3875	8.0E+08	8.2E+03
Simulation 6	22828	0.96	0.15	48.1	3876	5.7E+08	1.2E+04
Simulation 7	22845	2.80	0.98	48.2	3872	1.9E+08	3.0E+03
Mean	22839	2.10	0.65	48.2			
Std. Dev.	9.42	1.40	0.64	0.12			

* The models used in parameter identification are simplified trailer pitch plane models. There is no restriction for trailer pitch and vertical accelerations. The limitation for trailer longitudinal acceleration is $a_{x2} > 0.01\,g$.

If parameter identification windows for trailer vertical acceleration $a_{z2} < 0.0001\,g$, and pitch acceleration $\dot{P} < 0.0005\ rad/s^2$ in the above case were released, the results are listed in Table 3. Except for trailer mass m_2, very poor estimations for other trailer structural parameters can be obtained.

We may draw conclusions from the above case studies that no other useful information except trailer mass m_2 can be obtained from the trailer pitch plane model. Even for trailer mass m_2, we can only claim that we are able to obtain good estimation in simulation environments. It remains to be verified using the data from real world whether we can get good estimation for trailer mass m_2.

Since trailer wheelbase can be obtained from frequency domain analysis of F_{z5}, this information should be incorporated into the above analyses. In other words, we can set

trailer wheelbase to a known value, and estimate trailer mass m_2, CG height h_{CG}, and the distance from hitch to trailer CG in X direction b by analyzing the signals from the straight forward movements of the vehicle according to pitch plane models. Table 3.4 shows the results from some case studies. In Table 3.4, case 1 means we estimated parameters using the full pitch plane model with the condition of $a_{x2} > 0.01\,g$, without restriction on pitch and vertical accelerations. In case 2, the parameters are estimated using the simplified pitch plane model with the condition of $a_{x2} > 0.01\,g$, $a_{z2} < 0.0001\,g$ and $\dot{P} < 0.0005\,rad/s^2$. In case 3, we estimated parameters using the simplified pitch plane model, equation (A.1.13) and (A.1.14), with the condition of $a_{x2} > 0.01\,g$, without restriction on pitch and vertical accelerations. From Table 3.4, it can be seen that the estimations in case 1 are excellent no matter whether or not trailer wheelbase is known. The estimations in case 2 were greatly improved when L is known than L is not known, but the results are still not so good as that in case 1. However, these two cases are not feasible in the real word. Although the estimations in case 3 were improved when L is known than L is not known, the estimations are not adequate enough to be used in engineering analyses. Fortunately, the estimation for trailer mass was stable and accurate in all cases.

Table 3.4 Parameter identification of trailer with known wheelbase

Parameter	m_2	L	b	h_{CG}
Value used in simulations	22821	258.0	117.8	74.9
Case 1: unknown L	22758	254.9	116.7	74.6
Case 1: L=258 in	22758	258.0	118.1	75.5
Case 2: unknown L	22837	318.9	145.6	80.9
Case 2: L=258 in	22837	258.0	117.8	65.5
Case 3: unknown L	22840	8.5	3.6	48.8
Case 3: L=258 in	22840	258.0	109.3	148.1

3.5 IDENTIFICATION OF TRAILER CG HEIGHT

Since the roll moment at the fifth wheel can be expressed as

$$M_{x5} = (W_{2S} - W_{2STractor})a_y(h_{cg} - h_5) + (W_{2S} - W_{2STractor})\sin\phi(h_{cg} - h_5)$$

$$= (W_{2S} - W_{2STractor})(a_y + \sin\phi)(h_{cg} - h_5) \tag{3.17}$$

and the roll moment at the roll center of axle 2 can be expressed as

$$M_{x2} = W_{2S}a_y(h'_{cg} - h_{2r}) + W_{2S}\sin\phi(h'_{cg} - h_{2r})$$

$$= W_{2S}(a_y + \sin\phi)(h'_{cg} - h_{2r}) \tag{3.18}$$

where h'_{cg} is the CG height of lumped mass of sprung masses of tractor and trailer over axle 2, and

$$h'_{cg} = \frac{(W_{2S} - W_{2STractor})h_{cg} + W_{2STractor}h_{2STractor}}{W_{2S}}$$

Dividing equation (3.18) by equation (3.17) yields

$$\frac{M_{x2}}{M_{x5}} = \frac{W_{2S}(a_y + \sin\phi)(h'_{cg} - h_{2r})}{(W_{2S} - W_{2STractor})(a_y + \sin\phi)(h_{cg} - h_5)} \tag{3.19}$$

Substituting h'_{cg} into equation (3.19), we have

$$\frac{M_{x2}}{M_{x5}} = \frac{W_{2S}\left(\frac{(W_{2S} - W_{2STractor})h_{cg} + W_{2T}h_{2STractor}}{W_{2S}} - h_{2r}\right)}{(W_{2S} - W_{2STractor})(h_{cg} - h_5)}$$

$$= \frac{(W_{2S} - W_{2STractor})h_{cg} + W_{2T}h_{2STractor} - W_{2S}h_{2r}}{(W_{2S} - W_{2STractor})(h_{cg} - h_5)} \tag{3.20}$$

or

$$M_{x2} = \frac{(W_{2S} - W_{2STractor})h_{cg} + W_{2STractor}h_{2STractor} - W_{2S}h_{2r}}{(W_{2S} - W_{2STractor})(h_{cg} - h_5)}M_{x5} \tag{3.21}$$

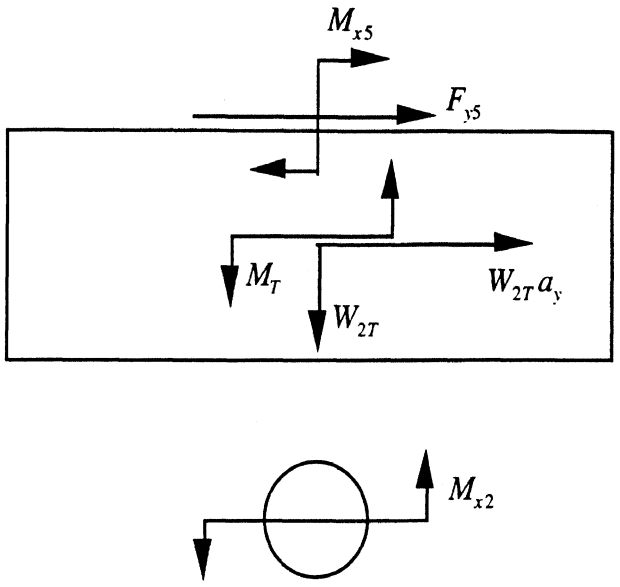

Figure 3.11 A diagram of the freebody of sprung mass of tractor over axle 2

Figure 3.11 is a diagram of the freebody of sprung mass of tractor over axle 2. According to it, we have

$$M_{x2} = M_{x5} + F_{y5}(h_5 - h_{2r}) + W_{2STractor}a_y(h_{2STractor} - h_{2r}) - M_T \tag{3.22}$$

where M_T is the roll moment sustained by tractor frame. Combining equation (3.21) and (3.22) produces

$$M_{x5} + F_{y5}(h_5 - h_{2r}) + W_{2STractor}a_y(h_{2STractor} - h_{2r}) - M_T$$

$$= \frac{(W_{2S} - W_{2STractor})h_{cg} + W_{2STractor}h_{2STractor} - W_{2S}h_{2r}}{(W_{2S} - W_{2STractor})(h_{cg} - h_5)} M_{x5}$$

or

$$h_{cg} = h_5 + \frac{M_{x5}W_{2S}(h_5 - h_{2r}) - M_{x5}W_{2STractor}(h_5 - h_{2STractor})}{\left[F_{y5}(h_5 - h_{2r}) + W_{2STractor}a_y(h_{2STractor} - h_{2r}) - M_T\right](W_{2S} - W_{2STractor})} \tag{3.23}$$

Since we know structural parameters of tractor h_5, $h_{2STractor}$, h_{2r} and $W_{2STractor}$, and we will measure signals M_{x5}, F_{y5} and a_y, the CG height of trailer h_{cg} can be estimated according to equation (3.23) if we know W_{2S} and M_T. W_{2S} can be estimated from the trailer pitch plane model. Because of low stiffness of tractor frame, M_T can be ignored.

M_T can also be set to different values to investigate its effect on estimating h_{cg}. In engineering application, M_T can be measured.

Figure 3.12 is a schematic representation of the vehicle dynamics simulation model. For the detailed data used in the simulations, see the PARSFILE in Appendix A.4. The known structural parameters of tractor in equation (3.23) are

h_5= 48 in

$h_{2STractor}$= 37.5 in

h_{2r}= 23 in

$W_{2STractor}$= 2500 lb.

Suppose that we know W_{2S} is 12000 LB (this is the value of W_{2S} used in simulation). From the simulation, we can obtain M_{x5}, F_{y5} and a_y that are shown in Figure 3.13, 3.14 and 3.15. The roll angle of trailer ϕ is also shown in Figure 3.16. When the roll moment sustained by tractor frame M_T linearly changes with the roll angle of trailer ϕ

$$M_T = K_T\phi \tag{3.24}$$

where K_T is about 3300 in-LB/deg. We can estimate the CG height of trailer according to equation (3.23). The estimated results are shown in Figure 3.17. The solid line in Figure 3.17 is the CG height of trailer used in the simulation which can be thought as a baseline. The thin solid line in Figure 3.17 is the estimated CG height of trailer when M_T is set to zero. It can be seen there is a good agreement between the estimation and baseline. The dashed line in Figure 3.17 is the estimated CG height of trailer when M_T in equation (3.24) is used. It shows that M_T will bias the estimation of the CG height of trailer.

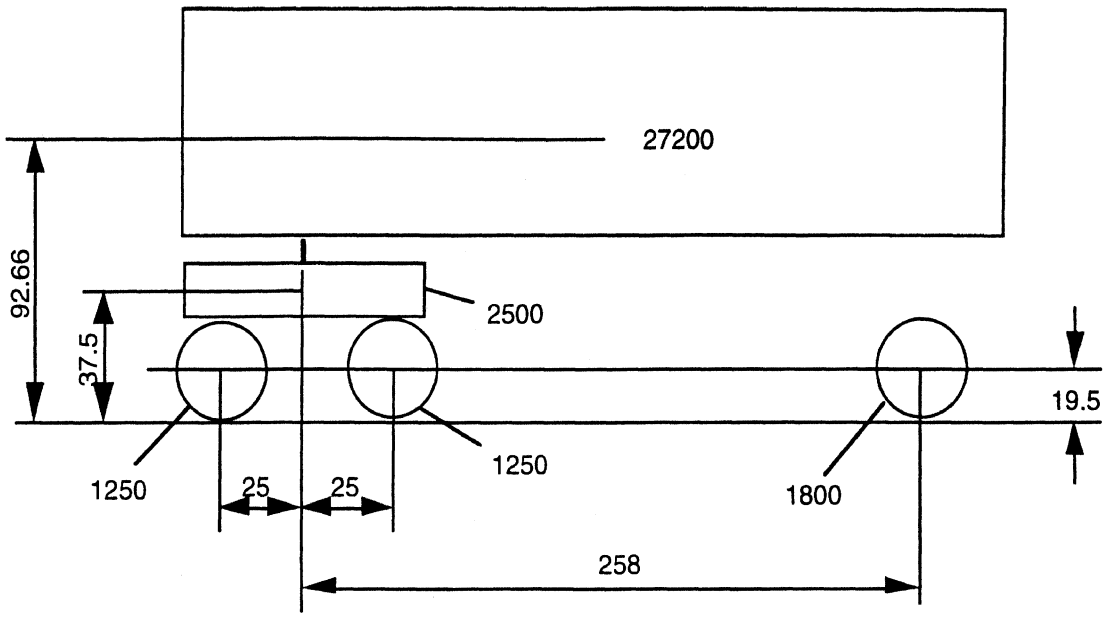

Figure 3.12 A schematic representation of the vehicle dynamics simulation model

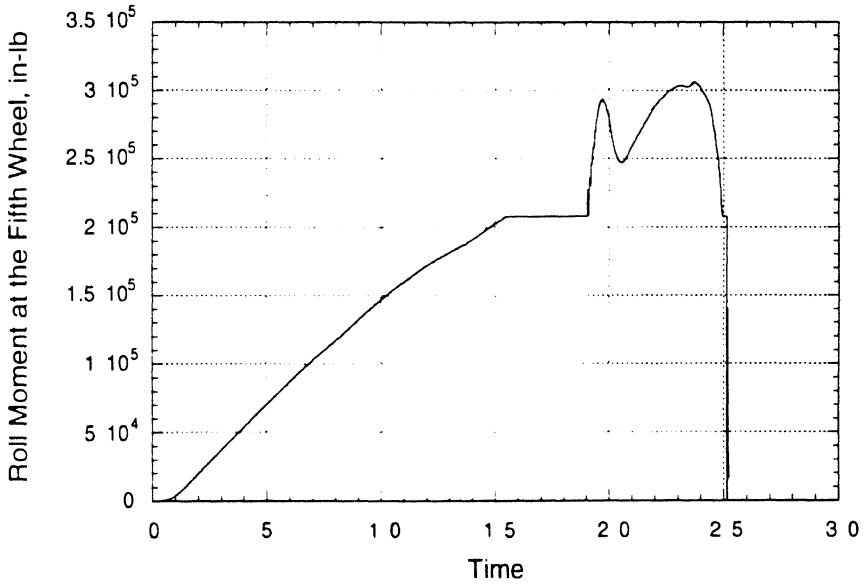

Figure 3.13 Simulation results: roll moment at the fifth wheel vs. time

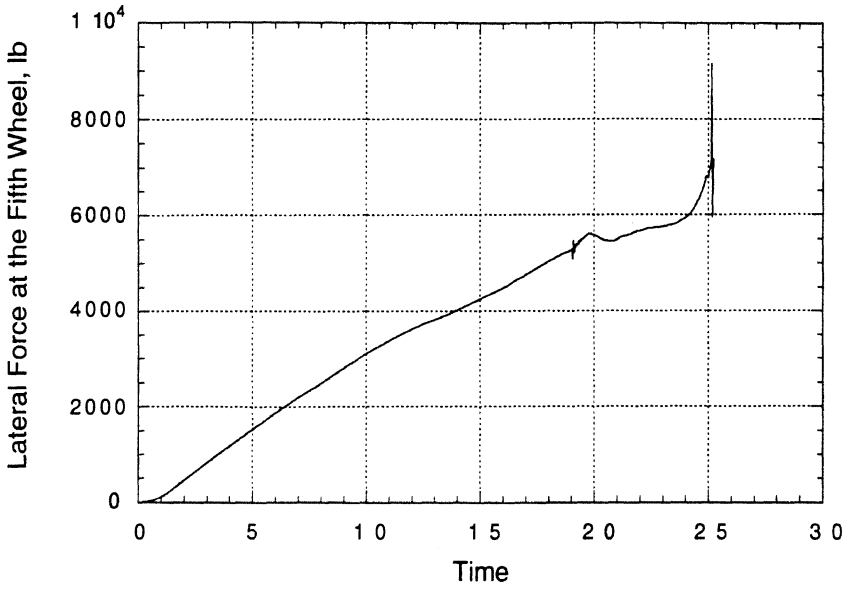

Figure 3.14 Simulation results: lateral force at the fifth wheel vs. time

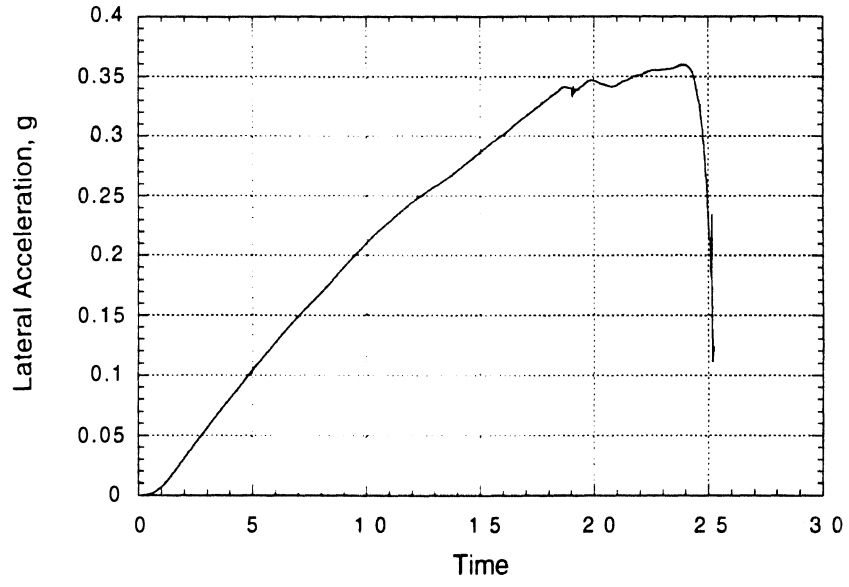

Figure 3.15 Simulation results: lateral acceleration vs. time

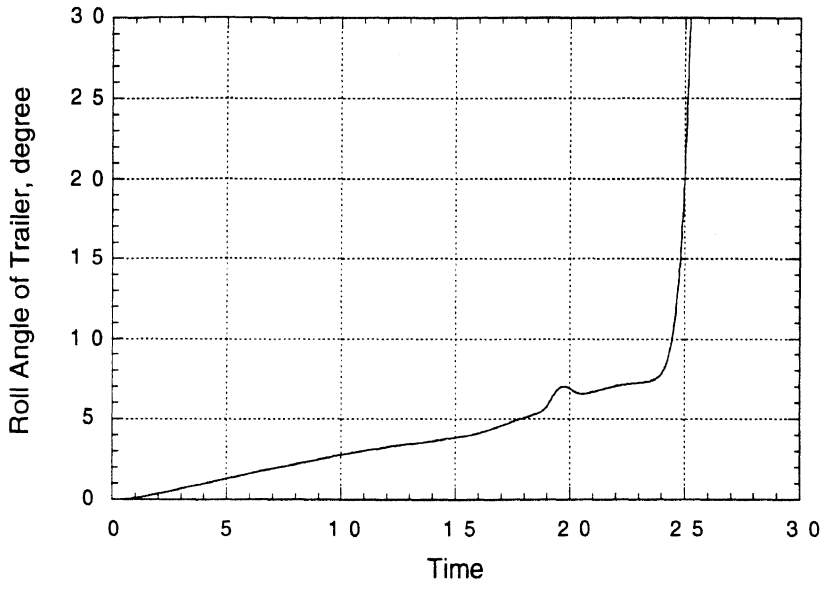

Figure 3.16 Simulation results: roll angle of trailer vs. time

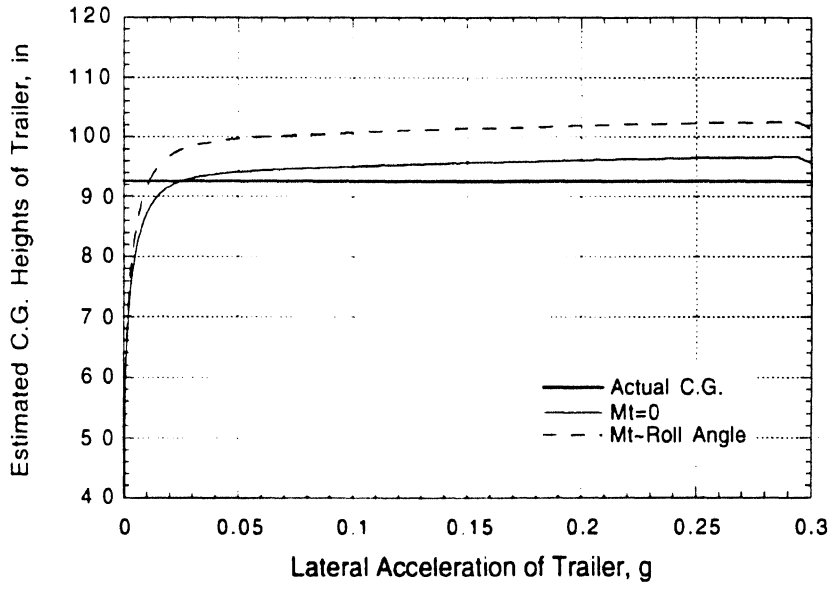

Figure 3.17 A comparison of estimated CG heights and actual CG height of trailer